FUNCTIONAL CHARACTERISTICS AND MOLECULAR REGULATION OF LYMPHANGIOGENESIS DURING GECKO TAIL REGENERATION: EVIDENCE FOR THE ROLES OF VEGF-C, VEGF-D AND THE RECEPTOR VEGFR-3

HELEN BLACKER
B.Sc. (Hons)

Department of Ecology and Evolutionary Biology
School of Earth and Environmental Sciences
The University of Adelaide
South Australia

August 2011

A thesis submitted for the degree of Doctor of Philosophy at The University of Adelaide

TABLE OF CONTENTS

Chapter Two

HOW REGENERATING LYMPHATICS FUNCTION: LESSONS FROM LIZARD TAILS

Chapter Three

DIFFERENTIAL mRNA EXPRESSION OF LYMPHANGIOGENIC GROWTH FACTORS (VEGF-C AND -D) AND THEIR RECEPTOR (VEGFR-3) DURING TAIL REGENERATION IN A GECKO

Chapter Four

ISOLATION AND CHARACTERISATION OF FULL LENGTH VEGF-C, VEGF-D AND VEGFR-3 SEQUENCES FROM THE GECKO *Christinus marmoratus*

Chapter Five

PROTEIN ANALYSIS OF gVEGF-C, gVEGF-D AND gVEGFR-3

Chapter Six
GENERAL DISCUSSION

Amendments to Thesis

Helen Blacker

Id: 1062833

Thesis title:

FUNCTIONAL CHARACTERISTICS AND MOLECULAR REGULATION OF LYMPHANGIOGENESIS DURING GECKO TAIL REGENERATION: EVIDENCE FOR THE ROLES OF VEGF-C, VEGF-D AND THE RECEPTOR VEGFR-3

Reviewer One

Reviewer one stated he/she was happy with the thesis as is and no changes were requested. However, suggestions were provided for future publications and future research and these have been gratefully received and noted. A reference was added as requested on Page 150, line 16 to provide clarification.

Reviewer Two

Some page changes have occurred as a result of amendments to the thesis. The paragraph and line changes requested by the reviewer are given first (P= paragraph, L= line) and then where applicable the new paragraph and line numbers are provided in brackets.

Abstract – Reworded section to strengthen the description of the justification for the study.

Chapter 1

P.1-2. (P.2.L.1, 3 and 7) References added as requested

P.7, L.11. Typo corrected

P.9, L.2. 'Aquatic' deleted as requested

P. 9-10. L.25.Deleted this statement, as difficult to clarify (for simplicity)

Fig. 1.3. 17 is in the figure but is obscured by dark shading of the pelvic area in this region. I have deleted the reference to 17 in the figure legend given that it is not readily obvious.

P. 10, l.6. Changed sentence to remove ambiguity

Fig. 1.7. Have deleted this figure due to poor quality and inability to get a better quality image

P.42, L.20. Changed to Gekkonidae

P.43, L.5. *Lacerta* Italicized as requested

Fig. 1.9. Changed to lower case r in Representation as requested

Chapter 4

P. 96 (and others). A global search was performed highlighting the word "insight" and sentences were recast removing this word where appropriate. In particular, as a result of making these changes the last paragraph of the introduction (P.97. L.5, 6 and 7) was changed.

P. 96. (P.97, L.11-14) Added in a sentence stating that RNA was the same as that extracted in Chapter 3 (and therefore animals were the same and tails collected in the same way)

P107, L.7-8. (P108. L.8) Wording changed to 'using these primers', as suggested

Figs. 4.5, 4.6 and 4.7. Abbreviation of 'g' for gecko added to figure caption as requested. Gecko data have been highlighted by the addition of an arrow at each row

P.149, 2nd last line and P. 15-, L.2. (P.150, last line; P.151, L.3) Figs. 5.10A and 5.10B changed to 4.10A and 4.10B as requested

P.151, L.13-17. (P.152, L.13, 18 and 25) References added as requested

P.152, L.15. (P.153, L18, 19) Deleted "has also been found to" and "is believed to" as requested. Likewise performed global search on these terms to remove them where appropriate

P.163, L.7. (P.164, L.7) Deleted second full stop

P.163, L.16. (P.164, L.16) Deleted 'highly' as requested

Chapter 5

P.167, 5.2.1. (P.168, L.3-6) Details of gecko tails used in this chapter added as requested

Fig.5.6. Changed caption as requested

P.203, L.8. (P.205, L.8) Changed 'vessles' to 'vessels' as requested

P.204. A discussion regarding the homology of the immunogenic sites of the antibodies in comparison to the gecko sequence is provided on P.206, L.3-16. The specific immunogenic region (sequences) for the VEGF-C and VEGF-D antibodies were unavailable due to patents by the developers. The sequence for the VEGFR-3 immunogen is accessible and is discussed on P.206, L.13-16.

Chapter 6

6.1. (P.209, L.17) Added that lymphangiogenesis could occur as a combination of both *de novo* or sprouting mechanisms

As earlier addressed have removed "have been shown to" statements where appropriate

P. 220, L.5. (P.222, L.5) Word wasn't missing but an extra word had not been deleted. Deleted to clarify the sentence as requested

Further suggestions for future work

I thank the reviewer for his/her interest in this study and for the valuable suggestions for future studies/publications.

Specifically, the *Anolis carolinensis* sequence will be included in the manuscript of the work described in Chapter 4 for publication.

Further work in this area would almost certainly be warranted on the suggested skink species to examine the process in an animal with fewer lipid stores. A paragraph with this suggestion has been included in the Future Directions section of the thesis (P.218, L.5-10)

ABSTRACT

The Australian marbled gecko, *Christinus marmoratus* has the ability to voluntarily shed its tail (autotomy) and subsequently regenerate the lost tail. The lymphatic vessels of the gecko tail are severed during autotomy and yet the regenerated tail is not lymphoedematous, indicating that the mechanisms for interstitial fluid drainage are maintained, presumably by the growth of new lymphatic vessels (lymphangiogenesis). In contrast, disruption to the lymphatic system in humans can readily result in lymphoedema due to inadequate lymphatic regenerative capacity. Hence, the regenerating gecko tail offers an excellent model to study the process of and fundamental molecular mechanisms behind lymphatic regeneration. Here, I examine lymphangiogenesis within regenerating gecko tails. I hypothesise that physiological function of lymphatic vasculature is recovered by tail regeneration. Further, I hypothesise that lymphatic regeneration is, in part, regulated by vascular endothelial growth factor C (VEGF-C) and VEGF-D via binding to their receptor, VEGFR-3, a key lymphangiogenic pathway in mammals.

Lymphatic uptake and transport, of different sized radiolabelled tracers, were examined using lymphoscintigraphy. Basic lymphatic function is apparent at 6 weeks of regeneration, however lymph clearance and velocity are not restored to near original levels until 12 weeks of regeneration. Differential clearance and lymph velocity between tracers are likely influenced by changes in the cellular matrix and lymphatic vessel permeability.

Molecular control of lymphangiogenesis within regenerating gecko tails was studied by identifying and characterising VEGF-C, VEGF-D and VEGFR-3 in gecko tail tissue extracts. This is the first study to demonstrate the presence of these genes within any reptile. Sequence alignments and molecular modelling highlight conservation of many lymphangiogenic functional residues within the gecko proteins at both a sequence and structural level.

Real time PCR established differential expression profiles of VEGF-C, VEGF-D and VEGFR-3 mRNA throughout tail regeneration, with up-regulation during the early, late and mid-phases of regeneration, respectively. These data are consistent with mammalian studies in wound healing and suggest differing roles during gecko tail regeneration and potentially the lymphangiogenic process following autotomy.

Sites of expression of VEGF-C and VEGF-D in regenerating gecko tails, demonstrated by immunohistochemistry, include keratinocytes and fibroblasts. Positive staining lining blood and lymphatic-like vessels is demonstrated for VEGF-D and VEGF-C, respectively indicating possible associations of the proteins with VEGFRs on endothelial cell surfaces and hence angiogenic and lymphangiogenic capabilities. Strong positive staining of VEGF-C and VEGFR-3 is also observed in adipose tissue in both regenerated and original tail tissue suggesting potential roles in adipogenesis and lymphangiogenesis during fat store expansion.

Positive immunostaining using the LYVE-1 lymphatic endothelium marker demonstrates that lymphangiogenesis does occur during tail regeneration. Technical limitations, possibly related to antibody cross-reactivity prevented detection of VEGFR-3 staining on lymphatic (or blood) endothelial cells in all regenerated and original tails. A suspected lack of mammalian-derived antibody reactivity to the reptilian proteins was also encountered with ELISA and western blotting analyses, with both yielding inconclusive results.

In conclusion, this study demonstrates that adequate lymphatic vasculature and function are restored during gecko tail regeneration. Furthermore, this study provides several lines of evidence, through sequence conservation and mRNA and tissue expression profiles, that VEGF-C, VEGF-D and VEGFR-3 play a role in lymphatic regeneration in a reptile.

DECLARATION

This work contains no material which has been accepted for the award of any other degree or diploma in any university or other tertiary institution and, to the best of my knowledge and belief, contains no material previously published or written by another person except where due reference has been made in the text.

I give consent to this copy of my thesis when deposited in the University Library, being made available for loan and photocopying, subject to the provisions of the Copyright Act 1968.

The author acknowledges that copyright of the published works contained within this thesis (see below*) resides with the copyright holder(s) of those works.

I also give permission for the digital version of my thesis to be made available on the web, via the University's digital research repository, the Library catalogue, the Australasian Digital Theses Program (ADTP) and also through web search engines, unless permission has been granted by the University to restrict access for a period of time.

Helen Blacker
August 2011

*Publications included within this thesis:

Blacker HA, Tsopelas C, Orgeig S, Daniels CB, Chatterton BE. How regenerating lymphatics function: Lessons from lizard tails. The Anatomical Record: Advances in Integrative Anatomy and Evolutionary Biology (2007) 290: 108-114. © 2006 Wiley-Liss, Inc.

Blacker HA and Orgeig S. Differential mRNA and tissue expression of lymphangiogenic growth factors (VEGF-C and –D) and their receptor (VEGFR-3) during tail regeneration in a gecko. Journal of Comparative Physiology B (2011) DOI 10.1007/s00360-011-0604-0. © Springer-Verlag 2011

ACKNOWLEDGEMENTS

I sincerely wish to thank my principal supervisor Associate Professor Sandra Orgeig for all your patience, guidance and support over the many long years of this project. Thankyou Sandy for your encouragement, your belief in me and for putting up with the many obstacles that came my way (even when they were obstacles I had created myself). Thanks also for being readily available whenever I needed assistance and in particular in the preparation and critical assessment of this thesis. I could not have completed this project without you.

Many thanks also to my co-supervisor Professor Christopher Daniels who was instrumental in the conceptualisation of this work. Thankyou Chris for developing my interest in the world of gecko tails, your enthusiasm and support.

I am grateful to the two best research assistants a lab could want, Ceilidh Marchant and Tamara Crittenden. Thankyou both for your technical expertise and assistance, I could not have gotten the results I did without you.

Thankyou also to past and present lab and office mates who have worked alongside me. In particular, Dr Carol Lang, Dr Natalie Foot, Dr Debra Gum, Suri Lakshmi, Srinivasa Kunchala and everyone in the UniSA Reid building 0-05 and 1-13 offices for their friendship and support and for listening to me whinge when things weren't going well and cheer when things were.

I also thank Frank Madaras for his invaluable knowledge of protein biochemistry and Andrew Beck for training in histology and immunohistochemistry techniques. Thankyou both also for sharing your knowledge on a wide range of topics, your advice and your interest in my work.

Thanks also to Rupal Pradhan for processing tissue samples and providing lab space for the histology and immunohistochemistry components of my work. Thanks to Jessica

Logan and Professor Tony Woods for use of reagents, lab space and training in the failed *in situ* hybridisation studies.

I also thank Chris Leigh and Dr Julie Haynes for helping me to determine the histology of the gecko tail sections I was working with. Thanks also to Dr Steve Donnellan for his critical review of the phylogenetic analysis work in this thesis.

I would like to thank my parents, Ron and Julie Blacker, and my parents in law, Clive and Cherylyn Harrison, for your love, support and many hours of babysitting you have provided over the years so that I could achieve this goal. I also acknowledge my sister Nicole Godfrey and very good friends Lori Pope and Nina Sweet along with my wider family and friends; thankyou for sharing my life and this experience with me.

Finally, I would like to thank my husband Chris and daughter Maya for your love, laughter and unwavering support throughout this journey. Thankyou for your patience, understanding, and encouragement even when things got tough and deadlines kept being passed without being met. Thankyou for sharing the ups and downs with me, continually helping me to see the bigger picture and making it all worthwhile.

All experiments were performed in accordance with the National Health and Medical Research Council guidelines for the use of animals and with approval from both the Adelaide University Animal Ethics Committee (S-18-2003) and Institute of Medical and Veterinary Sciences (IMVS) Animal Ethics Committee (47/04 and 117/08). Adult Australian marbled geckos were collected and housed with permission from South Australia National Parks and Wildlife (permit numbers: E24650 and A24420-7/8) This research was supported by Australian Research Council (ARC) grants to SO and also by a grant from the Breast Cancer Research Association Inc. as trustee for the Breast Cancer Research Trust.

BIBLIOGRAPHY

Journal Articles

Blacker, H.A., S. Orgeig and C.B. Daniels. Hypoxic control of the development of the surfactant system in the chicken: Evidence for physiological heterokairy. *American Journal of Physiology- Regulatory, Integrative and Comparative Physiology.* 2004 Aug; 287(2):R403-10

Blacker HA, Tsopelas C, Orgeig S, Daniels CB, Chatterton BE. How regenerating lymphatics function: Lessons from lizard tails. *The Anatomical Record: Advances in Integrative Anatomy and Evolutionary Biology* (2007) 290: 108-114.

Blacker HA and Orgeig S. Differential mRNA and tissue expression of lymphangiogenic growth factors (VEGF-C and –D) and their receptor (VEGFR-3) during tail regeneration in a gecko. *Journal of Comparative Physiology B* (2011) DOI 10.1007/s00360-011-0604-0

Published Abstract

Orgeig, S., C.B. Daniels, N.J Foot and **H.A Blacker**. 2009. The surfactant system and evolution of the blood-gas barrier. *In:* Perry, S.F., S. Morris, T. Breuer, N. Pajor and M. Lambertz (Eds.) *2nd International Congress of Respiratory Science. Abstracts & Scientific Program*, p. 81. Tharax Verlag.

Unpublished Abstracts

Blacker H, Tsopelas C, Orgeig S, Daniels C, Chatterton B. (2005). Physiological and molecular characterisation of lymphangiogenesis in regenerating gecko tails. 5th World Congress of Herpetology, Stellenbosch, South Africa.

Helen A. Blacker, Sandra Orgeig, Grant W. Booker. (2008). Presenting Vascular endothelial growth factor C (VEGF-C) of the gecko *Christinus marmoratus* – Sequence and model. Australian and New Zealand Society for Comparative Physiology and Biochemistry, Sydney, Australia.

Helen A. Blacker, Sandra Orgeig, Grant W. Booker. (2009). Presenting Vascular endothelial growth factor C (VEGF-C) of the gecko *Christinus marmoratus* – Sequence and model. The Australian Society for Medical Research (ASMR) SA Scientific Meeting, Adelaide, Australia.

Helen A. Blacker. (2009). Expression patterns of lymphangiogenic factors within the regenerating gecko tail. Royal Society of South Australia (RSSA) Post Graduate Student Prize, Adelaide, Australia.

Helen A. Blacker and Sandra Orgeig. (2011). Tissue localisation and mRNA expression of lymphangiogenic growth factors VEGF-C and -D and their receptor VEGFR-3 during tail regeneration in the gecko, *Christinus marmoratus*. The Australian Society for Medical Research (ASMR) SA Scientific Meeting, Adelaide, Australia.

LIST OF ABBREVIATIONS

µCT	Micro-computed tomography
^{99m}Tc-ATC	^{99m}Technetium-antimony trisulphide
^{99m}Tc-DTPA	99mTcdiethylenetriaminepentaacetic acid
^{99m}Tc-TFC	99mTc-tin fluoride colloid
ADSC	Adipose tissue derived stem cell
Ang-1	Angiopoietin-1
Ang-2	Angiopoietin-2
BCA	Bicinchoninic acid
BEC	Blood endothelial cell
CAM	Chorioallantoic membrane
cDNA	Complementary DNA
cVEGF-C(-D)(R-3)	Chicken VEGF-C, VEGF-D or VEGFR-3
ECM	Extracellular matrix
ELISA	Enzyme linked immunosorbent assay
FGFs	Fibroblast growth factors
Flt4	Fms-like tyrosine kinase 4
fVEGF-C(-D)(R-3)	Frog VEGF-C, VEGF-D or VEGFR-3
GSP	Gene specific primer
gVEGF-C(-D)(R-3)	Gecko VEGF-C, VEGF-D or VEGFR-3
HIER	Heat induced epitope recovery
hVEGF-C(-D)(R-3)	Human VEGF-C, VEGF-D or VEGFR-3
Ig-like	Immunoglobulin-like
IHC	Immunohistochemistry
LB	Luria-Bertani
LEC	Lymphatic endothelial cell
LYVE-1	Lymphatic endothelial hyaluronan receptor-1
MMF	Morgan-Mercer-Flodin
mVEGF-C(-D)(R-3)	Mouse VEGF-C, VEGF-D or VEGFR-3
NJ	Neighbour-joining
NRP	Neuropilin
PBS	Phosphate buffered saline

PBS-T	Phosphate buffered saline- Tween20
PCR	Polymerase chain reaction
PDB	Protein data base
PlGF	Placenta growth factor
QC	Quality control
qPCR	Quantitative real time PCR
rAAV	Recombinant adeno-associated virus
RACE	Rapid amplification of cDNA ends
rhVEGF-C	Recombinant human VEGF-C
rhVEGF-D	Recombinant human VEGF-D
rhVEGFR-3	Recombinant human VEGFR-3
rVEGF-C(-D)(R-3)	Rat VEGF-C, VEGF-D or VEGFR-3
rVEGF-C/D	Reptilian VEGF-C/VEGF-D homologue
SDS-PAGE	Sodium dodecyl sulfate polyacrylamide gel electrophoresis
SLC	Secondary lymphoid chemokine
SOC	Super optimal broth with carbolite repression
SS	Signal sequence
sVEGFR-2	Soluble VEGFR-2
TBS	Tris buffered saline
UTR	Untranslated region
VEGF(-A)	Vascular endothelial growth factor (-A)
VEGF-B	Vascular endothelial growth factor B
VEGF-C	Vascular endothelial growth factor C
VEGF-D	Vascular endothelial growth factor D
VEGF-E	Vascular endothelial growth factor E
VEGF-F	Vascular endothelial growth factor F
VEGFR-1	Vascular endothelial growth factor receptor 1
VEGFR-2	Vascular endothelial growth factor receptor 2
VEGFR-3	Vascular endothelial growth factor receptor 3
VHD	VEGF homology Domain
zVEGF-C(-D)(R-3)	Zebrafish VEGF-C, VEGF-D or VEGFR-3

Chapter One

INSIGHTS INTO LYMPHANGIOGENESIS AND LIZARD TAIL REGENERATION

1.1. OVERVIEW

Introducing the topics covered, and the aims addressed, in this thesis requires a wide range of background information. Therefore, in this chapter I provide background to the lymphatic system in mammals and other vertebrate groups and the process of lymphangiogenesis (lymphatic vessel growth) in different physiological and pathological states. I then introduce the vascular endothelial growth factor (VEGF) family and in particular the lymphangiogenic factors VEGF-C, VEGF-D and their receptor VEGFR-3 and discuss the evidence demonstrating their importance in the molecular regulation of lymphangiogenesis in mammals and also in birds, frogs and fish. I follow this with a description of the processes of tail autotomy (tail-loss) and subsequent regeneration in lizards along with previous work that suggests the probability of new lymphatic growth within regenerating tails and regulation by a potential reptilian VEGF-C/D homologue. I conclude with the rationale for choosing the Australian marbled gecko as my model and the aims that I will address in this thesis.

1.2. THE LYMPHATIC SYSTEM

1.2.1. LYMPHATIC SYSTEM STRUCTURE

The lymphatic system is a specialised component of the circulatory system consisting of a network of vessels that drains excess fluid and protein (termed lymph) from the tissues and returns them back into the blood circulation. In humans and other mammals, initial lymphatic networks are found in almost every tissue in the body with the exception of the brain and central nervous system and avascular organs such as the epidermis, the cornea (in non-

pathological states), cartilage and bone marrow (Alitalo et al. 2005). Tissues near the surface of the body for example the skin and mucous membranes of the gastrointestinal and respiratory tracts commonly have an abundance of lymphatic vessels supplying them (Jeltsch et al. 2003).

Lymphatic flow is unidirectional, beginning in small blind-ended lymphatic capillaries (initial lymphatics), draining into pre-collector vessels that then merge into larger collecting lymph vessels (Swartz 2001). Lymph from collecting vessels eventually empties into the thoracic and right lymphatic ducts where it's drained into veins (Fig. 1.1.).

Lymphatic capillaries (Fig. 1.2.) are comprised of a single-cell layer of thin-walled, non-fenestrated lymphatic endothelial cells (LECs). The capillaries are blind-ended vessels of approximately 30-80 μm in diameter with a discontinuous or absent basement membrane. Junctions between LECs within lymphatic capillaries are discontinuous or "button-like" (Baluk et al. 2007; Tammela et al. 2007), unlike the continuous interendothelial junctions of blood vessels. This structural organisation makes lymphatic capillaries highly permeable to protein-rich lymph uptake (Leak 1976) and facilitates leukocyte entry (Baluk et al. 2007). When interstitial pressure is reduced, overlapping junctions of the LECs are arranged such that they act as valves to prevent lymph escaping back into the interstitial spaces (Schmid-Schonbein 2003; Trzewik et al. 2001).

Figure 1.1. Organisation of mammalian lymphatic vasculature. Interstitial fluid, collected by initial lymphatic capillaries, is transported by pre-collector lymphatic vessels to larger collecting lymphatic vessels and returned to the circulation through the thoracic duct. Collecting lymphatic vessels have smooth muscle cell coverage (red) and luminal valves to propel and maintain unidirectional lymph flow. Deep lymphatic vessels run along arteries (A) and veins (V). Figure reproduced from Alitalo et al. (2005).

Lymphatic capillaries depend on specialised, sensitive, elastic structures, termed anchoring filaments, to link LECs to the extracellular matrix (ECM) framework (Gerli et al. 1991; Leak and Burke 1968). This connection between the lymphatic network and the ECM is vital to lymph uptake as the anchoring filaments prevent lymphatic capillaries from collapsing under increased interstitial pressure (arising from increased fluid build-up). Instead increased interstitial pressure results in increased tension on the anchoring filaments that in turn opens the intercellular junctions (Rossi et al. 2007). Opening of the junctions between the LECs creates a pressure gradient that drives interstitial fluid and cell influx into the vessel. The importance of the associations between lymph vessels and the ECM is highlighted in transgenic mice that are deficient in a primary anchoring filament component, ECM glycoprotein Emilin-1 (Danussi et al. 2008). Mice lacking adequate lymphatic/ECM associations as a result of Emilin-1 deficiency display impaired lymph drainage and increased lymphatic leakage.

Following lymph uptake by lymphatic capillaries, lymph is drained into pre-collecting vessels (Fig. 1.2.), which in-turn merge into larger collecting vessels. The pre-collectors and collectors, unlike capillaries, contain a basement membrane, continuous "zipper-like" interendothelial junctions and are surrounded by smooth muscle cells with intrinsic contractile activity to promote lymph flow (Alitalo et al. 2005; Baluk et al. 2007). Collectors also contain intraluminal valves that aid in lymph propulsion by preventing backflow (Petrova et al. 2004; Ryan 1989). Pre- and post-nodal collectors take lymph through at least one or several regional lymph nodes, where lymph is screened and filtered before being returned to the venous circulation. In humans, only two lymphatic/venous anastomoses exist; the thoracic duct draining into the left subclavian vein and the right lymphatic trunk draining into the right subclavian vein (Casley-Smith 1980).

Figure 1.2. Structure of the lymphatic vessels. Lymphatic vessels are thin-walled and have a relatively wide lumen. The endothelial cells of lymphatic capillaries (*green*) lack tight junctions. Instead, the neighboring endothelial cells partly overlap, forming valve-like openings, which allow easy access for fluid, macromolecules, and cells into the vessel lumen. Lymphatic capillaries lack vascular mural cells and have no or only an incomplete basement membrane. Elastic fibers known as anchoring filaments connect lymphatic capillary endothelial cells to the surrounding stroma and maintain vessel patency during increased interstitial pressure. The pre-collecting and collecting lymphatic vessels have a basement membrane, are surrounded by vascular smooth muscle cells (vSMCs; *red*) with intrinsic contractile activity to promote lymph flow, and contain valves that prevent backflow of the lymph. The valve regions are devoid of vSMCs. Figure reproduced from Karpanen and Alitalo (2008).

Lymph transport occurs via a passive drainage system. It is not “pumped” around the body as is the case for the blood circulatory system but rather lymph is moved as a result of contraction of smooth muscle in the walls of larger vessels and by indirect external pressure due to contraction of adjacent skeletal muscles (Bridenbaugh et al. 2003).

1.2.2. LYMPHATIC SYSTEM FUNCTION

The primary function of the lymphatic system is to maintain normal tissue fluid homeostasis by restoring excess interstitial fluid to the cardiovascular system. This interstitial fluid, along with extravasated plasma proteins and macromolecules (lymph), arises from blood capillary leakage as a result of the hydrostatic pressure differential between the arterial and venous ends of capillaries (Landis and Pappenheimer 1963). The return of fluid and plasma proteins into the blood stream ensures that osmotic and hydrostatic gradients between blood capillaries and tissues are sustained thereby guaranteeing adequate interstitial protein transport (see (Jeltsch et al. 2003; Swartz 2001) for reviews) and the maintenance of both plasma and tissue volume. Impaired lymphatic function, characterised by inadequate transport of fluid, macromolecules or cells can result in a number of pathologies characterised by oedema, impaired immunity, and fibrosis (Ryan 1989; Skobe and Detmar 2000) (further discussed in section 1.4.).

Another important function of the lymphatic system is in immune defence. The lymphatics are the main transport route of immune cells from peripheral tissues to the lymph nodes and into the blood circulation. Lymphoid organs such as the lymph nodes, tonsils, Peyer’s patches, spleen, and thymus, are all part of the lymphatic system and all play important roles in the immune response. Lymph nodes, in particular, are extremely important in the body’s defence as they filter and screen lymph for bacteria, viruses, cancer cells, and other unwanted substances and are the site where immune responses to these are initiated (Cavanagh and Von Andrian 2002). Within the lymph node, antigens are presented to B and T

cells, which, in collaboration with the antigen presenting cells, proliferate and mount an immune response against foreign pathogens, including inflammatory cell responses, killer T-cell activation and antibody production (Cavanagh and Von Andrian 2002). Activated B-cells produce antibodies that, along with other activated immune cells are delivered into the normal circulation by the lymphatics to begin their surveillance; additionally the immune cells use the lymphatic network to drain from peripheral tissues back to the lymph nodes.

The lymphatic system also plays a crucial role in intestinal absorption and transport of dietary lipids and the fat-soluble vitamins A, D, E and K from the digestive tract (Blomhoff et al. 1990). The intestinal villi of the digestive tract contain highly permeable lacteal lymphatic vessels, which preferentially take up large molecules and colloids. Up to 90% of dietry fat is absorbed from the gut via the lacetals (Casley-Smith 1962). Further links between lymph vessels, fat digestion and adipose tissue have recently been highlighted in Prox1 heterozygous mice. Prox1 is a homeobox gene that is a specific marker for LECs and is considered the master control gene for the specification of LEC fate and the maintenance of LEC identity (Wigle et al. 2002; Wigle and Oliver 1999). Mice heterozygous for Prox1 either die in the neonatal period (Wigle and Oliver 1999) or display adult onset obesity with fat deposits situated within tissues surrounding leaky lymphatics (Harvey et al. 2005).

The crucial role of the lymphatic system in returning excess interstitial fluid and escaped plasma proteins back into the blood, thereby maintaining tissue fluid balance and homeostasis, is highlighted when disruptions to the lymphatic system occur (discussed in section 1.4.1.).

1.2.3. LYMPHATICS IN OTHER VERTEBRATES

1.2.3.1. Fish

The existence of a lymphatic system in fish has been debated. It is thought that primitive fish species lack well-established lymph vasculature and instead possess a secondary vascular

system (described by (Steffensen and Lomholt 1992; Steffensen et al. 1986; Vogel 1985)) that has been hypothesised to be an evolutionary predecessor of the lymphatic system (Steffensen and Lomholt 1992). This secondary vascular system is proposed to function in skin respiration, osmoregulation and immune defence and the vessels are in open communication with arteries by multiple connections. In contrast, Kampmeier (1969) documented a detailed classification of the lymphatics of adult teleost fish, which consists of longitudinal superficial trunks (dorsalis, ventralis and laterale) and deeper trunks (spinal and subvertebral) along with profuse networks of smaller vessels on the surface of the organs. This work was supported by findings of Yaniv et al. (2006) in the adult zebrafish and in a recent review (Isogai et al. 2009) evidence was provided from both views, with the authors concluding that in zebrafish at least there is a well defined lymphatic system that shares many common features with those of other vertebrates (Isogai et al. 2009).

1.2.3.2. Amphibians

All amphibian orders have a lymphatic system that is analogous to the mammalian system except for a few key differences. Adult animals possess a system of interconnected cutaneous lymph sacs or sinuses rather than tubular lymphatic vessels (Kotani 1990). Amphibians also possess lymph hearts, positioned near lymphatico-venous communications. These hearts are muscular, contractile structures that receive many lymphatic vessels and act in facilitating the entry of lymph into the venous circulation and also to maintain lymph flow directionality. Frogs can have anywhere between 4 and 6 lymph hearts positioned in the jugular, lumbar and caudal regions of the body, whereas caecilians can have over two hundred.

1.2.3.3. Birds

Birds, like mammals, have lymph nodes and no lymph hearts. The number of lymph nodes present, however, is considerably lower than that in mammals. For example ducks have 4

lymph nodes (Jeltsch et al. 2003) compared to 400-500 in humans. Such few lymph nodes implies that not all lymph passes through a node before entering the venous circulation as is the case in humans. Only lymph vessels in the cervical and lumbar regions drain into lymph nodes before their junction with a vein. Similarly, birds also possess valves within the lymph vessels that ensure unidirectional lymph flow, however these are less numerous than in mammals.

1.2.3.4. Reptiles

Reptiles, like mammals, possess superficial lymphatic nets penetrating most organs and structures (Ottaviani and Tazzi 1977). These nets collect lymph from the intercellular spaces in preparation for delivery to the lymphatic sinuses via collecting vessels. Lymph is transported via the collectors to the principal (or main) trunks, which are large vessels that convey lymph to the venous system (Ottaviani and Tazzi 1977). Reptilian lymphatic flow is also unidirectional as a result of specialised valves within the lymphatic vessels (Kotani 1959) (quoted in (Ottaviani and Tazzi 1977)). Despite similarities in anatomy and function, several distinct differences between the reptilian and mammalian lymphatic systems exist. Reptiles appear to lack lymph nodes and instead have lymphatic sinuses (characteristic dilations of the vessels) occurring at the sites where lymph nodes are normally present in mammals and birds (Panizza 1833) (quoted in (Ottaviani and Tazzi 1977)). Reptiles also possess a single pair of pelvic lymphatic hearts acting to pump lymph into the venous system. Further differences are observed in lizards, which appear to have additional lymph drainage sites into the systemic blood circulation compared with mammals. The reptilian lymphatic system is also generally composed of relatively larger vessels than those of mammals (Panizza 1833) (quoted in (Ottaviani and Tazzi 1977)).

The basic anatomy of the major trunks of the lizard lymphatic system is shown in Fig. 1.3. (Ottaviani and Tazzi 1977). Evidence of lymph drainage at a site other than the thoracic

region (as is generally the case for mammals) is provided by visualisation of radiocolloid movement and migration following injection into the tail of the lizard *Pogona vitticeps*, which does not exhibit caudal autotomy. Colloid uptake and flow within the lizard tail shows emptying of lymph into the venous system near the cloacal plexus (Tsopelas et al. 2002). This transit pattern was also observed in the gecko *Christinus marmoratus* (Daniels et al. 2003). In comparison, visualisation of lymphatic flow following injection into the tail of mice shows drainage via the thoracic and right lymphatic ducts (Tsopelas et al. 2002). In general for the lizard, the *jugular trunks* drain lymph from the head and neck, the *subclavian trunk* drains the anterior limbs, the *lumbar trunks* drain the posterior limbs and organs of the pelvis and the *thoracic ducts* drain the trunk and coelom and continue caudally into the lumbar trunk (Ottaviani and Tazzi 1977). Along with these major trunks there are two major sinuses that convey lymph to the venous system; these are the pre-cardiac sinus and the ischiatic sinus. The pre-cardiac sinus, also known as the cardiac plexus (Panizza 1833) or jugular cistern (Chapman and Conklin 1935), occurs in all reptiles and is the site of confluence for the major lymphatic trunks in the anterior portion of the body that drain lymph to the venous system. The ischiatic sinus in lizards is the confluence of the lateral collectors of the tail and other collectors, branches and sinuses of the posterior portion of the body. It also marks the beginning of the lateral lymphatic trunk. The lymphatic hearts are found in the caudal part of the ischiatic sinus. In *Lacerta vivipara* and other lacertids the lymph heart pumps the lymph into the venous system at the ischiatic sinus at a rate of 50-78 pulses per minute (Spanner 1929) (quoted in (Ottaviani and Tazzi 1977)).

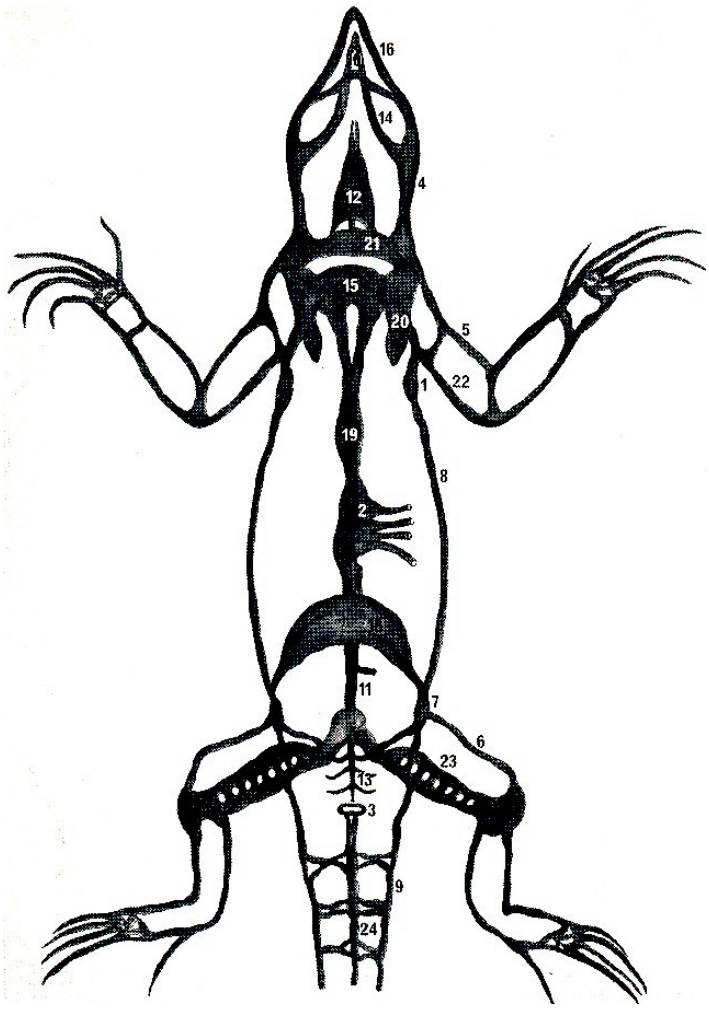

Figure 1.3. The Reptilian Lymphatic System. The major trunks of the lymphatic system in lizards. 1. Axillary sinus; 2, cisterna chyli with intestinal collectors; 3, cloacal plexus; 4, deep jugular trunk; 5, dorsal collector of anterior limb; 6, dorsal collector of posterior limb; 7, ischiatic sinus with lymphatic heart; 8, lateral trunk; 13, pelvic plexus; 14, perimasseteric lymphatic ring; 15, precardiac sinus; 16, submandibular trunk;; 18, subvesical sinus; 19, thoracic duct; 20, thoracic sinus; 21, transverse sinus; 22, ventral collector of anterior limb; 23, ventral collector of posterior limb with periglandular sinus; 24, ventral trunk of the tail. Figure reproduced from Ottaviani and Tazzi (1977).

1.2.4. LYMPHATICS OF THE LIZARD TAIL

The lymphatics in the subcutaneous layer of the ventral surface of the lizard tail are comprised of a set of paired, longitudinal, axial vessels that collect lymph from this region and drain it into the cloacal plexus (Ottaviani and Tazzi 1977). Along the lateral surfaces of the tail there are also lateral collectors, which enter the ischiatic sinus near the caudal base. The deeper part of the tail is drained by the perivertebral lymphatic vessels (Ottaviani and Tazzi 1977). The ventral and lateral lymphatic networks appear to be connected, although, while the lateral trunks in the tail connect with those in the upper body, the ventral trunk ceases near the cloaca. As previously described, radiocolloid injection into the tail of *P. vitticeps* (Tsopelas et al. 2002) and *C. marmoratus* (Daniels et al. 2003) shows migration along the ventral trunk alone, without any uptake of the lateral lymphatics suggesting that overall lymphatic flow in the tail is directed solely towards the ventral lymphatic vessel. Adipose tissue in the tail of certain reptiles has also been found to contain lymphatic vessels. Geckos, for example, have thick, spongy lymphatic nets within the fat bands of their tails (Ottaviani and Tazzi 1977), suggesting that the tail in general for these lizards is particularly rich in lymphatic vasculature.

1.3. LYMPHANGIOGENESIS

Lymphangiogenesis is a term that describes the growth of new lymphatic vessels, both during development and postnatally, by sprouting from veins and/or pre-existing lymphatic vessels and/or de novo growth from lymphangioblasts (Ji 2006).

1.3.1. FACTORS DRIVING LYMPHANGIOGENESIS

To fully discuss the process of lymphangiogenesis in development, normal physiology and in pathological conditions a brief introduction is necessary to the lymphangiogenic growth factors vascular endothelial growth factor C (VEGF-C), VEGF-D and their receptor VEGFR-

3 prior to a more detailed description in section 1.5. VEGF-C and VEGF-D, through binding and activation of the receptor VEGFR-3 have been suggested to constitute the key lymphangiogenic pathway (Achen et al. 1998; Joukov et al. 1997a; Joukov et al. 1996; Joukov et al. 1997b). VEGF-C and VEGFR-3 are essential for normal lymphatic development; inactivation of these genes prevents adequate lymphatic vessel production and function and is fatal as a result of severe lymphoedema (Karkkainen et al. 2004; Makinen et al. 2001a). VEGF-C and VEGF-D promote, via activation of VEGFR-3, migration, proliferation and survival of lymphatic endothelial cells (Jeltsch et al. 1997; Makinen et al. 2001b; Oh et al. 1997; Veikkola et al. 2001). In adults, up-regulation of VEGF-C, VEGF-D and VEGFR-3 stimulates lymphangiogenesis. This pathway is crucial to wound healing (section 1.3.3) and is also implicated in stimulating lymphangiogenesis in tumours (section 1.4.3) and inflammatory diseases (1.4.2).

1.3.2. EMBRYOGENESIS OF THE LYMPHATIC SYSTEM

The precise mechanism behind the embryogenesis of the lymphatic system remains unclear. Two opposing theories for the embryonic origin of the lymphatic vessels have been proposed; Sabin's centrifugal sprouting theory (Sabin 1902) and Huntington and McClure's centripetal theory (Huntington and McClure 1910).

In the centrifugal sprouting hypothesis, LECs are derived from the venous endothelium and bud off from veins during early development to form primitive lymph sacs in the jugular region. The peripheral lymphatic system develops from these embryonic lymph sacs exclusively by sprouting of endothelial cells into surrounding tissues and organs to produce an organised network of lymphatic capillaries and collecting lymphatic vessels. Most recent research appears to support Sabin's theory. For example, the lymphangiogenic receptor and a LEC marker, VEGFR-3, is expressed in the venous endothelium and by precursor lymphatic endothelial cells during early development (Dumont et al. 1998; Kaipainen et al.

1995; Kukk et al. 1996) and then becomes largely restricted to the lymphatic endothelium in adults (Kaipainen et al. 1995; Partanen et al. 2000). Similarly, expression patterns and gene knockouts of Prox1, the master control gene for lymphatic endothelial cell phenotype (Hong et al. 2002; Wigle et al. 2002; Wigle and Oliver 1999), demonstrate a venous origin of lymphatic development.

Conversely, the centripetal theory suggests lymphatic endothelial cells arise independently of the venous endothelium and instead derive from mesenchymal progenitor cells (lymphangioblasts). These cells fuse into primitive lymph networks, which subsequently spread centripetally and connect to the venous system. Evidence for this theory has been provided primarily in avian lymphatics, where lymph vessels in both the chorioallantoic membrane and also in early wing buds are derived not only from sprouting from the lymph sacs but also local lymphangioblasts (Papoutsi et al. 2001; Schneider et al. 1999; Wilting et al. 2006; Wilting et al. 2001). Similarly, lymphangioblasts have been documented in *Xenopus* tadpoles, and have been found to contribute to lymphatic vessel formation (Ny et al. 2005). These lymphangioblasts within the developing frogs where characterised as Prox1 positive mesodermal precursor cells, sharing a common origin with vascular progenitor cells (Ny et al. 2005).

Despite the fact that the precise nature of the origin of the first lymph vessels within the embryo remains unclear, a working model for embryonic lymphatic vasculature development has been proposed (Oliver 2004; Oliver and Harvey 2002) based on evidence from studies using molecular markers and transgenic mouse models. This model is highlighted in Fig. 1.4. and incorporates 4 steps: LEC competence, LEC bias, LEC specification and lymph vessel differentiation and maturation.

LEC competence is conferred by the expression of the endothelial cell surface marker lymphatic endothelial hyaluronan receptor-1 (LYVE-1) (Banerji et al. 1999; Jackson et al.

2001) on a small population of endothelial cells lining the cardinal vein (Oliver 2004; Wigle et al. 2002). In mice, this occurs at embryonic day E9 (Oliver 2004; Oliver and Alitalo 2005; Wigle et al. 2002) and indicates that the cells are now able to respond to a lymphatic-inducing signal.

LEC bias is signified by the expression of Prox1 on a subpopulation of LYVE-1 positive endothelial cells shortly after the expression of LYVE-1 (E9.5 in mice) (Wigle and Oliver 1999). Prox1 expression signifies that these cells are now biased towards the lymphatic lineage as this gene has been demonstrated to be required for the induction of LEC fate (Wigle et al. 2002; Wigle and Oliver 1999). Deletion of the Prox1 gene in mouse embryos prevents the formation of the lymph vasculature due to the failure of the appearance of lymphatic cell-type progenitor cells (Wigle and Oliver 1999). Furthermore, cultured blood vascular endothelial cells can be reprogrammed into LECs by increasing Prox1 expression (Hong et al. 2002; Petrova et al. 2002). Prox1 positive endothelial cells are polarised to one side of the cardinal vein and subsequent LEC budding, towards the region where the primary lymph sacs are formed, is also polarised (Wigle and Oliver 1999). Sabin's theory of a venous origin of lymph development is strongly supported by the specific polarised localisation of Prox1 expression in venous endothelial cells, which then go on to form the entire lymph system (Harvey and Oliver 2004).

Figure 1.4. Stepwise model for the development of the mammalian lymphatic vasculature. Early during mouse embryonic development (E9.0–9.5), Prox1 begins to be expressed in lymphatic endothelial cell (LEC) progenitors located in one side of the anterior cardinal veins. Following this expression, those progenitors acquire a LEC phenotype (LEC bias) and bud in a polarised manner. This budding, which is dependent on a VEGF-C signal in the surrounding mesenchyme, gives rise to the primary lymph sacs. Sometime during this process, the lymphatic and venous systems become separated in a process that involves the Syk/SLP-76 signalling pathway, and the sprouting of LECs from those sacs is initiated. Finally, lymphatic vessel maturation and remodeling occurs in a stepwise manner, leading to the formation of the complete lymphatic network. Reproduced from Oliver and Alitalo (2005).

During the stage of LEC specification a precise cascade of molecular steps occurs in which the lymphatic endothelial "precursor" cells decrease the expression of blood vascular endothelial cell specific markers such as CD34, collagen IV and laminin (Wigle et al. 2002) and begin to increase the expression of markers associated with LEC differentiation e.g. neuropilin 2 (NRP2), podoplanin and VEGFR-3. By E12.5 expression of CD34 and laminin is completely absent on the immature LECs and expression of VEGFR-3 by the blood vasculature is being down-regulated (Kaipainen et al. 1995; Wigle et al. 2002). The specification stage also sees budding of immature LECs, which are specified into the lymph programme, from the anterior cardinal vein and the appearance of the primary lymph sacs at E12.5 (Oliver 2004).

Lymph vessel differentiation and maturation is the final stage in the development of the lymphatic network. At this stage, lymph capillaries and vessels are forming and spreading around the developing embryo via budding and sprouting of immature LECs from the primary lymph sacs (Oliver 2004) but these vessels are not yet considered fully mature nor are the cells terminally differentiated (Oliver and Harvey 2002; Wigle and Oliver 1999). Further lymph-specific markers are expressed by the lymphatic vasculature as the immature LECs undergo terminal differentiation, for example podoplanin and secondary lymphoid chemokine (SLC) are detected around the time the LEC's bud from the cardinal vein (Schacht et al. 2003; Wigle et al. 2002). In this final phase of development the LECs are responsive to lymphangiogenic factors and express genes that are important in the final maturation and remodelling of the lymph vasculature. Only immediately prior to birth do lymphatic vessels express the complete profile of markers found in mature, terminally differentiated lymphatics (Oliver 2004; Saharinen et al. 2004).

The formation of the blood vasculature is dependent on vascular remodelling to achieve it's final mature state (Risau 1997). A recent report (Makinen et al. 2007) has

provided strong support for the idea that this process is also required during the maturation of the lymphatic system. Lymph vascular remodelling reorganises the system resulting in the formation of a hierarchically organised network of lymphatic capillaries and collecting lymphatic vessels. Remodelling ensures the development of competent luminal valves within and precise smooth muscle recruitment and coverage on collecting vessels. Crucial genes to this remodelling/ maturation process include angiopoietin-2 (Ang2) and the VEGF-C/D/R3 pathway (Maisonpierre et al. 1997; Veikkola and Alitalo 2002). These genes will be discussed in more detail in section 1.5.

1.3.3. WOUND HEALING AND REPAIR

Normal lymph function is thought to be crucial to wound healing and tissue repair following injury. Lymph vessels at wound sites remove protein-rich lymph and wound debris thereby maintaining tissue homeostasis as well as functioning to deliver cells that mediate the immune response. Impaired lymph function following injury has been implicated in delayed wound healing, persistent oedema and delayed removal of debris and inflammatory cells (Ji 2005). Lymphangiogenesis is therefore assumed to be a vital component of the wound healing process and is assumed to occur by sprouting from existing lymphatics, similar to embryonic development (Clark and Clark 1932; Paavonen et al. 2000; Shimoda et al. 2004). It is unknown whether lymphangiogenesis during tissue repair also involves the incorporation of progenitor cell populations, as is suggested in blood vessel angiogenesis (Rafii 2000). Lymphangiogenesis has been demonstrated in several wound healing studies. For example, wounds in pig skin (Paavonen et al. 2000), mice skin (Ji et al. 2004), rabbit ears (Bellman and Oden 1959; Oden 1960) and the muscle coat of the rat jejunum (Shimoda et al. 2004) all display sprouting and regeneration of lymphatic vessels. Lymphangiogenesis in pig skin punch biopsies was characterised by rapid growth of VEGFR-3 positive lymph vessels, followed by a regression in lymph vessel number. This transient increase in lymph vessels

was suggested to be an integral part of normal wound healing, whereby increased numbers of vessels are required early to promote lymph removal and lymphocyte trafficking and once healing is complete increased vessels are no longer needed (Paavonen et al. 2000). Impaired healing in chronic pig skin wounds showed an absence of lymph vessels (Paavonen et al. 2000). Likewise, mouse cornea excisional wounds show increased formation of lymphatics during the acute phases of healing, despite this tissue normally being devoid of lymphatic vessels (Maruyama et al. 2005). Similarly, lymphatic vessel regeneration is observed in unilateral autotransplantation of rat hindlimb tissue (Anthony et al. 1997) where a rapid return to near normal levels of lymph clearance is observed following replantation. The pattern of lymph flow in this model, however, was abnormal, relying on multiple small channels of the superficial lymphatic system bypassing the usual deeper routes of lymphatic drainage (Anthony et al. 1997). In humans, lymphatic imaging has shown a re-establishment of lymphatic pathways following replantation of amputated extremities (Smith et al. 1987) and following microvascular free-flap tissue transfer (Slavin et al. 1997). It is unclear whether the re-establishment of flow seen in many wound healing studies is through the same pathways as seen before the injury/trauma or whether new pathways are formed and similarly whether restored flow is due to passage through simple fluid channels within tissues, growth of new vessels and/or reconnection to existing vessels. More research into lymphatic regeneration and lymph flow re-establishment within the setting of wound healing is needed and could provide further knowledge into the mechanisms behind lymphangiogenesis.

1.4. PATHOLOGY OF THE LYMPHATIC SYSTEM

The lymphatic system and the lymphangiogenic process have recently been highlighted in several pathological conditions where there is either a malfunction in the process of

lymphangiogenesis (up or down-regulated) or a breakdown in the normal function of the lymphatic system.

1.4.1. LYMPHOEDEMA

Malfunctions of the lymphatic system can result in impaired lymphatic drainage and lead to excess fluid accumulation within the tissues, otherwise known as lymphoedema (Szuba and Rockson 1997). This painful and debilitating disorder is either an inherited disease where these is an underdevelopment of the lymphatic network (primary lymphoedema) or may be the result of lymphatic vessel trauma or obstruction as a result of infection, radiation therapy, or surgery (secondary/ acquired lymphoedema). While not life threatening, lymphoedema is often complicated by fibrosis and susceptibility to infections and inflammation (Tabibiazar et al. 2006).

The genetic basis for some primary lymphoedema diseases has recently been uncovered. Milroy disease (Milroy 1892) appears to be a result of mutations that lead to inactivation in the kinase region of the VEGFR-3 gene (Brice et al. 2005; Butler et al. 2007; Karkkainen et al. 2000). Inactivation in this part of the VEGFR-3 gene prevents adequate receptor phosphorylation and hence inhibits downstream signalling. Furthermore, the Chy mouse model, which displays a lymphoedema phenotype, was discovered to contain a heterozygous inactivating VEGFR-3 mutation in the germ line resulting in hypoplasia of the cutaneous initial lymphatics. This model is consequently being used for the design and testing of new therapeutic strategies for lymphoedema (Karkkainen et al. 2001; Kriederman et al. 2003; Pennisi et al. 2000). Encouraging results have already been obtained using VEGF-C gene therapy in animal models of lymphoedema (Karkkainen et al. 2001; Saaristo et al. 2002b; Szuba et al. 2002), which is discussed in more detail in section 1.5.2.1. Further understanding of the molecular control (up-regulation and inhibition) of the process of

lymphangiogenesis in both normal and pathological scenarios is needed to aid in therapy development.

Secondary (or acquired) lymphoedema occurs much more frequently than primary lymphoedema and is a consequence of lymphatic vessel damage or obstruction. The most common causes of secondary lymphoedema are parasitic infection (filariasis (Routh and Bhowmik 1994)) of the lymphatic vessels (in developing countries) and surgery or radiation (in developed countries).

Surgery to remove cancerous tissue and radiation are common therapies in cancer treatment. Surgery often results in resection of the lymphatic vessels and removal of lymph nodes impairing lymphatic drainage. Radiation therapy can induce tissue fibrosis, which can also compromise lymph flow (Petrek et al. 2000). A common example of post-cancer lymphoedema is seen in breast cancer treatment by either full or partial mastectomy. In this operation, several lymph nodes in the armpit are excised, (Mortimer et al. 1996), which can impair lymphatic drainage in the arm resulting in fluid accumulation and hence lymphoedema.

Untreated lymphoedema progressively worsens and can become excruciating, unsightly and incapacitating, which has both physical and psychological connotations for sufferers (Bianchi and Todd 2000). It can also make the affected limbs more susceptible to bacterial infection. Current treatments of lymphoedema (reviewed in (Board and Harlow 2002b)) include: compression therapy, massage, diuretics and surgery. These treatments aim to stabilise and restore the equilibrium between capillary filtration and lymphatic drainage (Badger et al. 2000; Leduc et al. 1998; Mortimer 1990; Todd 2000), however, none effectively address the cause of the lymphoedema and no curative therapies are currently available.

1.4.2. INFLAMMATION

An active involvement of lymphatic vessels in the regulation of inflammation and of lymphangiogenesis in certain inflammatory diseases has recently been demonstrated (reviewed by Ji (2007)). Pro-inflammatory cytokines can induce expression of the lymphangiogenic factors VEGF-C (Ristimaki et al. 1998) and VEGF-D (Watari et al. 2008). Activation of lymphangiogenic factor secretion by pro-inflammatory cytokines is presumably through promoter activation by NF-kB, a transcription factor typifying inflammation (Watari et al. 2008). Furthermore, cells involved in the inflammatory process such as dendritic cells, macrophages, neutrophils and epithelial cells also express VEGF-C and VEGF-D (Baluk et al. 2005; Watari et al. 2008).

Macrophages, when recruited to inflammation sites, are not only able to secrete lymphangiogenic growth factors VEGF-C and VEGF-D to induce lympangiogenesis (Schoppmann et al. 2002a) and chemotaxis of additional macrophages (Skobe et al. 2001a), but are also capable of trans-differentiating to LECs, which incorporate into the lymphatic endothelium (Kerjaschki 2005; Kerjaschki et al. 2006; Maruyama et al. 2005; Schledzewski et al. 2006).

Mouse models of chronic airway inflammation, stimulated by infection with *Mycoplasma pulmonis*, show vigorous lymphangiogenesis, driven by immune cell secretion of VEGF-C and VEGF-D (Baluk et al. 2005). This new lymph vessel growth within the airway inflammation model prevents mucosal oedema. Blocking the action of VEGF-C and VEGF-D results in bronchial lymphoedema, thus demonstrating the importance of the lymphatic vasculature in the removal of immune cells and excess fluid (Baluk et al. 2005).

Inflammation is stimulated in cases of rejected kidney transplants and is associated with increased lymphangiogenesis (relative to normal kidneys) of the host lymphatic vessels (Kerjaschki et al. 2006). Likewise, excess lymphangiogenesis is implicated in corneal

allograft rejection (Cursiefen et al. 2003). Lymphatic vessels are not normally present within the cornea unless stimulated under inflammatory conditions (Albuquerque et al. 2009; Cursiefen et al. 2002). Rabbit and mice corneal inflammation models demonstrate that inflammatory cells can respond to, and express, lymphangiogenic signals to mediate lymphangiogenesis (Cursiefen et al. 2004; Hamrah et al. 2003).

In the mouse corneal model a serendipitous discovery of a naturally occurring antagonist to VEGF-C was made which may prove useful in therapeutic strategies aimed at blocking lymphangiogenesis (Albuquerque et al. 2009). A soluble protein generated by alternative splicing of the gene encoding VEGFR-2, termed soluble VEGFR-2 (sVEGFR-2), was capable of binding to and blocking VEGF-C function and consequently inhibit lymphangiogenesis (Albuquerque et al. 2009).

In addition, other inflammatory diseases seem to be associated with lymphatic activation and dysfunction. For example, lymphatic hyperplasia is observed in UVB-irradiation induced skin inflammation resembling psoriasis and in human psoriatic skin lesions (Kajiya and Detmar 2006; Kunstfeld et al. 2004). A primary role for VEGF-C/D/R3 signalling in inflammatory lymphangiogenesis is also suggested by overexpression of VEGF-C in the joint synovium of rheumatoid arthritis patients (Paavonen et al. 2002). These studies underline the close relationship between inflammation, the immune response and the adaptability of a mature lymphatic network.

Further research into the molecular mechanisms behind lymphangiogenesis and the development of new tissue or animal models in which lymphangiogenesis occurs may uncover further agonists or antagonists to aid in therapies to treat lymphatic based pathologies. In the context of inflammatory lymphangiogenesis, for example, more knowledge on how to effectively block the process may help prevent graft rejection and allow the manipulation of certain inflammatory diseases.

1.4.3. TUMOUR LYMPHANGIOGENESIS

Research into the lymphatic system has recently attracted much interest due to the role of the lymphatic vasculature in metastatic dissemination of tumour cells. The lymphatic vasculature serves as a primary pathway for the initial metastasis of malignant tumour cells to regional lymph nodes (reviewed by (Stacker et al. 2002b). Tumour spread, as detected by the presence of tumour cells within lymph nodes, has long been used as a prognostic indicator of disease progression, dictating treatment options for human cancers and determining the likelihood of disease recovery. To enable metastatic spread, tumours must either invade pre-existing lymphatic vessels in the surrounding tissues or utilise peri-tumoural (vessels adjacent to the tumour) and/or intra-tumoural lymphatic networks (Cao 2008; Karpanen et al. 2001; Mandriota et al. 2001; Skobe et al. 2001b; Stacker et al. 2001).

Many studies performed over the past decade have suggested that tumour cell dissemination via the lymphatics occurs as a result of lymphangiogenesis, whereby tumours actively stimulate lymphatic vessel growth to gain access to pre-existing lymph vasculature. Experimental cancer models have provided evidence that lymphangiogenesis is associated with and may facilitate metastasis (Saharinen et al. 2004; Stacker et al. 2002a). Likewise, clinical findings have shown strong correlations between tumour lymphangiogenesis and metastasis to lymph nodes in tumours, including inflammatory breast carcinoma (Van der Auwera et al. 2005), non-small cell lung cancer (Renyi-Vamos et al. 2005) and cancers of the bladder (Fernandez et al. 2008), head and neck (Beasley et al. 2002). Furthermore, in some human cancers such as cutaneous melanoma, the presence of tumour lymphangiogenesis serves as a prognostic indicator for metastasis and survival (Dadras et al. 2003). However, metastasis is not always dependent on lymphangiogenesis. Tumour cell spread to lymph nodes has been observed in the absence of tumour lymphangiogenesis, presumably by tumour cells accessing pre-existing lymph vessels only (Wong et al. 2005).

Tumour lymphangiogenesis is likely to be induced via the production of lymphangiogenic growth factors by the tumour cells themselves and by tumour-associated cells such as macrophages (Hirakawa et al. 2007; Hirakawa et al. 2005; Schoppmann et al. 2002b). In addition to actively stimulating lymphatic vessel growth these factors could dilate pre-existing lymph vessels (making entry easier) and facilitate transmigration of tumour cells through the lymphatic endothelium (Alitalo et al. 2004). Studies in animal models of cancer have provided direct experimental evidence that VEGF-C or VEGF-D promote active tumour lymphangiogenesis and lymphatic tumour spread to regional lymph nodes (Karpanen et al. 2001; Mandriota et al. 2001; Skobe et al. 2001a; Stacker et al. 2001). Expression of VEGF-C and -D in transgenic mouse models or via xenotransplantation by tumour cells shows growth of new lymph vessels, mainly at the tumour margin as well as dilation of pre-existing lymphatic vessels draining the tumour. This VEGF-C/D driven lymphangiogenesis increased metastasis of the tumour cells (Kawakami et al. 2005; Mattila et al. 2002). Likewise, many clinicopathological studies report the expression of VEGF-C and/or -D by tumour cells along with positive correlations between increased lymphangiogenic factor expression, lymphatic invasion, lymph node metastasis and poor patient survival, but not necessarily with the density of tumour-associated lymphatic vessels (reviewed in ref (He et al. 2004; Pepper et al. 2003; Stacker et al. 2002a)). Conversely, VEGF-C expression was insufficient to induce lymphatic metastasis in human soft tissue sarcomas (Lahat et al. 2009).

Gaining a better understanding of the lymphatic system and the process of lymphangiogenesis could lead to effective strategies for the treatment of cancer. Despite strong evidence for the role of intra/extra-tumour lymphangiogenesis in cancer growth and metastasis, together with the correlations between lymphangiogenesis or lymphangiogenic factor secretion with lymph node metastasis and poor patient prognosis, the mechanisms of

tumour lymphangiogenesis are still poorly understood and are the focus of much research to aid in therapeutic development.

1.5. THE VEGF FAMILY: ANGIOGENIC AND LYMPHANGIOGENIC GROWTH FACTORS

Members of the VEGF family of growth factors and their receptors are essential components in guiding both blood and lymphatic vessel development and growth. The VEGF family consists of a group of homologous and evolutionarily conserved glycoproteins including, placenta growth factor (PlGF; (Maglione et al. 1991)), VEGF (also known as VEGF-A; (Leung et al. 1989)), VEGF-B (Olofsson et al. 1996), VEGF-C (Joukov et al. 1996), VEGF-D (Achen et al. 1998), VEGF-E (homologs of VEGF encoded by the orf virus) (Lyttle et al. 1994) and the most recently described VEGF-F (present in snake venom) (Suto et al. 2005). VEGF family members are encoded by separate genes (Stacker and Achen 1999) that demonstrate similarities to the primary structure of VEGF characterised by a highly conserved central VEGF homology domain (VHD), which includes six conserved cysteine residues making up the cysteine knot motif.

The VEGF family of proteins binds to specific receptors of the class III tyrosine kinase family. These receptors include VEGFR-1 (also known as FLT1), VEGFR-2 (KDR/FLK1) and VEGFR-3 (FLT4), which are almost exclusively found on endothelial cells (reviewed by (Jussila and Alitalo 2002)). Fig. 1.5. shows the interaction between the VEGFs and their receptors. All VEGF family members are dimeric, whereby, in mature proteins, monomers bind one another via disulphide bridges (VEGF, VEGF-B) or non-covalent bonds (VEGF-C, VEGF-D) to form anti-parallel homodimers before specific receptor binding. VEGF-A binds and activates both VEGFR-1 and –2 (Ferrara 2001), VEGF-B binds only to VEGFR-1 (Olofsson et al. 1996), while VEGF-C and –D are the major ligands for VEGFR-3 and can also bind and activate VEGFR-2 to a certain degree (Achen et al. 1998; Joukov et al.

1996). Each of these proteins and their receptors has different and specific roles. VEGF-A and VEGF-B are thought to be primarily angiogenic, controlling permeability and growth of blood vessels, via signalling through the primary angiogenic receptor VEGFR-2 and VEGFR-1, which are predominantly expressed on BECs (Mustonen and Alitalo 1995). VEGF-C and VEGF-D are thought to be lymphangiogenic via VEGFR-3, which is expressed by blood and lymphatic vasculature during embryogenesis and becomes largely restricted to lymphatic endothelial cells in adults (Dumont et al. 1998; Kaipainen et al. 1995; Partanen et al. 2000). As VEGFR-2 is also expressed on LECs VEGF-C and VEGF-D binding can also stimulate lymphangiogenesis through that receptor.

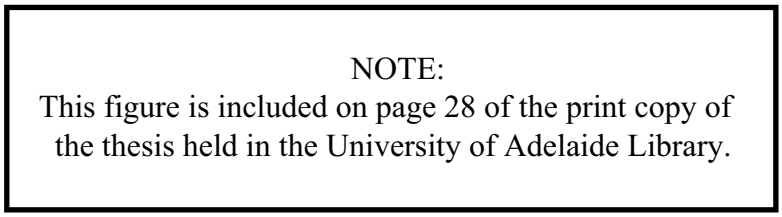

Figure 1.5. Interactions between VEGF family members and VEGF receptors. VEGF-A, VEGF-B and PlGF bind VEGFR-1 on blood vascular endothelium. VEGF-A and fully processed VEGF-C and VEGF-D are capable of binding VEGFR-2 on blood and (to a lesser extent) lymphatic endothelium. VEGF-C and VEGF-D primarily bind VEGFR-3 on lymphatic endothelium. Binding of ligand homodimers triggers receptor dimerisation, subsequent autophosphorylation and signal transduction. The specific actions of receptor binding on blood or lymphatic vessels are shown, along with the structures of the VEGF receptors. Neuropilins 1 and 2 (NRP-1 and NRP-2) are co-expressed with the VEGFR receptors on blood and lymphatic endothelium and interact directly with VEGFRs to guide vasculogenesis (NRP-1) lymphatic sprouting (NRP-2). Asterix denotes that VEGF-D binds VEGFR-2 in humans but not mice (Baldwin et al. 2001). Figure modified from Jussila and Alitalo (2002).

1.5.1. THE KEY LYMPHANGIOGENIC PATHWAY: VEGF-C, VEGF-D AND THEIR RECEPTOR VEGFR-3

VEGF-C and –D form a subfamily of the VEGF family, characterised in terms of their amino acid sequence, by the presence of N- and C-terminal extensions (propeptides) flanking the VHD, which are not present in other family members (Achen et al. 1998; Joukov et al. 1996). The full-length sequence identity between human VEGF-C and –D is 31%, whereas the VHD identity alone is 61%. On the other hand, VEGF-C has only 30% VHD sequence identity with VEGF-A (Joukov et al. 1996). Both VEGF-C and VEGF-D undergo proteolytic processing upon secretion (Fig. 1.6.) to generate mature versions of the proteins, which essentially consist of the VHD (Joukov et al. 1997b; Stacker et al. 1999). Proteolytic cleavage of the propeptides by proteases such as the intracellular secretory proprotein convertases, furin PC5 and PC7 (McColl et al. 2007; Siegfried et al. 2003) and plasmin (McColl et al. 2003) modulates the availability and bioactivity of both VEGF-C and VEGF-D (Baldwin et al. 2002). It is supposed that the C-terminal and N-terminal extensions are responsible for interactions of these ligands with the surrounding extracellular matrix, serving to retain these molecules close to their secretion sites, where they are needed. The C-terminals of both VEGF-C and VEGF-D contain C10XCXCXC motifs resembling the Balbiani ring 3 protein, a secretory protein and a component of silk produced in larval salivary glands of the midge (*Chrionomus tentans*) (Chilov et al. 1997). The silk-like nature of this region of the C-terminal suggests it would promote adhesion to tissues within the site of secretion. The N- and C- terminal extensions are also important in regulating receptor-binding affinities thereby modulating ligand action and function. VEGF-C and VEGF-D are both initially synthesised as pre-proteins with the N and C- terminal extensions intact. Stepwise processing (Fig. 1.6.) results in cleavage of the extensions and the generation of several forms of the proteins, which have sequentially increased binding affinity and activity for their receptors VEGFR-3 and

VEGFR-2. Only the mature fully processed forms of each of these proteins can bind and activate VEGFR-2 and hence promote angiogenesis (Achen et al. 1998; Joukov et al. 1997b; Stacker et al. 1999). Surprisingly, it appears that VEGF-D binds only to VEGFR-3 in mice and not VEGFR-2, but the mature human VEGF-D binds to and activates both VEGFR-2 and VEGFR-3 (Baldwin et al. 2001).

The secreted propeptide of VEGF-C consists of a 31kDa subunit and a 29kDa subunit bound together by disulphide bonds. This secreted form is able to bind VEGFR-3 without any further processing. The VEGF-C propeptide is then further proteolysed in the extracellular environment to generate the mature 21-kDa non-disulfide-linked, anti-parallel homodimeric protein with high affinity for both VEGFR-2 and VEGFR-3 (Otrock et al. 2007). The VEGF-C and VEGF-D receptors also dimerise upon ligand binding and can form homo-VEGFR-3 dimers, homo-VEGFR-2 dimers or hetero-VEGFR-3/VEGFR-2 dimers (Dixelius et al. 2003a) with each having different signal transduction properties.

Figure 1.6. Schematic model of the stepwise proteolytic processing of VEGF-C and VEGF-D. Stepwise proteolytic processing regulates VEGF-C and VEGF-D activity. Both factors are synthesised as precursor proteins (prepropeptides). The C-terminal cleavage occurs in all producing cells and activates binding to VEGFR-3 (lymphangiogenic receptor), which is the only signal needed for lymphangiogenic activity in vivo (Veikkola et al. 2001). After the N-terminus is fully processed, the short form binds to and activates VEGFR-2 (angiogenic receptor) as well, resulting in angiogenic activity (Cao et al. 1998). Thus, both angiogenic and lymphangiogenic signals can be generated from a single molecule depending on the degree of processing and the relative expression of the receptors. Abbreviations are as follows: VHD, VEGF homology domain; SS, signal sequence; N-term, amino-terminus; C-term, carboxy-terminus. Figure reproduced from Oliver and Alitalo (2005).

Proteolytic cleavage is an important regulator of lymphangiogenic and angiogenic processes. Both VEGF-C and VEGF-D acquire the ability to bind VEGFR-2 (in humans) only after proteolysis (Achen et al. 1998; Joukov et al. 1996; Joukov et al. 1997b; McColl et al. 2003). Mature VEGF-D has a 290-fold greater affinity for the VEGFR-2 receptor than unprocessed VEGF-D (Stacker et al. 1999). Similarly, VEGF-C and VEGF-D bind VEGFR-3 with far greater affinity following proteolytic maturation (Joukov et al. 1997b; Stacker et al. 1999). The importance of proteolysis in VEGF-C function is highlighted when mutations are made within cleavage sites. Lymphangiogenesis is greatly reduced in a mouse tumour model as a result of a mutation in a VEGF-C proteolytic cleavage site (Siegfried et al. 2003). The necessity for proteolysis in determining different receptor binding affinities and abilities means that a collection of inactive VEGF-C and VEGF-D molecules can be present at all times but are only activated when required. This allows for rapid lymphangiogenic responses when needed for example, following tissue damage (McColl et al. 2004).

1.5.1.1. VEGF-C

VEGF-C is a potent stimulator of survival, proliferation and migration of endothelial cells mediated through VEGFR-2 for BECs (Cao et al. 1998) and via VEGFR-3 for LECs (Makinen et al. 2001b; Taipale et al. 1999). The VEGF-C protein can exhibit angiogenic effects, in some circumstances; for example in the undifferentiated chorioallantoic membrane (CAM) model (Cao et al. 1998), mouse cornea (Cao et al. 1998) and rabbit hindlimb model of ischemia (Witzenbichler et al. 1998) through binding of VEGFR-2. Similarly, VEGF-C seems to be an inducer of vascular permeability (Joukov et al. 1997b). However, proliferative, mitogenic and angiogenic functions on BECs demonstrated by VEGF-C are far less potent than those induced by VEGF-A. Instead, the primary function of VEGF-C is as a lymphangiogenic factor through VEGFR-3 binding, as demonstrated in the differentiated CAM (Oh et al. 1997), ears of injected mice (Karpanen et al. 2001) and transgenic mice

(Jeltsch et al. 1997). The capacity of VEGF-C to be angiogenic in some circumstances and lymphangiogenic in others is determined by the location of its expression, whether lymph vessels are present at the site of expression, the developmental or pathological stage of the tissue and which receptor is available.

VEGF-C is essential for the development of the lymphatic system. It is produced by vascular smooth muscle cells and by mesenchymal cells in regions adjacent to the sites of initial sprouting of LECs from veins (Karkkainen et al. 2004; Kukk et al. 1996). Mice with homozygous deletions of the VEGF-C gene (VEGF-$C^{-/-}$) die around embryonic stage E15 due to failure of lymph vasculature development and subsequent oedema (Karkkainen et al. 2004). Heterozygous deletions (VEGF-$C^{+/-}$) in mice are not fatal, but adults display severe lymphatic hypoplasia (Karkkainen et al. 2004). It is suggested that VEGF-C expression is the signal responsible for the polarised sprouting and directed migration of lymphatic progenitor cells (cells that are $Prox1^{+}$, $LYVE1^{+}$, VEGFR-3^{+}) from the cardinal vein during development. These pre-LECs arise normally in VEGF-$C^{-/-}$ mice but do not bud from their initial location.

In adults, VEGF-C remains an important stimulator of lymphangiogenesis during wound healing, inflammation and certain pathological conditions (see section 1.4.). Overexpression of VEGF-C in the skin of transgenic mice induces lymphatic (but not vascular) endothelial cell proliferation and vessel enlargement (Jeltsch et al. 1997; Veikkola et al. 2001). Adenoviral expression of VEGF-C also stimulates the growth of functional lymphatic vessels in mice (Enholm et al. 2001; Saaristo et al. 2002a). However, blood vessel changes were also apparent as a result of adenoviral induced VEGF-C expression with veins being excessively leaky and enlarged (Saaristo et al. 2002a). Long term expression of activated and mature VEGF-C and VEGF-D induced by recombinant adeno-associated virus (rAAV) transduced in mouse skeletal muscle is both angiogenic and lymphangiogenic; resulting in functional growth of both blood and lymphatic vessels (Anisimov et al. 2009).

While both VEGFR-2 and VEGFR-3 are expressed on LECs it is suggested that the lymphangiogenic activity exerted by VEGF-C is purely through binding to VEGFR-3 and not VEGFR-2. Evidence for this is provided by overexpression of a mutant form of VEGF-C (designated VEGF-C156S with a mutation at cysteine residue 156, a crucial residue for structural integrity and biological activity) that is unable to bind VEGFR-2 (Saaristo et al. 2002b; Veikkola et al. 2001). The resultant lymphangiogenic effects generated by VEGF-C156S are no different to the action observed through expression of wild type VEGF-C, suggesting that VEGFR-2 does not contribute to normal lymphangiogenesis. Furthermore, adenoviral VEGF-C156S induced lymphangiogenesis has no effect on the blood vasculature, indicating that angiogenic effects of VEGF-C are driven only through VEGFR-2 binding (Saaristo et al. 2002b; Veikkola et al. 2001).

The lymphangiogenic capacity of VEGF-C has made it an attractive therapeutic candidate to ameliorate conditions of lymphatic dysfunction, such as lymphoedema, which currently has no cure. In a rabbit ear model of post-surgical lymphatic insufficiency, recombinant VEGF-C increased lymphatic vascularity and restored lymphatic function (Szuba et al. 2002). Similarly, in rabbit ear and mouse-tail secondary lymphoedema models, VEGF-C gene therapy improves fluid drainage from the accumulated site through the induction of lymphangiogenesis (Yoon et al. 2003). Other models of lymphoedema, for example the Chy mouse model, can be improved with the aid of VEGF-C gene therapy that stimulates functional lymphatic vessel growth (Karkkainen et al. 2001). However, while experimental studies have shown the promise of using growth factors for therapeutic neovascularisation, more knowledge is required for this process to work effectively in a clinical setting. The utilisation of angiogenic factor proteins or genes to rescue ischemic organs by stimulating angiogenesis has shown limited efficacy in clinical trials (Epstein et al. 2001a; Epstein et al. 2001b). Similarly, lymphangiogenic therapies have yet to be optimised

for use in clinical trials. Some VEGF-C induced lymphangiogenesis is transient with vessels regressing after the VEGF-C therapy has stopped and not displaying adequate function (Paavonen et al. 2000). New methods of protein delivery for example long lasting expression of growth factors via rAAV transduction at specific sites may overcome these issues; however whether these technologies are feasible in a clinical setting remains to be seen. Identification of the conditions required for lymphangiogenic factors to stimulate neovascularisation, including the choice of factor and their required expression levels will contribute to the understanding of the molecular and cellular mechanisms of functional, long-lasting lymphangiogenesis. Furthermore, while therapies targeting induction of VEGF-C are warranted the inhibition of VEGF-C could also be useful in blocking inflammatory pathologies and graft rejection and also in blocking cancer metastasis and growth. Further research examining the expression of lymphangiogenic factors may aid in the development of therapies that both promote and inhibit lymphangiogenesis within certain pathologies. Such research, including the use of multiple animal models and systems, may reveal new antagonists/stimulants in the regulatory mechanisms of such factors.

1.5.1.2. VEGF-D

In comparison to VEGF-C, relatively few studies have thoroughly examined the biological actions of VEGF-D, partly due to its later discovery (Achen et al. 1998), but also due to its apparent lack of importance in embryonic lymphatic development. Gene deletions of VEGF-D are not fatal in mouse embryos, as they are for VEGF-C (Baldwin et al. 2005), and little effect is observed in the lymphatic system as a result of a lack of VEGF-D except perhaps for some minor lymphatic vessel hypoplasia within the lung. VEGF-D delivery can, however, rescue the VEGF-$C^{-/-}$ phenotype and lead to adequate vessel development in the absence of VEGF-C (Karkkainen et al. 2004). VEGF-D is lymphangiogenic, although it appears to have certain, specific target tissues where it elicits a greater effect. VEGF-D is strongly expressed

in the developing lung during embryogenesis, and in the adult human, VEGF-D is found in many tissues, most abundantly in the lung and heart (Achen et al. 1998; Yamada et al. 1997). VEGF-D is the most potent inducer (of all VEGF family members) of lymphangiogenesis in skeletal muscle (Rissanen et al. 2003), where it also stimulates angiogenesis (Byzova et al. 2002). VEGF-D also induces lymphangiogenesis (but not angiogenesis) in subcutaneous tissues when expressed by skin keratinocytes (Veikkola et al. 2001) but here it appears to act to a lesser extent than VEGF-C. VEGF-D can also stimulate the migration of endothelial cells *in vitro* and can increase cell proliferation *in vitro* and *in vivo* (Marconcini et al. 1999). VEGF-D appears to be more angiogenic than VEGF-C; it induces angiogenesis in the rabbit cornea assay (Marconcini et al. 1999) and when injected in rat cremaster muscle. Similarly, VEGF-D is angiogenic (along with being lymphangiogenic) when injected into epigastric skin (Byzova et al. 2002). Human VEGF-D is mitogenic for endothelial cells and angiogenic as well as lymphangiogenic *in vivo* (Saharinen et al. 2004).

In experimental tumours VEGF-D plays a pivotal role in stimulating lymphangiogenesis and lymphatic metastasis (Stacker et al. 2001). VEGF-D has been proposed as a prognostic indicator as it is expressed by many tumour types and stimulates tumour angiogenesis and lymphangiogenesis in melanoma (Achen et al. 2001), pancreatic cancer (Von Marschall et al. 2005), oesophageal squamous cell carcinoma (Kleespies et al. 2005), breast cancer (Akahane et al. 2006) and lung cancers (Ishii et al. 2004). Because of this tumoural expression VEGF-D, along with VEGF-C, has been proposed as an attractive target for cancer therapies.

1.5.1.3. VEGFR-3

VEGFR-3 (fms-like tyrosine kinase 4, Flt4) is a member of the endothelial cell receptor tyrosine kinases. In contrast to VEGFR-1 and VEGFR-2, a disulphide bridge disrupts the fifth Ig domain of VEGFR-3 (Pajusola et al. 1994). The VEGFR-3 receptor was identified as one

of the first lymphatic endothelial markers and is a key signalling molecule for lymphangiogenesis. VEGFR-3 transduces mitogenic and migratory signals in LECs, and stimulation of the receptor blocks apoptosis induced by serum starvation (Makinen et al. 2001b). It is expressed by both BECs and LECs during development, however VEGFR-3 expression becomes restricted to the lymphatic endothelium as development advances and at birth is present only on lymphatic endothelia (Dumont et al. 1998; Kaipainen et al. 1995; Partanen et al. 2000). VEGFR-3 gene knockout mice die from cardiovascular failure early during development, prior to the formation of the lymphatic vasculature (Dumont et al. 1998). Blocking of VEGFR-3 function via transgenic expression of a soluble VEGFR-3 – immunoglobulin G Fc-domain fusion protein during development after the blood vascular system has formed, results in inhibition of lymphangiogenesis, regression of lymphatic vessels and subsequent lymphoedema (Makinen et al. 2001a), highlighting the importance VEGFR-3 signalling in the development of the lymphatic system. In adults, along with being a specific LEC marker, VEGFR-3 expression is up-regulated on many fenestrated endothelia for example within endocrine glands and the kidney (Partanen and Paavonen 2001). VEGFR-3 is also expressed by blood vascular endothelial cells in pathological states such as in chronic inflammatory wounds (Paavonen et al. 2000), tumour models (Kubo et al. 2000) and in human tumours (Partanen et al. 1999; Saaristo et al. 2000; Valtola et al. 1999). The crucial role played by VEGFR-3 in the development of the lymphatic system is also demonstrated when mutations of the VEGFR-3 gene occur. Missense mutations in the VEGFR-3 gene that reduce the biological activity of the protein are the leading cause of human primary lymphoedema as a result of deficient lymphatic vessel growth (Irrthum et al. 2000; Karkkainen et al. 2000). In adults, VEGFR-3 does not seem to have a role in the normal maintenance of the lymphatic vasculature, however it is up-regulated during lymphangiogenesis in wound healing (Paavonen et al. 2000), tumours (Petrova et al. 2008; Su

et al. 2007) and in inflammatory conditions (Flister et al. 2010) and as such is a crucial regulator of new lymphatic vessel growth.

1.5.3. VEGFs IN NON-MAMMALS

Members of the VEGF family have been identified in birds (Eichmann et al. 1998; Wilting et al. 2000), frogs (Ny et al. 2005) and fish (Ober et al. 2004; Song et al. 2007). In these animals they appear to exhibit the same functions as in mammals and display a high level of sequence conservation. For example, avian VEGF-C interacts with avian VEGFR-2 and VEGFR-3 (Eichmann et al. 1998) and in embryos is expressed in regions destined to be rich in lymph vessels (Wilting et al. 2001). VEGF-C and VEGF-D also have important roles in vasculogenesis in zebrafish (Ober et al. 2004; Song et al. 2007) and *Xenopus* tadpoles (Ny et al. 2005; Ny et al. 2008) with VEGF-C being crucial to the development of the lymphatic system in both species (Kuchler et al. 2006; Ny et al. 2005). VEGF-D is not critical for developmental lymphangiogenesis in frog embryos (Ny et al. 2008); however it does appear to enhance the function of VEGF-C. Combined knockdown of both genes in *Xenopus* results in greater lymphatic defects than single knockdowns of either gene (Ny et al. 2008). Correspondingly, VEGFR-3 expression is critical for lymphatic development and function in *Xenopus* (Ny et al. 2008). Zebrafish VEGF-C is proteolytically processed and the mature protein binds and induces autophosphorylation of both human (Ober et al. 2004) and zebrafish (Khatib et al. 2010) VEGFR-2 and VEGFR-3. Furthermore, proteolytic processing of VEGF-C is necessary for fin regeneration following injury (Khatib et al. 2010), though the precise role of mature VEGF-C in this process is yet to be elucidated.

Alignments of the amino acid sequences of zebrafish VEGF-C, human VEGF-C and mouse VEGF-C show many regions of identity, particularly in the VHD (Ober et al. 2004) . Similarly, zebrafish and *Xenopus* VEGF-D appear to share sequence similarity with their

mammalian counterparts (Ny et al. 2008). The wide variety of species from many branches of the vertebrate evolutionary tree which express both VEGF-C and VEGF-D suggests a high level of conservation throughout evolution and that these factors are likely to also be found in reptiles.

The only study that has examined the presence of VEGF-C or VEGF-D in reptiles has been from our laboratory and focused on the possible association of these factors with tail regeneration following autotomy (voluntary trail dropping; see section 1.6.) in the gecko *Christinus marmoratus*. Western blot analysis on protein extracted from regenerated tail tissue from *C. marmoratus* using a human reactive VEGF-C antibody indicated the presence of a reptilian homolog of mammalian VEGF-C (termed rVEGF-C/D) (Daniels et al. 2003). Semi-quantitation of the blot showed the presence of rVEGF-C/D at low levels in 6-week regenerates, increasing at 9 weeks and peaking at 12 weeks after regeneration commenced. rVEGF-C/D was not detected 3 weeks after autotomy, but levels at 9, 12 and 15 weeks were significantly up-regulated over basal levels in original tails (Daniels et al. 2003). This up-regulation correlates with the major proliferative phase of lymphangiogenesis in the regenerating tail and hence, rVEGF-C/D is likely to have a pivotal role in lymphatic regeneration.

1.6. REPTILIAN TAIL AUTOTOMY

The Australian marbled gecko, *Christinus marmoratus*, like many lizard species, has the ability to voluntarily shed its tail by active contraction of the caudal muscles, a process known as autotomy (Bellairs and Bryant 1985; Sheppard and Bellairs 1972). This controlled self-amputation is utilised as a method of predator escape, allowing the lizard to flee a predator that has grasped it by the tail (Daniels 1983). The writhing tail further acts to distract the predator while the lizard moves to safety (Dial and Fitzpatrick 1983). Studies examining the usage of caudal autotomy as an effective predator escape tactic (reviewed by (Bateman and

Fleming 2009)) demonstrate that the process significantly increases the chances of an individual's survival from a predatory encounter. However, several studies report 'costs' of autotomy whereby despite the obvious benefits, the process may significantly impact an individual's fitness (reviewed in (Arnold 1988; Bateman and Fleming 2009; McConnachie and Whiting 2003)). The loss of the tail has been demonstrated to negatively impact the animal in several ways. Firstly, it can increase the susceptibility of an animal to subsequent predation due to the lack of the tail to distract future predators (until tail regeneration is complete) (Daniels 1985; Daniels et al. 1986) and through decreased locomotor performance (decreased momentum and balance, running speed and endurance). Tail loss can also impact social interactions and behaviours (displays, status, and attractiveness to mates). Furthermore, there are significant metabolic costs associated with replacing the lost tissue (McConnachie and Whiting 2003) as well as the loss of fat stores within the tail (Daniels 1984a). These metabolic costs can lead to a reduction of female fecundity and also lead to animals having less energy and less time available (due to increased foraging requirements) for finding a mate (Bateman and Fleming 2009). All of these factors may ultimately lead to reduced survival and reduced reproductive fitness, which in part, explains why animals will sometimes exhibit other defence mechanisms before autotomy (rearing, biting, running, thrashing, excreting) and why autotomy generally takes place in an economical manner, where the tail is shed one to three vertebrae anterior to where it is grasped (Arnold 1984) to ensure minimal tail loss.

1.6.1. CAUDAL ADAPTATIONS TO AUTOTOMY

In lizards, autotomy occurs intravertebrally, as opposed to the intervertebral nature of autotomy in salamanders (Wake and Dresner 1967), and is associated with specialised adaptations of the vertebrae and various caudal tissues (Bellairs and Bryant 1985). Autotomous lizards possess modifications, known as fracture planes, in each of the caudal vertebrae (reviewed by (Etheridge 1967; Hoffstetter and Gasc 1969)), with the exception of

the first few vertebrae closest to the cloaca. The lack of fracture planes in this basal region of the tail prevents autotomy in this area and hence ensures protection of reproductive and digestive organs and also prevents damage to the lymphatic hearts of the pelvis and ischiatic sinus at the caudal base.

Fracture planes (Fig. 1.7.) are pre-determined sites of weakness within the vertebrae. The structural features of lizard tail fracture planes have been determined using histological, radiographic (Etheridge 1967) and more recently micro-computed tomography (μCT) methods (Kuhn et al. 2008), which provide a 3D evaluation of internal structures of small bones. Positions of the fracture planes within lizard vertebrae vary between different lizard families (Bellairs and Bryant 1985). For example in the Scincidae family the fracture planes typically split the transverse processes into a small proximal and a larger distal part (Bellairs and Bryant 1985; Etheridge 1967; Kuhn et al. 2008), whereas in Gekkonidae the autotomy planes lie distal to the split transverse processes (Fig. 1.7.) (Bellairs and Bryant 1985; Etheridge 1967; Kuhn et al. 2008). Each fracture plane within lizard vertebrae is represented by a split that divides the vertebrae into two parts, positioned such that it passes through the centrum (dividing it) and neural arch (Sheppard and Bellairs 1972). Regenerated portions of the tail do not contain intravertebral autotomy fracture planes and thus subsequent autotomies must occur proximal to the regenerated tissue.

Segmentation of the caudal muscles and fat bands is also present in the tails of autotomous lizards (see (Bellairs and Bryant 1985) for review). Figure 1.8. shows the basic arrangement of muscles, fat and longitudinal septa in the tail of *Lacerta vivipara*. Longitudinal bands of fatty tissue surround the vertebral column, with the muscles and skin lying superficial to them. The muscles and fat are subdivided into four segments by sheets or septa of connective tissue. This arrangement of the caudal muscles and fat bands provides

appropriate partitions such that the tissues are effectively separated (rather than torn) upon autotomy, thus retaining their integrity.

Figure 1.7. Fracture planes of autotomous lizard vertebrae. A. Representation of the mid-caudal vertebrae of *Lacerta vivipara*, lateral aspect (Pratt 1946). B. 3D micro-computed tomography (μCT) reconstruction of *Christinus marmoratus* vertebral column. C. 3D μCT reconstruction of dorsal half of *Christinus marmoratus* caudal vertebrae, view from inside. B. and C. taken from Kuhn et al. (2008). Arrows point to the autotomy planes that run distal of the transverse process. Scale bars indicate 1 mm.

A

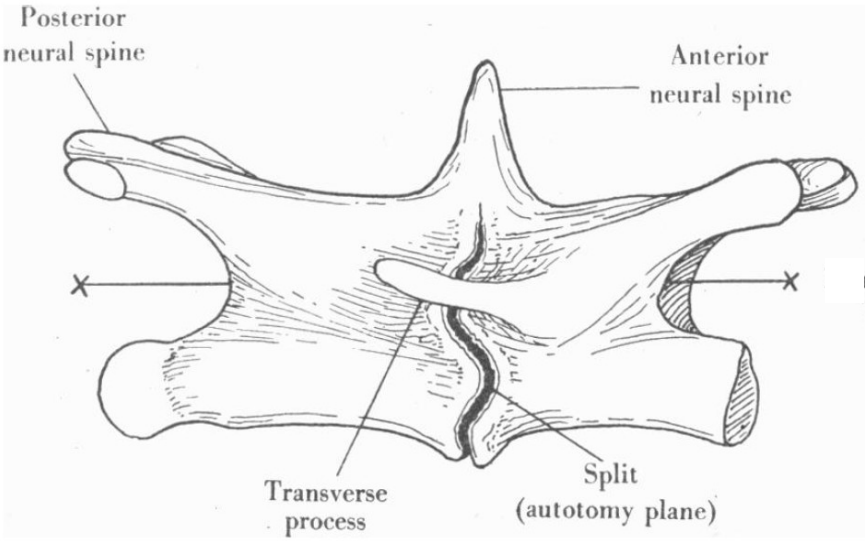
Posterior
neural spine
Anterior
neural spine
Transverse
process
Split
(autotomy plane)

B

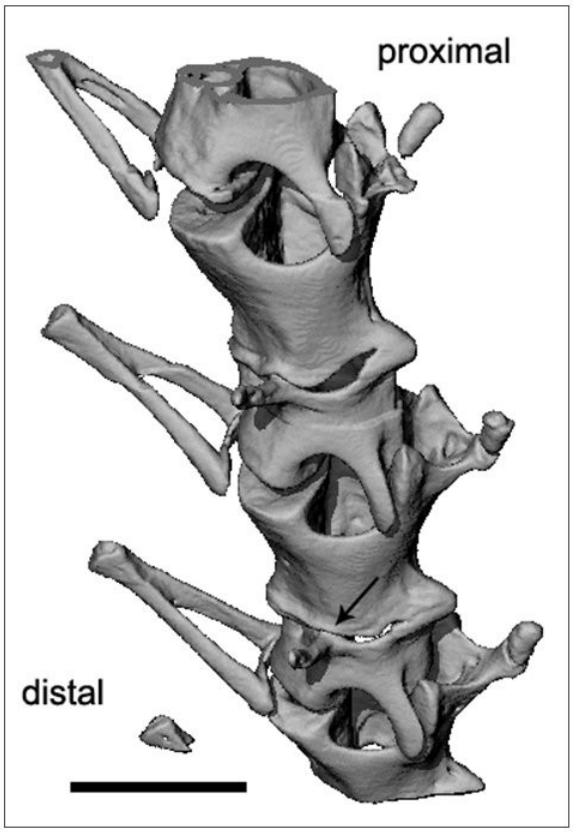
proximal
distal

C

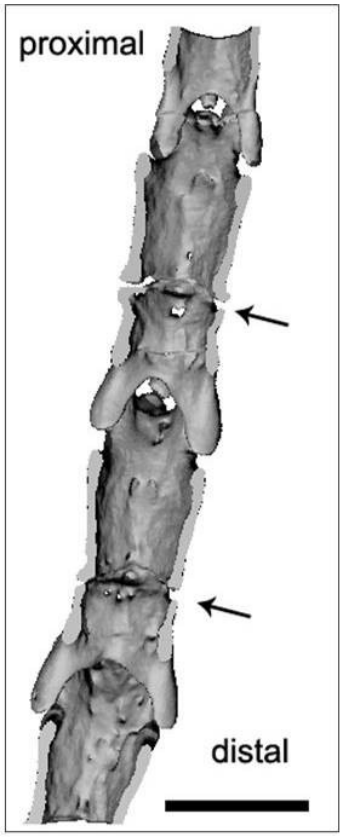
proximal
distal

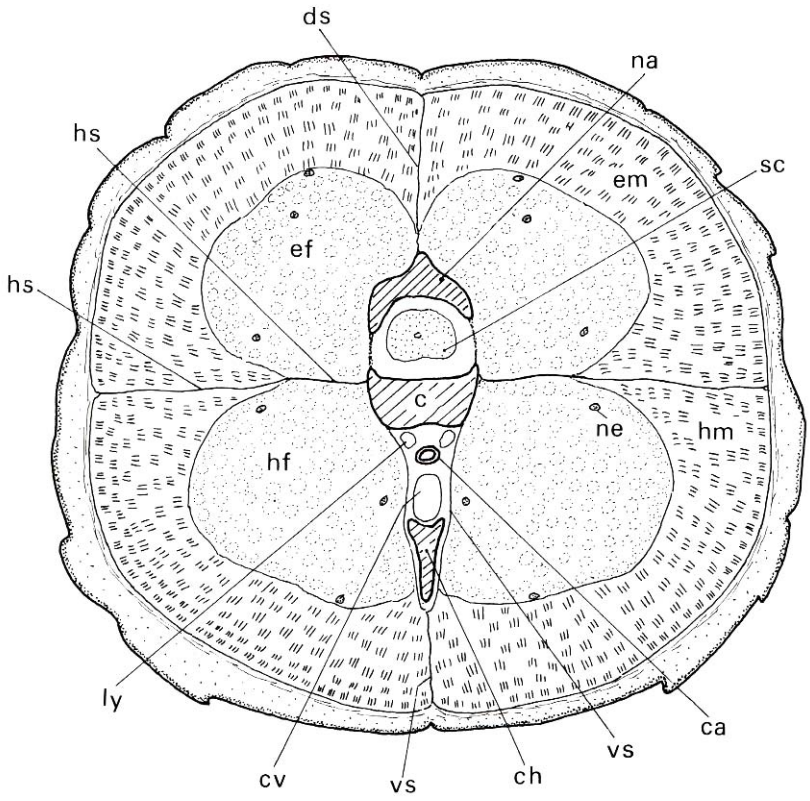

Figure 1.8. Schematic representation of the transverse section through the autotomous part of the lizard tail. The basic arrangement of muscles, fat, and longitudinal septa is shown in an autotomous section of the tail in *Lacerta*. Abbreviations are as follows: c, Centrum; ca, caudal artery; ch, chevron (a series of small bones that protect blood vessels and nerves of the underside of the tail); cv, caudal vein; ds, dorsal median longitudinal septum; ef, epaxial fat band; em, epaxial muscle; hf, hypaxial fat band; hm, hypaxial muscle; hs, horizontal longitudinal septum; ly, caudal lymphatic; na, neural arch; ne, nerve; sc, spinal cord; vs, ventral median longitudinal septum. Figure reproduced from Bellairs and Bryant (1985).

1.6.2. THE MECHANISM OF AUTOTOMY

Flexion of the tail occurring via active contraction of the tail muscles, and sometimes assisted by the tail being grasped, concentrates pressure onto one particular vertebral fracture plane. The caudal muscles are arranged such that they are able to contract sufficiently to result in breakage and separation of the fracture plane to trigger autotomy and allow the tail to be shed at one of a number of points along its length. As the tail flexes the skin is split on the stretched, convex aspect of the tail (Sheppard and Bellairs 1972), and the nearby muscles on this side also separate from their weak anterior attachments. The split then appears to travel right across the remaining tissues of the tail. The vertebra is disjointed and requires little force at this stage due to the presence of the fracture plane; separation of the fat bands surrounding the vertebrae is readily enabled due to their segmented arrangement. There is little to no blood loss due the presence of valves and/ or sphincters within arterial and venous walls (Sheppard and Bellairs 1972).

1.7. LIZARD TAIL REGENERATION FOLLOWING AUTOTOMY

Following autotomy, many lizard species are able to regenerate a replacement tail. Given the high number of potential costs discussed in section 1.6. it is understandable that a new and complex tail is, often rapidly, regenerated. In the gecko, movement and function are recovered within the regenerated tail along with the relevant cardiovascular, neural, muscular, lymphatic, adipose, structural and integumentary systems. Obvious differences do however exist between original and regenerate tails; for example, the skeleton of the regenerate consists of a simple cartilage tube as opposed to new bony vertebrae (Werner 1967). The cartilage tube lacks fracture planes and is therefore incapable of further autotomy (Bellairs and Bryant 1985). However, it is still possible for additional breaks to occur on the proximal portion of the original tail or at the junction between the original and regenerate tissue.

Regenerated muscles within the tail have no attachment to the skeleton as they do in original tails and the muscle arrangement is more simplified with no clearly defined horizontal and median longitudinal septa to separate them into four quadrants (Bellairs and Bryant 1985). Similarly, regenerated fatty tissue is unsegmented and instead fat masses surround and support the cartilage tube. The regenerated tail is often not as long as the original and often presents with less flexibility (Daniels 1984b), but is, however, capable of mobility and can facilitate locomotion and balance. Dorsal scale pattern on regenerated tails is often less complex and can be one of the distinguishing features for identifying a regenerate (Daniels 1984b). A beneficial characteristic of the regenerated tail is that it can be more efficient as a site for fat storage (Daniels 1984a), often resulting in a regenerated tail that is broader in appearance than the original.

There are three principal phases to reptilian tail regeneration. These are wound healing, blastema formation and differentiation and growth (see (Alibardi 2010; Bellairs and Bryant 1985; Bryant 1970) for reviews on tail regeneration). Natural autotomy causes relatively little damage to the local tissues. The spinal cord and meninges, the peripheral nerves, caudal blood vessels and lymphatics along with the skin are severed by autotomy. However, the integrity of the muscles, fat bands and vertebrae are maintained, despite being detached, due to their specialised adaptations. The first steps occurring within the first few minutes following autotomy are the cessation of bleeding (which is usually minimal due to arterial sphincters and venous valves), along with the contraction of the skin around the breakage site. The skin, along with clotted blood and necrotic tissue form a scab, which protects the wound surface from infection and triggers immune cell migration to the site to contribute to effective wound healing (Bellairs and Bryant 1985). Epidermal cells migrate beneath the scab (which is then shed) to cover the wound surface. Here they proliferate such

that the epidermis becomes stratified and thickened forming the wound epithelium (or apical cap), which is essential to tail regeneration (Alibardi 2010; Bellairs and Bryant 1985).

As the damaged tissues in the stump break down, they release dedifferentiated cells, which appear to have lost their morphological identity and possess none of the recognisable characteristics of their tissues of origin (Bryant 1970). These cells congregate beneath the wound epithelium and form the blastema, or regenerative bud (Fig. 1.9.). It has recently been suggested that the blastema may also consist of stem cells that have been retained in the tail following embryonic development (Alibardi 2010). Most tissues found in the regenerated tail are thought to arise from these dedifferentiated and potentially embryonic sources. This early phase of blastema formation is called the latent period, because the autotomised tail does not elongate during this stage. The conclusion of the latent period is signalled by the visible outgrowth of the blastema, due to the accumulation of new cells derived from tissues in the vicinity of the wound and also by mitosis (Bryant 1970).

The differentiation and growth phase of tail regeneration sees the differentiation of blastema cells back into the tissues of the tail (Fig. 1.10.). The cartilage tube is one of the first structures to appear. This merges with the last vertebrae of the stump as a continuation of the original skeleton and surrounds the ependymal tube (containing the regenerating spinal cord) (Bryant 1970). Muscles, fat, connective tissue, epidermis, blood vessels, and nerves are also formed in this time (see (Alibardi 2010) for an ultrastructural and cytological review). The tail lengthens as a result of this differentiation until eventually the new tail is produced and regeneration is complete.

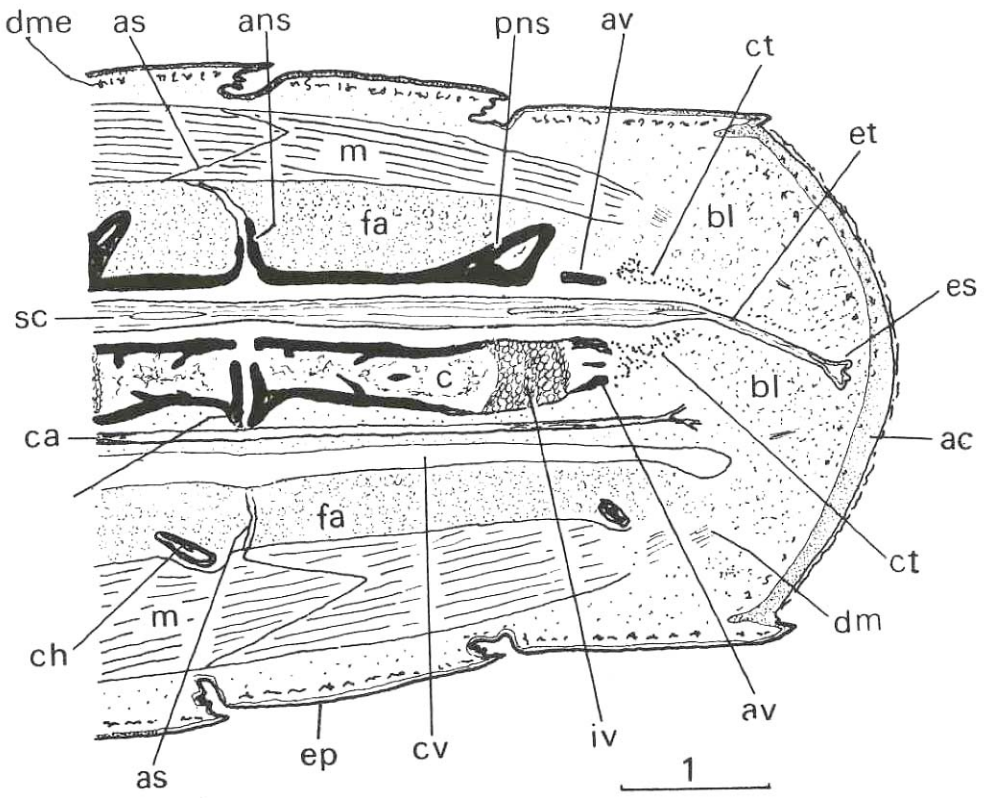

Figure 1.9. Early regenerate tail of *Lacerta vivipara.* Longitudinal, nearly median section through regenerating tail 2-3 weeks after autotomy and shortly after end of latent period. An apical cap and ependymal tube have formed and the blastema is well developed. Ac, Apical cap; ans, anterior neural spine (split by fracture plane); as, connective tissue autotomy septum (bilaminar through fat layer); av, autotomised vertebra, probably after ablation; bl, blastema; c, centrum; ca, caudal artery; ch, chevron; ct, developing cartilage tube; cv, caudal vein; dm, developing muscle (pro-muscle aggregate); dme, dermal melanophore; ep, epidermis; es, ependymal sac; et, ependymal tube; fa, fat layer; iv, intervertebral pad; m, original muscle; pns, posterior neural spine; sc, spinal cord. Figure reproduced from Bellairs and Bryant (1985).

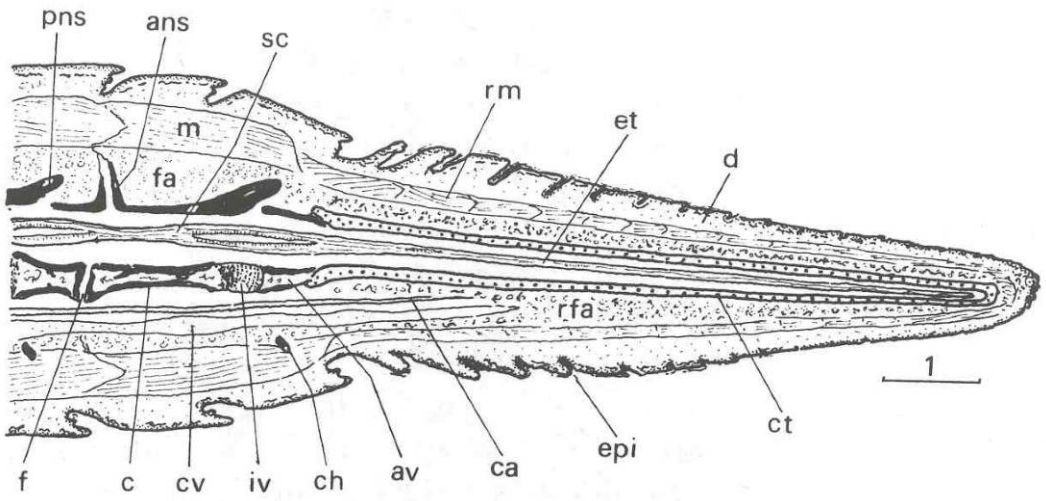

Figure 1.10. Late stage regenerate tail of *Lacerta vivipara.* Longitudinal section near the midline through an advanced, but not completely mature regenerate. Scale in mm. ans, anterior neural spine (split by fracture plane); av, autotomised vertebra; c, centrum; ca, caudal artery; ch, chevron; ct, cartilage tube; cv, caudal vein; d, dermis; epi, epidermal ingrowth forming new scale; et, ependymal tube; f, fracture plane in centrum; fa, fat (label on epaial fat band); iv, intervertebral pad; m, original muscle; pns, posterior neural spine; rfa, regenerated fat interspersed with pigment cells; rm, regenerated muscle; sc, spinal cord. Figure reproduced from Bellairs and Bryant (1985).

The regenerative capacity of the tail appears to be dependent on two major factors. The first is the apical cap of cells covering the developing blastema. The apical cap is crucial as tail regeneration is hindered when the cap and adjacent skin are removed (Quattrini 1955) (quoted in (Bellairs and Bryant 1985)). Similarly, tail regeneration does not occur if the apical cap is replaced by a graft of mature skin (Whimster 1978). The second important factor in regeneration is the presence of an adequate nervous supply near the site of injury (Kamrin and Singer 1955; Simpson 1977; Singer 1980), without which the tail will not successfully regenerate (Simpson 1970). For example damaging the spinal cord in the lizard *Anolis carolinensis* near the autotomy site inhibited tail regeneration. However, Simpson (1964, 1977) and others (Cox 1969; Whimster 1978) found that it was not so much the spinal cord itself that is critical for normal regeneration but rather the ependymal cells, which line the spinal cord. Transplanting autografts of cartilage tube and ependyma, in which no nerve cell bodies are present and with no residual influence of nerve fibres, from a regenerating tail into wounds inflicted in the dorsum of the tail, resulted in a complete regenerate from the dorsum of the tail (Simpson 1964).

It is also likely that tissue regeneration is subject to the control of hormones and other growth factors. For example, removal of the pituitary gland prevents blastema formation and tail regeneration in the lizard *Anolis carolinensis* (Licht and Howe 1969). Subsequent injections of the growth hormones, prolactin, gonadatropin and thyrotropin following pituitary removal restore tail regeneration to nearly normal levels (Licht and Howe 1969). Similarly, calcium ion antagonists have been used to determine roles for intracellular calcium ions in fibroblast collagen production, neurogenesis, and angiogenesis during lizard tail regeneration (Turgut et al. 2007). Recent studies have begun measuring the expression levels of certain regulatory genes to determine the molecular mechanisms behind tail regeneration. Such work has highlighted the importance of specific genes such as brain protein 44-like gene (Jiang et

al. 2009) and platelet-derived growth factor C (Liu et al. 2009) in the regeneration of the spinal cord of *Gekko japonicus* following autotomy. Gene expression of beta-keratins and tissue localisation of alpha-keratins likewise implies potential roles within regenerating lizard tail scales (Alibardi et al. 2000; Dalla Valle et al. 2005). Additionally, tissue distribution, particularly within regenerating nervous tissue, suggests potential trophic roles for fibroblast growth factors (FGFs) in stimulating tail regeneration (Alibardi and Lovicu 2010).

Few studies have examined the regeneration of the blood and lymphatic vasculature following autotomy. Previous work has shown that the main blood vessels of the lizard tail regenerate as a continuation of the pre-existing vessels of the stump (Quattrini 1954) (quoted in (Alibardi 2010)). Blood vessels appear in the early stages of tail regeneration within the blastema close to the wound epithelium (Hughes and New 1959). Endothelial cells derived from differentiation of blastema cells have been suggested to make up these new blood vessels during angiogenesis (Alibardi et al. 1993), which must then undergo some form of reconnection to the damaged blood vessels in the stump. However, it is possible that sprouting angiogenesis from pre-existing vessels (as is the case in mammalian wound healing (Gerhardt et al. 2003)) may also take place along with the recruitment of endothelial cells from the blastema comparable to a proposed method of blood vessel growth (with recruitment of endothelial precursors) in mammals (Rafii 2000). Little is known about the regeneration of the lymphatic system. The lymphatic vessels are severed during autotomy and yet the regenerated tail is not lymphoedematous, indicating that the mechanisms for draining tissue fluids are restored, presumably by the creation of new (de novo lymphangiogenesis), or the extension of pre-existing (sprouting lymphangiogenesis), lymphatic vessels.

Basic histological analysis of original, partial and fully regenerated tails of *C. marmoratus* demonstrates different lymphatic characteristics in original and regenerating tails (Daniels et al. 2003). Original tailed geckos appear to have a greater number of lymphatic

vessels, with a larger diameter, than full regenerates. Early regenerates (3 weeks following autotomy) have fewer lymphatic vessels than originals and have vessels of a wider diameter (Daniels et al. 2003). As regeneration proceeds, lymphatic vessel number increases and vessel diameter decreases. In particular, the number of both lymphatic and blood vessels increase significantly between three and six weeks of regeneration, indicating that this is a major proliferative phase of angiogenesis and lymphangiogenesis. The diameter of lymphatic vessels within full regenerates is less than that in original gecko tails; however an organised lymphatic network is apparent within the regenerated tails (Daniels et al. 2003). Findings of this study go further to suggest that this lymphangiogenesis in the regenerating lizard tail may be caused by a reptilian homolog of VEGF-C and/or VEGF-D (Daniels et al. 2003), as this protein has been found to play important roles in embryogenesis and growth of the lymphatic system in mammals (reviewed by (Jussila and Alitalo 2002) and see also section 1.5.). However, this work was performed using basic histology staining, as specific molecular markers were not available at the time to accurately identify lymphatic vessels. Whether the same pattern would be observed utilising LEC specific markers remains to be seen. Similarly, the functionality of the regenerating lymphatic vessels within the gecko tail is unclear – the tails do not appear lymphoedematus and hence restoration of lymph drainage pathways appears likely. However, whether the route of fluid drainage is through the apparent newly formed lymph vessels or instead through simple fluid channels is unknown.

Likewise it is unknown whether re-established flow in regenerates has the same physiological characteristics as the system in the original tails. Daniels et al. (2003) did find significant differences between regenerate and original tailed geckos in lymphatic transport of the radiocolloid ^{99m}Technetium-antimony trisulphide (^{99m}Tc-ATC) following subdermal administration. Differences in small particle transport between the two tail states indicates that differences may exist with respect to the lymphatic network and/or surrounding tissues,

however these differences were not elucidated. Further work to clarify these functional and structural aspects of lymphatic regeneration within the gecko tail may provide further details of the process of lymphangiogenesis. Furthermore, studies into tail regeneration in the gecko can provide knowledge into the molecular basis of the regeneration mechanism.

1.8. PROJECT RATIONALE

Two decades ago virtually nothing was known about the lymphatic system or the process of lymphangiogenesis. Despite multiple advances in the field in recent years, primarily brought about by the discovery of specific lymphatic vessel molecular markers and identification of some core lymphangiogenic genes, much remains to be discovered. The molecular regulators driving lymphangiogenesis and the precise roles these genes play are not fully understood, in particular the molecular mechanisms driving lymph vessel growth following trauma are unclear. The importance of lymphangiogenesis in wound healing and several pathologies including tumour metastasis highlights the need for further understanding. New animal models, particularly, adult models of lymphatic regeneration, would be beneficial in investigating this process. The regenerating lizard tail offers an excellent model of tissue regeneration in an adult system that is more closely related to mammalian systems in terms of phylogeny (both groups are amniotes and evolved from a common ancestor) and histology compared to amphibians, which are extensively used for regeneration studies (Mescher 1996; Odelberg 2005). Therefore, this thesis aims to determine how lymphangiogenesis is controlled following tail autotomy in lizards.

I aim to describe the physiological process and molecular mechanisms of lymphangiogenesis during tail regeneration in the gecko *C. marmoratus* with a focus on the lymphangiogenic growth factors, VEGF-C and VEGF-D, together with the receptor VEGFR-3. I hypothesise that VEGF-C, VEGF-D and VEGFR-3 will be present within the gecko tail

and that lymphangiogenesis during tail regeneration is driven by VEGF-C and VEGF-D through binding and activation of VEGFR-3. Additionally, I aim to highlight the potential of the regenerating gecko tail as a new model to investigate the lymphangiogenic process, which may further provide insights into this complex mechanism and hence facilitate the development of new therapeutic strategies.

1.8.1. USE OF *C. MARMORATUS* AS AN ANIMAL MODEL OF LYMPHANGIOGENESIS

Here, I study the Australian marbled gecko, *Christinus marmoratus*. This species was selected on the basis that its tail regeneration time is relatively short (approximately 24 weeks to reach full regeneration), it is commonly found in Adelaide parks and gardens and is easy to house and maintain.

While other models of lymphangiogenesis are available the regenerating gecko tail is novel in that it potentially allows the study, in an adult animal, of the de novo synthesis of permanent lymph vessels into an area devoid of them. Other animal models for lymphangiogenesis often require invasive manipulation such as surgery (e.g. epigastric flaps in mice (Saaristo et al. 2004), punch biopsy wounds in the skin of pigs (Paavonen et al. 2000) and mice (Saaristo et al. 2006)), specialised materials (e.g. the collagen dermal equivalent (Boardman and Swartz 2003; Goldman et al. 2007; Rutkowski et al. 2006)) or expert handling (e.g. transgenic mice development, small animal dissections) and expensive housing (e.g. aquariums, sterile/contamination free animal house facilities). Zebrafish (Isogai et al. 2009; Kuchler et al. 2006; Yaniv et al. 2006; Yaniv et al. 2007) and *Xenopus laevis* tadpoles (Kalin et al. 2009; Ny et al. 2006; Ny et al. 2005; Ny et al. 2008) have both recently been validated as excellent models for examining the molecular mechanisms underlying embryonic lymphangiogenesis, but the findings in development may not hold true postnatally. In addition, the reptilian lymphatic network has been described as being structurally more

similar to that of mammals compared to other non-mammals (Ottaviani and Tazzi 1977) and so is more suited to studies in lymphangiogenesis. Furthermore, gecko tail autotomy and regeneration are natural processes that occur readily, and for which the tail tissues are well adapted. Hence, there is no concern about potential issues of infection or inflammation or the need for administration of medications such as pain relief, anaesthetics and antibiotics.

1.9. AIMS OF THE THESIS

1. To examine the functional and structural characteristics of the regenerating gecko tail lymphatic network and surrounding tissues.
2. To identify and characterise the expression profiles and genetic sequences of the lymphangiogenic growth factors VEGF-C, VEGF-D and their receptor VEGFR-3 throughout tail regeneration in the gecko *C. marmoratus*.
3. To use the molecular marker LYVE-1 to conclusively identify lymphatic vessels and hence prove that lymphangiogenesis occurs within the regenerating tail.
4. To determine tissue localisation and protein expression profiles of VEGF-C, VEGF-D and VEGFR-3 within regenerating gecko tail tissue and provide evidence for their roles in lymphangiogenesis.

Chapter Two

How regenerating lymphatics function: Lessons from lizard tails

Blacker, H.A.[1], Tsopelas, C.[2], Orgeig, S.[1], Daniels, C.B.[1], Chatterton, B.E.[2]

[1]Environmental Biology, School of Earth and Environmental Sciences, University of Adelaide, Adelaide, Australia
[2]Department of Nuclear Medicine, Royal Adelaide Hospital, Adelaide, Australia

The Anatomical Record: Advances in Integrative Anatomy and Evolutionary Biology
(2007) 290: 108-114.

2.1. STATEMENT OF AUTHORSHIP

How regenerating lymphatics function: Lessons from lizard tails

The Anatomical Record ***(2007) 290: 108-114.***

Authors were arranged in order of extent of contribution to the work.

Blacker, H.A. (Candidate)

Performed analysis on all data, handled/ prepared animals for data acquisition, assisted in experimental design, interpreted data and wrote manuscript

I hereby certify that the statement of contribution is accurate

[redacted]

Tsopelas, C.

Assisted in obtaining funding for research, concept development and experimental design, supervised data acquisition, handled radiolabels and performed injection into gecko tail, showed how to analyze data and assisted in manuscript evaluation

I hereby certify that the statement of contribution is accurate and I give permission for the inclusion of the paper in the thesis

Signed..... [redacted] Date. 15 APR 11

Orgeig, S.

Major contribution to concept development and experimental design, obtained funding for research, supervised conduct of the work, manuscript evaluation and acted as corresponding author

I hereby certify that the statement of contribution is accurate and I give permission for the inclusion of the paper in the thesis

Signed..... [redacted] Date. 3/8/11

Daniels, C.B.

Major contribution to concept development, assisted in experimental design and obtaining funding for research and manuscript evaluation

I hereby certify that the statement of contribution is accurate and I give permission for the inclusion of the paper in the thesis

Signed..... [redacted] .....Date.....5/4/11

Chatterton, B.E.

Provided access to laboratory and equipment to perform experiments, assisted in obtaining funding for research, experimental design, concept development and manuscript evaluation

I hereby certify that the statement of contribution is accurate and I give permission for the inclusion of the paper in the thesis

Signed..... [redacted] .....Date.....15 APR 2011

2.2. SUMMARY AND CONTEXTUAL LINKAGE

Lymphoedema is defined as excess fluid accumulation in the tissues and arises as a result of lymphatic system trauma or malfunction (Board and Harlow 2002a). In the gecko tail, the lymphatic vessels are severed by autotomy and yet the regenerating gecko tail shows no sign of swelling. Hence, fluid transport within the tail must be reinstated. Excess fluid could be removed from the regenerated tissues either via flow through simple fluid channels or through newly formed lymphatic capillaries and collecting vessels that have the capacity to take up excess interstitial fluid and transport it to the venous/lymphatic anastomoses near the cloacae. Previous work has shown the likely presence of new lymphatic vessels within regenerating and fully regenerated tails (Daniels et al. 2003), but the functional characteristics of these vessels were not fully elucidated.

In this chapter I present my published paper *'How regenerating lymphatics function: Lessons from lizard tails'* in which I describe studies performed to determine the physiological functionality of the lymphatic vessels and surrounding tissues throughout different stages of regeneration. I used the nuclear medicine technique of lymphoscintigraphy to measure the parameters of lymph clearance and lymph velocity of three different radio-labelled tracers at different stages of tail regeneration and in original tails. The tracers used included two non-soluble colloids of differing sizes and one soluble molecule. Examining the ability of the lymphatic vessels to take up both large and small particles was used to gain details of the changes in permeability of both the lymphatic vessels and the connective tissue (extracellular matrix) surrounding the lymph network throughout regeneration. This technique also provides information regarding the capabilities of the regrowing and regenerated lymphatic vessels in transporting 'lymph' to the venous circulation.

Results from this paper show that basic lymphatic function is restored by 6 weeks of regeneration where large non-soluble colloids can be taken up by the vessels from the

interstitial spaces and transported to the venous circulation. As regeneration proceeds this uptake becomes more selective, vessels become less permeable to large colloids presumably as a result of maturation of the lymphatic vessels along with increasing density of the extracellular matrix due to re-growth of connective tissue. By 12 weeks of regeneration tracer clearance and lymph velocity are restored to near original levels, highlighting that lymphatic regeneration takes place and the functional lymphatic network is likely to be restored to the pre-autotomy structure. The regenerating gecko tail therefore offers an advantageous model to study lymphangiogenesis. Recent discoveries have highlighted the importance of lymphangiogenesis in many pathological conditions and stimulation of lymphangiogenesis offers potential benefits for disorders involving lymphatic dysfunction. However, the molecular mechanisms behind lymphangiogenesis are unclear. The regenerating gecko tail model offers a system whereby the molecular mechanisms controlling the re-growth of a whole functional lymphatic network, including vessel maturation and remodelling, may be elucidated.

Helen A. Blacker, Chris Tsopelas, Sandra Orgeig, Christopher B. Daniels and Barry E. Chatterton (2007)
How regenerating lymphatics function: Lessons from lizard tails.
The Anatomical Record: Advances in Integrative Anatomy and Evolutionary Biology, v. 290 (1), pp. 108-114, January 2007

Chapter Three

Differential mRNA and tissue expression of lymphangiogenic growth factors (VEGF-C and –D) and their receptor (VEGFR-3) during tail regeneration in a gecko

Blacker, H.A.[1]and Orgeig, S.[2]

[1]Ecology and Evolutionary Biology, School of Earth and Environmental Sciences, University of Adelaide, Adelaide, AUSTRALIA, SA, 5005
[2]Sansom Institute for Health Research, School of Pharmacy and Medical Sciences, University of South Australia, Adelaide, AUSTRALIA, SA 5000.

Journal of Comparative Physiology B (2011) *DOI 10.1007/s00360-011-0604-0*

3.1. STATEMENT OF AUTHORSHIP

Differential mRNA expression of lymphangiogenic growth factors (VEGF-C and –D) and their receptor (VEGFR-3) during tail regeneration in a gecko

Journal of Comparative Physiology B (2011) DOI 10.1007/s00360-011-0604-0

Blacker, H.A. (Candidate)

Performed analysis on all samples, developed and validated all experiments, performed all technical aspects of work, interpreted data and wrote manuscript.

I hereby certify that the statement of contribution is accurate.

Signed…….Date……

Orgeig, S.

Major contribution to concept development and experimental design, obtained funding for the research, supervised conduct of the work, contributed to manuscript preparation and acted as corresponding author.

I hereby certify that the statement of contribution is accurate and I give permission for the inclusion of the paper in the thesis.

Signed…….Date……

3.2. SUMMARY AND CONTEXTUAL LINKAGE

In the previous chapter it was demonstrated that the regenerating lymphatic network within the gecko tail recovers the same functional characteristics as those seen in original tails by 12 weeks of regeneration, with basic fluid transport capabilities present at 6 weeks following autotomy. Thus, a functional lymphatic system is regenerated that appears to have recovered a similar structure and arrangement as was present prior to autotomy. However, the molecular mechanisms driving lymphangiogenesis within the regenerating gecko tail are unknown.

In mammals, the growth factors VEGF-C and VEGF-D have been identified as primary regulators of lymphangiogenesis, during both embryogenesis and in adults. These growth factors induce endothelial cell survival, proliferation, migration, induction and permeability (Jeltsch et al. 1997; Kukk et al. 1996; Makinen et al. 2001b; Veikkola et al. 2001) upon binding to their receptor VEGFR-3. While these molecules are predominantly regarded as lymphangiogenic they are also capable of stimulating angiogenesis via binding to the blood endothelial receptor VEGFR-2 or by binding to VEGFR-3 which although generally restricted to the lymphatic epithelia following development (Kaipainen et al. 1995) is also expressed on blood endothelial cells in certain conditions (Petrova et al. 2008; Tammela et al. 2008).

In 2003 Daniels et al. reported the presence of a homologue of VEGF-C and/or VEGF-D within protein extracts from the regenerating gecko tail based on their findings using western blotting. Two positive bands were identified by binding of an anti-human VEGF-C antibody at 58 and 43 kDa which is similar to those reported in other studies (Joukov et al. 1997b). This was further confirmed by an absence of bands in the presence of a VEGF-C blocking peptide. In their paper, Daniels et al. termed this homologue reptilian VEGF-C/D (rVEGF-C/D) as the amino acid sequence of the protein identified was never determined. It is highly likely however, that reptiles, and in particular the regenerating gecko

tail, possess both VEGF-C and VEGF-D along with their receptor as they have been identified in all other vertebrate groups including mammals (Achen et al. 1998; Fitz et al. 1997; Joukov et al. 1996), birds (Eichmann et al. 1998; Wilting et al. 2001), fish (Kuchler et al. 2006; Ober et al. 2004; Song et al. 2007) and amphibians (Ny et al. 2005; Ny et al. 2008).

In this chapter I present my published paper 'Differential mRNA and tissue expression of lymphangiogenic growth factors (VEGF-C and –D) and their receptor (VEGFR-3) during tail regeneration in a gecko'. This paper first describes the identification and isolation of partial cDNA sequences for gecko VEGF-C, VEGF-D and VEGFR-3 that are highly similar to those of other vertebrate species. Phylogenetic analysis confirms the high level of sequence conservation in these partial sequences and shows that the gecko sequence is evolutionarily most closely related to the chicken sequence. Secondly, we have developed and validated a quantitative real-time PCR (qPCR) method to quantify mRNA expression of lymphangiogenic growth factors and their receptor within the regenerating gecko tail. This method was used to identify and examine the precise timing of expression of the lymphangiogenic factors VEGF-C and VEGF-D and the receptor, VEGFR-3 throughout tail regeneration. Expression profiles show up-regulation of VEGF-C, VEGF-D and VEGFR-3 mRNA expression in early, late and mid-regeneration respectively. This differential expression could have implications for potential roles of these factors in the tail regenerative process and more specifically in lymphangiogenesis throughout tail regeneration. Thirdly, immunohistochemistry was used to positively confirm the identity of lymphatic vessels in regenerated gecko tail tissue and hence provide conclusive evidence of lymphangiogenesis occurring within the tails. LYVE-1 positive staining was observed in full regenerate gecko tail tissue on endothelial cells lining vessels with characteristic lymphatic architecture. Sites of expression of VEGF-C and VEGF-D in regenerating gecko tails, obtained using immunohistochemistry, occur in regions rich in lymphatic vasculature and are consistent with

sites of expression in mammalian studies of wound healing where they do stimulate lymphangiogenesis (Bauer et al. 2005; Kivelä et al. 2007; Trompezinski et al. 2004).

However, quantitative protein expression profiles need to be performed to corroborate mRNA expression data to verify the conclusions that up-regulation of gene expression is capable of producing a functional response. Furthermore, full-length sequences of gecko VEGF-C, VEGF-D and VEGFR-3 are required to further explore the evolutionary relationships of these genes to other vertebrate species and provide further evidence for their roles in lymphangiogenesis within the regenerating gecko tail.

Helen A. Blacker and Sandra Orgeig (2011) Differential mRNA and tissue expression of lymphangiogenic growth factors (VEGF-C and –D) and their receptor (VEGFR-3) during tail regeneration in a gecko.
Journal of Comparative Physiology B: Biochemical, Systemic and Environmental Physiology, v. 182 (1), pp. 109-126, January2011

Chapter Four

ISOLATION AND CHARACTERISATION OF FULL-LENGTH VEGF-C, VEGF-D AND VEGFR-3 CDNA SEQUENCES FROM THE GECKO *CHRISTINUS MARMORATUS*

4.1. INTRODUCTION

Partial gene sequences (145 bases) of gVEGF-C, gVEGF-D and gVEGFR-3 were identified in the previous chapter that appear to be highly similar to other vertebrate species. Sequence analysis, mRNA expression profiles and tissue localisation suggest that these factors play a role in tail regeneration and more specifically in lymphangiogenesis. However, the gVEGF-C, gVEGF-D and gVEGFR-3 sequences obtained in Chapter 3 only represent 11, 14 and 3.5 % respectively of the total expected protein coding sequence. Therefore, more sequence information is required to accurately analyse these genes in the gecko.

The growth factor VEGF-C and its receptor VEGFR-3 are crucial for lymphatic system development (Karkkainen et al. 2004; Makinen et al. 2001a) and both VEGF-C, and its closely related homologue, VEGF-D are capable of stimulating lymphangiogenesis and angiogenesis in adult tissues (Anisimov et al. 2009; Cao et al. 2004; Cao et al. 1998; Karpanen and Alitalo 2008; Marconcini et al. 1999; Rissanen et al. 2003). Lymphangiogenic and angiogenic functions of VEGF-C and VEGF-D are driven by binding and activation of the endothelial cell specific receptors VEGFR-3 and VEGFR-2 leading to endothelial cell migration and proliferation. Key steps are crucial for these processes to occur and are governed by specific functionally important sites on both the ligands and receptors.

Proteolytic cleavage of VEGF-C and VEGF-D is an important regulator of bioactivity. Both VEGF-C and VEGF-D acquire the ability to bind VEGFR-2 only after proteolysis (Achen et al. 1998; Joukov et al. 1996). Mature VEGF-D has a 290-fold greater affinity for the VEGFR-2 receptor than unprocessed VEGF-D (Stacker et al. 1999). Similarly, VEGF-C

and VEGF-D bind VEGFR-3 with far greater affinity following proteolytic maturation (Joukov et al. 1997b; Stacker et al. 1999). Lymphangiogenesis is reduced by approximately 4-fold in a mouse tumour model as a result of a mutation in a VEGF-C proteolytic cleavage site (Siegfried et al. 2003).

Binding and activation of VEGFR-2 and VEGFR-3 also require ligand (and subsequent receptor) dimerisation, whereby each monomer contributes one receptor binding site. In the case of VEGF-C and VEGF-D, fully processed, mature monomers bind one another via non-covalent (Joukov et al. 1997b; Stacker et al. 1999) and/or covalent (Leppänen et al. 2010) bonds in an antiparallel fashion, before specific receptor binding can take place. Thus residues required in the formation of the dimer interface are essential to VEGF-C and VEGF-D function. VEGFR-3, being a tyrosine kinase receptor, follows a specific pattern of intracellular signalling upon activation (Fig. 4.1.). Dimeric ligand binding triggers receptor dimerisation resulting in transphosphorylation between the receptor monomers, which regulates kinase activity and creates docking sites for specific signal transduction molecules. Thus, specific tyrosine residues within the VEGFR-3 tyrosine kinase domain that are capable of phosphorylation are essential for receptor activity (Dixelius et al. 2003b).

Figure 4.1. VEGFR-3 phosphorylation sites and signal transduction pathways. Intracellular domains of dimerised and activated vascular endothelial growth-factor receptor 3 (VEGFR-3) are shown with tyrosine-phosphorylation sites that are indicated by numbers (from human sequence). Binding of dimerised VEGF-C or VEGF-D triggers receptor dimerisation and autophosphorylation. Circled R indicates that use of the phosphorylation site is dependent on heterodimerisation (VEGFR-2/VEGFR-3 heterodimers are possible along with VEGFR-3 homodimers). Dark blue squares in the receptor molecules indicate positions of tyrosine residues. Binding of signalling molecules (dark blue ovals) to certain phosphorylation sites (boxed numbers), initiates signalling cascades (light blue ovals), which leads to the establishment of specific biological responses (pale blue boxes). The mode of initiation of certain signalling chains is unclear (dashed arrows). Final biological outcomes that are coupled to the respective receptors are indicated in pink boxes. MAPK, mitogen-activated protein kinase; PI3K, phosphatidylinositol 3′ kinase; PKC, protein kinase C. Figure adapted from Olsson et al. (2006).

Amino acid sequence mutations, occurring either naturally or artificially, highlight the functional importance of specific residues within VEGF-C, VEGF-D and VEGFR-3 proteins. For example several forms of hereditary lymphoedema arise due to missense mutations within the VEGFR-3 gene encoding the tyrosine kinase domain. Such mutations inhibit receptor transphosphorylation upon ligand binding and thus prevent downstream signalling to endothelial cells leading to the development of a lymphoedema phenotype (Butler et al. 2007; Karkkainen et al. 2000). Similarly, the transgenic Chy mouse model, which displays hypoplasia of the cutaneous lymphatic vessels, also possesses a heterozygous mutation rendering the tyrosine kinase domain inactive (Karkkainen et al. 2001). Mutations in residues of VEGF-C and VEGF-D important in the receptor-binding interface likewise prevent or reduce receptor binding and signalling. In VEGF-C, mutations of only three amino acids (Cys156, Phe151 and Pro198) are sufficient to inhibit binding to VEGFR-3 (Jeltsch et al. 2006). Likewise, VEGFR-2 binding by VEGF-C is reduced by alanine mutations in three VEGF-C residues (Cys 156, Pro 155, Phe 151) (Jeltsch et al. 2006) and is completely abolished when Cys 156 is mutated into a serine residue (Joukov et al. 1998).

High levels of similarity were reported in the previous chapter between the VEGF-C, VEGF-D and VEGFR-3 nucleotide sequences of the gecko and other species. However, given that only a small amount of sequence information was available it was unclear whether this similarity was limited only to the identified regions or whether it was representative for the whole molecule. Nor was it determined whether functionally important residues are conserved or whether the gecko proteins possess similar structural features to those of other species. Furthermore, phylogenetic analysis of the partial sequences provided evidence for differing modes of evolution of VEGF-C (stabilising selection) compared to VEGF-D and VEGFR-3 (directional selection). However, again as only a small amount of sequence information was

present the results may have been biased and thus more sequence information may aid in clarifying these evolutionary relationships.

In this chapter I aim to further characterise the VEGF-C/D/R3 pathway within the gecko by describing the cDNA and translated protein sequences. Sequence alignments, phylogenetic analysis and molecular modelling have been used to provide evidence that the gecko proteins would act in a functionally similar way as they do in mammals, fish, birds and frogs i.e. they are likely to be lymphangiogenic.

4.2. MATERIALS AND METHODS

4.2.1. RNA EXTRACTION

Total RNA extracted in Chapter 3 was used for sequence determination in this chapter. Briefly, gecko tails were stimulated to autotomise and then left to regenerate for either 4, 5, 6, 7, 9, 10 or 12 weeks after which the regenerated portion of the tails was once again autotomised and immediately snap frozen in liquid nitrogen until required. Total RNA was isolated from snap frozen gecko tails using TRIzol (Astral Scientific Pty Ltd), following the manufacturer's instructions. Briefly, gecko tail tissue was pulverised to a fine powder using a mortar and pestle in the presence of liquid nitrogen to prevent any tissue thawing. Up to 100 mg of crushed tissue was then added to a sterile 1.5 ml screw cap eppendorf tube containing 1 ml of chilled TRIzol and half-filled with 1.0 mm diameter Zirconia/silica beads (Daintree Scientific). Homogenisation was performed using a Mini-Beadbeater (Daintree Scientific) for 3 x 60 sec at 4800 rpm with cooling on ice in between each homogenisation step. The homogenate was centrifuged at 12,000 g for 10 min at 4°C to remove insoluble material and beads. Chloroform was added to the supernatant of the homogenate followed by vortexing for 15 s and incubating at room temperature for 5 min. The upper aqueous phase containing RNA was transferred to a fresh tube and RNA was precipitated by the addition of 500 µl of

isopropanol. The resultant pellet was washed using 75% ethanol and finally resuspended in 100 µl of diethyl pyrocarbonate (DEPC) -treated water. RNA concentration and purity were measured using a NanoDrop spectrophotometer (NanoDrop Technologies Inc.).

4.2.2. cDNA SYNTHESIS

Complementary DNA (cDNA) was synthesised with the Superscript™ III First-Strand Synthesis System (Invitrogen) using 1 µg of DNase-treated total RNA and Oligo-dT priming in a final volume of 20 µl as per the manufacturer's guidelines. Controls containing no RNA transcript were performed to test for reagent contamination.

4.2.3. DEGENERATE POLYMERASE CHAIN REACTION (PCR)

Partial lymphangiogenic cDNA sequences were obtained using degenerate primers designed from consensus vertebrate sequence alignments of the different genes (Table 4.1.) in a degenerate polymerase chain reaction (PCR) using AmpliTaq® Gold DNA Polymerase enzyme with GeneAmp® 10X PCR Buffer (Applied Biosystems) according to the manufacturer's instructions. Each 25 µl reaction mix, in 0.2 ml microfuge tubes, contained 0.4 µM of forward and reverse degenerate primer, 200 µM dNTPs, 0.1 µl AmpliTaq® Gold DNA polymerase, 2.5 µl GeneAmp® 10X PCR buffer, 2.5 mM $MgCl_2$ and 2.5 µl of cDNA template. PCRs were performed in a Peltier Thermal Cycler (MJ research), under the following conditions:

Initial denaturation and enzyme activation - 95°C for 10min

Denaturation - 94°C for 30 sec
Annealing - 53°C for 30 sec
Extension - 72°C for 30 sec
} 35 Cycles

Final extension - 72°C for 7min

A lower annealing temperature allows for a lower stringency reaction and thus enables degenerate primers to bind.

Several different combinations of degenerate primers were used to amplify several sequence fragments of different sizes for each gene to attempt to determine as much of the protein coding sequence as possible.

Table 4.1. Degenerate primers used in successful PCR reactions to obtain partial cDNA sequences of lymphangiogenic factors VEGF-C, VEGF-D and the receptor VEGFR-3

Gene name	Primer sequence FWD 5'- 3'	Primer sequence REV 5' – 3'	Region to amplify
VEGF-C	ATCACACKTCCTGCMGRTGC	ACARCGRCAYACTTCTTCAC	5' end (to gain sequence for design of qPCR and RACE primers)
VEGF-C	CCACCATGCACTTGCTGG	TGTTACGGGTTTGGGACCAT	3' UTR and start of translated region
VEGF-D	TGGCARARGACTCAGTGTGTGC	TCTCTTCATTGCAGCAKCC	Middle (for qPCR primer design)
VEGF-D	GGACTGGAAGCTGTGGARATGC	AAGGTGGCTTGAAGAATTTGTTG	Middle (gain sequence for design of RACE primers)
VEGF-D	AGCTGTSTGVTAHYAACTG	AAGGTGGCTTGAAGAATTTGTTG	5' UTR and start of translated region
VEGFR-3	TCACCTGCACVGYCTAYGG	CTTGTGCTCACTTGCAGTCG	Middle (for design of RACE primers)
VEGFR-3	ACAGARCTCTCYAGCATCC	CTTGTGCTCACTTGCAGTCG	Middle (for design of RACE primers)
VEGFR-3	AAGTGCATCCACMGAGAYCTGG	CGGGCACTGCCTTTCCKG	Middle (for qPCR primer design)

Abbreviations are as follows: FWD, forward primer; REV, reverse primer; PCR, polymerase chain reaction; qPCR, quantitative real time PCR; UTR, untranslated region; RACE, rapid amplification of cDNA ends; VEGF-C, vascular endothelial growth factor C; VEGF-D, vascular endothelial growth factor D; VEGFR-3, vascular endothelial growth factor receptor 3. Mixed base codes: R (AG) Y (CT) M (AC) K (GT).

4.2.4. AGAROSE GEL ELECTROPHORESIS

Detection of the correctly sized PCR products was performed using agarose gel electrophoresis. Electrophoresis was performed using specific volumes of DNA diluted in 6X DNA loading dye (New England Biolabs). Pre-stained 100 bp or 1 kb molecular weight markers (New England Biolabs) were always run in conjunction with DNA solutions (marker chosen dependent on expected size of product). All samples were run on set 1% agarose gels containing 1 μg/ml ethidium bromide at 130 volts (v) in 1X Tris-borate-EDTA (TBE) buffer. Gels were visualised under UV light using the GelDoc EQ Trans UV imaging system (Bio-Rad).

4.2.5. PCR CLEAN-UP, CLONING AND DNA SEQUENCING

Amplicons of the expected size obtained in degenerate PCRs were gel purified using QIAquick Gel Extraction Kit (QIAGEN) as per the manufacturer's instructions. Briefly, PCR products were examined by agarose electrophoresis (see above) on a UV box and bands of expected size were excised using a scalpel blade. The excised gel slices were then weighed and incubated at 50°C in 3 volumes of solubilisation and binding buffer (buffer QG) until the agarose was completely dissolved. DNA was then isolated and purified on the provided spin columns and eluted with 30 μl of buffer EB (10 mM Tris·Cl, pH 8.5). Elution buffer was left to stand on the membrane for 1 min before centrifugation to increase DNA concentration. Cleaned DNA was then stored at -20°C until required.

DNA was then ligated into a pGEM-T Easy vector using the pGEM-T Easy Vector System (Promega), according to the supplier's recommendations. Ligation reactions were performed in a 10 μl volume containing 5 μl of 2X Rapid Ligation Buffer, 1 μl of T4 DNA ligase and a 1:1 vector: insert molar ratio and left to incubate overnight at 4°C. Ligated plasmids were transformed into Subcloning Efficiency™ DH5α™ Competent Cells (Invitrogen) following the manufacturer's guidelines with a few modifications. Briefly, 3 μl

of the ligation reaction was added to 25 µl of thawed competent cells, mixed gently and left to incubate on ice for 30 min. Cells were then heat-shocked in a 42°C waterbath for 20 sec and returned to ice for 2 min followed by incubation in 950 µl of pre-warmed culture media (super optimal broth with carbolite repression (SOC, Invitrogen) or Luria-Bertani (LB) without antibiotic) at 37°C for 1 h with shaking. Following this cellular recovery period the transformations were spun at 6,000 g for 1 min to pellet bacterial cells and most of the supernatant was removed leaving approximately 150 µl with the bacterial pellet. Bacteria were then re-suspended and 8 µl of 50 mg/ml X-gal (Subcloning Efficiency™ DH5α™ Competent Cells do not require IPTG for blue/white selection) was added directly to the cell suspension for blue/white screening for recombinants. The entire cell suspension was then spread onto pre-warmed LB plates containing 100 µg/ml ampicillin and left overnight at 37°C. Positive clones were identified as being white (due to disruption of the LacZ gene, thus no β-galactosidase is present to form a blue precipitate in the presence of X-gal), and were picked using a sterile toothpick and cultured in 2 ml of LB media containing ampicillin overnight at 37°C with shaking. Plasmids from positive colonies were isolated using the QIAprep Spin Miniprep Kit (QIAGEN) and the clones sequenced using sequence BigDye® Terminator v3.1 Cycle Sequencing (Institute of Medical and Veterinary Sciences, Adelaide). Sequences were confirmed to be the genes of interest by using a Basic Local Alignment Search Tool (BLAST, www.ncbi.nlm.nih.gov/blast/Blast.cgi).

4.2.6. 5’ AND 3’ RAPID AMPLIFICATION OF cDNA ENDS (RACE)

Where full protein coding sequences could not be obtained using degenerate PCR, rapid amplification of cDNA ends (RACE) was utilised to acquire the 5’ and 3’ ends of the partial cDNA’s. The 5’/3’ RACE kit, 2nd Generation (Roche) was used for first strand cDNA synthesis, Poly(A) tailing of first-strand cDNA (for 5’ RACE) and PCR amplification of cDNA using gene specific primers designed from the partial sequences (Table 4.2.). Both gVEGF-C and gVEGF-D 5’ends could be obtained using degenerate PCR, while gVEGFR-3 required 5’ RACE. All three genes required 3’ RACE to obtain the 3’ ends of the protein-coding gene sequences.

First-strand synthesis of cDNA for 5’ RACE was performed using 2 µg of total RNA extracted from *C. marmoratus* tails (section 4.2.1.) according to the manufacturers’ instructions. Briefly, 2 µg of total RNA was added to 0.625 µM of gene specific cDNA synthesis primer (VEGFR-35RACE_GSP1), 4 µl of cDNA synthesis buffer, 2 µl of dNTPs and 25 U of Transcriptor Reverse Transcriptase in a total reaction volume of 20 µl. Reverse transcription was then performed by incubation for 60 min at 55°C followed by inactivation of the enzyme by incubation at 85°C for 5 min. Single stranded cDNA was then cleaned up (removal of excess primer, dNTPs, buffer salts etc.) using the High Pure PCR Product Purification Kit (Roche) via the special protocol specified in the RACE manual. Next, a homopolymeric A-tail was added to the 3’end of the cleaned first-strand cDNA using recombinant Terminal Transferase and dATP. dA-tailed cDNA was then PCR amplified using an oligo-dT anchor primer plus reverse gene specific primer (VEGFR3_RACE_GSP5; designed 5’ to GSP6) in a PCR reaction using the FastStart High Fidelity PCR System (Roche). FastStart reactions were carried out in a final volume of 50 µl, with 5 µl of 10x FastStart High Fidelity Reaction Buffer (final $MgCl_2$ concentration 1.8 mM), 1 µl PCR grade

nucleotide mix (200 µM of each dNTP), 0.4 µM final forward and reverse primer concentration and 1 µl of dA-tailed cDNA template. PCR cycling conditions were as follows:

Initial denaturation and enzyme activation - 95°C for 2 min

Denaturation - 95°C for 30 sec
Annealing - 60°C for 30 sec
Extension - 72°C for 90 sec
} 35 Cycles

Final extension - 72°C for 7 min

A second round PCR was then used to further amplify specific cDNA using a further 5' designed gene–specific primer (VEGFR3_RACE_GSP4) and PCR anchor primer (from RACE kit). 5' RACE products were confirmed using agarose gel electrophoresis, gel extraction, cloning and sequencing as described above.

First-strand synthesis of cDNA for 3' RACE was performed using 2 µg of total gecko RNA in a 20 µl reaction consisting of 4 µl cDNA synthesis buffer, 2 µl dNTP mix, 1 µl oligo-dT-anchor primer and 1 µl of Transcriptor Reverse Transcriptase. This reaction mixture was then incubated for 60 min at 55°C then 5min at 85°C. The resulting single stranded cDNA (sscDNA) was then directly used in a PCR reaction using the FastStart High Fidelity PCR System (Roche) with the PCR anchor primer as reverse and gene- specific forward primer (Table 4.2.) under the same reaction and cycling conditions as described above. Second-round PCR was then performed using a second gene-specific primer further 3' to the first. 3' RACE products were confirmed using agarose gel electrophoresis, gel extraction, sub-cloning and sequencing as described above.

Table 4.2. Gene-specific primers used in successful 5' and 3' RACE cDNA synthesis and PCR to obtain full-length protein-coding sequences of lymphangiogenic factors VEGF-C, VEGF-D and the receptor VEGFR-3

Gene	Primer name	Primer Use	Primer sequence 5' – 3'
VEGF-C	VEGFC_3RACE_FWD	3' RACE 1st round PCR	ACTGCTGCCTAGCTCATGTGGACCC
VEGF-C	VEGFC_3RACE_FWD2	3' RACE 2nd round PCR	TGTACAGTCCGAACGAAACG
VEGF-D	VD_3RACE_JUN10	3' RACE 2nd round PCR (qPCR_FWD_VEGF-D used in 1st round PCR)	GAAGGACTTCCTCCACTTGC
VEGFR-3	RACE_VR3_FWD	3' RACE 2nd round PCR (qPCR_FWD_VEGFR_3 used in 1st round PCR)	TTATGTCAGGAAAGGCAGTGCCC
VEGFR-3	VEGFR-3_5RACE_GSP6	5' RACE cDNA synthesis primer	AGATGATAGAGGTTGTCGAGAGC
VEGFR-3	VEGFR-3_5RACE_GSP5	5' RACE 1st round PCR	TGAGGTCTGGAATGGATACC
VEGFR-3	VEGFR-3_5RACE_GSP4	5' RACE 2nd round PCR	ATGGGATGCAGATATTCTCC

Abbreviations are as follows: RACE, rapid amplification of cDNA ends; VEGF-C, vascular endothelial growth factor C; VEGF-D and VD, vascular endothelial growth factor D; VEGFR-3, vascular endothelial growth factor receptor 3; PCR, polymerase chain reaction; GSP, gene specific primer; FWD, forward primer

4.2.7. SEQUENCE ANALYSIS AND BIOINFORMATICS

Sequence data and chromatograms were returned in ab1 file format and viewed and edited using the BioEdit software package (Hall 1999). Nucleotide sequences were translated to amino acids using the BioEdit sorted six-frame translation tool. Sequence alignments to other vertebrate genes (obtained from GenBank, NCBI) were carried out using the ClustalW multiple alignment application. Similarity and difference scores were calculated using the sequence identity matrix and sequence difference matrix tools in BioEdit.

4.2.7.1. Phylogenetic analysis

To examine the phylogenetic relationships between different species, phylogenetic trees of the VEGF-C, VEGF-D and VEGFR-3 protein sequences were constructed from a ClustalW amino acid alignments using the Neighbour-Joining (NJ) method within the MEGA 4.1 software package (Tamura et al. 2007). The NJ method uses a distance-based algorithm to make pair wise comparisons of whole sequences. Thus evolutionary divergence is determined based on a single coefficient of sequence similarity or difference. Evolutionary distances were computed using the Poisson correction method (Zuckerlandl and Pauling 1965). Bootstrap analysis based on 1200 pseudo-replicates was performed to assess support for nodes. For the expanded phylogenetic analysis of the VEGF-C, VEGF-D and VEGFR-3 nucleotide sequences (in section 4.4.2.), NJ trees were constructed with pair wise evolutionary distances between sequences computed using the maximum composite likelihood method which reduces standard errors that can typically be generated by the NJ method and hence improves the accuracy of the constructed trees (Tamura et al. 2004). Sequences included in the expanded NJ trees were selected by a BLAST search using the gVEGF-C, gVEGF-D and gVEGFR-3 sequences as the query. Only sequences with Expect (E) values lower than e^{-5} and that were not named as a different sequence (e.g. a different VEGF family member or receptor) were included in the ClustalW alignment used to generate NJ trees.

4.2.7.2. Molecular Modelling

Comparative homology models were generated and partially assessed in the Swiss-Model workspace (first approach mode) (Arnold et al. 2006). Swiss-Model selects tertiary structure templates based on sequence alignments between the query and template. Analysis of the models to assess model accuracy and viability performed by Swiss-Model includes Anolea (atomic empirical mean force potential, used to assess the packing quality of the models) (Melo and Feytmans 1998), GROMOS (analysis of conformations in biomolecular systems) and Verify 3D (Eisenberg et al. 1997) which analyses the compatibility of a 3D atomic model with its own amino acid sequence (1D). Homology models with a sequence identity of less than 50% to the selected template were further assessed for model quality using QMEAN (Benkert et al. 2008) and DFire (Zhou and Zhou 2002). Molecular graphics images were produced using the UCSF Chimera package from the Resource for Biocomputing, Visualisation, and Informatics at the University of California, San Francisco (http://www.cgl.ucsf.edu/chimera, supported by NIH P41 RR001081) (Pettersen et al. 2004).

4.3. RESULTS

4.3.1. ISOLATION OF NUCLEOTIDE SEQUENCES ENCODING FULL-LENGTH PROTEIN CODING REGIONS FOR gVEGF-C, gVEGF-D AND gVEGFR-3

Full-length protein coding cDNA sequences were obtained for the VEGF-C (Fig. 4.2), VEGF-D (Fig. 4.3) and VEGFR-3 (Fig. 4.4) genes of the Australian marbled gecko (*Christinus marmoratus*) using both degenerate PCR and 5'/3' RACE. Degenerate primers were first designed based on the sequence of highly conserved regions within each of the genes. Using these primers, partial sequences were acquired and based on these partial sequences gene-specific primers for 3' and 5' RACE and further degenerate primers (for PCR with one degenerate and one specific primer) were designed. Degenerate PCR was sufficient to obtain 5' ends for both VEGF-C and VEGF-D due to high levels of similarity in mixed vertebrate species alignments in the 5' untranslated region (UTR) of these genes. That is, conserved nucleotide sequences in the 5' UTR of different species enabled a degenerate primer to be designed within this region that was capable of annealing to the gecko sequence allowing amplification of the 5' region when used with a gecko-specific reverse primer. 5' RACE was used for gVEGFR-3 to obtain the full 5' UTR and 5' end of the protein-coding region. Several attempts and re-designing of 3' RACE primers enabled 3' RACE to be used for all 3 genes to obtain the 3' ends including the poly (A) tail.

The sequences obtained contain protein-coding regions of 1272, 1056 and 4157 bp for gVEGF-C, gVEGF-D and gVEGFR-3 respectively, which upon translation encode proteins of 424, 351 and 1385 amino acids respectively. There is a poly-adenylation signal (AATAAA) within the 3' UTR for both VEGF-C and VEGF-D, but an authentic poly-adenylation signal was not present in the VEGFR-3 sequence.

Figure 4.2. Nucleotide and deduced amino acid sequences of gecko VEGF-C cDNA. Start and stop codons are shaded in yellow. The full 5' untranslated region (UTR) was not deduced. The total cDNA sequence obtained was 1722 bp and includes the 3' UTR (1282-1723 bp) and full protein-coding region (7-1281 bp), which codes for 424 amino acids. The poly-adenylation signal is underlined.

```
CCACCATGCACTTGCTGGGATCCCTCTCTCTGGGTTGCTATCTGGCTGCT 50
      M  H  L  L  G  S  L  S  L  G  C  Y  L  A  A

GCGACTCTGGGGCTGCTGGGAGCGAGGCGCGAGCCGGCCACCGCCGCTGC 100
 A  T  L  G  L  L  G  A  R  R  E  P  A  T  A  A  A

CTATGAGTCCGGGCAGGGCTACTACGAGGAGGAGCCCGAGCTGGGCGAGA 150
  Y  E  S  G  Q  G  Y  Y  E  E  E  P  E  L  G  E

CGAAGCAGGCTCATGCAAGCAAAGAGCTGGAAGAACAGTTGCGATCTGTA 200
T  K  Q  A  H  A  S  K  E  L  E  E  Q  L  R  S  V

TCCAGTGTGGATGAACTTATGACAGTACTTTATCCAGAATACTGGAAAAT 250
 S  S  V  D  E  L  M  T  V  L  Y  P  E  Y  W  K  M

GTTCAAATGTCAGTTGAGAAAAGGGAGCTGGCAACATAGTAGGGAACAAG 300
  F  K  C  Q  L  R  K  G  S  W  Q  H  S  R  E  Q

CCAGCTTCGATGCAAGATCAGAAGATTCAAATCCAATAAAATTTGCTGCA 350
A  S  F  D  A  R  S  E  D  S  N  P  I  K  F  A  A

GCACATTATAATGCAGATATCTTGAAAAGTATTGATAATGAGTGGAGAAA 400
 A  H  Y  N  A  D  I  L  K  S  I  D  N  E  W  R  K

AACTCAATGCATGCCACGTGAGGTATGTGTAGATGTGGGGAAAGAATTTG 450
  T  Q  C  M  P  R  E  V  C  V  D  V  G  K  E  F

GAGCAACAACAAACACCTTCTTTAAACCTCCATGTGTGTCCATCTACAGA 500
G  A  T  T  N  T  F  F  K  P  P  C  V  S  I  Y  R

TGTGGAGGTTGCTGCAATAGCGAGGGCCTGCAGTGTATGAATATCAGCAC 550
 C  G  G  C  C  N  S  E  G  L  Q  C  M  N  I  S  T

AAGCTACATCAGCAAAACGTTGTTTGAAATAACTGTGCCACTGTCTCATG 600
  S  Y  I  S  K  T  L  F  E  I  T  V  P  L  S  H

GTCCCAAACCCGTAACAATCAGTTTTGCCAATCACACATCTTGCCGATGC 650
G  P  K  P  V  T  I  S  F  A  N  H  T  S  C  R  C

ATGTCCAAACTGGATGTCTACAGACAAGTTCATTCCATCATTAGACGCTC 700
 M  S  K  L  D  V  Y  R  Q  V  H  S  I  I  R  R  S

CTTGCCACTGACACAACCGCAGTGTCAAGTGGCAAACAAAACTTGTCCAA 750
  L  P  L  T  Q  P  Q  C  Q  V  A  N  K  T  C  P

AAAGCTATATCTGGAATAACCACATCTGCAGATGTCTGGCACAACATGAC 800
K  S  Y  I  W  N  N  H  I  C  R  C  L  A  Q  H  D

TTCAGTTTCTCTTCCCACCTTGGGGATACAGACTCTACTGAAGGATTCCA 850
 F  S  F  S  S  H  L  G  D  T  D  S  T  E  G  F  H
```

TGATATCTGTGGACCTAACAAGGAGCTTGATGAAGAAACATGTCAGTGTG 900
D I C G P N K E L D E E T C Q C

TCTGCAAAGGGGGAGTGAGACCTTCCAGCTGTGGAGCCCACAAAGAATTA 950
V C K G G V R P S S C G A H K E L

GACAGAACATCCTGCCAGTGCACATGTAAAAATAAACTGCTGCCTAGCTC 1000
D R T S C Q C T C K N K L L P S S

ATGTGGACCCAACAAAGATTTTGATGAAGAAAGATGCCATTGTGTATGTA 1050
C G P N K D F D E E R C H C V C

AAAAAACATGCCCTAAACATCAACCGCTAAATCCTGCAAAATGTATCTGT 1100
K K T C P K H Q P L N P A K C I C

GAATGTGCAGAATCTCCAAACAAGTGCTTCTTGAAAGGAAAAAGATTTCA 1150
E C A E S P N K C F L K G K R F H

TCAGCAAACATGCAGTTGCTATAGACCACCATGTACAGTCCGAACGAAAC 1200
Q Q T C S C Y R P P C T V R T K

GCTGTGAGTCTGGATTTTATTACAGTGAAGAAGTATGTCGTTGCGTCCCC 1250
R C E S G F Y Y S E E V C R C V P

ATATATTGGAAAAGACCATTTATCAATTAG**TGAAGAAACCGTCATCTGAT** 1300
I Y W K R P F I N *

ATTCTGGTGTACATTTTTCCTTTTTTTAAAAAAAAGAAAAAGACTTCTAA 1350
CATTTTGAACTTCCTGTGCACTAGAGACCCTATGGGCTTATAAGAGACAG 1400
ACTTATTTGTGCTCTTCCTGAGACCCACAAAAAGCAAATGTAGGGAAAAT 1450
GGACTTTCTTCATATAAAGAATTCAATAAGGACTTGATTCTTGCCAATGA 1500
CCAGACAACTTAGGTTTTCTTCCATGTGATTTTTAAAAAAATAATGACTA 1550
TATAATTTATTTCCATAAAAATATTGTTCTGCATTCCTGTTTATAGCAGT 1600
AACAATTGTTAAATCTCACTGTGATCAATATTTTTATATCATGCAAAGTA 1650
TGTTTAAAATAAAATGAAATTGTATTATATACTGCTAAGAATAAAAAAAA 1700
AAAAAAAAAAAAAAAAAAAAA 1722

Figure 4.3. Nucleotide and deduced amino acid sequences of gecko VEGF-D cDNA. Start and stop codons are shaded in yellow. The full 5' untranslated region (UTR) was not deduced. The total cDNA sequence obtained was 2122 bp and includes the 3' UTR (1100-2122 bp) and full protein-coding region (43-1099 bp), which codes for 424 amino acids. The poly-adenylation signal is underlined.

```
GTGCTACCAACTGTGTAGTAAAGTGTGGATTTGAAAAACAAGGATGTACA 50
                                              M  Y

AGCTGTGGACAGCTGTGAACGTATTCATGGTGTCCTTTCTGCATCTGTTG 100
K  L  W  T  A  V  N  V  F  M  V  S  F  L  H  L  L

CAAGGTTCTGAGCATGGTTCTGTAAAGAGACCATCGCTTTCTGCACTGGA 150
 Q  G  S  E  H  G  S  V  K  R  P  S  L  S  A  L  E

ATGGTCAGAGCAGCAGATCAGGAAAGCCGCCAGTCTGGAAGAACTCCTTC 200
  W  S  E  Q  Q  I  R  K  A  A  S  L  E  E  L  L

GAATTACCCACTCCGAGGATTGGAAGCTATGGAAGTGCCGTCTAAAACTC 250
R  I  T  H  S  E  D  W  K  L  W  K  C  R  L  K  L

AAGAGTGTGGCCACCTTGGATTCCAGATCTGCATCGCATCGCTCCACGAG 300
 K  S  V  A  T  L  D  S  R  S  A  S  H  R  S  T  R

ATTCGCTGCGGCTTTTTATGATATAGAGATACTCAAAGTTATAGATGAGG 350
  F  A  A  A  F  Y  D  I  E  I  L  K  V  I  D  E

AGTGGCAGAGRACTCAGTGTGTGCCAAGGGAGACCTGCGTTGACGTTGCA 400
E  W  Q  X  T  Q  C  V  P  R  E  T  C  V  D  V  A

AAGGACCTGGGCACCACCACCAACAAATTCTTCAAGCCACCTTGTGTGAA 450
 K  D  L  G  T  T  T  N  K  F  F  K  P  P  C  V  N

TGTCTACAGATGTGGAGGCTGCTGTAATGAAGAGAGCCGGAGCTGCATGA 500
  V  Y  R  C  G  G  C  C  N  E  E  S  R  S  C  M

ACACAAGTACATCTTATGTTTCCAAAATGCTCTTTGAAATTTCAGTTCCT 550
N  T  S  T  S  Y  V  S  K  M  L  F  E  I  S  V  P

TTAACAAATGTGCCTGACCCAATTCAAGTCAAAATTGCGAACCACACAGG 600
 L  T  N  V  P  D  P  I  Q  V  K  I  A  N  H  T  G

TTGTAAGTGTATATCAAATGTTCAGCACCAACCATATTCCATCATAAGAA 650
  C  K  C  I  S  N  V  Q  H  Q  P  Y  S  I  I  R

GATCTGTCCTGTATTCAGAGGAGGATCGTTGTTCTCATTTAAAAAAACTG 700
R  S  V  L  Y  S  E  E  D  R  C  S  H  L  K  K  L

TGTCACAATGGCTGGATATGGGACATCAATAAATGTGAATGTGTTGAAAA 750
 C  H  N  G  W  I  W  D  I  N  K  C  E  C  V  E  N

TGAGGATCATCCTAGCAGAAGAGAAGGACTTCCTCCACTTGCTGAACTTG 800
  E  D  H  P  S  R  R  E  G  L  P  P  L  A  E  L

CTATGTGTGCRCCAAATATGGACTTTGATGAAGAGAACTGTGAGTGCATC 850
A  M  C  X  P  N  M  D  F  D  E  E  N  C  E  C  I
```

TGTAAATGGAAGTGTGCTGGCAATTTATTTCAGAACAAAGAGAATTGCAG 900
C K W K C A G N L F Q N K E N C S

CTGTTACTTGTGCACAGAGAACCAGGACAGCTGCTTTCAGAAACATAAGA 950
C Y L C T E N Q D S C F Q K H K

CATTTAATGCAGAAACGTGCAGTTGTGAAGACAAATGCCCATTCCAGGCC 1000
T F N A E T C S C E D K C P F Q A

AGAACGTGCCCAACTGCTAGGCCAGCGTGTTCAAGGCACTGTCGCTGTGT 1050
R T C P T A R P A C S R H C R C V

CAAGGGGGGAAGAGGCCCTCATGGGTCCCAAAGCAAAGAAAACCCTTGAT 1100
K G G R G P H G S Q S K E N P *

CAAGCTTTCGTTACACTTGGACAAAACATGCACTCTCTGCTTTGCAACGT 1150
AGGTGTYTTCTGCCACAAGCTATTCATCTATAATAATCATGGGATATGAG 1200
TGACATTACTAGTTTTAAAAAAAAATCAAATCGGTATTCATGATGAAGAG 1250
TGGGTGTGCAAGGACATTACCATCTGGCTTCAGRTGTCTGCTGCAACAGA 1300
TTATYCTTGTTCTGCAAAGGGTCACTAAAAGGACCTCTATCCATCACAGC 1350
TGTCAGGAAGAAACTGGTATGCTTGTTGCAGGAGGACAGTCAACATCCAG 1400
CATTTTGGAAATGCAGAAGAAAAATAGTTCTACAGCATCAACCCATAGAT 1450
GTTAATGAGCATATTTTTTTTAGAGCAGGGGTCCCTAACCTTTTTGAGCC 1500
TGCGGGCATCTTTGTAATTCTGCCACAGGGTGGTGGGCGCAATCACAAAA 1550
CGGTTGCTGCAGGAGGCAGAGCCAGCCACCAAATATCAGGGAGTGAGGGT 1600
ATGTACAGCTCTTAATAGTAACTCTTCAACATTTCCAGGCAGAAGCTATG 1650
TTTAACAGGATGTCTTTTAAAGTGAACGTATCATTTAAAGCTATTTTCTC 1700
GAACACACACAGTTTACCTTCAGTCACACGCTGAAGATCCTTGCTGCTGT 1750
GGTGGCAGCTGCTGCCGAAGCAATGTTTTTAAAAGTCTGCACAGCCAATC 1800
AGAAGCCCTGCTGAGCAAAAGCCCTGCCTACTTCCTAAAAACACTTGGCG 1850
GGCCCCAGGAAAGGTGTCGGCGGGCACCATGGTGCCCCTCGGGCATCACG 1900
TTGAGGATCCCTGATTTAGTGCAAACTTCCATGTTTGTATTCATATGTTC 1950
AGCACTGAATTAGTTGATCTACTGTCAATTTTTATTATTTAGATTTATTG 2000
TAGAACTACTGTCCGATGTTCCATATTTAAAATGTATATAGGAAAATAAA 2050
TGCATTGGTTATTAATAAATGTATATTGCCATATGTCATTTGGCAAGAAA 2100
TCTTAATCACAAAAAAAAAAA 2122

Figure 4.4. Nucleotide and deduced amino acid sequences of gecko VEGFR-3 cDNA. Start and stop codons are shaded in yellow. The cDNA of gecko VEGFR-3 is 4517 bp long, and its longest open reading frame (122-4279 bp) codes for 1385 amino acids. The 5' untranslated region (UTR) spans 1-121 bp. There was no authentic polyadenylation signal in the 3' UTR (4280-4517 bp).

```
TGAGGGAGGCAGGGAGGGAAGCTTTGCGCCGGCCCGGGCTGCCCGCCGCC 50
ACTCGCCGCCTCCGCCTCCGCCGCCGCCCCCGGGCCAGCCTTCCCCGCGG 100
ACCCTCGTCCCGGCGCTGGAGATGAAGAGAGCGTGCACGTGGTGCCTCTG 150
                      M  K  R  A  C  T  W  C  L  W

GCTCTGGATCGGGATCGTCTCTGAAGCGGATTTGGTGAGAAGCTATTCTA 200
  L  W  I  G  I  V  S  E  A  D  L  V  R  S  Y  S

TGACCCCACCCACACTCAGCACCGCAGAAGAGGAATACGTGATCAACACT 250
M  T  P  P  T  L  S  T  A  E  E  E  Y  V  I  N  T

AAAGATACCCTGAATATTACTTGCAGAGGACAGCATCCCCTGGAGTGGTC 300
 K  D  T  L  N  I  T  C  R  G  Q  H  P  L  E  W  S

GTGGCCTGGAGGCCAAGAGGACACTGTCCAGATTGGAAAGGACAGCGAAT 350
  W  P  G  G  Q  E  D  T  V  Q  I  G  K  D  S  E

CAGTGGTGTTGGTGAGTCTCGACGGCGTCCGAACAGTCAAGGAAGAAGAT 400
S  V  V  L  V  S  L  D  G  V  R  T  V  K  E  E  D

TGTGAGGGCACTGACACAAAGCCCTACTGCAAGGTCTTGACACTGACAGG 450
 C  E  G  T  D  T  K  P  Y  C  K  V  L  T  L  T  G

GACTCAGGCTAACGACACAGGCTACTACCGCAGTCACTACAAGTACATCA 500
  T  Q  A  N  D  T  G  Y  Y  R  S  H  Y  K  Y  I

GTGCCAAAATCGAGGGCACCACTGCAGTCAGCACCTATGTGTTTGTGAGA 550
S  A  K  I  E  G  T  T  A  V  S  T  Y  V  F  V  R

GATTTTCAACAGCCATTTATCAATAAACCAGAAACTCTTCTTATCTACAA 600
 D  F  Q  Q  P  F  I  N  K  P  E  T  L  L  I  Y  N

TAAGGAGAATATCTGCATCCCATGCCTGGTATCCATTCCAGACCTCAACA 650
  K  E  N  I  C  I  P  C  L  V  S  I  P  D  L  N

TCACTTTGCTCTCGACAACCTCTATCATCTACCCAGATGGAAAGAGCATT 700
I  T  L  L  S  T  T  S  I  I  Y  P  D  G  K  S  I

ATCTGGGACAATAAAAGAGGAATGTTGGTTCCCACCTTACTGATCAAGGA 750
 I  W  D  N  K  R  G  M  L  V  P  T  L  L  I  K  D

TTCCTTATATGTTCAATGTGAAACTTTAATTGACAGGAAATCCTTCAAAT 800
  S  L  Y  V  Q  C  E  T  L  I  D  R  K  S  F  K

CCAGTTTCTTCCTTGTCCACATTGCAGGAAATGAACTTTATGACATTCAG 850
S  S  F  F  L  V  H  I  A  G  N  E  L  Y  D  I  Q

TTGTTTCCAAGGAAAGCCATGGAACTGCTTGTTGGAGAAAAGCTAGTTAT 900
 L  F  P  R  K  A  M  E  L  L  V  G  E  K  L  V  I

CAACTGCACAGTATGGGCCGAGTTTAATTCTGGAGTAGATTTCCAGTGGG 950
```

N C T V W A E F N S G V D F Q W

ACTACCCTGCAAAACAGATGAATCGGGAAGTCACAGAAATGCCTGAGAGG 1000
D Y P A K Q M N R E V T E M P E R

CGCTCCCAGCAGACACACACTGAGCTCTCCAGCATCCTGATCATCCAAAA 1050
R S Q Q T H T E L S S I L I I Q N

TGTGAGCCAGCAAGATGTGGGGAAATATACGTGCCTGGCTAGCAATGGGG 1100
V S Q Q D V G K Y T C L A S N G

AACAGATCTTCAAGGAAAGCATAGATGTCATCGTACATGAGAAGCCTTTC 1150
E Q I F K E S I D V I V H E K P F

ATCAGTGTGGAGTGGAAGAAGGGCCCGATAATAGAAGCAACAGCAGGAGA 1200
I S V E W K K G P I I E A T A G D

TGAAATTGTGAAGCTGCCAGTGAAAAGTGTTGCGTACCCTCAGCCTGAGT 1250
E I V K L P V K S V A Y P Q P E

TTCAGTGGTTTAAGGATGGAAAGTTAATTTCCAACAGACAATCTCAGTAT 1300
F Q W F K D G K L I S N R Q S Q Y

TCCCTGCATATCAAGGATGTGACAGAGCAGAACTCTGGCACTTATACATT 1350
S L H I K D V T E Q N S G T Y T L

GGTTCTTAGGAATGGGCCGGCCGGCCTAGAGAAGCACATTCGCCTCCATC 1400
V L R N G P A G L E K H I R L H

TGGTGGTCAATGTTCCTCCACAAATCCATGAGAAAGAAGCCTCTTCACCA 1450
L V V N V P P Q I H E K E A S S P

AACATCTATTCCCGTAAAAGTCGGCAAGCACTCACCTGCACTGTCTATGG 1500
N I Y S R K S R Q A L T C T V Y G

CGTCCCAGCACCAGAAAAAATCCAGTGGCAATGGAGGCCTTGGACACCCT 1550
V P A P E K I Q W Q W R P W T P

GCCGGATGTTCTCCCACCGCAGTCTTAGCAGGAGGAGGGCTGCACGGCGC 1600
C R M F S H R S L S R R R A A R R

CATCAACGGGACCGGATGCCCGAATGTAAGGACTGGAAGGATGTATTGCA 1650
H Q R D R M P E C K D W K D V L Q

GCAGGATGCTGTGAACCCCATTGAGAGTATTGACACCTGGACAGAGTTCG 1700
Q D A V N P I E S I D T W T E F

TGGAAGGAAGGAACAAGACGGTCAGCAAACTGGTCATCCAAGAAGCAAGC 1750
V E G R N K T V S K L V I Q E A S

ATATCTGTTATGTACAAGTGTGTAGCCTCCAACAAAGTTGGTCGCGATGA 1800

I S V M Y K C V A S N K V G R D E

ACGCCTGATCTATTTCTATGTGACCACCATTCCAAATGGATTTGAAATTG 1850
R L I Y F Y V T T I P N G F E I

AGTCGCAGCCTTCGGAAGACCCCATTGAAGGACAAGACCTGAGGCTCAGC 1900
E S Q P S E D P I E G Q D L R L S

TGCAATGCTGATAATTACACCTATGAGAACCTGCAGTGGTACCGGCTCAA 1950
C N A D N Y T Y E N L Q W Y R L N

CCTCTCGAAGCTGCATGATGAAGAGGGCAACCCGCTGGTCCTGGATTGCA 2000
L S K L H D E E G N P L V L D C

AGAATGTCCATCACTATGCAACCAAAATGCAAGGCGAGCTGCACTTCAAA 2050
K N V H H Y A T K M Q G E L H F K

CCTAATTCCAACTATGCCACCTTGACACTTACAATCCCAAATATCTCACT 2100
P N S N Y A T L T L T I P N I S L

AGAGGATGAGGGAGACTATGTCTGTGAGGTGCAGAACCGGGAGAACAGTG 2150
E D E G D Y V C E V Q N R E N S

AGAAACATTGCCACAAAAAGTATATTTCTGTGCACGCTTTGGAAGTCCCA 2200
E K H C H K K Y I S V H A L E V P

AGGCTGAAGCAGAACCTGACAGACATCTTGGTGAATGTGAGTGATTCCAT 2250
R L K Q N L T D I L V N V S D S I

AGAGATGCGCTGCAAGGTTGATGGCACGCATGTTCCGAACATCAACTGGT 2300
E M R C K V D G T H V P N I N W

ATAAGGATGAGAAGCTTGTACAAGAGGTGTCAGGGATTGATCTGGAAGAT 2350
Y K D E K L V Q E V S G I D L E D

TCCAATCAGAGGCTGAGTATCCAGAGGGTGAGAGAAGAGGACGCTGGCCT 2400
S N Q R L S I Q R V R E E D A G L

CTACTTGTGTAGTGTCTGCAATGCCAAGGGTTGTGTGAATTCTTCTGCCA 2450
Y L C S V C N A K G C V N S S A

GTGTTTCTGTAGAAGGCTCAGATGACAGGACCAATGTGGAAATTGTTATC 2500
S V S V E G S D D R T N V E I V I

TTAATTGGGACTGGTGTCATTGCCATCTTCTTCTGGATTCTCCTAATCCT 2550
L I G T G V I A I F F W I L L I L

GATTTTCTGCAACATTAAGAGACCTGCTCATGCTGACATCAAGACTGGCT 2600
I F C N I K R P A H A D I K T G

ACCTTTCCATCATTATGGACCCAGGTGAAGTTCCCTTGGAGGAGCAATGT 2650

```
Y  L  S  I  I  M  D  P  G  E  V  P  L  E  E  Q  C

GAATACCTACCTTATGATTCTAGCAAATGGGAGTTCCCTCGAGAACGGCT 2700
 E  Y  L  P  Y  D  S  S  K  W  E  F  P  R  E  R  L

CCGGCTAGGTAAAGTCCTAGGCCATGGAGCCTTTGGGAAAGTGATTGAAG 2750
  R  L  G  K  V  L  G  H  G  A  F  G  K  V  I  E

CCTCTGCATTTGGAATTAATAAGAGTAACAGCTGTCAGACTGTAGCAGTT 2800
A  S  A  F  G  I  N  K  S  N  S  C  Q  T  V  A  V

AAAATGCTCAAAGAGGGAGcgactgcaaGTGAGCACAAGGCACTCATGTC 2850
 K  M  L  K  E  G  A  T  A  S  E  H  K  A  L  M  S

AGAGCTGAAGATCCTTATCCACATAGGGAACCACCTCAATGTCGTCAACC 2900
  E  L  K  I  L  I  H  I  G  N  H  L  N  V  V  N

TGTTGGGTGCCTGCACCAAACCTAATGGTCCCCTGATGGTTATTGTTGAA 2950
L  L  G  A  C  T  K  P  N  G  P  L  M  V  I  V  E

TTCTGTAAATATGGAAACCTCTCGAATTATCTGCGAACCAAACGAGAAGG 3000
 F  C  K  Y  G  N  L  S  N  Y  L  R  T  K  R  E  G

ATTCAGTCCTTATAGGGAGAAGTCTCCCAGATTGCGCATCCAGGTTCAAT 3050
  F  S  P  Y  R  E  K  S  P  R  L  R  I  Q  V  Q

CCATTGTGGAGGCTGCCAGAGCTGACAGAAGGAGCCGTTCTGGTACCAGT 3100
S  I  V  E  A  A  R  A  D  R  R  S  R  S  G  T  S

GAAAGTGCAATTCTTAATAGACTTCTGATGAACAAGAGCCAGCCAGCACC 3150
 E  S  A  I  L  N  R  L  L  M  N  K  S  Q  P  A  P

ACCACCGCCTCCTCTCCTACCAGAAGTGGATGACTTGTGGCAAAGCCCTC 3200
  P  P  P  P  L  L  P  E  V  D  D  L  W  Q  S  P

TGACAATGGAAGACCTGATCTGCTACAGCTTTCAGGTGGCCCGTGGTATG 3250
L  T  M  E  D  L  I  C  Y  S  F  Q  V  A  R  G  M

GAGTTTCTGGCATCCAGAAAGTGCATCCACAGAGACTTGGCAGCTCGTAA 3300
 E  F  L  A  S  R  K  C  I  H  R  D  L  A  A  R  N

CATCTTACTGTCAGAAAACAATGTGGTCAAGATTTGTGACTTTGGGCTGG 3350
  I  L  L  S  E  N  N  V  V  K  I  C  D  F  G  L

CCCGGGACATCTACAAGGATCCTGATTATGTCAGGAAAGGCAGTGCCCGC 3400
A  R  D  I  Y  K  D  P  D  Y  V  R  K  G  S  A  R

CTCCCACTAAAGTGGATGGCTCCAGAAAGCATCTTTGACAAAGTCTATAC 3450
 L  P  L  K  W  M  A  P  E  S  I  F  D  K  V  Y  T

CACACAGAGTGATGTCTGGTCATTTGGAGTCCTCCTGTGGGAGATCTTCC 3500
```

T Q S D V W S F G V L L W E I F

CTTTAGGTGCCTCCCCATACCCTGGAGTCCAAATCAATGAAGAATTTTGC 3550
P L G A S P Y P G V Q I N E E F C

CAGAGACTGAAAGATGGTACCAGGATGAGAGCCCCAGAATATGCAACTGC 3600
Q R L K D G T R M R A P E Y A T A

AGAAATTTACCGTATAATGCTAAGCTGCTGGCACGGTGATCCTAAGGAGA 3650
E I Y R I M L S C W H G D P K E

GACCAACATTCTCTGATTTGGTGGAGATTCTGGGGTACCTTCTTCAGGAG 3700
R P T F S D L V E I L G Y L L Q E

AATGTCCAGCATGAGGGGAAACACTATATCCCCCTGAATGACTCTCAGAG 3750
N V Q H E G K H Y I P L N D S Q S

CTCTGAAGATGATGGCTTCTCCCAGGTGGCTTCATCCATCCAGCAGAACT 3800
S E D D G F S Q V A S S I Q Q N

CTGATGAAGAGGAATTTGATATGAGAATGCACTGTCACAATATAGCAGCA 3850
S D E E E F D M R M H C H N I A A

AGATACTATAACTGTGTGTCCTTCCCTGGCTGTTTGACTGGTGGGAATCA 3900
R Y Y N C V S F P G C L T G G N Q

GATAAGGTGTCCATCTAGAATAAAGACTTTTGAAGAATTTCCTATGACAC 3950
I R C P S R I K T F E E F P M T

AAACCATGTATAAAGCACATCCGGACAATCAGACAGACAGTGGGATGGTC 4000
Q T M Y K A H P D N Q T D S G M V

TTGGCGTCTGAAGAGTTTGAGAGAATAGAAAATAGACACAGAAAAGAAGG 4050
L A S E E F E R I E N R H R K E G

TGCATTCAGCAGTAAAGGATCCAATCAAAATGCAGAATCAACCATGGAAC 4100
A F S S K G S N Q N A E S T M E

AGTCAGACCTGAGGGGTCGGGGTCGGCCACCGTATCAGTCCCAGCTCAGA 4150
Q S D L R G R G R P P Y Q S Q L R

GGTCAGACTTTTTATAACAGTGAATATGGGGAACTGTCAGAACAATCTGA 4200
G Q T F Y N S E Y G E L S E Q S E

AGAAGTCAGCTGCTCTCCACCCACTGAGGGAGCCAGTCCCTCTCTCCTTC 4250
E V S C S P P T E G A S P S L L

ATGCTTCATTCTTTTCAGACCAATACTAA**AGACGAACTGATTGAGAAGAC** 4300
H A S F F S D Q Y *

ACCAGGCAGAGATACCATCTTTCACCACTTCTGAGGCCTTGTTTTTGTTC 4350

TATTGAGTCACATCCCATTATCTTAGAAGAAGACCCAATGGGGGAGCCTG 4400
AGGAACAGACGGCAATGCTCCTTGGATATGAAAATGGATGCCAAGCATTT 4450
CAGCAGGGGACCCGGTTCTTGCATTTGGCACAAATACACTCTTGATAGTG 4500
CTAAAAAAAAAAAAAAA 4517

4.3.2. ANALYSIS OF gVEGF-C, gVEGF-D AND gVEGFR-3 AMINO ACID SEQUENCES

The VEGF-C, VEGF-D and VEGFR-3 amino acid sequences of different species including *Homo sapiens*, *Mus musculus*, *Rattus norvegicus*, *Gallus gallus*, *Xenopus laevis, Danio rerio* and *Christinus marmoratus* were aligned using the ClustalW multiple alignment method in the BioEdit (Hall 1999) software package (Figs 4.5A, 4.6A and 4.7A). Analysis of the predicted gecko proteins (by analogy to the other vertebrate sequences) illustrates gVEGF-C is a 424a.a.-long polypeptide comprising an initial signal sequence (a.a. 1-33), a VHD (a.a. 117-231) and N- and C-terminal domains (a.a. 34-116 and a.a. 232-424, respectively). Similarly, gVEGF-D is a 351a.a.-long polypeptide, also containing an initial signal sequence (a.a. 1-21), with a VHD (a.a. 87-203), N-terminal (a.a.22-86) and C-terminal (a.a. 204-351). For both proteins, within the VHD region, the eight cysteine residues (gVEGF-C: Cys135, 160, 166, 169, 170, 177, 213 and 215; gVEGF-D: Cys109, 134, 140, 143, 144, 151, 187 and 189) common to all VEGF family members are present in the gecko sequence. Six of these eight cysteines make up the cysteine knot motif (gVEGF-C: Cys135, 166, 170, 177, 213 and 215; gVEGF-D: Cys109, 140, 144, 151, 187 and 189), which is crucial for the structural integrity of VEGF (Muller et al. 2002). The free cysteine common to only VEGF-C and VEGF-D (gVEGF-C: Cys141; gVEGF-D: Cys115) is also present in geckos (Figs. 4.5A and 4.6A). The repetitive cysteine pattern homologous to a motif found in the silk-like secretory Balbiani ring 3 protein (BR3P) is also present within the C-terminal of the gecko growth factors.

Figure 4.5. *(A)* VEGF-C amino acid sequence of the Australian marbled gecko (*Christinus marmoratus*) aligned with other vertebrate species using the CLUSTALW multiple sequence alignment method (BioEdit). Residues are shaded with a residue-specific colour only if they are identical or similar to the consensus. Non-conservative substitutions are unshaded. Protein sequences were obtained from previously reported sequences in Genbank. The positions of the putative signal sequence (line above the hVEGF-C), N-terminal propeptide, VEGF homology domain (VHD) and C-terminal are labelled. Arrows denote positions of cleavage in proteolytic processing to generate the mature protein. In the VHD, the eight cysteine residues conserved in VEGF/PDGF family members are boxed, the cysteine residue conserved only in VEGF-C and VEGF-D is marked by an arrowhead, and the hash marks (#) show the position of the residues involved in the cysteine knot motif. Solid circles above the alignment denote conserved cysteine residues resembling the Balbiani ring 3 protein motif ($CX_{10}CXCXC$). Residues crucial for receptor binding are denoted by a bold B above the alignment; a red B signals importance in both VEGFR-2 and VEGFR-3 binding (Phe 151 and Cys 156 in the human sequence), blue denotes importance in binding VEGFR-3 only (Pro198 in human) and black denotes VEGFR-2 binding (Pro 155 in human). *(B)* Phylogenetic analysis of VEGF-C a.a. sequences. Neighbour-joining trees were constructed with the Mega 4.1 program (Tamura et al. 2007). The numbers on the branches represent confidence levels of 1200 bootstrap replications. The tree is drawn to scale, with branch lengths in the same units as those of the evolutionary distances used to infer the phylogenetic tree. The evolutionary distances were computed using the Poisson correction method (Zuckerlandl and Pauling 1965) and are in the units of the number of amino acid substitutions per site (shown on the scale bar). Abbreviations are as follows; g = gecko (horizontal arrow), c = chicken, h = human, m = mouse, r = rat, z = zebrafish, f = frog. Genbank accession numbers are as follows: cVEGF-C isoform 1: XM_001232468.1, cVEGF-C isoform 2: XM_420532.2, hVEGF-C: NM_005429.2, mVEGF-C: NM_009506.2, rVEGF-C: NM_053653.1, fVEGF-C: NM_001095814.1, zVEGF-C: NM_205734.1

A

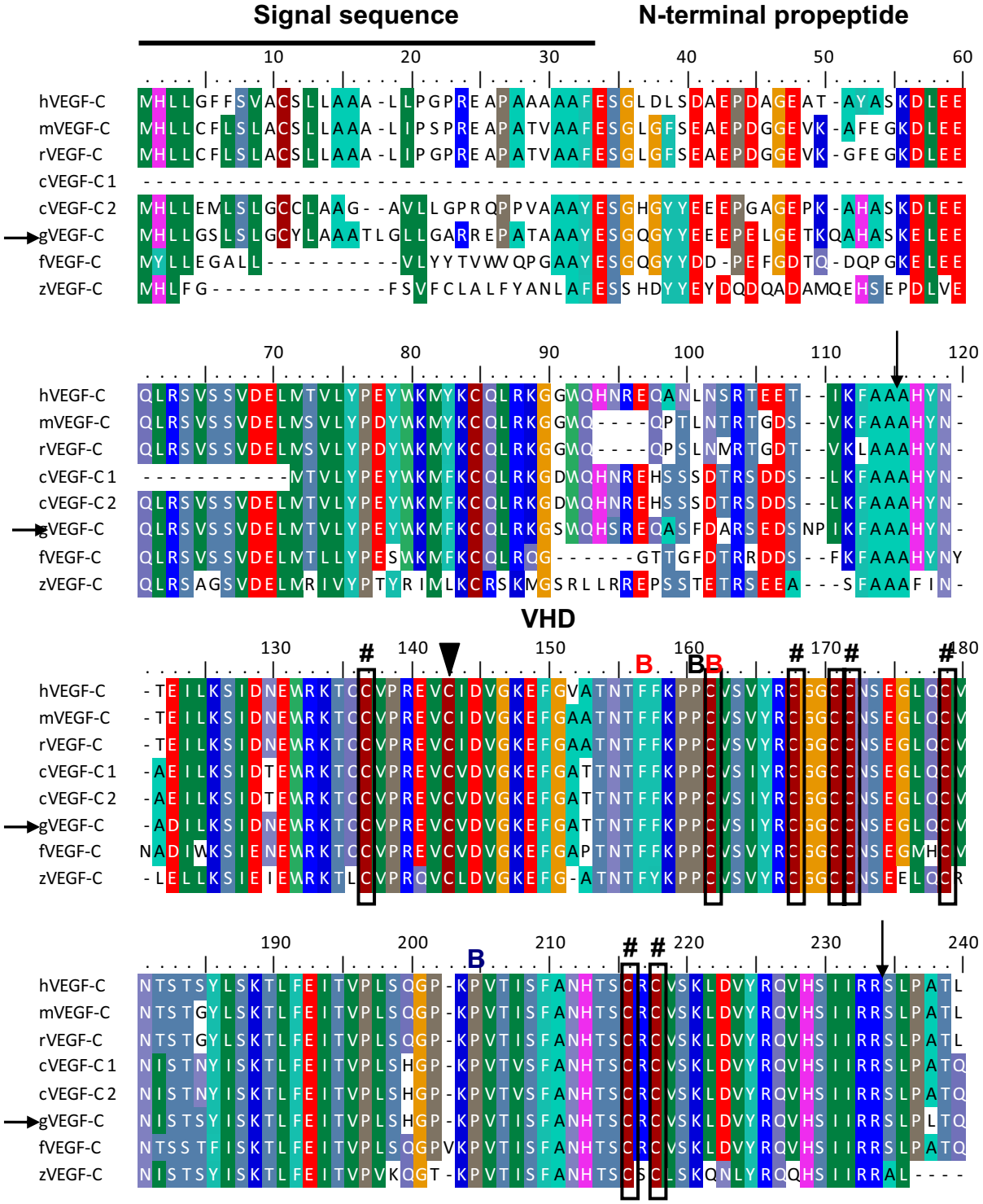
Signal sequence
N-terminal propeptide
VHD
hVEGF-C
mVEGF-C
rVEGF-C
cVEGF-C 1
cVEGF-C 2
gVEGF-C
fVEGF-C
zVEGF-C

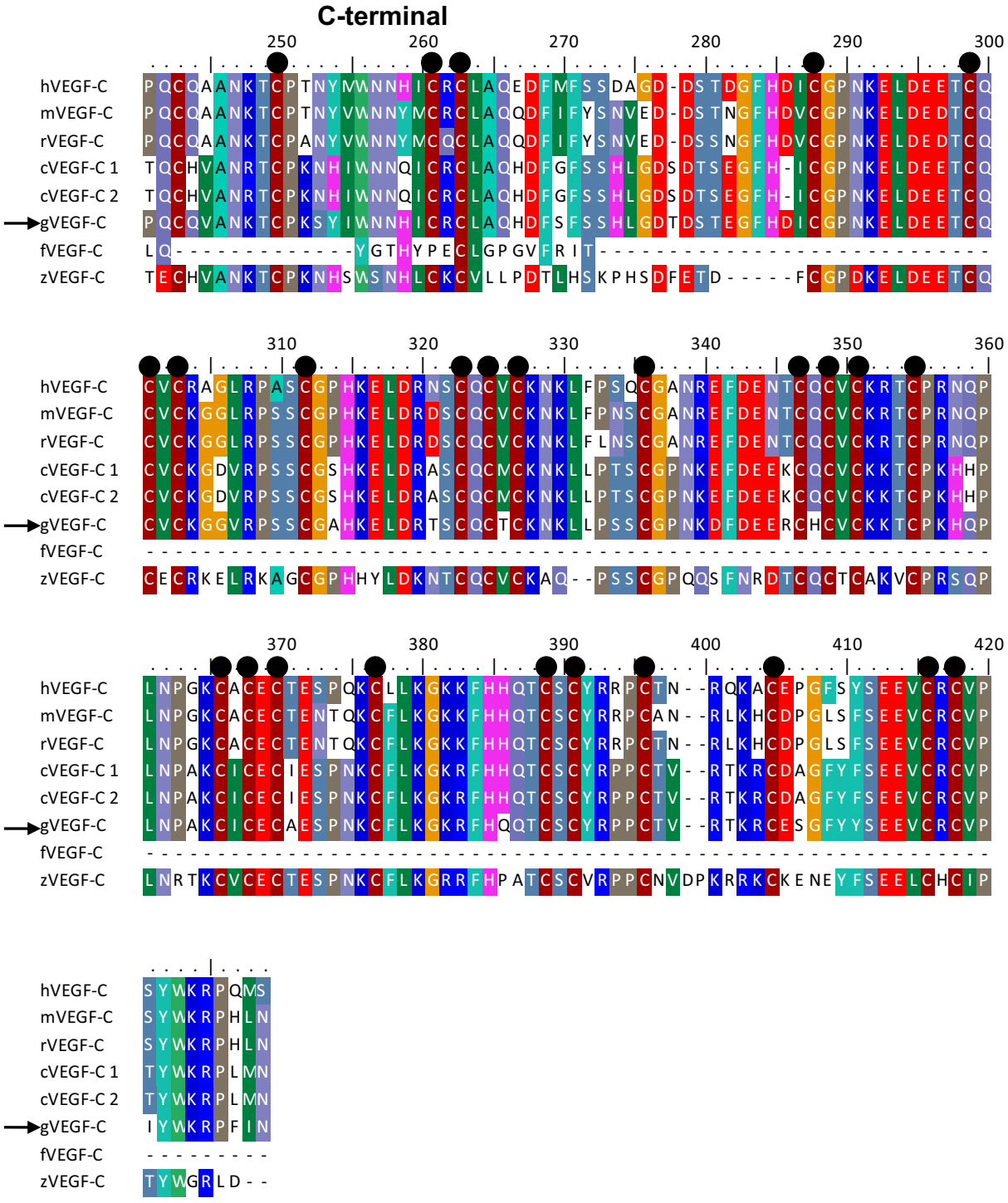
C-terminal
250
260
270
280
290
300
hVEGF-C
mVEGF-C
rVEGF-C
cVEGF-C 1
cVEGF-C 2
gVEGF-C
fVEGF-C
zVEGF-C
310
320
330
340
350
360
370
380
390
400
410
420

B

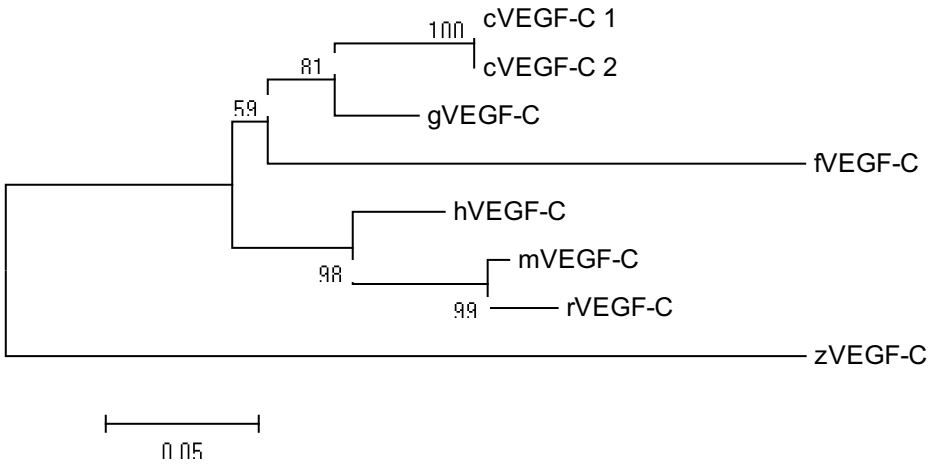
100
cVEGF-C 1
81
cVEGF-C 2
59
gVEGF-C
fVEGF-C
hVEGF-C
98
mVEGF-C
99
rVEGF-C
zVEGF-C
0.05

Figure 4.6. (A) VEGF-D amino acid sequence of the Australian marbled gecko (*Christinus marmoratus*) aligned with other vertebrate species using the CLUSTALW multiple sequence alignment method (BioEdit). Residues are shaded with a residue-specific colour only if they are identical or similar to the consensus. Non-conservative substitutions are unshaded. Protein sequences were obtained from previously reported sequences in Genbank. The positions of the putative signal sequence (line above the hVEGF-D), N-terminal propeptide, VEGF homology domain (VHD) and C-terminal are labelled. Large arrows denote major positions of cleavage in proteolytic processing to generate the mature protein and a smaller arrow denotes a minor (i.e. less frequently used) cleavage position. In the VHD, the eight cysteine residues conserved in VEGF/PDGF family members are boxed, the cysteine residue conserved only in VEGF-C and VEGF-D is marked by an arrowhead, and the hash marks (#) show the position of the residues involved in the cysteine knot motif. Solid circles above the alignment denote conserved cysteine residues resembling the Balbiani ring 3 protein motif ($CX_{10}CXCXC$). Residues crucial for receptor binding are denoted by an asterix. *(B)* Phylogenetic analysis of VEGF-D a.a. sequences. Neighbour-joining trees were constructed with the Mega 4.1 program (Tamura et al. 2007). The numbers on the branches represent confidence levels of 1200 bootstrap replications. The tree is drawn to scale, with branch lengths in the same units as those of the evolutionary distances used to infer the phylogenetic tree. The evolutionary distances were computed using the Poisson correction method (Zuckerlandl and Pauling 1965) and are in the units of the number of amino acid substitutions per site (shown on the scale bar). Abbreviations are as follows; g = gecko (horizontal arrow), c = chicken, h = human, m = mouse, r = rat, z = zebrafish, f = frog. Genbank accession numbers are as follows*:* cVEGF-D: NM_204568.1, hVEGF-D: NM_004469.2, mVEGF-D: NM_010216.1, rVEGF-D: NM_031761.1, fVEGF-D: NM_001127797.1, zVEGF-D: NM_001040178.1.

A

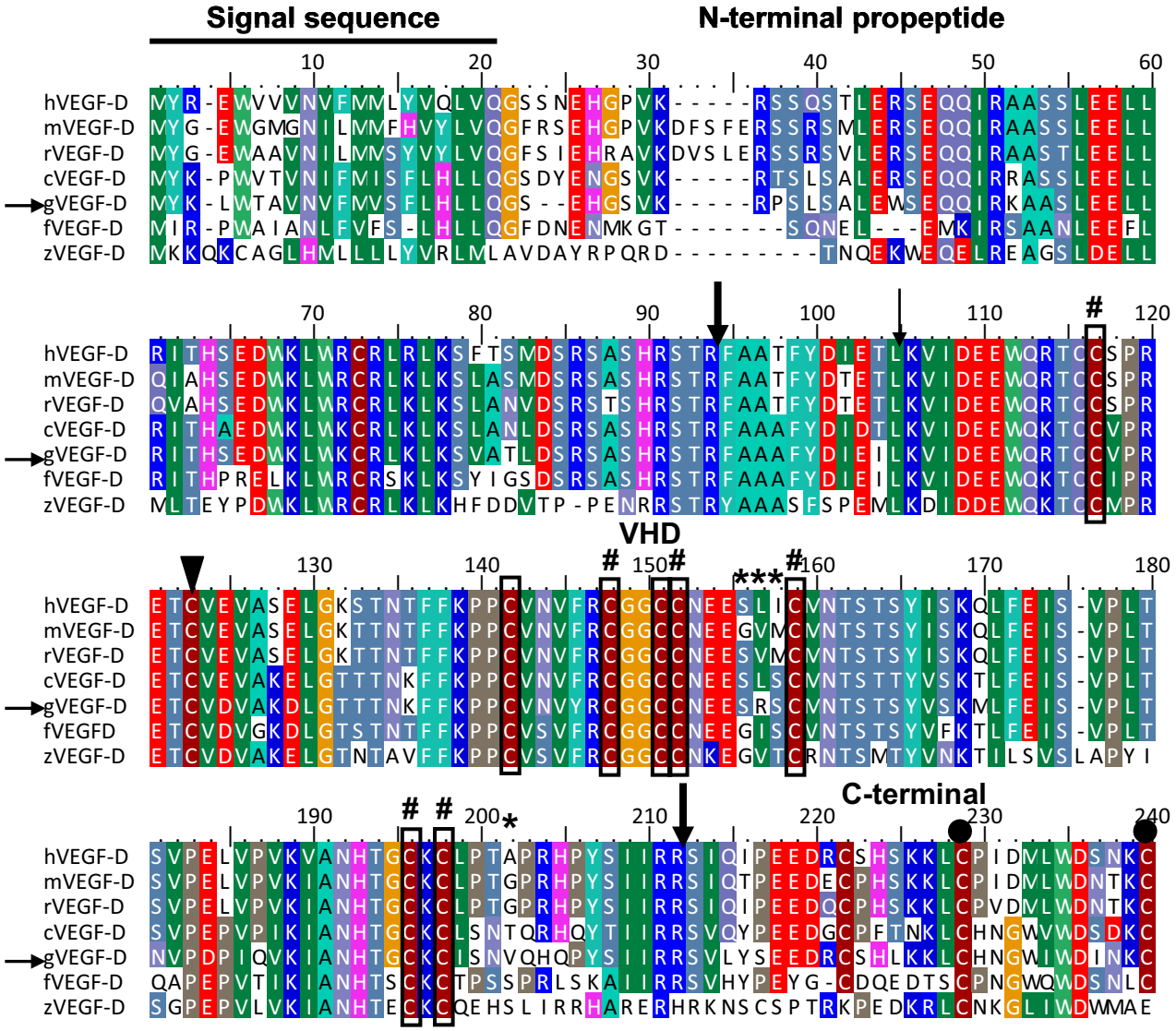
Signal sequence
N-terminal propeptide
VHD
C-terminal
hVEGF-D
mVEGF-D
rVEGF-D
cVEGF-D
gVEGF-D
fVEGF-D
zVEGF-D

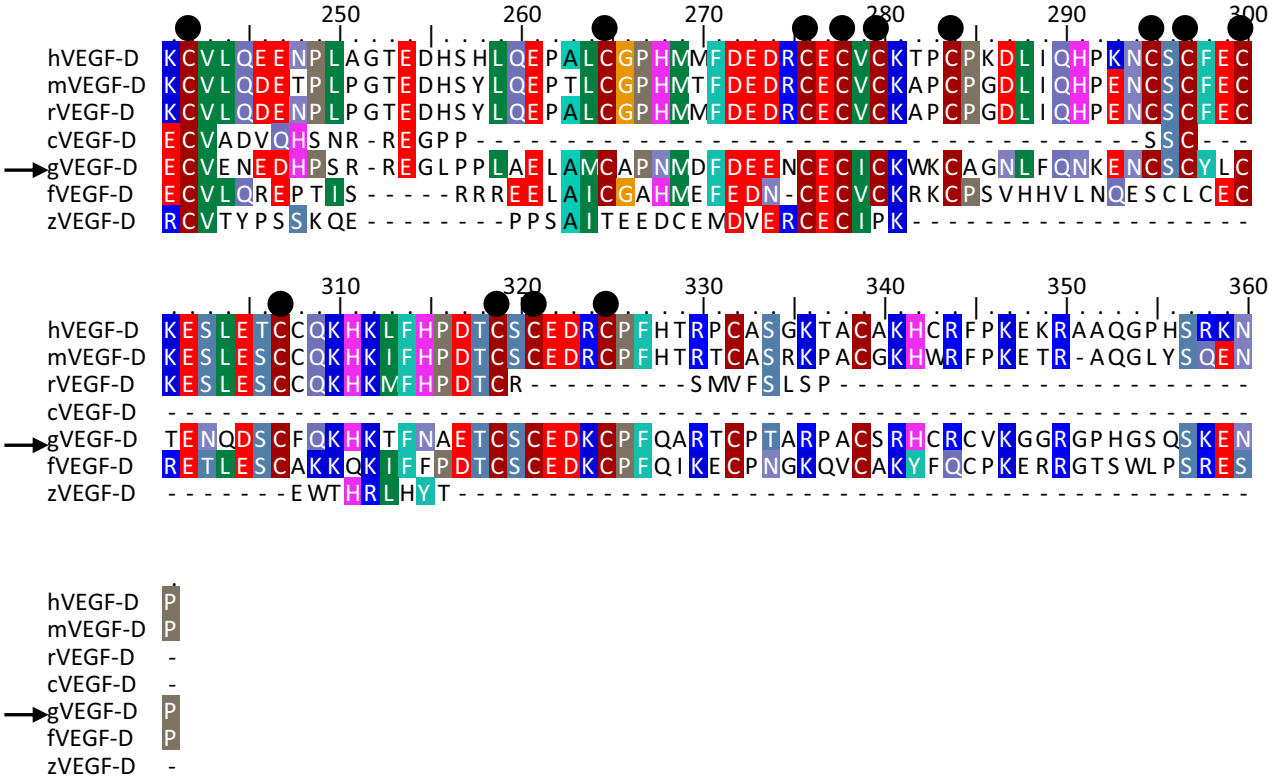
250
260
270
280
290
300
hVEGF-D KCVLQEENPLAGTEDHSHLQEPALCGPHMMFDEDRCECVCKTPCPKDLIQHPKNCSCFEC
mVEGF-D KCVLQDETPLPGTEDHSYLQEPTLCGPHMTFDEDRCECVCKAPCPGDLIQHPENCSCFEC
rVEGF-D KCVLQDENPLPGTEDHSYLQEPALCGPHMMFDEDRCECVCKAPCPGDLIQHPENCSCFEC
cVEGF-D ECVADVQHSNR-REGPP----------SSC---
gVEGF-D ECVENEDHPSR-REGLPPLAELAMCAPNMDFDEENCECICKWKCAGNLFQNKENCSCYLC
fVEGF-D ECVLQREPTIS-----RRREELAICGAHMEFEDN-CECVCKRKCPSVHHVLNQESCLCEC
zVEGF-D RCVTYPSSKQE--------PPSAITEEDCEMDVERCECIPK----------
310
320
330
340
350
360
hVEGF-D KESLETCCQKHKLFHPDTCSCEDRCPFHTRPCASGKTACAKHCRFPKEKRAAQGPHSRKN
mVEGF-D KESLESCCQKHKIFHPDTCSCEDRCPFHTRTCASRKPACGKHWRFPKETR-AQGLYSQEN
rVEGF-D KESLESCCQKHKMFHPDTCR---------SMVFSLSP----------
cVEGF-D ----------
gVEGF-D TENQDSCFQKHKTFNAETCSCEDKCPFQARTCPTARPACSRHCRCVKGGRGPHGSQSKEN
fVEGF-D RETLESCAKKQKIFFPDTCSCEDKCPFQIKECPNGKQVCAKYFQCPKERRGTSWLPSRES
zVEGF-D -------EWTHRLHYT----------
hVEGF-D P
mVEGF-D P
rVEGF-D -
cVEGF-D -
gVEGF-D P
fVEGF-D P
zVEGF-D -

B

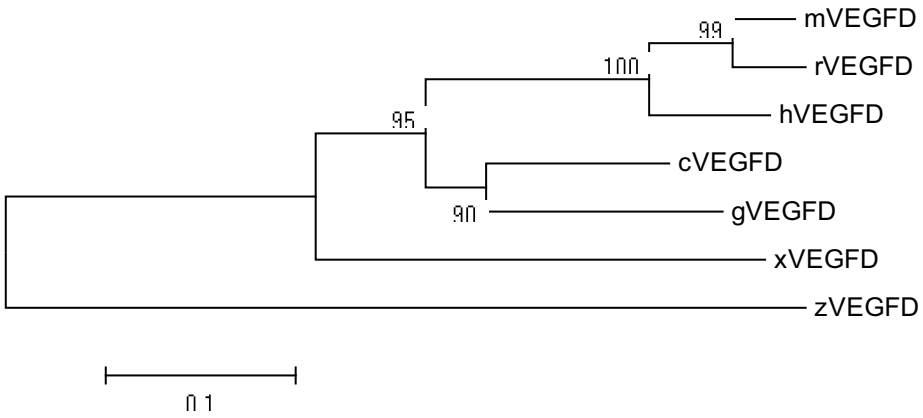
99
100
95
90
mVEGFD
rVEGFD
hVEGFD
cVEGFD
gVEGFD
xVEGFD
zVEGFD
0.1

Figure 4.7. (A) VEGFR-3 amino acid sequence of the Australian marbled gecko (*Christinus marmoratus*) aligned with other vertebrate species using the CLUSTALW multiple sequence alignment method (BioEdit). Residues are shaded with a residue-specific colour only if they are identical or similar to the consensus. Non-conservative substitutions are unshaded. Protein sequences were obtained from previously reported sequences in Genbank. The positions of the putative signal sequence, the seven immunoglobulin like domains (Ig-like 1-7), transmembrane region and protein kinase domain are labelled. The ATP binding site is boxed in black. Tyrosine residues suggested to be important in receptor phosphorylation are boxed in red. Receptor domains important for ligand binding are highlighted as Ig-like 1 and Ig-like 2. (*B*) Phylogenetic analysis of VEGFR-3 a.a. sequences. Neighbour-joining trees were constructed with the Mega 4.1 program (Tamura et al. 2007). The numbers on the branches represent confidence levels of 1200 bootstrap replications. The tree is drawn to scale, with branch lengths in the same units as those of the evolutionary distances used to infer the phylogenetic tree. The evolutionary distances were computed using the Poisson correction method (Zuckerlandl and Pauling 1965) and are in the units of the number of amino acid substitutions per site (shown on the scale bar). Abbreviations are as follows; g = gecko (horizontal arrow), c = chicken, h = human, m = mouse, r = rat, z = zebrafish, f = frog. Genbank accession numbers are as follows*:* cVEGFR-3: XM_414600.2, hVEGFR-3 isoform 1: NM_182925.4, hVEGFR-3 isoform 2: NM_002020.4, mVEGFR-3: NM_008029.3, rVEGFR-3: NM_0536521, fVEGFR-3: ENSXETT00000008399 (listed in Ensembl not Genbank), zVEGFR-3: NM_130945.1

A

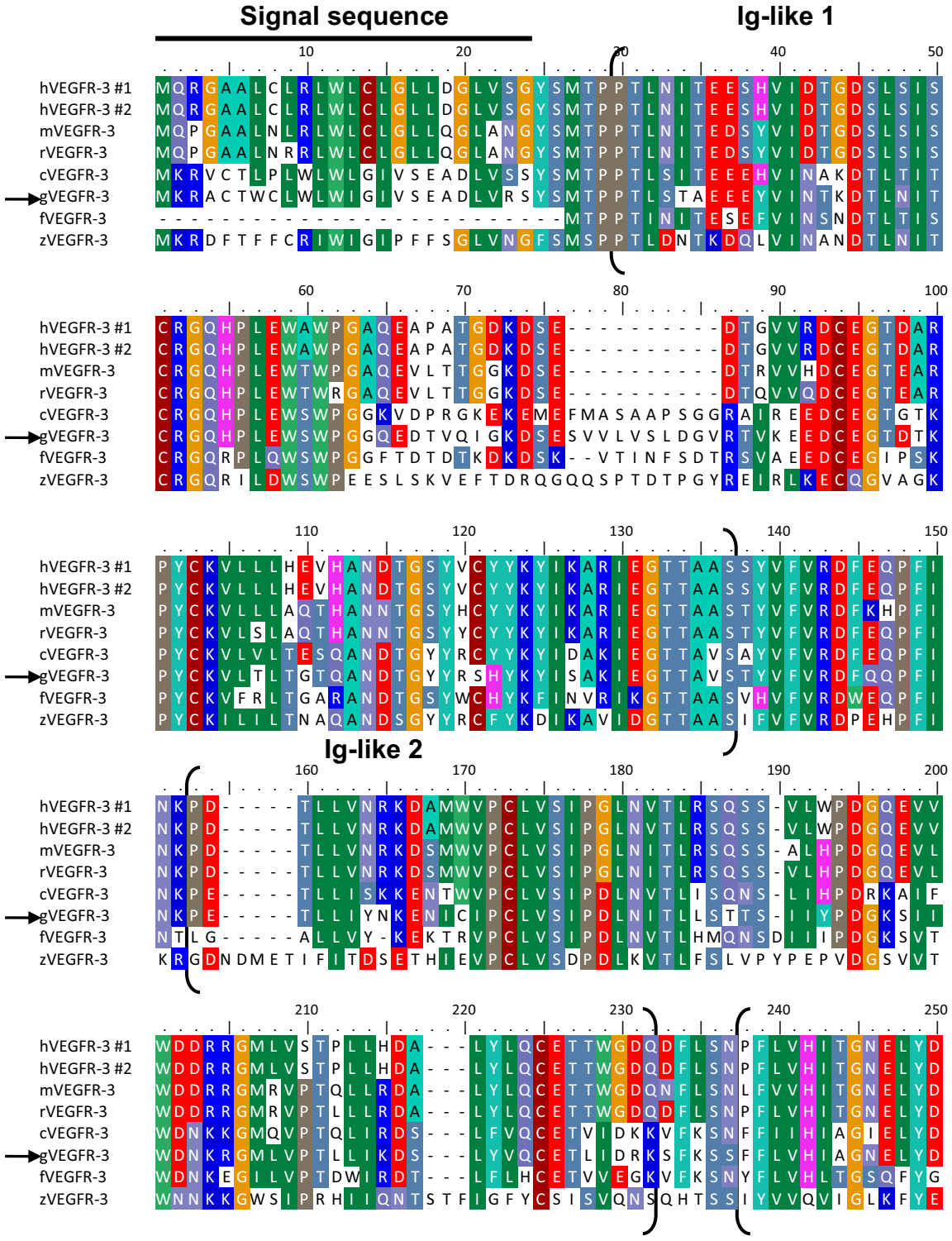
Signal sequence
Ig-like 1
Ig-like 2
hVEGFR-3 #1
hVEGFR-3 #2
mVEGFR-3
rVEGFR-3
cVEGFR-3
gVEGFR-3
fVEGFR-3
zVEGFR-3

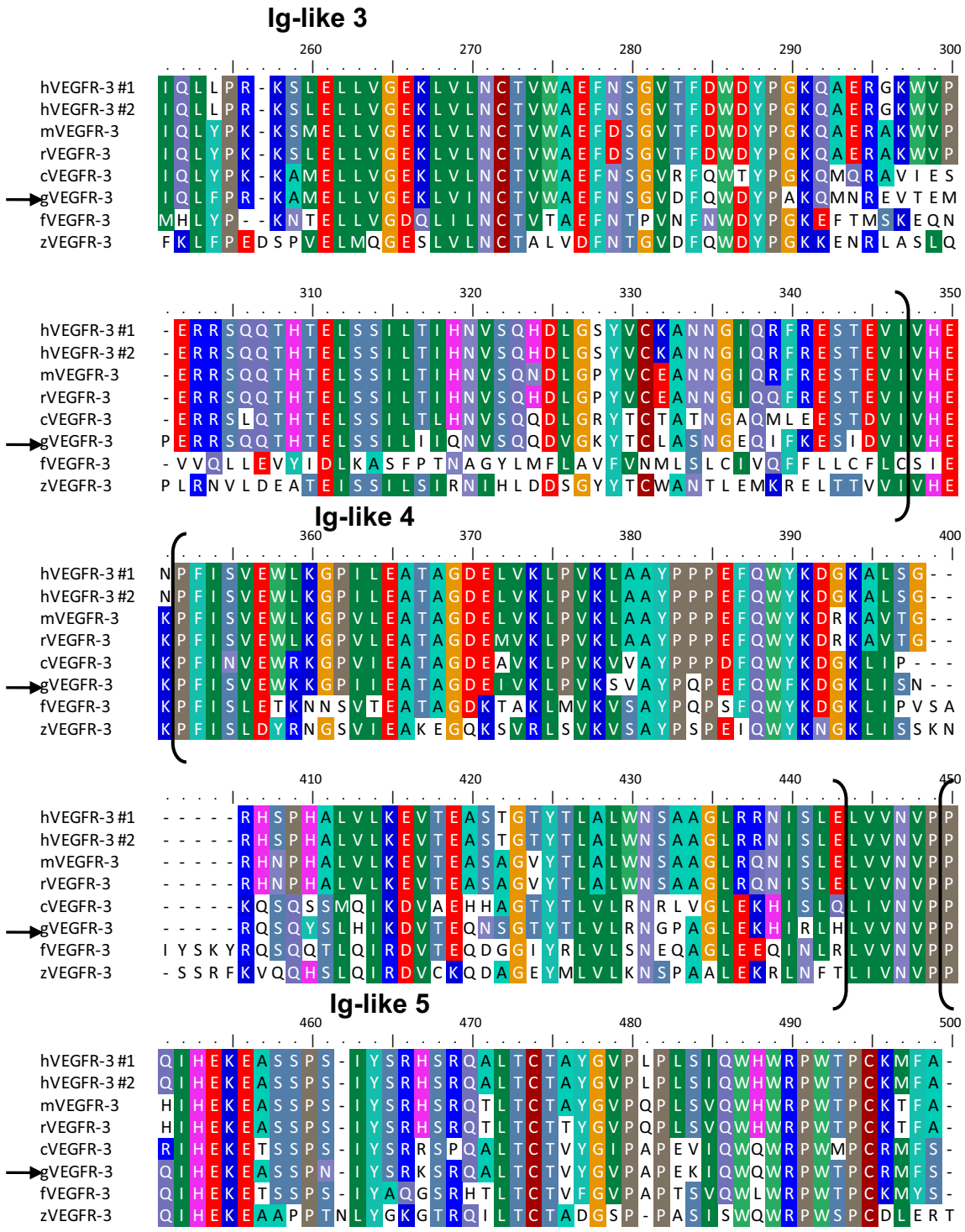
Ig-like 3
Ig-like 4
Ig-like 5
hVEGFR-3 #1
hVEGFR-3 #2
mVEGFR-3
rVEGFR-3
cVEGFR-3
gVEGFR-3
fVEGFR-3
zVEGFR-3

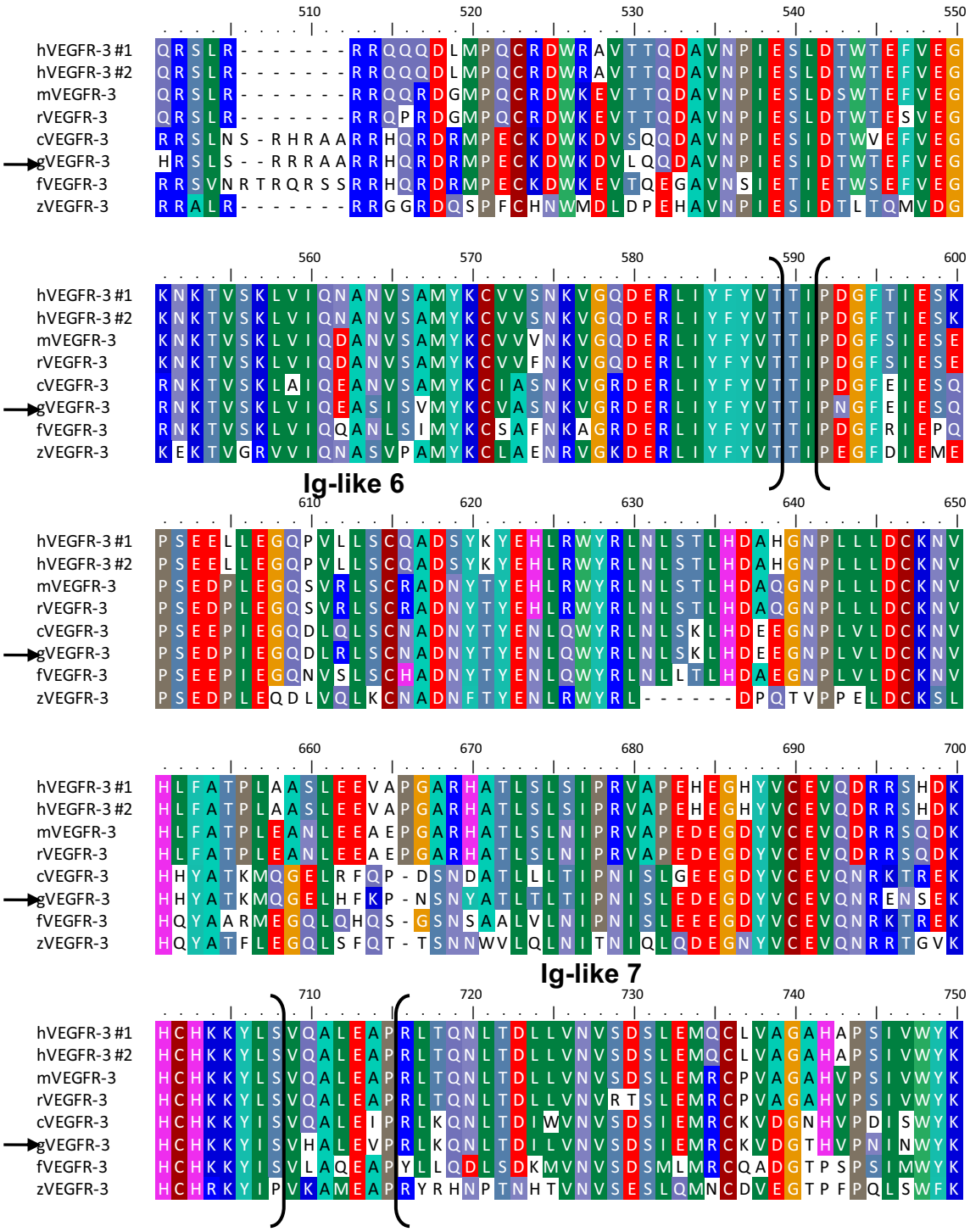
510
520
530
540
550
hVEGFR-3 #1
hVEGFR-3 #2
mVEGFR-3
rVEGFR-3
cVEGFR-3
gVEGFR-3
fVEGFR-3
zVEGFR-3
560
570
580
590
600
Ig-like 6
610
620
630
640
650
660
670
680
690
700
Ig-like 7
710
720
730
740
750

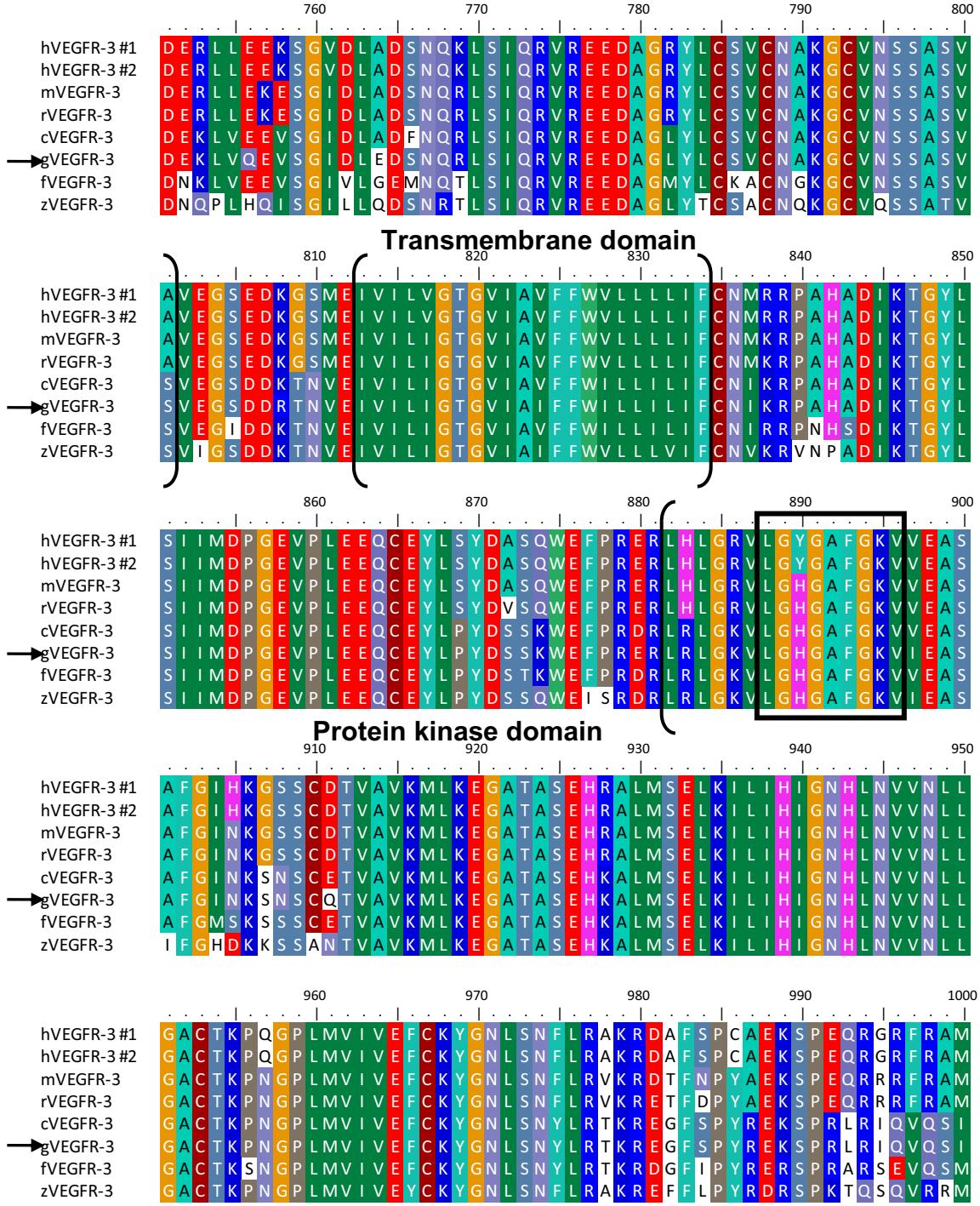
760
770
780
790
800
hVEGFR-3 #1
hVEGFR-3 #2
mVEGFR-3
rVEGFR-3
cVEGFR-3
gVEGFR-3
fVEGFR-3
zVEGFR-3
Transmembrane domain
810
820
830
840
850
860
870
880
890
900
Protein kinase domain
910
920
930
940
950
960
970
980
990
1000

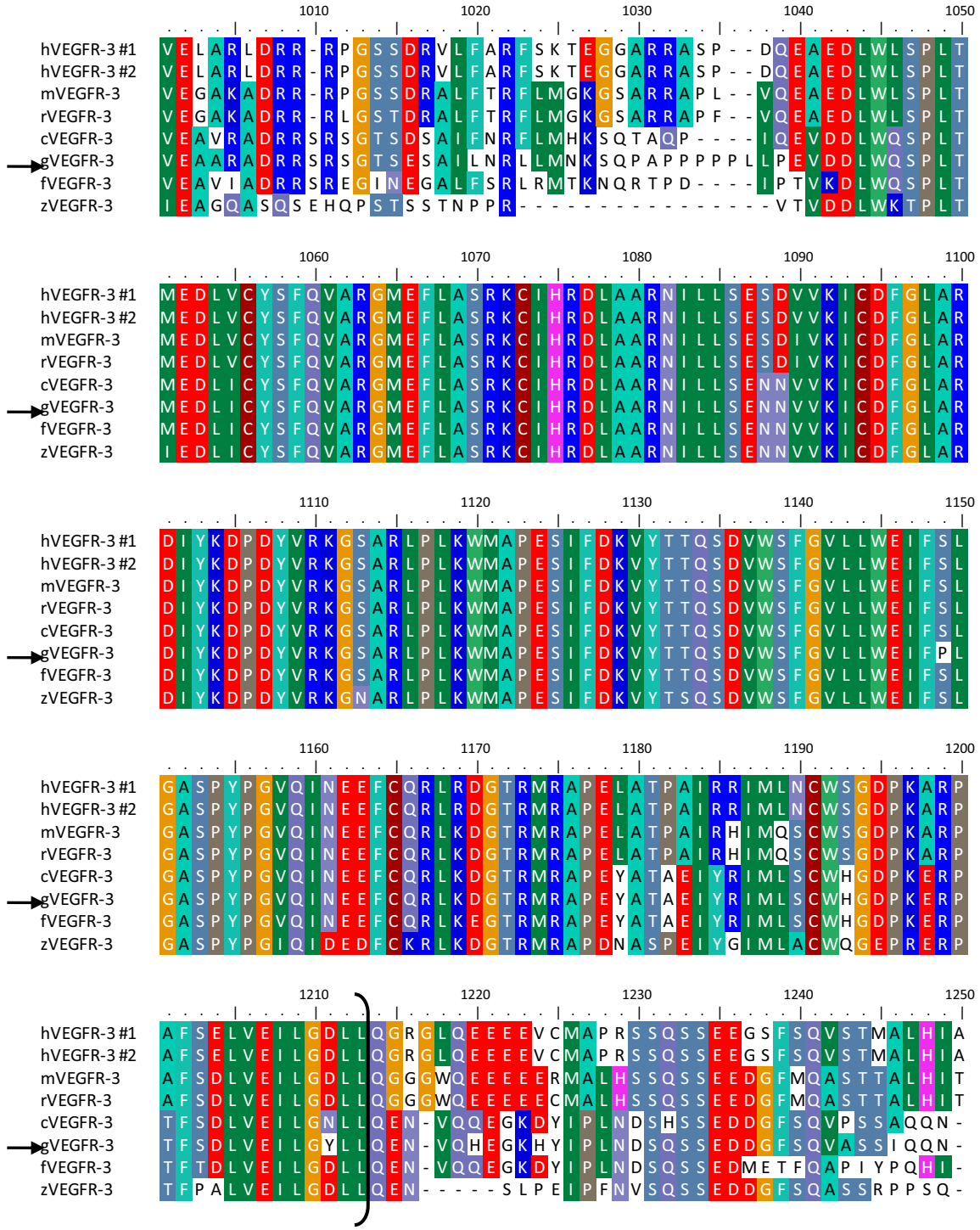
1010
1020
1030
1040
1050
hVEGFR-3 #1
hVEGFR-3 #2
mVEGFR-3
rVEGFR-3
cVEGFR-3
gVEGFR-3
fVEGFR-3
zVEGFR-3
1060
1070
1080
1090
1100
1110
1120
1130
1140
1150
1160
1170
1180
1190
1200
1210
1220
1230
1240
1250

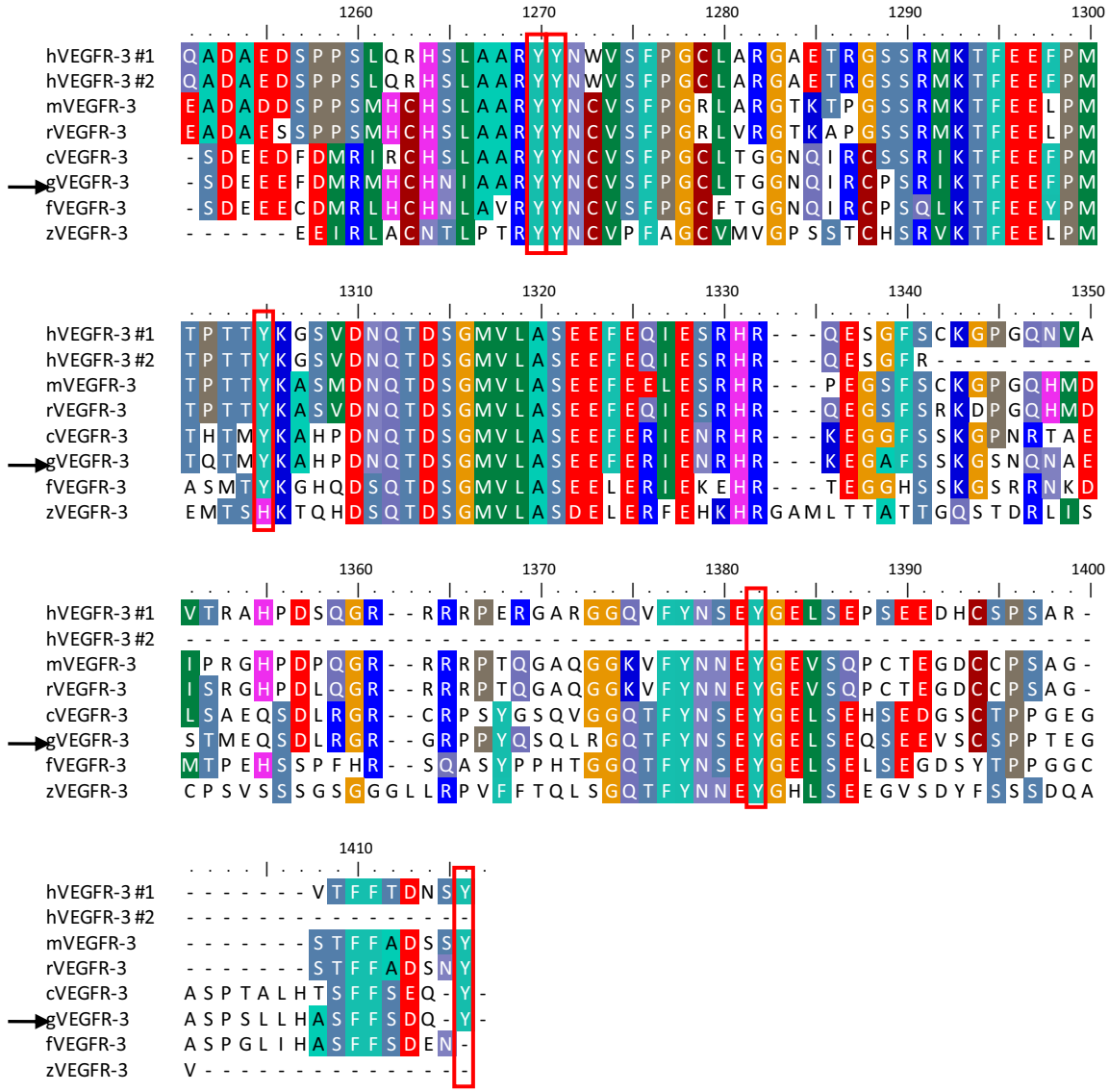
1260
1270
1280
1290
1300
hVEGFR-3 #1
hVEGFR-3 #2
mVEGFR-3
rVEGFR-3
cVEGFR-3
gVEGFR-3
fVEGFR-3
zVEGFR-3
1310
1320
1330
1340
1350
1360
1370
1380
1390
1400
1410

B

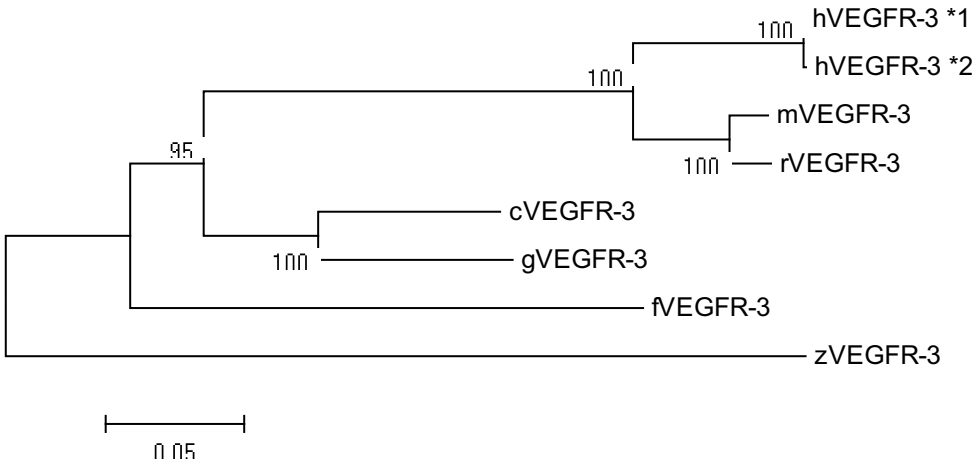
100
hVEGFR-3 *1
hVEGFR-3 *2
100
mVEGFR-3
95
100
rVEGFR-3
cVEGFR-3
100
gVEGFR-3
fVEGFR-3
zVEGFR-3
0.05

In terms of proteolytic processing, all specific residues of proteolytic cleavage sites previously identified in humans and mice (Joukov et al. 1997b; Stacker et al. 1999) are conserved within the gVEGF-C and gVEGF-D sequences (gVEGF-C: C-terminal cleavage Arg231-Ser232, N-terminal cleavage Ala115-Ala116; gVEGF-D: C-terminal cleavage Arg203-Ser204, N-terminal major cleavage Arg86-Phe87, minor cleavage Leu97-Lys98). Similarly, residues in the gVEGF-C sequence demonstrated to be important in receptor binding (gVEGF-C: Phe155, Cys160, Pro159 and Pro202) are conserved (see Fig. 4.5A). Receptor binding sites in gVEGF-D (Ser148, Arg149, Ser150 and Val193) are not identical to those suggested in humans (Ser150, Leu151, Ile152 and Ala195). Of these four residues implicated in receptor binding, only two are conserved. Differences between Arg-Leu and Ser-Ile are non-conservative, while Val-Ala is considered conservative. This region is quite variable between all vertebrate species in the alignment (Fig. 4.6A).

gVEGFR-3 is a 1385 a.a. long polypeptide, with corresponding regions to the seven Ig-like domains (Ig-like 1: a.a. 30-137; Ig-like 2: a.a. 161-223; Ig-like 3: a.a. 229-337; Ig-like 4: a.a. 342-426; Ig-like 5: 433-568; Ig-like 6: 571-686; Ig-like 7: 693-779), the transmembrane domain (a.a. 801-822) and protein kinase domain (a.a. 860-1191) known in other vertebrate sequences all present (Fig. 4.7A). Similarly, the gVEGFR-3 protein sequence appears to contain all tyrosine residues implicated in receptor phosphorylation (Tyr1352, Tyr1081 and Tyr1086 in gVEGFR-3) (Dixelius et al. 2003b), along with high sequence conservation within domains (Ig-like 1 and Ig-like 2) implicated as being crucial for ligand binding (Jeltsch et al. 2006).

The deduced amino acid sequences of the gecko proteins were further analysed by the ProtParam tool in EXPASY (http://cn.expasy.org/) and the predicted molecular weights of gVEGF-C, gVEGF-D and gVEGFR-3 were 47.8 kDa, 40 kDa and 157.6 kDa respectively.

The theoretical pI of each protein was calculated as 8.22 for gVEGF-C, 7.87 for gVEGF-D and 5.76 for gVEGFR-3.

4.3.3. SEQUENCE COMPARISON OF gVEGF-C, gVEGF-D AND gVEGFR-3 WITH OTHER KNOWN VERTEBRATE SEQUENCES

Identity and similarity scores derived from the ClustalW multiple alignments between the gecko VEGF-C (Fig. 4.5A), VEGF-D (Fig. 4.6A) and VEGFR-3 (Fig. 4.7A) proteins and different vertebrate sequences are highlighted in Tables 4.3. and 4.4.

For both VEGF-C and VEGFR-3, at an amino acid level, the chicken sequences had the highest identity score with the gecko sequence (85%). Two isoforms of VEGF-C have been identified in chickens, a longer form that is representative of other VEGF-C sequences and a truncated form missing the signal sequence and majority of the N-terminus. The un-truncated form of cVEGF-C shows the highest identity to the gecko sequence. Interestingly, for VEGF-D, the human (64%) and mouse (62%) sequences had higher identity scores with the gecko sequence than the chicken (57%). However, when conservative substitutions are included, as is the case in the similarity scoring, the chicken sequences are the most similar to all three gecko proteins (VEGF-C similarity 94/92 %, VEGF-D 88% similar and VEGFR-3 91% similar).

NJ trees of the amino acid sequences of VEGF-C, VEGF-D and VEGFR-3 vertebrate sequences, including the gecko, were constructed based on the similarity of their amino acid sequences. Bootstrap analysis was performed to determine the reliability of the constructed trees. Phylogenetic analysis of the amino acid sequences of the gecko and other species confirms the alignment data. Among the species selected for analysis, the chicken sequences show the closest relationship to the gecko sequences for all three proteins with high bootstrap confidence for all (81%, 90% and 100% confidence for VEGF-C, VEGF-D and VEGFR-3

respectively) (Figs. 4.5B, 4.6B and 4.7B). All three NJ trees generated from a.a. sequence data show distinct clusters of mammals separated from non-mammals.

Table 4.3. Percent of sequence identity (% of identical residues between all ungapped positions between the pairs) between deduced amino acid sequences of the gecko and chicken, human, mouse, rat, frog and zebrafish sequences.

	Chicken	Human	Mouse	Rat	Frog	Zebrafish
Gecko VEGF-C	(1) 73/ (2) 85	77	74	74	41	54
Gecko VEGF-D	56	64	62	56	54	32
Gecko VEGFR-3	85	(1) 68/ (2) 66	68	68	69	57

Note: Two identity scores are present for chicken VEGF-C and human VEGFR-3 sequences due to the presence of two isoforms.

Table 4.4. Percent of sequence similarity (% of both identical and similar amino acids among all ungapped positions between the pairs) between deduced amino acid sequences of the gecko and chicken, human, mouse, rat, frog and zebrafish sequences.

	Chicken	Human	Mouse	Rat	Frog	Zebrafish
Gecko VEGF-C	(1) 94/ (2) 92	86	85	84	81	70
Gecko VEGF-D	88	77	73	76	70	65
Gecko VEGFR-3	91	(1) 80/ (2) 82	81	81	85	73

Note: Two identity scores are present for chicken VEGF-C and human VEGFR-3 sequences due to the presence of two isoforms

4.3.4. MOLECULAR MODELLING OF gVEGF-C, gVEGF-D AND gVEGFR-3

The tertiary structure of the three gecko protein sequences was modelled using the Swiss-Model server workspace (Arnold et al. 2006). The quality, viability and accuracy of the models were assessed by Swiss-Model using Anolea, GROMOS and Verify 3D. The modelling template selected by the Swiss-model program to provide molecular models for both gVEGF-C and gVEGF-D was the crystal structure of hVEGF-C in complex with domains 2 and 3 of VEGFR-2. The specific template entry number for modelling of the VHD (mature protein) of gVEGF-C was PDB entry 2x1wC and for gVEGF-D was PDB entry 2x1wA. The gVEGF-C (Fig. 4.8) and gVEGF-D (Fig. 4.9) mature protein models both scored positively on all three parameters assessed and indicated a favourable energy environment for the majority of amino acids in the protein chain suggesting the amino acids can conform to the predicted model.

Figure 4.8. Molecular models of gecko VEGF-C (gVEGF-C). (A) A ribbon model of gVEGF-C generated by Swiss-Model (Arnold et al. 2006) and Chimera (Pettersen et al. 2004) showing positions of α-helices, β-sheets and loop regions. (B) Comparison of the gVEGF-C model (red) with the crystal structure template hVEGF-C (blue). Superimposition of the gecko model with template shows no variation in structure. (C) Front and back views of gVEGF-C modeled homodimers. The molecular surface of the individual monomers (one shown in red, and the other in yellow) making up the dimer is shown. Structural positions of divergent residues in the gecko sequence are shown in blue (i.e. residues that are not identical to other species in a VEGF-C alignment). Receptor binding sites are also highlighted. Residues involved in VEGFR-2 binding only, are in orange. Those crucial for VEGFR-3 binding only are shown in purple and residues important in both VEGFR-2 and VEGFR-3 binding are in green.

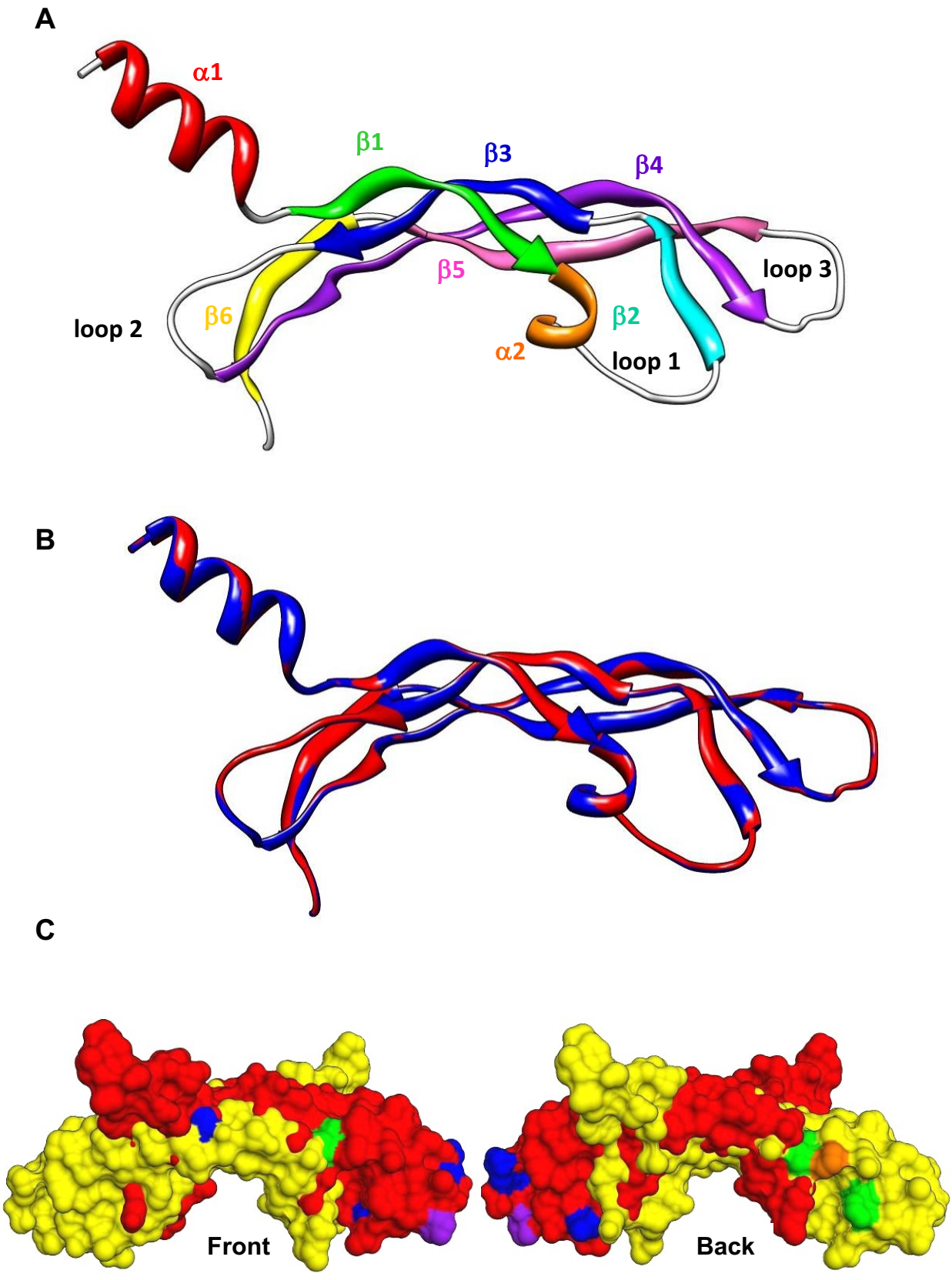
A
α1
β1
β3
β4
β5
loop 3
β6
loop 2
β2
α2
loop 1
B
C
Front
Back

Figure 4.9. Molecular models of gecko VEGF-D (gVEGF-D). (A) A ribbon model of gVEGF-D generated by Swiss-Model (Arnold et al. 2006) and Chimera (Pettersen et al. 2004) showing positions of α-helices, β-sheets and loop regions. (B) Comparison of the gVEGF-D model (red) with modelled hVEGF-D (blue) and cVEGF-D (white). Superimposition of the gecko model with human and chicken models shows slight variations in structure that overall do not appear to significantly alter the protein shape. (C) Front and back views of gVEGF-D modeled homodimers. The molecular surface of the individual monomers (one shown in red, and the other in yellow) making up the dimer is shown. Structural positions of divergent residues in the gecko sequence are shown in blue (i.e. residues that are not identical to other species in a VEGF-C alignment). Residues necessary for receptor binding (both VEGFR-2 and VEGFR-3) are shown in orange. A putative receptor binding interface (Baldwin et al. 2001) is also displayed (black line).

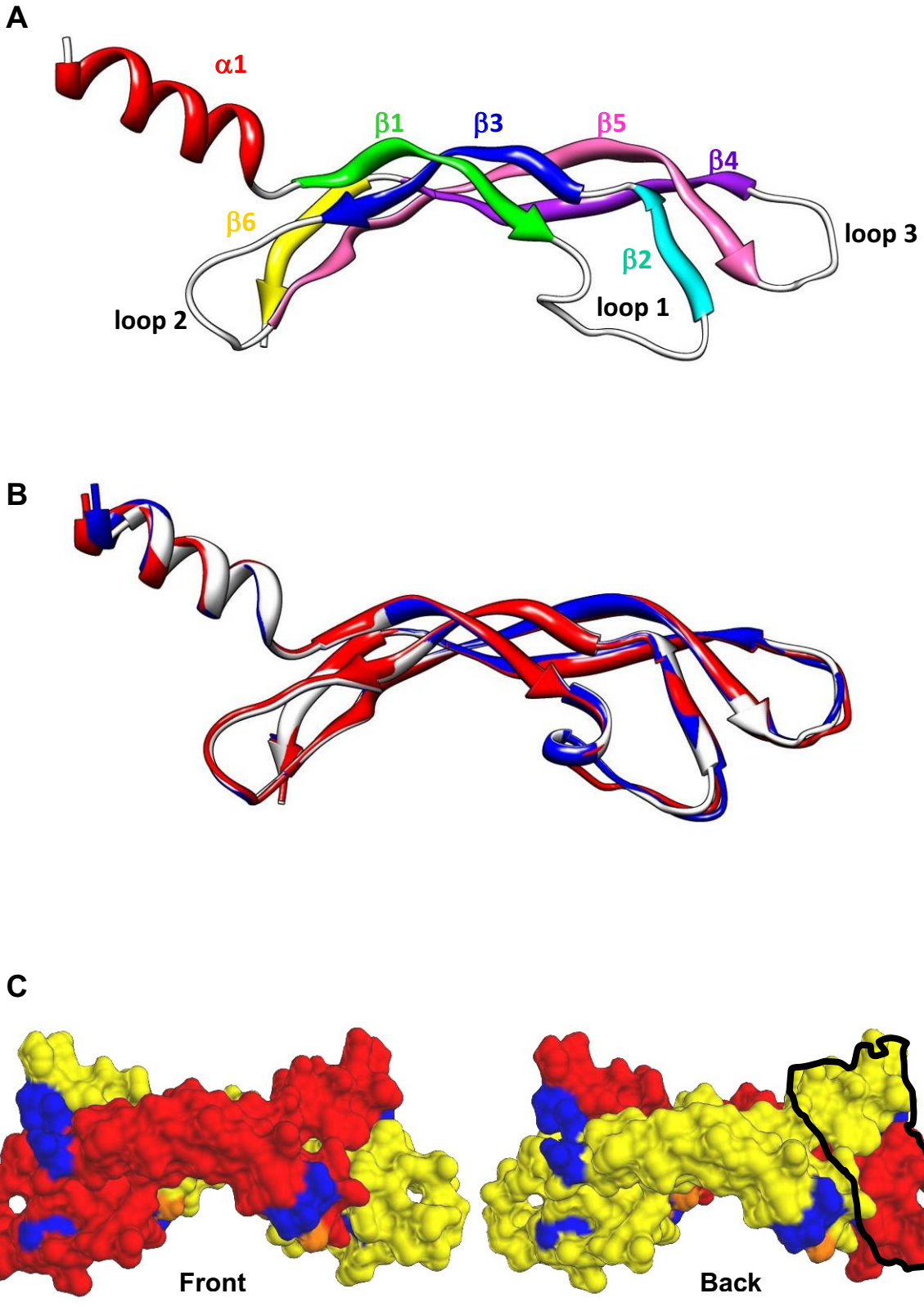
A
α1
β1
β3
β5
β4
β6
β2
loop 3
loop 1
loop 2
B
C
Front
Back

Figure 4.10. Molecular models of gecko VEGFR-3 (gVEGFR-3). Ribbon models of three (4.9. A-C) gVEGFR-3 models generated by Swiss-Model (Arnold et al. 2006) and Chimera (Pettersen et al. 2004). Model 1 (A left) and model 2 (B left) of gVEGFR-3 were both based on the modelling template of the crystal structure of the intracellular kinase region of VEGFR-2 with benzimidazole inhibitor (PDB entry 2oh4A) with model 1 mapping residues 1027-1198 of the gecko protein sequence and model 2 corresponding to residues 842-964. Model 3 (left) corresponds to residues 841-1202 of the gecko sequence and was modelled on the template of the VEGFR-2 kinase domain in complex with pyridyl-pyrimide benzimidazole inhibitor (PDB entry 3ewhA). Left images are ribbon representations for the specific gVEGFR-3 models and right images show comparisons of modelled gVEGFR-3 (red) with modelled hVEGFR-3 (blue) and cVEGFR-3 (white). Superimposition of the gecko model with human and chicken models shows variations in structure, with the chicken model appearing the most divergent and the gecko model appearing most similar to the human model.

A

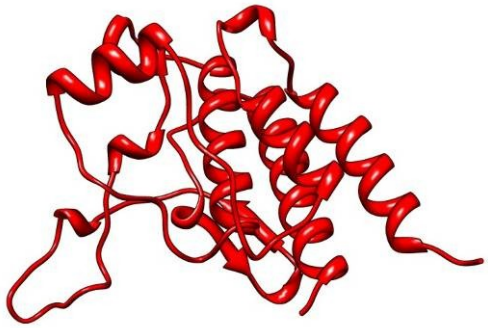

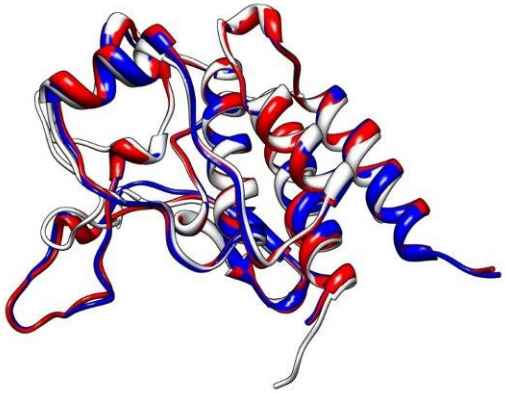

B

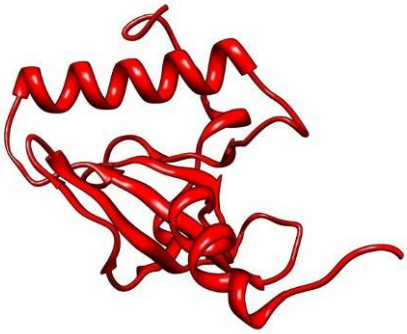

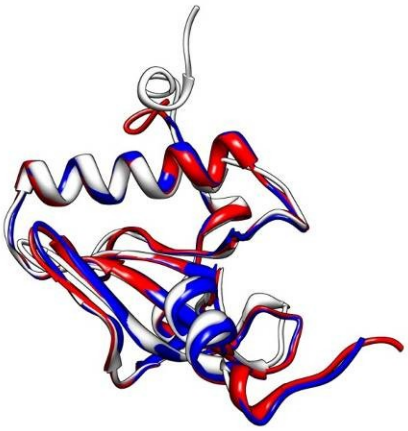

C

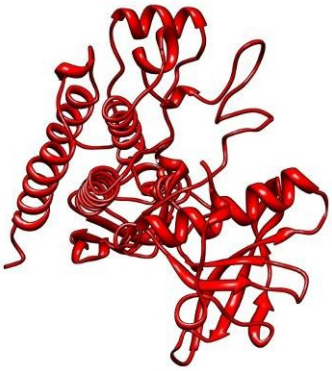

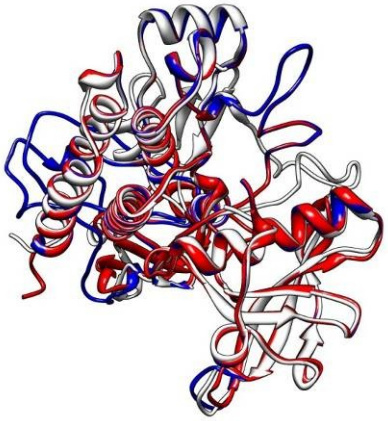

gVEGF-C produced a model consisting of 2 α-helices, a β-sheet comprised of 6 β-strands and 3 loop regions (Fig. 4.8A). Modelled gVEGF-C superimposed with the crystal structure of hVEGF-C generates a perfect fit (Fig.4.8B). There are no structural differences apparent between the gecko model and human crystal structure and the sequence alignment of this region used to generate the model shows only 3 different residues between gVEGF-C and the 2x1wC human VEGF-C template. Furthermore, residues considered essential in receptor binding (shown in Fig. 4.8C) are all positioned such that they would be available for this purpose. Loops 1 and 3 of VEGF-C, which are necessary for VEGFR-3 receptor binding in the human protein (Jeltsch et al. 2006), are present in the gecko and possess the same structural organisation.

gVEGF-D was modelled based on the human VEGF-C template, as a VEGF-D crystal structure is unavailable. Modelled gVEGF-D is made up of 6 β-strands, 1 α-helix and 8 loop regions (Fig. 4.9A). To make judgements on modelled gVEGF-D it was therefore necessary to model hVEGF-D and cVEGF-D such that structural comparisons could be made between the gecko model and VEGF-D proteins of different species. Superimposition of gVEGF-D onto the modelled structures of hVEGF-D and cVEGF-D shows several structural differences, mainly within the loop regions of the molecules (Fig. 4.9B). Modelled hVEGF-D and cVEGF-D in comparison to gVEGF-D possess a short extra α-helix in the region directly after β-sheet 1 corresponding to a segment of loop 1 in gVEGF-D. All three structures appear to have minor shape differences within the loops as a result of a few amino acid substitutions in these regions; however loop lengths are the same and the overall folding of the proteins does not appear to be significantly altered between models. Receptor binding residues have not been as well described for VEGF-D as for VEGF-C. A putative receptor-binding interface has been suggested for VEGF-D that is likely to interact with VEGFR-2 and VEGFR-3 (Baldwin et al. 2001). The putative receptor binding interface and three crucial binding residues are

highlighted on a homodimer model of gVEGF-D displaying the protein surface (Fig. 4.9C). While some residues within the gecko protein that are different to the consensus do appear within the assumed receptor binding interface, the majority of this region is structurally conserved in gVEGF-D and appears to be accessible. Homology modelling of gVEGF-D also produced a model from the C-terminal sequence based on the template of the heparin-binding domain from VEGF (PDB entry 1vghA). The sequence identity for this region with the given template is 23%, indicating a model of medium to low accuracy. Only models generated from an alignment with greater than 50% identity are predicted to have greater than medium accuracy. Therefore, additional quality checks were performed including QMEAN (Benkert et al. 2008) and DFire (Zhou and Zhou 2002). Anolea and GROMOS assessments of this model show that most amino acids within the sequence modelled have favourable energy characteristics to comply with the predicted model outcome. However, the QMEAN score is 0.402 and Dfire energy of the model is -33.38, indicating that the model reliability is not high.

As for VEGF-D there is no crystal structure available for VEGFR-3. Therefore, models generated are based on small segments of sequence homology to the VEGFR-2 receptor which has had its tertiary structure (in complex with other molecules) resolved (Hasegawa et al. 2007). Homology modelling of gVEGFR-3 generated 20 models (based on different templates) of different sites within the protein sequence. No models covered the entire length of the primary sequence and only three models had a sequence identity higher than 50% for the alignment between the template and query. Further examinations (viability testing) of gVEGFR-3 models with lower than 50% template identity revealed no models of acceptable accuracy and so these were not included in further analysis and are not shown. All three of the models with above 50% template identity (denoted gVEGFR-3 model 1-3) are in the intracellular kinase region of the receptor. gVEGFR-3 models 1 (Fig. 4.10A left) and 2 (Fig. 4.10B left) were based on the template of the crystal structure of VEGFR-2 with

benzimidazole urea inhibitor (PDB entry 2oh4A) with model 1 mapping residues 1027-1198 of the protein sequence and model 2 corresponding to residues 842-964. The third model (Fig. 4.10C left), corresponding to residues 841-1202 of the gVEGFR-3 protein sequence, was based on the template of the crystal structure of VEGFR-2 kinase domain in complex with a pyridyl-pyrimide benzimidazole inhibitor (PDB entry 3ewhA). Model comparisons were made between modelled human, chicken and gecko VEGFR-3 (Fig. 4.10A-C right). Of the three modelled proteins cVEGFR-3 appears to be the most different structurally, with gVEGFR-3 appearing quite similar to hVEGFR-3 particularly in models 1 and 2. However differences are predominantly confined to the loop regions and do not appear to change the protein structure dramatically.

4.4. DISCUSSION

4.4.1. gVEGF-C, gVEGF-D AND gVEGFR-3: CONSERVATION OF FUNCTIONALLY IMPORTANT RESIDUES

This chapter describes the isolation and characterisation of the full-length cDNA and translated amino acid sequences of the lymphangiogenic growth factors VEGF-C and VEGF-D and their receptor VEGFR-3 in the Australian marbled gecko *(C. marmoratus)*. All three gecko proteins appear to contain the specific-characteristic domains that are present in other species. gVEGF-C and gVEGF-D, based on analogy to the other species, contain putative signal sequences and a VHD flanked by C- and N-terminal propeptides. Likewise, by comparison to other species, gVEGFR-3 has a signal sequence, seven immunoglobulin-like domains, a transmembrane domain and an interrupted protein kinase domain. VEGF-C and VEGF-D, in mammals, function by binding to VEGFR-2 and VEGFR-3 to stimulate both angiogenesis and lymphangiogenesis (Otrock et al. 2007). For adequate receptor binding and activation several key steps are necessary and include: ligand dimerisation, proteolytic processing, receptor binding, receptor dimerisation, tyrosine transphosphorylation of the intracellular domains leading to activation of the tyrosine kinase and the creation of docking sites for downstream signalling proteins (Olsson et al. 2006). Activated signal transduction pathways then lead to specific responses in blood and lymphatic endothelial cells. Absence or mutations of any of the residues critical in these processes leads to ineffective responses in target cells resulting in proteins that are incapable of inducing angiogenic and lymphangiogenic responses (Cueni and Detmar 2006; Irrthum et al. 2000; Jeltsch et al. 2003; Karkkainen et al. 2000; Karkkainen et al. 2001; Khatib et al. 2010; Leppänen et al. 2010; Siegfried et al. 2003). The gecko VEGF-C, VEGF-D and VEGFR-3 translated amino acid sequences include all functionally important residues previously identified in other species (discussed further below). If the actions involving these residues occur in the gecko as they do

in other animals, it is likely that the gecko proteins would function similarly as they do in other species. We therefore hypothesise that binding of gVEGF-C and gVEGF-D to gVEGFR-3 would induce lymphangiogenesis. In particular, these proteins could therefore be key regulators in stimulating the growth of new lymphatic vessels within the regenerating gecko tail.

Crystallisation and determination of the VEGF-C structure (bound to VEGFR-2) has recently revealed that VEGF-C dimerisation can occur in mature proteins by disulphide bonding, as is the case for most other members of the VEGF family. VEGF-C and VEGF-D had previously been thought to only form non-covalently bound dimers (Achen et al. 1998; Joukov et al. 1996). Cysteine residues implicated in the formation of the dimerisation interface of other VEGF family members (Muller et al. 2002), and in human VEGF-C (Leppänen et al. 2010), are conserved in the gVEGF-C and gVEGF-D protein sequences (Cys156 and Cys165 of hVEGF-C corresponds to gVEGF-C Cys160 and Cys169; Cys 142 and Cys153 of hVEGF-D corresponds to gVEGF-C Cys140 and Cys151. Figs 4.5A and 4.6A). In contrast the free cysteine common only to VEGF-C (human Cys137), VEGF-D (human Cys117), and the PVF-1 protein, a recently characterised VEGF/PDGF homologue from *Caenorhabditis elegans* (Tarsitano et al. 2006) is also present in gVEGF-C (Cys141) and gVEGF-D (Cys115). As PVF-1 also exists predominantly as a non-covalent dimer this free cysteine may be important in maintaining these growth factors as non-covalent dimers. While it is not clear how a cysteine residue could prohibit covalent dimerisation, a study has shown that mutation of this residue in recombinant VEGF-D variants increases the number of VEGF-D dimers in the protein solution (Toivanen et al. 2009). Thus, the gecko proteins may have both the capacity to form covalent and non-covalent associations to generate homodimers.

gVEGF-C and gVEGF-D both contain proteolytic cleavage sites known to be essential for processing the mature forms of both proteins (Figs. 4.5A and 4.6A). In gVEGF-C, cleavage of the C-terminal is possible at Arg231-Ser232, which corresponds to the known human cleavage site of Arg227-Ser228 (Joukov et al. 1997b). Mutation of Arg226 and Arg227 of human VEGF-C into serine residues abolishes proteolytic processing of the protein resulting in an unprocessed form with reduced receptor affinity and weaker receptor autophosphorylation capability (Joukov et al. 1997b). Following C-terminal cleavage, the N-terminal of gVEGF-C could be cleaved at Ala115-Ala116, which likewise corresponds to the cleavage site in humans of Ala111-Ala112. Similarly, in gVEGF-D, the C-terminal cleavage site of Arg203-Ser204 analogous to the known human site Arg205-Ser206, is present and both the major (Arg86-Phe87 in gecko, Arg88-Phe89 in human) and minor (Leu97-Lys98 in gecko, Leu99-Lys100 in human) N-terminal cleavage sites are conserved. Thus, sequential cleavage of both the C- and N- terminal propeptides of gVEGF-C and gVEGF-D could result in mature bioactive forms of the proteins. Furthermore, the N- and C-terminal extensions of the VEGF-C and VEGF-D pro-peptides are hypothesised to be important for associations with the extracellular matrix, restricting them to remain close to secretion sites and thus modulating bioavailability and bioactivity. The silk-like BR3P motif, C_{10}XCXCXC, found in the C-terminal of both VEGF-C and VEGF-D in other species is conserved in the gecko proteins (Figs. 4.5A and 4.6A), potentially allowing the gecko proteins to adhere to the surrounding tissues until proteolytic cleavage releases active receptor binding forms when they are needed.

Mutation studies have previously identified residues critically important for receptor binding of VEGF-C and VEGF-D, and correspondingly regions important for ligand binding in VEGFR-3. The gecko sequences for VEGF-C and VEGFR-3 proteins are highly homologous to other species within these binding specificity regions (Figs. 4.5A. and 4.7A.).

gVEGF-C contains all residues implicated in VEGFR-3 and VEGFR-2 binding in mammals and gVEGFR-3 contains both Ig-like domains 1 and 2 which are highly similar to those of other species, and have been found to be essential for VEGF-C binding (Jeltsch et al. 2006). These similarities indicate that gVEGF-C is likely to be able to bind gVEGFR-3. However, further studies on expressed gecko proteins in receptor binding and activation are needed to ascertain this. Residues suggested to be important in human VEGF-D receptor binding are not fully conserved in the gecko sequence and are variable along the whole vertebrate alignment. However, this may not necessarily reflect an inability of gVEGF-D to bind gVEGFR-3 and gVEGFR-2 (if present) as mVEGF-D can bind and activate hVEGF-D (Baldwin et al. 2001) and rabbit VEGFR-2 (Marconcini et al. 1999) despite sequence variability. Surprisingly, mVEGF-D does not bind mVEGFR-2 as would be expected (Baldwin et al. 2001). Three residues are different between human (Ser150, Leu151 and Ile152) and mouse (Gly155, Val156 and Met157) sequences in the putative receptor-binding sites and mutations of the mouse residues to the corresponding human residues allows mVEGF-D to bind mVEGFR-2 (Baldwin et al. 2001). Therefore, the inability of mVEGF-D to bind and activate mVEGFR-2 may be more a result of specific issues with the interaction between the ligand and receptor only in the mouse, and not a specific issue with differences in the VEGF-D a.a. sequences.

Binding of dimerised ligand to the VEGFR-3 receptor results in receptor dimerisation, which allows for trans-phosphorylation between the partners of the dimer and activation of kinase activity and receptor signalling. Tyrosine residues specified as potential phosphorylation sites are therefore crucial in receptor activity. All tyrosine residues capable of phosphorylation in hVEGFR-3 (Dixelius et al. 2003a) are present in gVEGFR-3. In particular, Tyr1337 (in hVEGFR-3) is conserved in the gecko (Tyr1352) and this residue is required for binding of the signalling complex SHC (a transforming protein)-growth factor receptor bound protein-2 (Gbr2) to VEGFR-3 (Fournier et al. 1995). Similarly, Tyr1063 and Tyr1068 in

hVEGFR-3 within the kinase domain, which most likely regulate the kinase activity of the receptor, are present in the gecko protein sequence (Tyr1081 and Tyr1086). It, therefore, is possible that gVEGFR-3 is capable of transphosphorylation upon ligand binding and therefore also potentially capable of kinase activity, signal transduction and eliciting a response in the cells expressing the receptor.

Mutations in the protein kinase domain of VEGFR-3 inactivate the receptor and lead to reduced lymphangiogenesis and subsequent lymphoedema (Irrthum et al. 2000; Karkkainen et al. 2000; Karkkainen et al. 2001). The gVEGFR-3 protein kinase domain shows greater identity to other species than is the case for the whole protein, with 79% identity to both human isoforms, 81% to both mouse and rat sequences, 95% to chicken, 88% to frog and 76% identity to the zebrafish sequence. Furthermore, known residues linked to mutations that cause lymphoedema phenotypes are unchanged between all species aligned. For example, Gly857, Arg1041, Leu1044 and Pro1114 in hVEGFR-3, all of which are sites of mutation identified in patients with primary lymphoedema (Karkkainen et al. 2000), correspond to Gly872, Arg1059, Leu1062 and Phe1132 in the gecko receptor, suggesting that gVEGFR-3 appears to contain residues critical for tyrosine kinase activity. It is therefore possible that gVEGFR-3 may be capable of kinase signalling and consequently eliciting a response, within receptor expressing cells, as a result of VEGF-C/ VEGF-D binding.

4.4.2. COMPARISON OF gVEGF-C, gVEGF-D AND gVEGFR-3 WITH OTHER SPECIES

In the previous chapter we identified that partial cDNA sequences of gVEGF-C, gVEGF-D and gVEGFR-3 were highly similar to those of other species. This similarity is upheld by the full cDNA sequence data available in this chapter with a.a. sequence similarity scores ranging from 70-94% for VEGF-C, 65-88% for VEGF-D and 73-91% for VEGFR-3. The full-length gecko protein sequences are more similar to the chicken sequences than to human, mouse, rat, frog and zebrafish. This homology is consistent with the close phylogenetic relationship of

reptiles and birds (Hedges 1994) and was confirmed by phylogenetic analysis using the NJ algorithm (Figs. 4.5B, 4.6B and 4.7B). For all three-proteins the reptilian sequences reliably cluster tightly with the chicken sequences and are less closely related in terms of evolutionary history to the other species examined. NJ trees generated from sequence alignments of partial cDNA sequences of the VEGF-C, VEGF-D and VEGFR-3 genes showed essentially the same relationships (Chapter 3) except with lower bootstrap confidence scores for the relationship of chicken and gecko VEGF-D (78% compared to 90%) and VEGFR-3 (86% compared to 100%) sequences and slightly higher for VEGF-C (87% compared to 81%). In the previous chapter, expanding the phylogenetic analysis to include more species gave results that suggested differing modes of evolution of VEGF-C from VEGF-D and VEGFR-3. In these previous trees (Chapter 3: Fig. 7), the evolutionary history of VEGF-C appeared to be driven by stabilising selection forces, whereby non-synonymous substitutions have been limited resulting in high levels of sequence conservation resulting in a phylogenetic tree with short branch lengths, lack of resolution between clusters and poor confidence values. Alternatively, the NJ trees generated from partial sequence data for VEGF-D and VEGFR-3 conformed to the expected relationships of vertebrate evolution, suggesting that directional selection may be the dominant driving force behind the evolution of these genes. We suggested that using the full-length nucleotide sequences may help to reinforce these proposed evolutionary histories. Thus, the full gecko sequence data was used in a wider comparative analysis (Fig 4.11) in a manner similar to that previously described (Chapter 3). Phylogenetic analysis of the full-length gecko nucleotide sequences for VEGF-C, VEGF-D and VEGFR-3 within the expanded NJ trees (Fig. 4.11) appears to strengthen the previously observed relationships. Gecko sequences for all three genes still reliably cluster most closely with bird orthologues, although bootstrap confidence values are increased. This is particularly the case for VEGF-C, where bootstrap confidence at the node of the gecko and bird branches is increased from the

unreliable value of 15% reported previously to the much stronger value of 67%. The resolution of the NJ tree for VEGF-C is clearer using the full-length sequence data, however confidence values are still lower than expected (32-99%) and branch lengths are still quite short (many less than 0.05 base substitutions per site) for most relationships. Thus, this tree appears to support the stabilising selection theory proposed previously, and combined with the observed higher levels of a.a. sequence similarity between species for the VEGF-C protein (Table 4.4.), suggests that the sequence has been strongly conserved throughout evolution presumably due to high functional importance. Likewise, VEGF-D and VEGFR-3 NJ trees generated using full-cDNA sequence data comply with the theory of directional selection as the driving force of evolution for these genes. Both expanded NJ trees for these genes show clear separate clusters between different vertebrate groups with strong bootstrap scores (VEGF-D: 76-100%, VEGFR-3: 67-100%) for all divergences and branches that correspond to expected vertebrate evolution patterns (Fig. 4.11). More sequence data for a greater variety of species may help to increase the resolution of the different relationships, particularly the relationship between reptilian and bird VEGF-C, VEGF-D and VEGFR-3 sequences. The gecko is the only reptile for which sequence data is available for these genes and thus the ability of phylogenetic analysis to fully resolve the evolutionary histories of these genes is limited.

Figure 4.11. Expanded phylogenetic analysis of VEGF-C (A), VEGF-D (B) and VEGFR-3 (C) gene sequences utilising full-length cDNA sequence data. NJ trees were constructed from a ClustalW alignment of vertebrate sequences found from a BLAST search using the gecko sequence as the query. The numbers on the branches represent the confidence level of 1200 bootstrap pseudo-replicates. The tree is drawn to scale, with branch lengths in the same units as those of the evolutionary distances used to infer the phylogenetic tree. The evolutionary distances were computed using the Maximum Composite Likelihood method (Tamura et al. 2004) and are in the units of the number of base substitutions per site (shown on the scale bar).

A

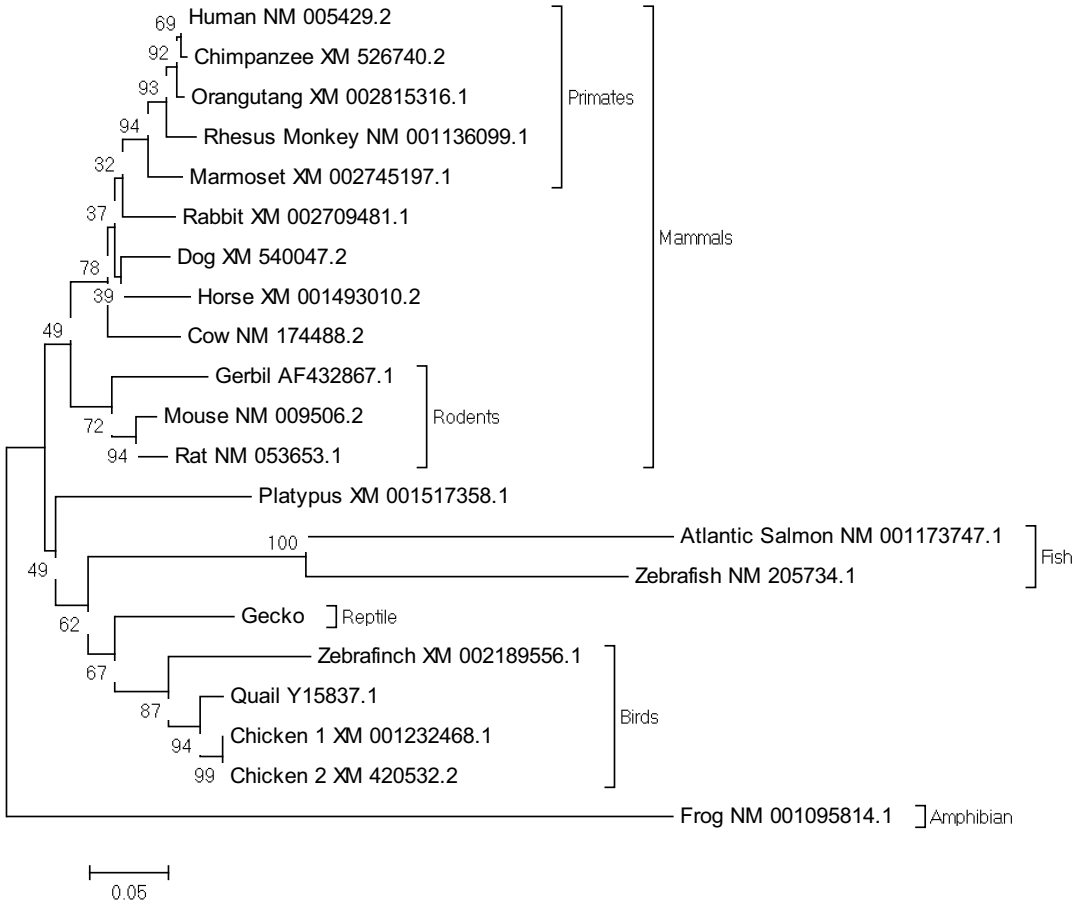
69
Human NM 005429.2
92
Chimpanzee XM 526740.2
93
Orangutang XM 002815316.1
Primates
94
Rhesus Monkey NM 001136099.1
32
Marmoset XM 002745197.1
37
Rabbit XM 002709481.1
Mammals
78
Dog XM 540047.2
39
Horse XM 001493010.2
49
Cow NM 174488.2
Gerbil AF432867.1
72
Mouse NM 009506.2
Rodents
94
Rat NM 053653.1
Platypus XM 001517358.1
100
Atlantic Salmon NM 001173747.1
Fish
49
Zebrafish NM 205734.1
62
Gecko
Reptile
Zebrafinch XM 002189556.1
67
Quail Y15837.1
87
Birds
Chicken 1 XM 001232468.1
94
99
Chicken 2 XM 420532.2
Frog NM 001095814.1
Amphibian
0.05

B

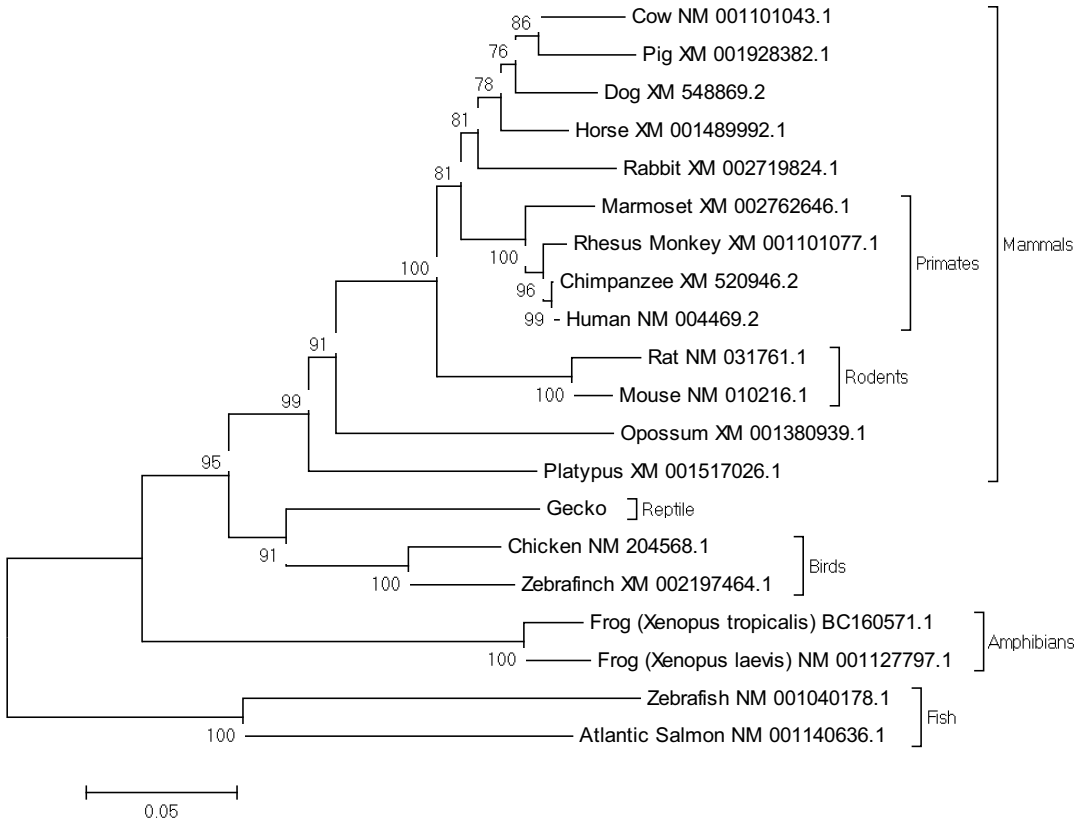
Cow NM 001101043.1
Pig XM 001928382.1
Dog XM 548869.2
Horse XM 001489992.1
Rabbit XM 002719824.1
Marmoset XM 002762646.1
Rhesus Monkey XM 001101077.1
Chimpanzee XM 520946.2
Human NM 004469.2
Primates
Mammals
Rat NM 031761.1
Mouse NM 010216.1
Rodents
Opossum XM 001380939.1
Platypus XM 001517026.1
Gecko
Reptile
Chicken NM 204568.1
Zebrafinch XM 002197464.1
Birds
Frog (Xenopus tropicalis) BC160571.1
Frog (Xenopus laevis) NM 001127797.1
Amphibians
Zebrafish NM 001040178.1
Atlantic Salmon NM 001140636.1
Fish
86
76
78
81
81
100
100
96
99
91
100
99
95
91
100
100
100
0.05

C

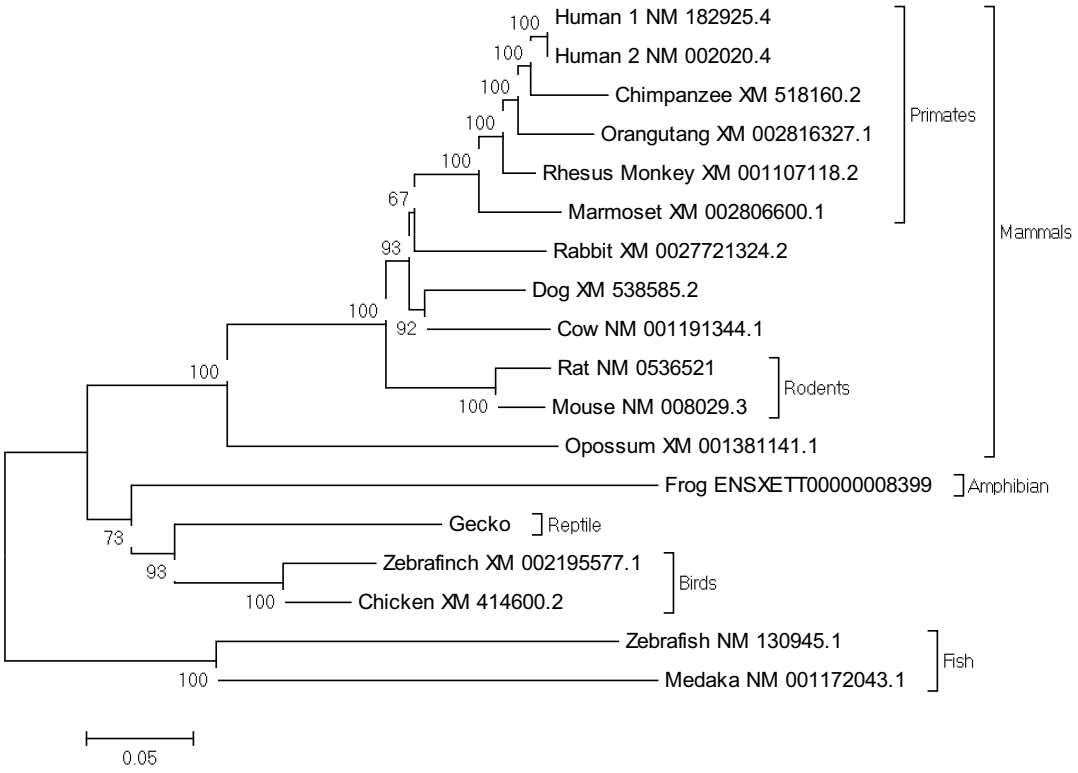
Human 1 NM 182925.4
Human 2 NM 002020.4
Chimpanzee XM 518160.2
Orangutang XM 002816327.1
Rhesus Monkey XM 001107118.2
Marmoset XM 002806600.1
Rabbit XM 0027721324.2
Dog XM 538585.2
Cow NM 001191344.1
Rat NM 0536521
Mouse NM 008029.3
Opossum XM 001381141.1
Frog ENSXETT00000008399
Gecko
Zebrafinch XM 002195577.1
Chicken XM 414600.2
Zebrafish NM 130945.1
Medaka NM 001172043.1
100
100
100
100
100
67
93
100
92
100
100
73
93
100
100
Primates
Rodents
Mammals
Amphibian
Reptile
Birds
Fish
0.05

4.4.3. STRUCTURAL ANALYSIS OF gVEGF-C, gVEGF-D AND gVEGFR-3

Predicted tertiary structures of gVEGF-C, gVEGF-D and gVEGFR-3 were produced using the Swiss-Model Server (Arnold et al. 2006). The crystal structure for hVEGF-C has recently been deduced and thus gVEGF-C was modelled directly on this molecular structure. Tertiary structures have not been experimentally resolved for VEGF-D or VEGFR-3, thus models were based on homology to other known crystal structures and as such the accuracy of these models is reduced. This may result in the discrepancies observed between the human, chicken and gecko models for these proteins. Re-modelling the proteins once the crystal structures are known for VEGF-D and VEGFR-3 may change the results obtained in this study.

Mature gVEGF-C appears to be identical to hVEGF-C at a structural level. The gVEGF-C models are capable of forming anti-parallel homodimers necessary for receptor binding. Residues and regions implicated in both VEGFR-2 and VEGFR-3 binding are positioned to allow for receptor binding, which would allow for subsequent receptor dimerisation and activation. Similarly, while modelled mature gVEGF-D shows some small differences when compared with models of hVEGF-D and cVEGF-D, the molecular complex as a whole appears largely unchanged and receptor binding regions appear to be positioned in such a way that they are available for VEGFR-2 and VEGFR-3 binding. However, the structural determinants for receptor binding in VEGF-D have not been as well established as for VEGF-C and thus other regions not highlighted in this study may also be important. The generation of a heparin binding domain model for the C-terminal region of gVEGF-D, based on sequence identity to the tertiary structure of VEGF, is interesting. Modelling of the human and mouse VEGF-D amino acid sequences also generates this model, however neither have previously been described as having a heparin binding domain. This domain in VEGF functions to bind heparin and heparan sulfate glycosaminoglycans, located on cell surfaces and in the ECM (Sasisekharan and Venkataraman 2000), thus determining the localisation of

VEGF proteins within the extracellular space (Houck et al. 1992; Poltorak et al. 1997). Heparin binding assays on unprocessed gVEGF-D would conclude whether this model is an artefact based purely on coincidental sequence similarity or whether it is a true representation of the protein.

Homology modelling of gVEGFR-3 produced many models from a variety of templates. However, only models based on the protein kinase region were considered to be accurate as determined by the Anolea, GROMOS and verify3D analysis tools. Models generated in the Ig-like domains were not considered reliable, and thus this analysis was unable to determine structurally whether gVEGFR-3 is capable of binding gVEGF-C and gVEGF-D. Comparisons of the viable protein kinase models with human and chicken modelled structures show small differences that do not appear to greatly alter the molecular organisation of the protein, indicating that structurally the protein kinase region of gVEGFR-3 may be capable of the actions displayed in humans and chickens such as dimer transphosphorylation and docking for signal transduction molecules.

4.4.4. CONCLUSION

Gecko cDNA sequences that are similar to other species have been isolated for the lymphangiogenic and angiogenic growth factors VEGF-C, VEGF-D and their receptor VEGFR-3. For all three translated protein sequences, functionally important residues are conserved in the gecko sequences, corresponding to the sequence of events necessary for specific target cell responses, at both a sequence and structural level. This study therefore provides evidence for the hypothesis that gVEGF-C and gVEGF-D, via binding to gVEGFR-3, contribute to lymphangiogenesis within the regenerating gecko tail. Further studies are needed to confirm this hypothesis and would include bioassays on either isolated or recombinant proteins to determine receptor binding and activation profiles along with determining sites of expression of gVEGFR-3 within the regenerating tissues. *In vivo*

expression analysis would establish whether gVEGFR-3 is restricted to lymphatic endothelial cells throughout regeneration, with activation triggering a lymphangiogenic response, or whether it may be expressed by blood endothelial cells, as is the case for tumours (Petrova et al. 2008), thereby triggering an angiogenic response upon ligand binding.

Chapter Five

PROTEIN ANALYSIS OF gVEGF-C, gVEGF-D AND gVEGFR-3

5.1. INTRODUCTION

Endogenous or exogenous overexpression of VEGF-C, VEGF-D and/or VEGFR-3 protein triggers lymphangiogenic responses. For example, lymphatic vessel density and/or vessel volume are increased in adult tissues treated with adenoviral expression of VEGF-C and VEGF-D and lymphangiogenesis is stimulated upon delivery of recombinant VEGF-C (Enholm et al. 2001; Jin da et al. 2009; Rissanen et al. 2003; Saaristo et al. 2002b; Szuba et al. 2002). Previous work utilising western blotting within regenerating gecko tail extracts suggests gVEGF-C protein expression is up-regulated between 3 and 6 weeks after autotomy and then remains increased in 9, 12 and 15 week regenerates (Daniels et al. 2003). Early up-regulation of VEGF-C during gecko tail regeneration is consistent with mammalian wound healing studies (Ling et al. 2009; Rutkowski et al. 2006; Shimoda et al. 2004; Uzarski et al. 2008). However, specific timings within the early regenerative phase were not examined nor were the expression patterns of gVEGF-D or gVEGFR-3 protein. Furthermore, sites of expression of gVEGFR-3 within regenerating tail tissues are unknown.

In Chapter 3, I showed differential expression profiles of gVEGF-C, gVEGF-D and gVEGFR-3 mRNA throughout tail regeneration, with up-regulation of all three genes at differing stages of the regeneration process signalling potentially different roles. While mRNA expression is commonly used to make inferences about protein function, and increased mRNA expression is required to produce a protein product, adequate protein translation from expressed mRNA is required to truly bring about cellular and tissue responses. Many studies do show positive correlations between expression of specific mRNAs and corresponding proteins that result in a clear biological response (Asplund et al.

2008; Dhanasekaran et al. 2001; Fu et al. 2007; Mousses et al. 2002). However, others show inconsistencies (Chen et al. 2002; Gry et al. 2009; Guo et al. 2008). Therefore, functional inferences made from mRNA expression data, while useful for showing potential for biological actions, are more reliable when corroborated with protein analysis.

Obtaining protein expression profiles will provide more evidence for the hypothesis that the VEGF-C/D/R3 pathway plays a key role in lymphatic regeneration within gecko tails following autotomy. Surprisingly, despite the results of Chapter 4 showing strong sequence and structural homology between the gecko and mammalian proteins, many problems were encountered in the protein analysis. In hindsight, this is presumably as a result of low affinity of the antibodies generated against mammalian proteins for the gecko proteins.

In this chapter I describe attempts made to quantify the protein expression of gVEGF-C, gVEGF-D and gVEGFR-3 within protein extracts from regenerating gecko tails using ELISA as well as attempts to show protein presence and size using western blotting. I also describe troubleshooting of the immunohistochemistry method described in Chapter 3 with the aim to gain information on gVEGFR-3 expression within gecko tail tissues. In Chapter 3 I showed no positive staining in gecko tail tissue sections on lymphatic or blood endothelial cells using an anti-VEGFR-3 antibody, despite these cells being major sites of expression in other species and despite the observation of potential associations of gVEGF-C and gVEGF-D with VEGFRs on lymphatic-like and blood vasculature. However, despite extensive troubleshooting, these techniques were largely unsuccessful in achieving the aims of this chapter.

5.2. MATERIALS AND METHODS

5.2.1. PROTEIN EXTRACTION

Gecko tails were obtained as described in Chapter 3. Briefly, gecko tails were stimulated to autotomise and then left to regenerate for either 4, 5, 6, 7, 9, 10 or 12 weeks after which the regenerated portion of the tails was once again autotomised and immediately snap frozen in liquid nitrogen and stored at -80°C until needed. Tails were then ground using a mortar and pestle under liquid nitrogen to a fine powder. Two different protein extraction methods were used due to issues with yield, suspected inhibiting factors within extracts and issues encountered due to the highly fatty nature of the gecko tails.

5.2.1.1. Tri-reagent extraction of protein

Following tail crushing, 100mg of crushed tissue was added to 1ml of Tri-reagent (Sigma) and RNA, DNA and protein were extracted predominantly according to the manufacturer's instructions. Briefly, tissue and tri-reagent mixture were homogenised using a Mini-Beadbeater (Daintree Scientific) and then spun at 12,000 x *g* for 10 min at 4°C to remove insoluble material and beads. 0.2 ml of chloroform was added to the supernatant, left for 15 min at room temperature and then spun at 12,000 x *g* for 15 min at 4°C to separate out the mixture into an upper colourless aqueous phase and a lower red phenol/chloroform phase. Three volumes of acetone were added to the phenol/chloroform phase and incubated at room temperature for 5 min to precipitate the protein, then spun at 12,000 x *g* for 10 min at 4°C. The resulting protein pellet was washed three times using 500 µl of 0.3 M guanidine hydrochloride in 95% ethanol plus 2.5% glycerol (V:V). A final wash in 1 ml of ethanol containing 2.5% glycerol (V:V) was performed and the dried protein pellet was re-solubilised in 1 ml of 1% SDS.

5.2.1.2. Guanidine and triton extraction of protein

100 mg of crushed tissue was measured into a 1.5 ml eppendorf tube and taken through a freeze-thaw process to fully disrupt the cells and tissues. Tubes were placed in ethanol that had been supercooled using dry ice, and then left until frozen and then placed at 37°C until thawed. This freeze-thaw process was cycled 5 times. 1 ml of 6 M Guanidine-HCl + 0.1% triton-X100 was then added to the pulped tissue and homogenised using the Mini-Beadbeater method. Following homogenisation and the removal of beads and insoluble material by centrifugation, the homogenate was incubated at 60°C for 2 h, centrifuged at 13,000 x g for 20 min and the supernatant was collected and stored at -20°C until needed. High levels of fat were detected within samples that prevented sample filtering. Hence, several methods were used to attempt to either remove the fat or precipitate the protein. A chloroform extraction method was attempted whereby chloroform was added to the supernatant in a ratio of 1:2 and left for 2 h at 4°C then centrifuged at maximum speed for 15 min to separate the chloroform from the aqueous layers. The resulting solution was then filtered as described in 5.2.2. Precipitation of proteins within the guanidine supernatant was also tried using ice-cold acetone (4 x volume of sample), ethanol, and various ratios of acetone: ethanol. Samples were left for 2 h at -20°C and centrifuged at 13,000 x *g* for 15 min. 0.2% SDS, 1% SDS and 0.3 M guanidine-HCl solutions were then used to attempt to re-solubilise protein pellets.

5.2.2. PROTEIN FILTRATION TO REMOVE CONTAMINANTS AND CONCENTRATE PROTEIN

Microcon centrifugal filter devices (Millipore) with a 10 kDa MW cut-off were used to concentrate protein extracts. 500 µl of protein sample was added to the sample reservoir and centrifuged at 14,000 x *g* for 30 min. The retentate was then recovered by placing the sample reservoir upside down in a new vial and centrifuging at 1,000 x *g* for 3 min.

To remove guanidine from samples, 400 µl of 0.1% triton-X100 in PBS was added to the retentate and filtered again through the microcon filter. This was repeated several times.

5.2.3. TOTAL PROTEIN QUANTIFICATION

Total protein concentration was determined using bicinchoninic acid (BCA) protein assay (Pierce) and absorbance values read at 595 nm on a GENios microplate reader (TECAN).

5.2.4. SDS-PAGE AND WESTERN BLOTTING ON GECKO TAIL EXTRACTS

50 µg of gecko tail protein extract was analysed on a precast NuPAGE® 4–12% Bis-Tris gel (Invitrogen). Samples were incubated for 10 min at 70°C with 4 x NuPAGE ® LDS sample buffer (Invitrogen, Carlsbad, CA) and 1 µl of 50 mM dTT prior to loading. Gels were run using the XCell SureLock™ Mini-Cell (Invitrogen, Carlsbad, CA) at 200 V for 30 min and transferred to nitrocellulose membrane (0.2 µm) using the XCell II™ blot module and NuPAGE® transfer buffer (Invitrogen). Membranes were blocked with 5% skim milk TBS-T (10 mM Tris, 0.9% NaCl, pH 7.4, with 0.1% Tween 20) and incubated with primary antibody directed against VEGF-C, VEGF-D or VEGFR-3 (Table 5.1.) overnight at 4°C. α-Actin polyclonal antibody (Sigma-Aldrich) was used at 1:5,000 as the internal loading control standard. Blots were incubated with secondary antibody (Goat anti-rabbit IgG, Invitrogen; 1:5,000) for 1 h at room temperature. Immunoreactive bands were visualised with chemiluminescence (using luminol solution, see Appendix Three) on HT-G orthofilm. Films were photographed and densitometry performed in an Alpha Innotech FluorChem 8900 using the AlphaView SA software. Samples were randomised before loading onto gels and were quantified using densitometry. Inter-gel expression was normalised to a specific quality control sample run on every gel. Intra-gel expression was normalised to α-actin. The average of two separate experiments for each sample was used for analysis. Results are given as the mean ± SEM. Expression data for each protein across regeneration time points were analysed

using a one-way ANOVA with a posthoc Dunnett multiple comparison test using expression levels of the original tailed geckos as the control. Differences were considered significant if $P < 0.05$.

5.2.5. ELISA VALIDATION AND ATTEMPTS TO QUANTIFY gVEGF-C, gVEGF-D AND gVEGFR-3 WITHIN PROTEIN EXTRACTS

To determine the concentration of VEGF-C, VEGF-D and VEGFR-3 within gecko tail protein extracts two ELISA methods were performed - a direct method and a sandwich ELISA method. Recombinant human protein standards (rhVEGF-C, R&D systems, Cat# 2179-VC; rhVEGF-D, R&D systems, Cat# 622-VD and rhVEGFR-3, R&D systems, Cat# 349-F4) were used to try and establish standard curves for quantification. rhVEGF-D and rhVEGFR-3 did not react with the antibodies used and so only rhVEGF-C could be used for assay development. In setting up the VEGF-C ELISA protocols several validation steps were undertaken using rhVEGF-C to ensure results for this standard were optimal. For example, concentrations of coating antibody (IgG plate saturation), primary antibody, secondary antibody and samples were all assayed to identify those that gave the greatest absorbance value for the samples and the lowest background (zero absorbance values).

5.2.5.1. Sandwich ELISA

High binding 96-well ELISA plates (Greiner) were coated for 1 h at room temperature and then overnight at 4°C with 100 µl of coating antibody (see Table 5.1.) at a 1:500 dilution in 50 mM sodium bicarbonate, pH 9.6. Coating solution was removed from the wells by gently flicking the plates upside down. The plates were washed with 200 µl of wash buffer (PBS-T; phosphate buffered saline, pH 7.4, 0.1% Tween 20, 0.01% thimerosal) and blotted onto paper towel. Blocking buffer (1% skim milk in PBS-T; 100 µl) was added to each well using an 8-well multi-channel pipette to block non-specific binding. The plates were then incubated at room temperature for at least 1 h. For VEGF-C ELISAs, a standard curve was prepared using rhVEGF-C diluted in PBS as follows 1/1000, 1/8000, 1/32000, 1/64000, 1/128000. Standard curves were not prepared for VEGF-D and VEGFR-3 ELISAs due to non-reactivity of the recombinant proteins with the antibodies. Each standard and sample (up to 200 µg, also

diluted in PBS) were added to the plate in duplicate and incubated for 3 h at 37°C with shaking. After incubation with samples and standards, the plate was washed three times with washing buffer, after which the primary antibody (see Table 5.1.) was added (1:1000 in blocking buffer). This was then incubated for 1 h at room temperature and then overnight at 4°C. The plate was washed again three times with washing buffer and incubated with secondary antibody (1:1000 goat anti-rabbit IgG-HRP conjugate (Zymed/ Invitrogen) in blocking buffer) for 1 h at room temperature. The plate was then washed three times in washing buffer, with the final wash left for 3 min to soak. 100 µl of TMB substrate (1 tablet of 3',3',5',5'-Tetramethylbenzidine.2HCl substrate in 10 ml phosphate citrate buffer with sodium perborate, Sigma) was added to each well for the final colour reaction, which was stopped after 20 min with 1 M HCl. Absorbance was then read on the GENios microplate reader (TECAN) at 450 nm and the final concentrations of the samples were calculated using the standard curve. Standard curves using rhVEGF-C dilutions were generated in the CurveExpert 1.38 software utilising the Morgan-Mercer-Flodin (MMF) sigmoidal model.

5.2.5.2. Direct ELISA

A direct ELISA protocol was attempted for all three proteins, in particular for VEGFR-3 where a suitable coating antibody could not be identified. Samples (up to 200 µg, in duplicate) were diluted in coating buffer and 100 µl was dispensed into a high binding 96-well ELISA plate (Greiner) and left overnight at 4°C. The following day excess coating buffer was removed by inverting the plate, flicking out the solution and tapping on paper towel. Plates were then washed with 200 µl of washing buffer three times and 100 µl of blocking buffer was added to each well and incubated at room temperature with shaking for 1 h. Following blocking, primary antibody was added and the protocol was followed as for the sandwich ELISA.

Table 5.1. Antibodies used for all protein analysis studies.

Antibody	Catalogue Number and Supplier	Immunogen	Purpose	Dilution Used
Goat anti-human VEGF-C (A-16)	sc-27128 (Santa Cruz)	A peptide mapping near the N-terminus of VEGF-C of human origin	Coating antibody ELISA Unsuccessful WB	1:500 1:500, 1:1000
Goat anti-human VEGF-C (C-20)	sc-1881 (Santa Cruz)	A peptide mapping at the C-terminus of VEGF-C of human origin	Unsuccessful WB	1:500, 1:1000
Goat anti-human VEGF-D (N-19)	sc-7603 (Santa Cruz)	A peptide mapping at the N-terminus of VEGF-D of human origin	Coating antibody ELISA Unsuccessful WB	1:500, 1:1000
Rabbit polyclonal to VEGF-C	ab9546 (abcam)	Highly pure recombinant full length dNdC-VEGF-C protein (Rat)	Primary antibody ELISA, WB, IHC	1:1000 ELISA 1:500 WB 1:200, 1:100, 1:50 IHC
Rabbit polyclonal to VEGF-D	ab63068 (abcam)	KLH conjugated synthetic peptide selected from the C-terminal region of human VEGF-D	Primary antibody ELISA, WB, IHC	1:1000 ELISA 1:500 WB 1:200, 1:100, 1:50 IHC
Rabbit polyclonal to VEGF Receptor 3	ab27278 (abcam)	Synthetic peptide corresponding to C terminal amino acids 1279-1298 of Human VEGF Receptor 3	Primary antibody ELISA, WB, IHC	1:1000 ELISA 1:500 WB 1:200, 1:100, 1:50 IHC

Abbreviations are as follows: *ELISA*, Enzyme linked immunosorbance assay; *WB*, western blotting; *IHC*, immunohistochemistry; dNdC, deltaN-terminal deltaC-terminal (i.e. lacking N- and C-terminals)

5.2.6. IMMUNOHISTOCHEMISTRY ON FIXED GECKO TAIL TISSUE

Following on from unsuccessful efforts to identify cellular and tissue expression sites of gVEGFR-3 described in Chapter 3, troubleshooting was performed on this technique to increase antibody specificity and cross-reactivity. Much of the immunohistochemical method was performed as per Chapter 3, including tissue fixation and preparation, slide dewaxing and rehydration and visualisation of immunostaining using the Dako Envision+® kit and DAB+ substrate chromogen solution (Dako). Immunostaining using varying concentrations of an antibody directed against VEGFR-3 along with various antigen retrieval, blocking and antibody incubation steps was undertaken with regenerating gecko tail tissue sections (listed in Table 5.2.). Following attempts at all of the protocols described in Table 5.2. the only change to the method described in Chapter 3 that was found to produce a positive staining result with the anti-VEGFR-3 antibody was in the primary antibody incubation temperature regime. Following blocking, the diluted primary antibody was added to tissue sections and incubated in a humid chamber for 3 h at 37°C, then overnight at 4°C. Negative control slides were incubated in antibody diluent only (1% normal goat serum in TBS). Slides were then washed, peroxidase quenched, incubated with labelled polymer as per the Dako EnVision+® kit instructions and visualised as described in Chapter 3.

Table 5.2. Troubleshooting of the immunohistochemical process for detection of VEGF-C, VEGF-D andVEGFR-3 in regenerating gecko tails.

Immunohistochemical detection step	Protocols tested	Result
Antigen Retrieval	Proteinase K digestion (Dako® Ready to Use Proteinase K solution, incubated for 6, 15 and 30 min)	No specific binding was visualised for proteinase K and EDTA antigen retrieval. EDTA retrieval resulted in higher levels of non-specific general staining, particularly in muscles. Positive staining was observed using citrate buffer HIER, though in unexpected sites.
	HIER using Tris-EDTA Buffer, pH 9.0 (10 mM Tris, 1 mM EDTA, 0.05% Tween 20; heated using microwave, 4 min HIGH, 14 min MED-LOW)	
	HIER using sodium citrate buffer, pH 6.0 (10 mM sodium citrate, 0.05% Tween 20; heated as above)	
Blocking solutions	**5% normal goat serum (GS), 1% BSA in TBS**	Less non-specific colour detection for bolded blocking solution
	5% GS, 1% BSA, 0.1% forscolin (cold water fish skin gelatin)	
	10% GS +/- 1% BSA	
	5% normal sheep serum +/- 1% BSA	
Primary antibody concentration	**1:200**, 1:100, 1:50	Less non-specific binding with higher dilution, no increase in specific binding for lower dilutions.
Primary antibody protocol	1 h at RT, overnight at 4°C	Only the bolded protocol showed any positive brown staining. All others were negative.
	1 h at RT	
	3 h at 37°C	
	1 h at RT, 3 h at 37°C, overnight at 4°C	
Secondary antibody	***Envision Kit*** Anti-rabbit IgG – HRP conjugated	No difference.

Bolded protocols for each step are those that were chosen for final immunostaining runs. *HIER*, heat induced epitope recovery; *RT*, room temperature.

5.3. RESULTS

5.3.1. PROTEIN EXTRACTION AND FILTRATION

Gecko tails are highly fatty and highly muscular tissues and thus require a relatively harsh method of protein extraction. Tail tissues need to be mechanically and chemically disrupted to obtain protein and thus protein yield can be lower than in other tissues and more prone to difficulties associated with the extraction process (e.g. degradation of proteins, lack of re-solubilisation of protein). Tri-reagent extraction of proteins from crushed gecko tail resulted in a protein pellet that was difficult to dissolve following precipitation and washing, thus requiring a high concentration of SDS in the solubilisation buffer. Therefore, this method resulted in low protein yields (due to difficulties in full solubilisation) and samples that were dissolved in a relatively high concentration of SDS, which could potentially alter protein conformations and inhibit antibody interactions. Furthermore, analysis on tri-reagent extracted protein gave variable results, particularly in ELISAs, suggesting the presence of potential inhibiting factors within the extract (see section 5.3.3.).

In an attempt to improve extracted protein yields and reduce the variability observed in tri-regent extracted samples, a different protein extraction method was undertaken utilising a guanidine/ triton extraction buffer. However, this extraction method was also problematic. Higher protein yields were obtained but guanidine had to be removed from the sample, as it is not compatible with SDS-PAGE and ELISA. Attempts to filter and wash out the guanidine from the sample were unsuccessful, as large fatty deposits within the sample blocked the filter. To remove the fat from the sample, chloroform extractions were performed, leaving an aqueous protein supernatant above a chloroform and fat layer after centrifugation. Although fatty globules were observed within the discarded chloroform layer, fat was nevertheless present within the aqueous supernatant and blocked the filter even after several sequential chloroform extractions on the protein sample. Acetone and ethanol precipitation of the protein

from the guanidine extract resulted in a protein precipitate that could not be dissolved, thus guanidine could not be fully removed from the sample and this extraction method was not utilised for further analysis. Hence, only tri-reagent extracted proteins were used for ELISA and western blotting analysis.

Tri-reagent extracts were filtered using microcon 10 kDa centrifugal filters (Millipore). Filtration allowed all proteins below 10 kDa along with other small molecules (potentially excess/unbound SDS) to be filtered out of the sample, while retaining all protein above 10 kDa. The concentrated retentate could then be recovered for further analysis. Filtering in this way concentrated gecko tail protein extracts approximately 10-fold, but it was not known whether filtering out some SDS may have affected the solubility of some proteins within the extract. However, a percentage of SDS could still be detected within filtered sample, as these samples still displayed frothing/ bubbling upon agitation, characteristic of the presence of SDS.

5.3.2. WESTERN BLOTTING

Gecko tail protein extracts were run under reducing conditions in SDS-PAGE. α-actin was used as an internal loading control to standardise target protein results. However, significant variability was apparent in actin-blotted samples. This variability appeared to be due to errors in the quantitation of total protein, rather than to differences in actin expression between gecko tail extracts. Despite loading 50 μg of total protein for all samples some would occasionally show no actin and no target protein expression. This was not limited to a certain experimental group but was a random occurrence. Variability was not just limited to between experimental groups (i.e. different regeneration stages) but intra group variability was also observed. Coomassie staining of these samples resolved by SDS-PAGE would also show little to no protein present (data not shown) despite the BCA assay showing high total protein content. Therefore, for some samples something within the protein sample was interfering

with the quantitation of total protein providing false results. Samples used for quantitative analysis were those, which showed consistent protein concentration by Coomassie staining.

5.3.2.1. VEGF-C

Filtered protein extracts were subjected to western blotting using an antibody directed against recombinant full-length mature rat VEGF-C. A main band was observed for the majority of positive samples at approximately 64 kDa and minor bands were observed for some samples at 48, 56 and 80 kDa (Fig. 5.1A). Banding patterns were generally similar, but some samples did display an absence of one or more of these 4 bands and/or the presence of extra bands. Likewise, the relative intensity of the bands differed between samples. In some samples the 64 kDa band was the most intense, whereas in others one of the lower molecular weight bands showed higher densitometry values. A band representing the fully processed (mature) form of the VEGF-C protein, expected to be 21 kDa in size if comparable to other vertebrates, was not observed by western blotting. Densitometry analysis of the major 64 kDa band standardised to α-actin and the quality control, revealed that VEGF-C protein expression is higher in 4 week regenerates than in original tails ($P < 0.01$, Fig. 5.1.B). VEGF-C protein expression remains unchanged between all other regenerate time points and original tails.

Figure 5.1. Western blotting analysis of gecko vascular endothelial growth factor C (gVEGF-C). (A) Representative western blot images for anti-VEGF-C and anti-actin in all regeneration stages and in original tails. Images are from different blots. (B) Normalised expression of gVEGF-C within protein extracts from regenerating gecko tails was determined by densitometry of western blots. Time points selected were 4 (n=6), 5 (n=5), 6 (n=6), 7 (n=5), 8 (n=3), 9 (n=4), 10 (n=6), 12 (n=5) weeks following autotomy and fully regenerated (FR; >24 wks, n=7) and original tails (OR, n=6). Protein expression was standardised to a quality control sample run on each gel and normalised to α-actin and data are expressed as mean ± SEM. Comparisons of experimental groups were performed using a 1-way ANOVA ($P < 0.0001$), followed by Dunnett multiple comparisons tests. *$P < 0.01$ compared to OR.

A

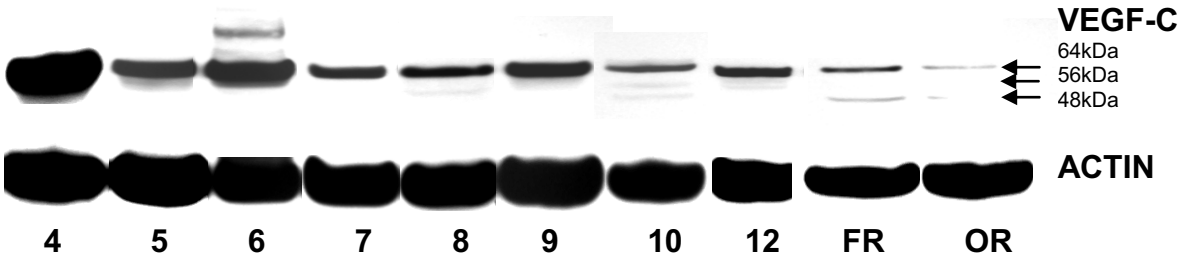
VEGF-C
64kDa
56kDa
48kDa
ACTIN
4
5
6
7
8
9
10
12
FR
OR

B

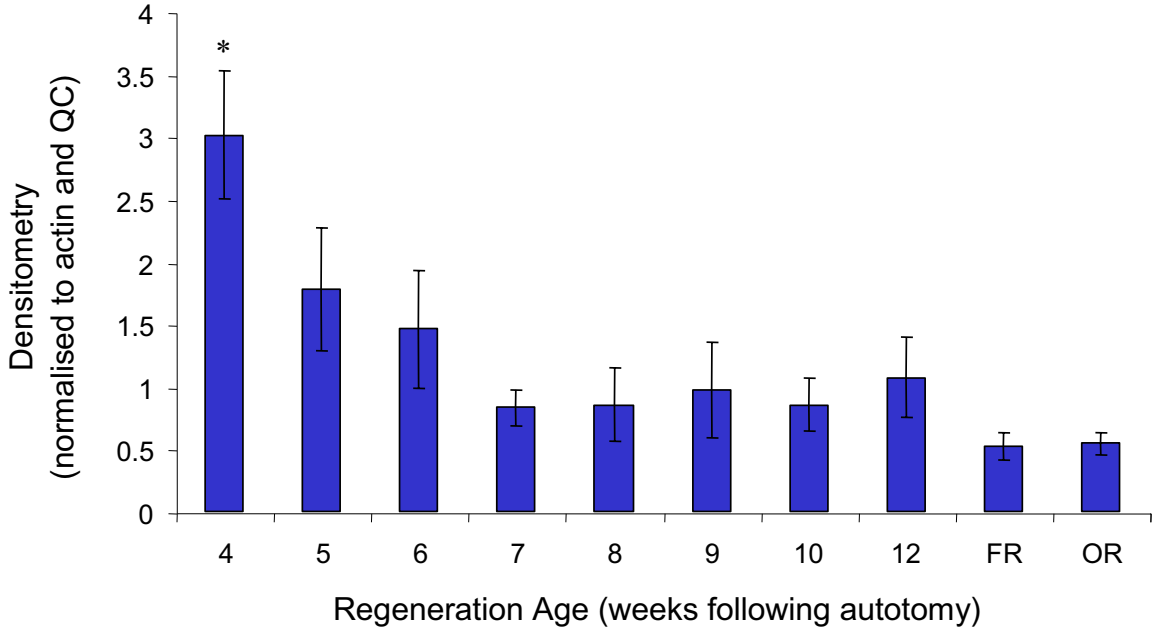
Densitometry
(normalised to actin and QC)
4
3.5
3
2.5
2
1.5
1
0.5
0
*
4
5
6
7
8
9
10
12
FR
OR
Regeneration Age (weeks following autotomy)

5.3.2.2. VEGF-D

Resolved protein samples were probed with an antibody directed against a synthetic peptide selected from the C-terminal region of human VEGF-D. Banding patterns of VEGF-D in gecko tail extracts showed multiple bands and were highly variable between samples (Fig. 5.2A). Generally 4 darker bands were observed at approximately 65, 60, 55 and 43kDa. However, the intensity of each of these bands differed between samples and was not limited to inter-experimental group variation. VEGF-D detection was not as intense as for VEGF-C and often required longer exposure times. Furthermore, VEGF-D staining appeared to be less precise, less reproducible and often very faint or undetectable, requiring many blots to be repeated. This reduced the available sample size, as there was not always sufficient protein to repeat gels more than twice. When enough sample was available and both duplicate runs worked then replicate blots were comparable. As no clear main band could be distinguished, densitometry analysis was performed on all bands present within each lane (Fig. 5.2B). Standard deviations between samples within experimental groups were high, suggesting that western blot analysis for this protein was not very accurate. No significant differences were observed in protein expression between regenerates and original tails.

Figure 5.2. Western blotting analysis of gecko vascular endothelial growth factor D (gVEGF-D). (A) Representative western blot images for anti-VEGF-D and anti-actin in all regeneration stages and in original tails. Images are from different blots. (B) Normalised expression of gVEGF-D within protein extracts from regenerating gecko tails was determined by densitometry of western blots. Time points selected were 4 (n=6), 5 (n=4), 6 (n=5), 7 (n=5), 8 (n=3), 9 (n=4), 10 (n=4), 12 (n=4) weeks following autotomy and fully regenerated (FR; >24 wks, n=4) and original tails (OR, n=3). Protein expression was standardised to a quality control sample run on each gel and normalised to α-actin and data are expressed as mean ± SEM. Comparisons of experimental groups were performed using a 1-way ANOVA ($P > 0.05$, considered not significant).

A

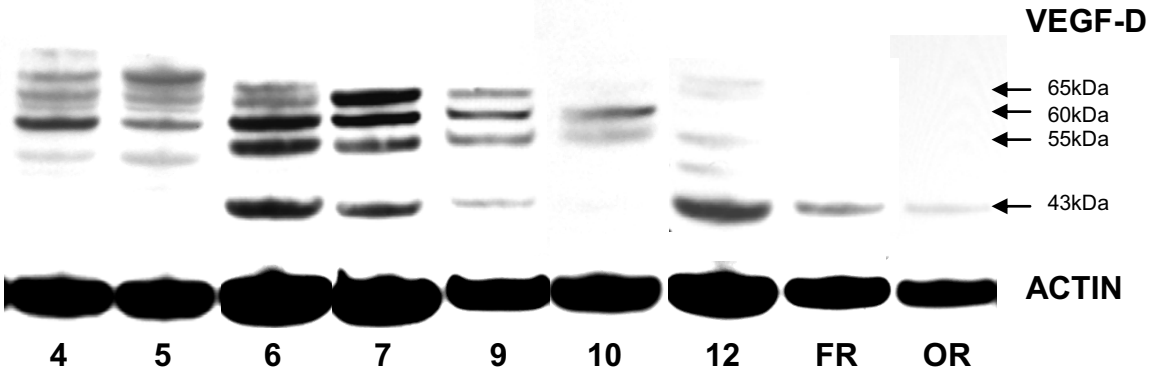
VEGF-D
65kDa
60kDa
55kDa
43kDa
ACTIN
4
5
6
7
9
10
12
FR
OR

B

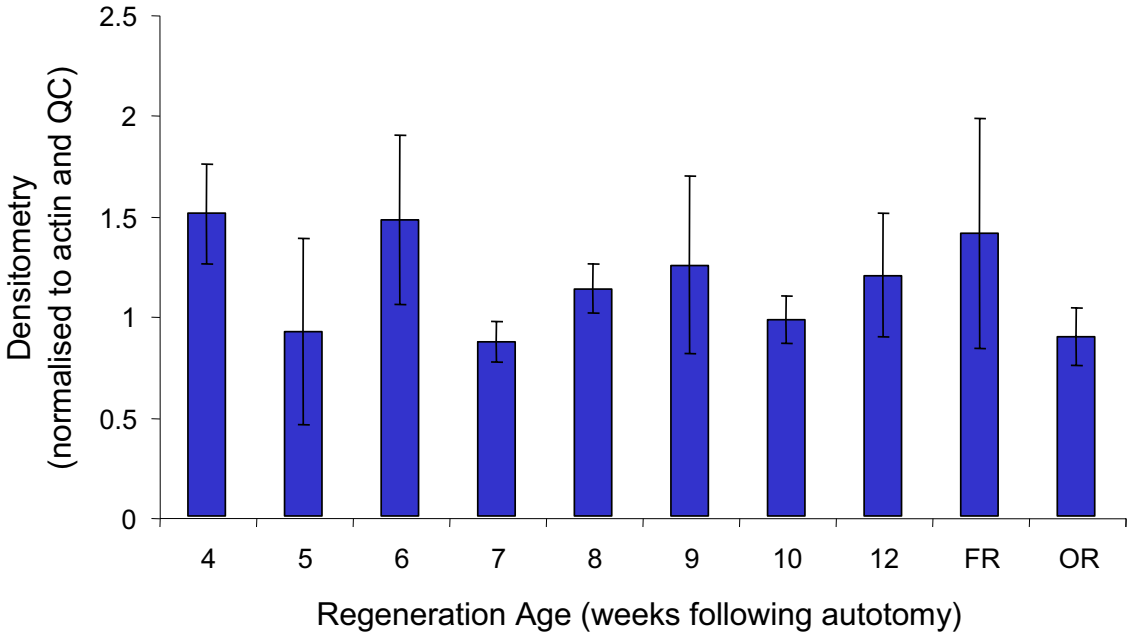
Densitometry
(normalised to actin and QC)
2.5
2
1.5
1
0.5
0
4
5
6
7
8
9
10
12
FR
OR
Regeneration Age (weeks following autotomy)

5.3.2.3. VEGFR-3

To analyse VEGFR-3 protein expression in gecko tail extracts, western blotting was performed using an antibody directed against a synthetic peptide selected from the C-terminal region of human VEGFR-3. Multiple bands were observed in VEGFR-3 probed blots ranging from 100 kDa to 240 kDa (Fig. 5.3A). Banding pattern profiles were highly variable between samples, making it difficult to distinguish major bands and high levels of band smearing was also apparent. As for VEGF-D, densitometry analysis of VEGFR-3 protein expression was performed on all bands within the lane due to a lack of one specific sized major band for all samples (Fig. 5.3B). No significant differences were observed for VEGFR-3 protein expression between different regeneration stages and original tails.

Figure 5.3. Western blotting analysis of gecko vascular endothelial growth factor receptor 3 (gVEGFR-3). ***A.*** Representative western blot images for anti-VEGFR-3 and anti-actin in all regeneration stages and in original tails. Images are from different blots. ***B.*** Normalised expression of gVEGFR-3 within protein extracts from regenerating gecko tails determined by densitometry on western blots. Time points selected were 4 (n=6), 5 (n=4), 6 (n=6), 7 (n=5), 8 (n=3), 9 (n=4), 10 (n=4), 12 (n=5) weeks following autotomy and fully regenerated (FR; >24 wks, n=7) and original tails (OR, n=2). Protein expression was standardised to a quality control (QC) sample run on each gel and normalised to α-actin and data are expressed as mean ± SEM. Comparisons of experimental groups were performed using a 1-way ANOVA ($P > 0.05$, considered not significant).

A

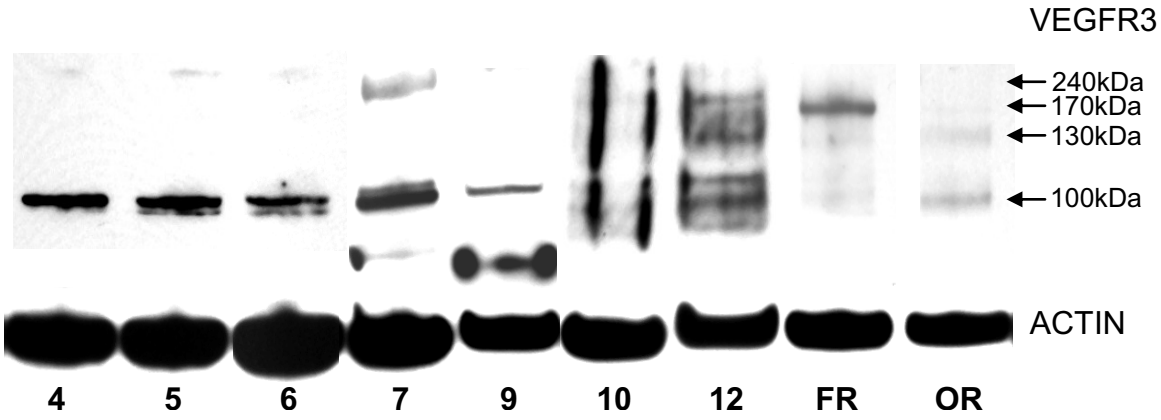
VEGFR3
240kDa
170kDa
130kDa
100kDa
ACTIN
4
5
6
7
9
10
12
FR
OR

B

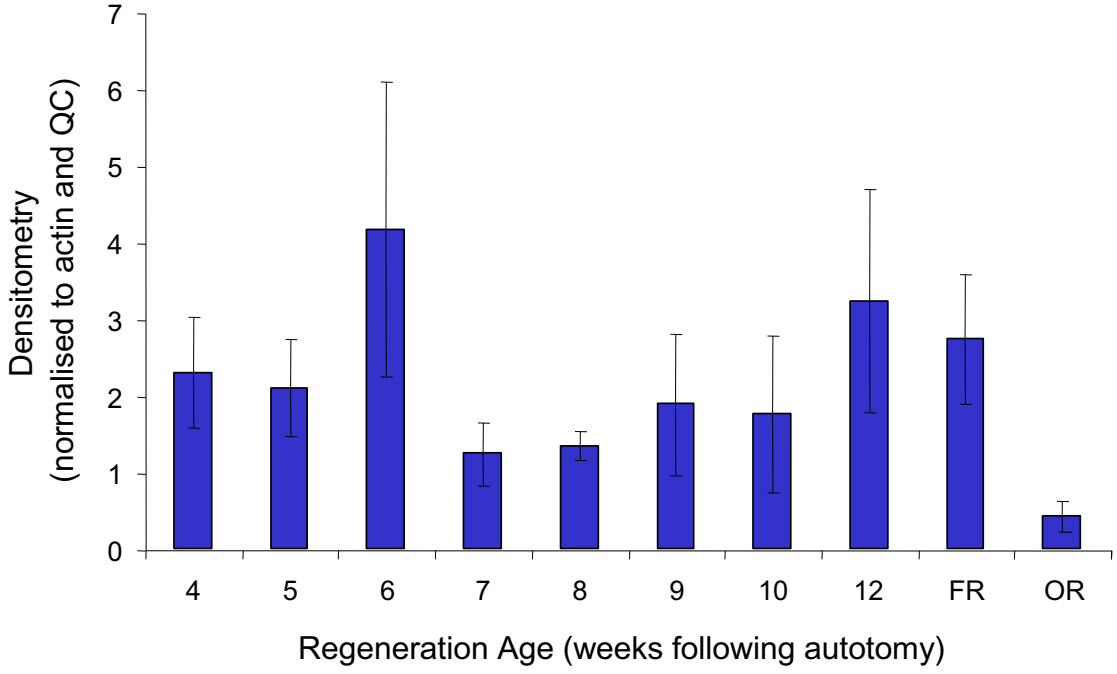
Densitometry
(normalised to actin and QC)
0
1
2
3
4
5
6
7
4
5
6
7
8
9
10
12
FR
OR
Regeneration Age (weeks following autotomy)

5.3.3. ELISA

Direct and indirect ELISA methods were attempted to gain measures of protein concentration for gVEGF-C, gVEGF-D and gVEGFR-3. Many protocols were attempted for both methods (sections 5.2.5.1. and 5.2.5.2.), but despite altering blocking conditions, protein concentrations, antibody concentrations and incubation times, the gecko proteins were either expressed in too low a concentration, were not bound by the antibodies used or were contaminated with factors capable of inhibiting either the antibody/antigen interaction or the enzymatic colour development reaction. Therefore, no reliable results were obtained for any of the three proteins.

5.3.3.1. VEGF-C

A standard curve was generated using serial dilutions of the recombinant hVEGF-C standard (an example is provided in Fig. 5.4.A) using the sandwich ELISA protocol. Correlation coefficients for this MMF model curve (R^2=0.998) suggest a high probability of predicting reliable and accurate estimations for VEGF-C protein quantitation. Absorbance values generated from several gecko protein extracts are shown in Fig. 5.4.B. gVEGF-C values were either too low to fit on the standard curve or varied greatly between experiments. In many cases serially increasing protein concentrations resulted in serially decreasing absorbance values, suggesting the presence of an inhibiting factor in the protein extract.

Figure 5.4. VEGF-C ELISA on extracted protein from original and regenerated gecko tails. (A) Representative image of rhVEGF-C standard curve generated using CurveExpert 1.38 software and utilising the Morgan-Mercer-Flodin sigmoidal Model. Values for the rhVEGF-C dilution series are 1000 for 1/1000 dilution, 125 for 1/8000, 31.25 for 1/32000, 15.625 for 1/64000 and 7.8125 for 1/128000 dilution. (B) Examples of absorbance and concentration values from gecko tail extracts. Many values are either indistinguishable from zero or display distinct levels of inhibition with increasing protein concentration.

A

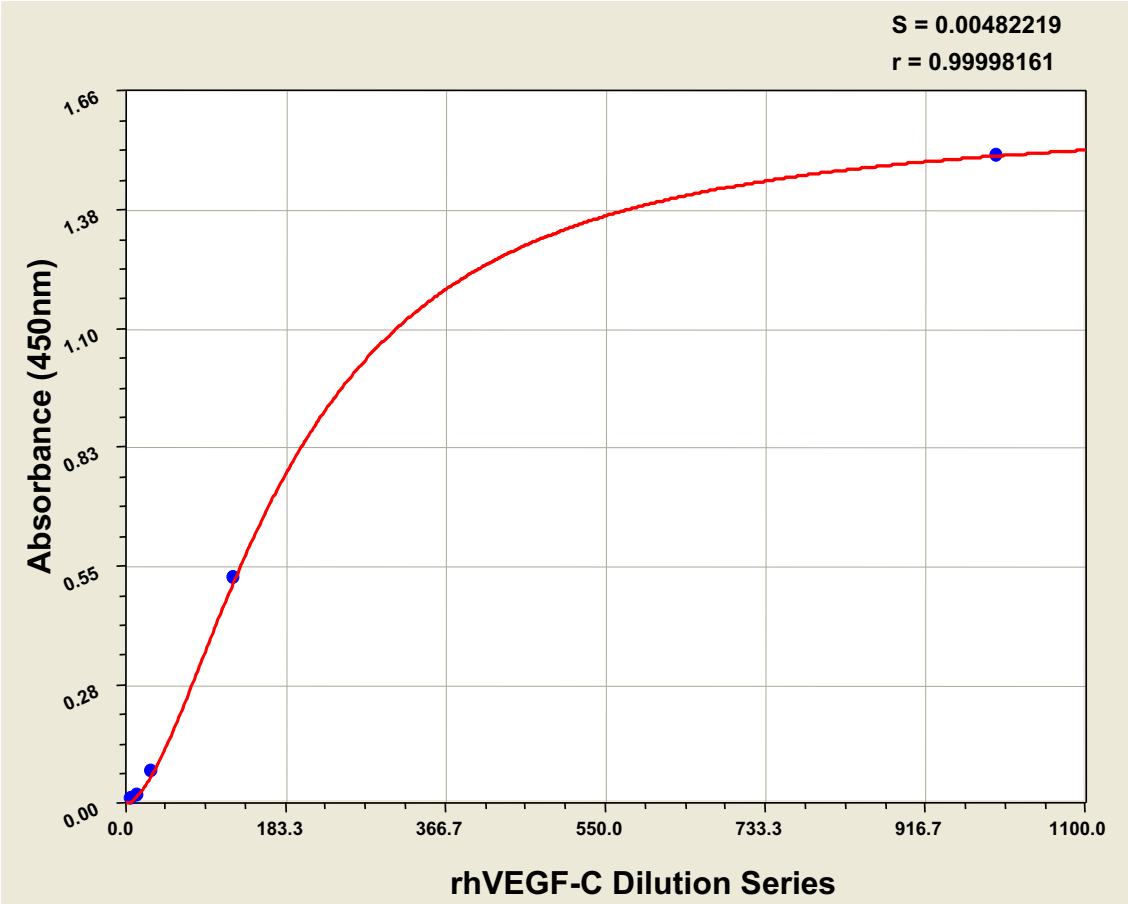
S = 0.00482219
r = 0.99998161
Absorbance (450nm)
1.66
1.38
1.10
0.83
0.55
0.28
0.00
0.0
183.3
366.7
550.0
733.3
916.7
1100.0
rhVEGF-C Dilution Series

B

Target Protein	Sample	Sample Concentration (μg total protein/well or dilution factor)	ELISA Absorbance (corrected for Zero)	Concentration based on standard curve
VEGF-C	V1	1/1000	1.5053	1000.10
VEGF-C	V2	1/8000	0.5216	124.97
VEGF-C	V3	1/32000	0.0744	31.99
VEGF-C	V4	1/64000	0.0158	12.59
VEGF-C	V5	1/128000	0.0105	9.92
VEGF-C	11wk	150	0.0620	28.58
VEGF-C	11wk	50	0.0679	30.23
VEGF-C	11wk	17	0.0468	24.065
VEGF-C	11wk	4	0.0198	14.37
VEGF-C	13wka	13	0.0301	18.44
VEGF-C	13wka	7	0.0148	12.11
VEGF-C	13wka	2.2	0.0163	12.82
VEGF-C	10wkb	60	0.0181	13.63
VEGF-C	10wkb	30	0.0232	15.79
VEGF-C	10wkb	5	0.0315	18.95
VEGF-C	13wkb	65	0.1410	47.99
VEGF-C	13wkb	33	0.1299	45.50
VEGF-C	12wk	70	0.1856	57.54
VEGF-C	12wk	50	0.1990	60.32
VEGF-C	12wk	35	0.1969	59.88
VEGF-C	12wk	20	0.1704	54.35
VEGF-C	FR2	30	0.0632	28.92
VEGF-C	FR2	15	0.0716	31.24
VEGF-C	FR5	30	0.0187	13.90
VEGF-C	FR5	15	0.0270	17.28

5.3.3.2. VEGF-D

Recombinant hVEGF-D did not react with anti-VEGF-D (either in the ELISA or on a dot blot) and thus a standard curve could not be generated. Absorbance results for gecko samples used in direct and indirect ELISAs are shown in Table 5.3. and as for VEGF-C were not reliable and could not be used for VEGF-D quantitation.

Table 5.3. VEGF-D ELISA on protein extracts from regenerating gecko tails.

Target Protein	Sample	Sample Concentration (μg total protein/well or dilution factor)	ELISA Absorbance (corrected for Zero)
VEGF-D	10wka	50	0.0201
VEGF-D	10wka	140	0.0056
VEGF-D	13wka	26	0.0126
VEGF-D	13wka	13	0.0124
VEGF-D	13wka	4.3	0.0156
VEGF-D	13wkb	18	0.0095
VEGF-D	13wkb	9	0.0029
VEGF-D	13wkb	3	0.0099
VEGF-D	10wkb	7	0.0762
VEGF-D	10wkb	3.5	0.0832
VEGF-D	10wkb	1.725	0.1073
VEGF-D	FR1	30	0.0234
VEGF-D	FR1	15	0.0050
VEGF-D	OR2	30	-0.0011
VEGF-D	OR2	15	-0.0017
VEGF-D	VD1	1/10	-0.0023
VEGF-D	VD2	1/20	0.0056
VEGF-D	VD3	1/40	0.0032

Examples are provided of absorbance values from a sandwich ELISA protocol of serial dilutions of protein extracts from original tailed geckos (OR2), full regenerates (FR1), several different regenerates (10, 13 and 14 weeks following autotomy) and the rhVEGF-D standard (VD1-3). Many values can be seen to be either indistinguishable from zero or displaying increased absorbance values for decreasing sample concentration i.e. inhibition of the ELISA.

5.3.3.3. VEGFR-3

Recombinant hVEGFR-3 did not react with the anti-VEGFR-3 antibodies (either in ELISA or a dot blot), thus no standard curve was produced. Results for gecko samples are shown in Table 5.4. and show a lack of/ or inhibition of antibody binding to the gecko protein.

Table 5.4. VEGFR-3 ELISA on protein extracts from regenerating gecko tails.

Target Protein	Sample	Sample Concentration (dilution factor)	ELISA Absorbance (corrected for Zero)
VEGFR-3	9wka	Neat	0.0277
VEGFR-3	9wka	1/4	0.0174
VEGFR-3	9wka	1/16	0.0019
VEGFR-3	9wka	1/64	-0.0028
VEGFR-3	7wka	Neat	0.0121
VEGFR-3	7wka	1/4	0.0024
VEGFR-3	7wka	1/16	-0.0032
VEGFR-3	7wka	1/64	-0.0086
VEGFR-3	13wka	Neat	0.0147
VEGFR-3	13wka	1/3	0.0056
VEGFR-3	13wka	1/6	0.0071
VEGFR-3	7wka	Neat	0.0160
VEGFR-3	7wka	1/2	0.0116
VEGFR-3	7wka	1/6	0.0134
VEGFR-3	14wka	Neat	0.0145
VEGFR-3	14wka	1/2	0.0115
VEGFR-3	14wka	1/6	0.0099

Examples are provided of absorbance values from a direct ELISA protocol of serial dilutions of protein extracts from several different regenerates (7, 9, 13 and 14 weeks following autotomy). Many values can be seen to be either indistinguishable from zero, unreproducible in different assays for the same protein sample or displaying increased absorbance values for decreasing sample concentration i.e. inhibition of the ELISA.

5.3.4. IMMUNOHISTOCHEMISTRY TO DETECT gVEGFR-3

In Chapter 3, immunostaining of gVEGFR-3 within gecko tail tissue sections yielded no positive staining. Troubleshooting performed to detect gVEGFR-3 expression is described in this chapter. An antibody directed against human VEGFR-3 was used on paraffin embedded sections with ultimately limited success in terms of obtaining positive staining of gVEGFR-3 on gecko lymphatic and/or blood endothelial cells. Negative controls, consisting of the antibody diluent without primary antibody, were performed for each tissue section and were always devoid of staining. As for the ELISAs many different protocols were attempted (listed in Table 5.2.). These included changing antigen retrieval conditions, altering blocking conditions, increasing antibody incubation times and temperatures and changing detection systems. However, none of these factors was successful in yielding positive results on endothelial cells. Initial results for VEGFR-3 staining showed dark positive staining over the entire tissue section that did not appear to be specific, despite negative controls being clear. However, refining antibody concentration and blocking conditions reduced this problem to display what appeared to be highly specific staining that was limited purely to adipose tissue and in particular appeared to be on adipocytes themselves. Figs 5.5. and 5.6. display examples of adipocyte staining in original and regenerating tissues, respectively, using the anti-VEGFR-3 antibody. Dark positive staining is evident in adipose deposits in subcutaneous tissue in original and to a lesser extent regenerate tail tissue sections, where fewer subcutaneous adopose deposits are apparent. Positive staining is also observed deeper within the central region of the tail, between the muscle bands surrounding the vertebrae of original tails and the cartilage tube of regenerating and fully regenerated tails. Neither lymphatic nor blood endothelial cells were specifically stained in gecko tail tissue.

Figure 5.5. VEGFR-3 positive immunostaining within adipose tissue of original gecko tails. Specific positive staining (brown) of VEGFR-3 was seen surrounding adipocytes in fat masses in both subcutaneous tissues (A) and within muscle bands and central connective tissue surrounding the vertebrae (C). H&E staining of a serial section shows the histology of these regions highlighting aggregated adipocytes and blood vessels within the fat masses (B and D). Muscle tissue (m) displays a light brown stain. It is unclear if this is specific positive staining. Lymphatic and blood endothelial cells do not appear to show any positive staining. Arrows indicate obvious vessels of lymphatic characteristics and arrowheads indicate obvious blood vessels. Scale bars represent 200 μm in A and B and 100 μm in C and D.

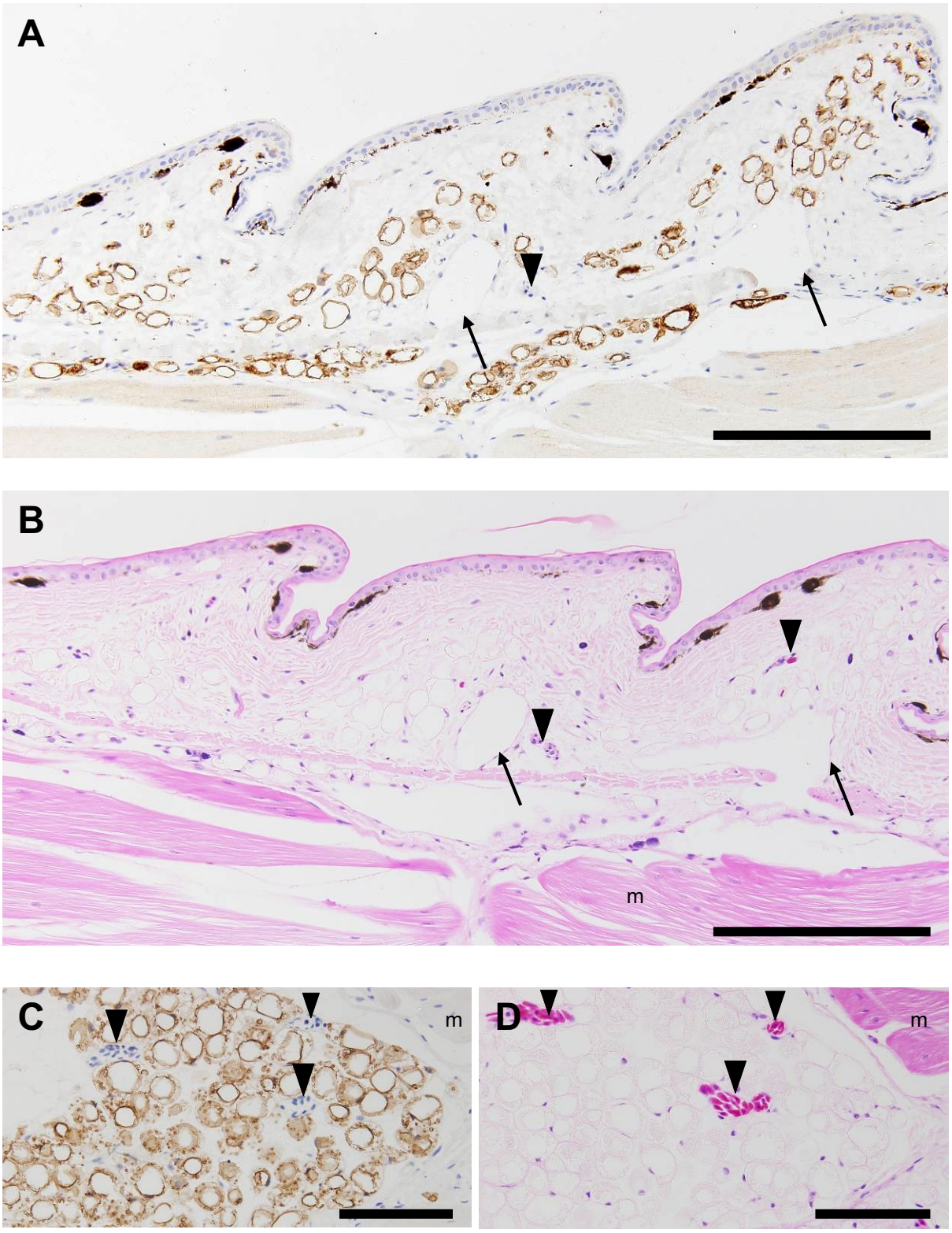
A
B
m
C
m
D
m

Figure 5.6. VEGFR-3 positive immunostaining within adipose tissue of regenerating gecko tails. Specific positive staining (brown) of VEGFR-3 was seen surrounding adipocytes in fat masses in 5 week (A), 9 week (C) and full regenerates (D) within central connective tissue surrounding the vertebrae. H&E staining of a serial section shows the histology of these regions highlighting aggregated adipocytes and blood vessels within the fat masses (B, D and F). Adipocytes within subcutaneous tissues also stained positively for VEGFR-3 in full regenerates (G). Earlier regenerates did not appear to have as much subcutaneous fat as full regenerates and thus did not have positive staining in this region. Muscle tissue (m) displays a light brown stain. It is unclear if this is specific positive staining. Lymphatic and blood endothelial cells do not appear to show any positive staining. The caudal artery (a) is seen in images C and D. Nervous tissue (n) is apparent in images E and F. Arrows indicate obvious vessels of lymphatic characteristics and arrowheads indicate obvious blood vessels. Scale bars represent 200 μm in A, B, E, F and G and 100 μm in C and D.

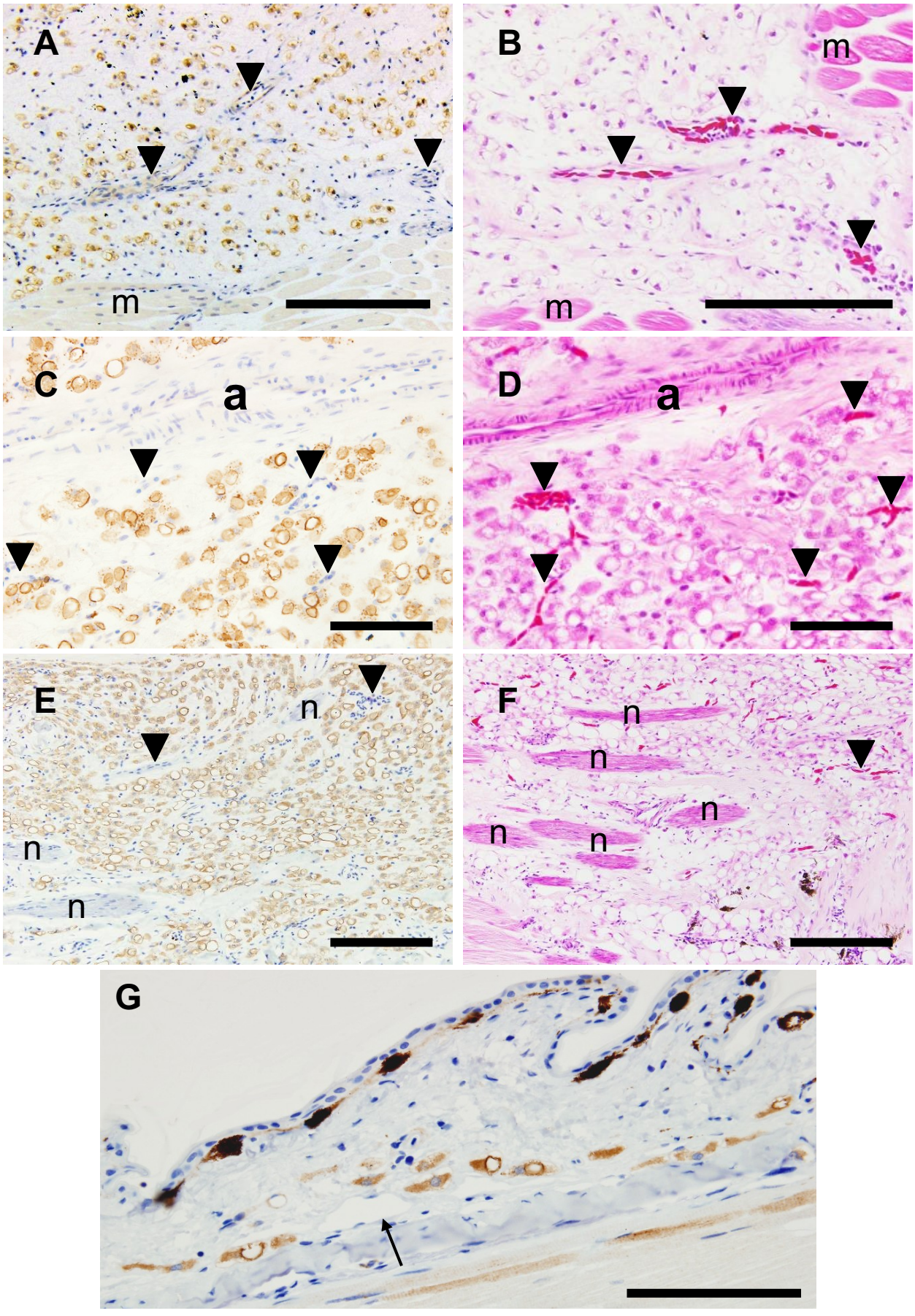
A
m
B
m
m
C
a
D
a
E
n
n
n
F
n
n
n
n
n
G

5.4. DISCUSSION

In this chapter I aimed to confirm the presence of gVEGF-C, gVEGF-D and gVEGFR-3 proteins within protein extracts from original and regenerating gecko tails and corroborate mRNA expression data by determining protein expression profiles of these growth factors and their receptor throughout tail regeneration. Identifying the location of expression of gVEGFR-3, matching protein expression profiles with different lymphangiogenic states, along with the locations of gVEGF-C and gVEGF-D protein expression identified in Chapter 3, would provide more evidence for the role of the VEGF-C/ -D/R-3 pathway in the growth of new lymphatic vessels throughout gecko tail regeneration. The results of this work, however, remain largely inconclusive either due to problems with inhibiting factors in protein extracts or due to a lack of antibody specificity for the target antigens on the gecko proteins.

Protein extraction from the gecko tails appeared to be suboptimal in that both protein extraction methods had significant limitations. The tri-reagent extraction suffered from low protein yields, high SDS concentrations required for protein pellet solubilisation and the presence of inhibiting factors that prevented the accurate determination of total protein concentration and ELISA analyses for the proteins of interest. While the guanidine/triton extraction process provided higher yields, it resulted in fat deposits within the sample making filtering and washing out the guanidine unachievable. Thus, guanidine/ triton extracted samples could not be used in downstream analyses.

The apparent presence of an unknown compound or substance within the tri-reagent extracted samples that yielded false measurements of total protein concentration in the case of some samples (observed by Coomassie staining of SDS-PAGE gels and by underexpression or absence of the actin loading control) is puzzling. False BCA results are particularly perplexing given that not all samples reacted in the same fashion and the majority of samples did appear to be accurately quantitated. There are some substances that are known to interfere

with the BCA assay including those with reducing potential, chelating agents, and strong acids or bases. However, we would not expect that any of these would be present within properly extracted gecko protein SDS has been known to be an inhibiting factor of the BCA assay, however; only concentrations above 5% are incompatible with the kit used.

Lipids may also interfere with the BCA assay and while it is unlikely that lipid would remain after the tri-reagent extraction process (given that protein is precipitated using acetone, a method recommended for removing conflicting substances by the BCA protocol, and vigorously washed), even minute amounts of lipid or lipoproteins could result in higher absorbance values and thus higher calculated concentrations. Further studies aimed at optimising protein extraction and total protein concentration assays and eliminating any incompatible substances, need to be performed. Use of the Bradford method for quantifying total protein concentration was not possible due to its incompatibility with concentrations above 0.1% of SDS. Dialysis of the phenol-ethanol supernatant (from the tri-reagent method) against 0.1% of SDS may reduce potential problems with high SDS concentrations. However, this may also reduce the solubility of some proteins. Another potential extraction buffer could include lysis buffer (8M Urea, 50 mM Tris-HCl, pH 7.6, 0.1 M 2-mercaptoethanol, 1 mM DTT and 1mM phenylmethylsulphonyl fluoride) using the extraction protocol of Sybert (1985). However, given that high urea concentrations can also interfere with total protein quantitation and western blotting and ELISA protocols, extracts from this method would also require further filtering and may be problematic.

Inhibition within ELISA assays was apparent for some (but not all) tri-reagent extracted proteins. Despite increasing the amount of total protein in some samples, absorbance values were reduced. However, whether this was true inhibition or more a result of the very low absorbance values detected for most samples is unclear. Further, the precise nature of the substances that could be present within the extract capable of inhibiting the

ELISA reaction is unclear. It is also possible that it is not inhibition of the ELISA that is causing these results but an issue with the specificity and/or strength of the antibody-antigen interaction. The strength of the standard curve relationship for the rhVEGF-C dilution series (R^2=0.9999632) demonstrates the validity of the ELISA methodology. Hence it is possible that the lack of detection of VEGF-C in the gecko protein extracts is due to poor antibody specificity.

All results from western blotting, ELISAs and IHC showed a high level of variability. Potentially positive results were obtained for all techniques but suffered from lack of reproducibility (both in the same and in different samples) and reliability. Western blotting appeared the most successful technique and banding patterns observed for gVEGF-C, gVEGF-D and gVEGFR-3 were all within expected size ranges indicating firstly that these proteins are indeed present within the gecko tail extracts and that the antibodies used can, at least to some extent, recognise the gecko proteins. Bands of approximately 64 kDa, 56 kDa and 48 kDa for gVEGF-C are consistent with different sized propeptides of the protein at different stages of proteolysis. These band sizes resemble those of proVEGF-C precursors detected previously in gecko samples using a different VEGF-C antibody (58 kDa and 43 kDa) (Daniels et al. 2003), in recombinant human proVEGF-C expressed in different cell types (Joukov et al. 1997b; Zeng et al. 2004) and in zebrafish cells transfected with proVEGF-C cDNA (approximately 59kDa) (Khatib et al. 2010). Furthermore, the detected 48 kDa band in this study corresponds to the predicted 47.8 kDa MW from the translated amino acid sequence of gVEGF-C (see Chapter 4). Mature, fully processed, gVEGF-C protein (expected at 21 kDa) was not detected by western blotting, despite the fact that the antibody was raised against recombinant ΔNΔC –VEGF-C (i.e. protein without N- and C- terminals). It is possible that fully processed forms are present within the gecko samples at very low concentrations so that they are not detectable by western blotting. It may also be possible that

mature gVEGF-C is not present within samples, as the extraction process may not have efficiently recovered extracellular secreted proteins. Alternatively, smaller proteins may have been lost in the extraction and filtration processes. It is unlikely; however, that geckos would not possess mature VEGF-C as the gecko sequence obtained in Chapter 4 does contain amino acid sequences corresponding to proteolytic cleavage sites in similar relative positions as in mammals.

Banding patterns for gVEGF-D (approximately 65, 60, 55 and 43 kDa) and gVEGFR-3 (approximately 100, 130, 179 and 240 kDa) detected by western blotting, are consistent with the predicted MW from amino acid sequences (40 kDa for VEGF-D and 157.6 kDa for VEGFR-3). Furthermore, some of these bands are consistent with previous studies. For VEGF-D, bands of approximately 60 kDa and 53 kDa, corresponding to unprocessed VEGF-D (in cell media) have been identified (Stacker et al. 1999; Zeng et al. 2004) and the VEGF-D antibody specification sheet lists expected sizes of 40 and 72 kDa. Given that the VEGF-D antibody used is directed against the C-terminal of the protein it would not be expected to detect the mature VEGF-D protein. Previous studies examining VEGFR-3 have described bands at 125, 175 and 195 kDa from specific cell lysates and in recombinant human and mouse proteins that reflect a proteolytically cleaved form, an intracellular unglycosylated precursor and the uncleaved form, respectively (Bando et al. 2004; Breslin et al. 2007; Kukk et al. 1996; Pajusola et al. 1994). The bands observed for gVEGFR-3 are not too dissimilar to these different forms of VEGFR-3. Differing band sizes above the predicted size (140kDa from the antibody datasheet and 157.6kDa from amino acid sequence prediction) for gVEGFR-3 may represent glycosylated forms of the protein (band smearing was apparent in many samples as further evidence of glycosylation) and band sizes below may be a result of proteolysis of the receptor.

Positive detection with human antibodies at sizes comparable to those identified in other studies provides evidence for the presence and expression in regenerating tail tissue of gecko VEGF-C, VEGF-D and VEGFR-3. However, densitometric analysis performed to quantify relative expression of these proteins at different stages of regeneration displayed high levels of variation (high standard deviations) and poor reproducibility, particularly for VEGF-D and VEGFR-3. Given the observed variability along with potential issues in total protein quantitation, data obtained from the western blot analyses cannot be taken as conclusive.

As for ELISAs, high levels of variability in densitometric analysis may be a result of issues in the specificity of the antibody-antigen reaction. Many factors can impact on the antibody-antigen reaction and can include temperature, pH, ionic strength, relative concentration of antigen and antibody, antigen density (number of antigen sites per protein) and the antibody affinity/ specificity for the given antigen (Reverberi and Reverberi 2007). If antibody affinity is low, these other factors can have a greater impact on the antibody-antigen reaction, than if the affinity were high. In Chapter 4, I showed that gVEGF-C, gVEGF-D and gVEGFR-3 are highly similar both structurally and at a sequence level to their mammalian orthologues. It was therefore assumed that commercial antibodies directed against mammalian proteins (no reptilian or even bird antibodies are commercially available at present to the best of my knowledge) would be sufficiently homologous to allow gecko protein binding. Other studies examining specific protein expression in regenerating lizard tissues has shown sufficient cross-reactivity using mammalian antibodies. Fibroblast growth factor-1 (FGF1) and FGF2 have both been accurately immunolocalised in regenerating tail sections of the lizard *Lampropholis guichenoti* utilising antibodies directed against mammalian FGFs (Alibardi and Lovicu 2010). It appears that high levels of antibody cross-reactivity predicted by homology to the antibody target species may not be the case for the VEGFs and VEGFRs. Very slight differences in the conformation of proteins can alter the

degree of fit between the antibody and antigen and result in a much lower affinity reaction (Absolom and van Oss 1986; Braden and Poljak 1995; Collawn et al. 1988), thus binding may either not take place or may not occur to a degree that is detectable or may easily be disrupted by other factors. Thus, while the VEGF-C, VEGF-D and VEGFR-3 antibodies do appear to be sufficiently cross-reactive to display the presence of the reptilian proteins, the antibody-antigen interaction may not be to a high enough affinity to be quantifiable.

Densitometric analysis of VEGF-C provided the least variability and demonstrated a pattern of higher protein expression in early tail regeneration, with significantly increased levels in tails at 4 weeks of regeneration compared to original tails. This pattern is consistent with mRNA expression data (Chapter 3) and indicates that highly expressed mRNA (at least in 4 week regenerates) is being translated effectively into protein. Tissue expression sites of gVEGF-C include keratinocytes, fibroblasts and adipose tissue (Chapter 3), sites that are consistent with a role for gVEGF-C in lymphangiogenesis within the regenerating tail. Increased levels of VEGF-C protein expression may therefore lead to LEC survival, proliferation and migration (Makinen et al. 2001b) and lymphatic vessel formation (Anisimov et al. 2009; Szuba et al. 2002) in subcutaneous tissue and in internal adipose deposits.

Immunolocalisation of gVEGFR-3 in original and regenerating gecko tail tissues is puzzling. Positive binding that appears highly specific was observed in adipose tissue only, and appeared to be restricted to adipocytes. Endothelial cell binding was not observed. Sites of expression of VEGFR-3 in other species have been limited to lymphatic endothelia in embryonic and adult tissues and blood endothelia in embryonic tissues, some tumours and wounds (Petrova et al. 2008; Witmer et al. 2001). VEGFR-3 expression has also occasionally been observed on macrophages and dendritic cells (Berggreen et al. 2009; Hamrah et al. 2003; Maruyama et al. 2005; Schoppmann et al. 2002a). VEGFR-3 mRNA has been detected in adipose tissue of mice (Voros et al. 2005). However, the subcutaneous and gonadal fat pads

extracted were not purely made up of adipocytes and may also have included lymphatic and blood vasculature. Adipocytes express VEGF-A (Zhang et al. 1997) and both angiogenesis and lymphangiogenesis have been suggested to be regulated by adipose tissue at times of fat deposition to maintain adequate blood supply and homeostasis in the growing fat deposit (Harvey 2008; Hausman and Richardson 2004). Therefore, adipose tissue in regenerating gecko tails may contain lymphatic vasculature and thus express VEGFR-3, however, it is unclear whether it is realistic for adipocytes themselves to express VEGFR-3. Geckos contain a meshlike arrangement of lymphatic vessels within the tail fat deposits (Ottaviani and Tazzi 1977), however the observed staining does not appear to be vascular. gVEGF-C expression was also observed in adipose tissue in original and regenerating tails (Chapter 3). This expression pattern may either indicate adipose secretion of gVEGF-C or associations of gVEGF-C with gVEGFR-3 on cell surfaces. Thus, adipose deposits may secrete and/ or bind this growth factor and VEGF-C/VEGFR-3 binding may play an important role in lymphangiogenesis, angiogenesis and/or adipogenesis during times of fat store expansion. Alternatively, positive immunostaining of VEGFR-3 may be due to antibody cross-reactivity with an adipocyte specific protein and may not truly reflect the presence of VEGFR-3 in these cells. However, western blotting did identify VEGFR-3 positive bands at realistic sizes and so did appear to accurately identify VEGFR-3 in gecko tail extracts (although not to a level that was quantifiable).

gVEGFR-3 expression was not observed on lymphatic or blood endothelial cells, or on LYVE-1 positive vessels in full regenerates as identified in Chapter 3. This result could be due to either a lack of gVEGFR-3 expression on gecko endothelial cells, a lack of antibody specificity or expression below the level of detection of the assay. Consequently, further studies need to be performed using specific reptilian VEGFR-3 antibodies to examine specific

sites of expression within regenerating gecko tails and to identify the phenotype of both gecko lymphatic endothelial cells and gecko tail adipocytes (see section 6.4).

The immunogenic sites of the antibodies used in this study may impact on the ability of the antibody to cross-react with non-target species. The polyclonal anti-rat VEGF-C antibody used to analyse gVEGF-C protein expression was directed against the whole recombinant mature protein (ΔNΔC –VEGF-C). Protein analysis of gVEGF-C did appear to be more successful than for gVEGF-D and gVEGFR-3. This may be a result of the larger immunogen allowing for more antigenic sites to be available for antibody production. Furthermore, this region is also more homologous (compared to the N- and C- terminals) between the gecko and rat sequences. In the case of gVEGF-D and gVEGFR-3 the antibodies used were generated against small synthetic peptides. Hence, there would be fewer available antigenic sites and any sequence differences within these regions are more likely to impact antibody specificity. In particular, the anti-VEGFR-3 immunogenic site has 6 residues different between the gecko and human sequence within the 20-residue peptide. These residue differences are generally conservative but may nevertheless impact the conformation of the protein, thereby preventing antibody binding.

In conclusion, protein expression analysis demonstrated the expression of gVEGF-C, gVEGF-D and gVEGFR-3 within regenerating and original gecko tails. However, quantifying this expression was problematic and largely inconclusive using densitometric analysis of western blots and ELISA, likely owing to poor antibody specificity and affinity. Repeating this analysis using specific reptilian antibodies is necessary to identify if protein expression profiles of gVEGF-C, gVEGF-D and gVEGFR-3 match the mRNA expression profiles obtained in Chapter 3. Similarly, specific reptilian antibodies are needed to confirm the localisation of gVEGFR-3 to adipocytes in regenerating and original tailed geckos and to identify whether gecko LECs express gVEGFR-3.

Chapter Six

General Discussion

6.1. FUNCTIONAL EVIDENCE FOR THE PRESENCE OF LYMPHANGIOGENESIS IN THE REGENERATING GECKO TAIL

The lymphatic system is crucial in maintaining homeostasis within organisms by removing excess interstitial fluid from tissues, trafficking of immune cells and absorption of fat and fat-soluble vitamins. Accordingly, malformation or dysfunction of the lymphatic system results in many pathological conditions such as lymphoedema and certain inflammatory diseases. Furthermore, cancer cells can utilise the lymphatic vasculature for metastatic spread around the body. Thus, maintaining the structure and function of the lymphatic network is essential, particularly following injury. In this study, I have examined the lymphatic system at different stages within the unique setting of the regenerating gecko tail, with the focus being to describe the functional process and potential molecular regulation of lymphangiogenesis within the tails. The initial question stimulating this research was why are gecko tails not lymphoedematus given that the original lymphatic network is severed by autotomy? Chapter 2 of this thesis shows that lymphatic transport is restored by tail regeneration; lymph is cleared from the distal portion of the tail and delivered to the blood circulation from as early as 6 weeks of regeneration and lymphatic clearance and flow are returned to near normal levels by 12 weeks. While the transport characteristics change throughout the regeneration process the ability of excess interstitial fluid to be removed from tissues prevents lymphoedema. I have hypothesised that adequate fluid drainage from the tail is a consequence of lymphangiogenesis. The functional characteristics of lymph transport within regenerating tails observed in Chapter 2, along with the presence of LYVE-1 positive vessels that resemble the

architecture of mammalian lymphatics in fully regenerated tails (Chapter 3) confirms the regeneration of a new, functional lymphatic network.

Functional data suggest that lymphatic vessel regeneration within the tails begins with large, highly permeable vessels (and/or open fluid channels throughout the tissues) surrounded by a loose extracellular matrix enabling easy uptake and transport of large particles. As regeneration progresses, the uptake and transport of very large particles is restricted, presumably (but not specifically studied in this work) due to maturation of the lymphatic vessels and surrounding network including tightening of junctions between LECs in capillaries, smooth muscle recruitment to collecting lymphatics, formation of extracellular matrix attachments and increased cell and connective tissue density surrounding the vessels. Twelve week regenerates display the same lymph clearance and velocity measures as full regenerates and so it is likely that lymphangiogenesis is largely complete by this stage. In a mouse tail model of skin regeneration lymphangiogenesis begins with and is initiated by interstitial fluid flowing from the direction of the tail tip towards the body across the wound site along simple non-vascular fluid channels (Boardman and Swartz 2003; Goldman et al. 2007; Rutkowski et al. 2006; Uzarski et al. 2008). The direction of interstitial flow in the mouse tail is the driving force behind the formation of pre-lymphatic channels, transport of factors that promote lymphangiogenesis (e.g. VEGF-C) and extracellular matrix remodeling (e.g. metalloproteinases) along with unidirectional migration and organisation of LECs (derived from pre-existing vessels in the tail tip) into a functional lymphatic network. In the gecko there are no upstream lymphatics to collect lymph in the regenerating region of the tail; however interstitial fluid may begin pooling in the distal portion of the blastema or elongating tail preceding new vessel growth. Thus distal to proximal interstitial flow would occur and lymphangiogenesis may follow the pattern shown in the mouse tail model. Certainly, from 6 weeks of regeneration lymphatic flow in the regenerating gecko tail is directed from the tail

tip, towards the venous/lymphatic communications near the cloaca and into the blood circulation (Chapter 2). For gecko tail lymphangiogenesis to follow the mouse tail model, LECs or progenitor cells capable of differentiating to the lymphatic lineage would be required within the distal region of the tail that could migrate proximally along the direction of lymph flow. LECs or progenitor cells in this case would have to arise from the blastema of the regenerating gecko tail rather than from pre-existing vessels in the original portion of the tail. Blood vessels are formed from blastema derived endothelial cells in the early stages of tail regeneration (Hughes and New 1959; Quattrini 1954). LECs may also differentiate from blastema derived cells and lymphatic vessel growth in tail regeneration would thus arise from *de novo* lymphangiogenesis. However, this is in contrast to the sprouting lymphangiogenesis seen in development (Karkkainen et al. 2004), wound healing (Paavonen et al. 2000; Shimoda et al. 2004) and is assumed in tumours (Achen and Stacker 2008; Sleeman et al. 2009; Sleeman and Thiele 2009) where specific factors (e.g. VEGF-C and VEGF-D) stimulate LECs of pre-existing vessels to proliferate, migrate, bud and extend outwards to form new vessels. Knowledge on the origin of cells of the newly formed lymphatic vasculature is required to further describe and establish the suitability of the regenerating gecko tail as either a *de novo* or spouting model for adult lymphangiogenesis or a combination of both.

6.2. MOLECULAR EVIDENCE FOR THE PRESENCE AND ROLE OF THE VEGF-C/D/R3 PATHWAY IN THE REGULATION OF LYMPHANGIOGENESIS IN THE REGENERATING GECKO TAIL

The activation of the tyrosine kinase receptor VEGFR-3, by binding of its ligands VEGF-C and/or VEGF-D, is considered crucial for lymphangiogenesis (Alitalo et al. 2005; Olsson et al. 2006; Tammela and Alitalo 2010). This pathway was chosen to examine in this study due to the critical importance of VEGFR-3 and VEGF-C in the lymphangiogenic process and due to the likely presence of a VEGF-C homologue within gecko tails (Daniels et al. 2003).

Therefore, I wanted to confirm and characterise the presence of VEGF-C within the regenerating gecko tail along with its receptor VEGFR-3 and the other known VEGFR-3 ligand and lymphangiogenic factor VEGF-D. My major aim was to determine whether these factors were responsible for the molecular regulation of lymphangiogenesis within regenerating gecko tails.

The Australian marbled gecko does express VEGF-C, VEGF-D and VEGFR-3 both at a gene and protein level (Chapters 3, 4 and 5). Gene sequences of these molecules are highly homologous to other vertebrates at nucleotide, amino acid sequence and structural levels and in particular are most closely related in an evolutionary sense to the chicken sequences (Chapters 3 and 4). Sequence and structural alignments highlight the conservation of most major functionally important residues (Chapter 4). Proteolytic cleavage sites are available in gVEGF-C and gVEGF-D sequences that would enable processing of the gecko prepropeptides to occur. Hence, N- and C- terminal cleavages could generate mature peptides with increased affinity for the receptors gVEGFR-3 and gVEGFR-2 (currently unidentified in reptiles). Residues involved in ligand dimerisation and receptor and ligand binding sites are also conserved in the gecko protein sequences. Thus, the formation of gVEGF-C and gVEGF-D homo- and/or hetero-dimers is possible enabling precise receptor/ligand interactions. Further, sequences important in signal transduction upon receptor binding are present in the gVEGFR-3 sequence, thus autophosphorylation of dimerised receptors could occur resulting in activation of the correct signal transduction pathways to produce a cellular response e.g. migration, proliferation. The presence of functional residues in gecko sequences theoretically demonstrates that these proteins have the capacity to generate a biological response upon binding of gVEGF-C and/or gVEGF-D to gVEGFR-3 and/ or gVEGFR-2 (if present) in cells expressing these receptors.

Gene expression profiles of gVEGF-C, gVEGF-D and gVEGFR-3 throughout gecko tail regeneration show differential expression patterns between the three genes that are largely consistent with the proposal that these three gene products have roles in lymphatic regeneration (Chapter 3). High levels of mRNA expression for all three genes frequently correlate with lymphangiogenesis in many previous studies (Anisimov et al. 2009; Enholm et al. 2001; Flister et al. 2010; Ji et al. 2004). Further, localisation of gVEGF-C and gVEGF-D primarily within lymphatic-rich subcutaneous tissues of regenerating gecko tails (Chapter 5) supports lymphatic functions.

Up-regulation of VEGF-C mRNA expression suggests a role in the early stages of tail regeneration and likely functions in the initiation of lymphangiogenesis (Chapter 3). Tissue expression of VEGF-C appears to follow a similar pattern, although not quantitated, with more prolific staining observed in early regenerates (Chapter 3). Darker staining, compared to 12 week, full regenerate and original tissues, was apparent in keratinocytes and fibroblasts from 3-9 weeks of regeneration. In particular the secreted form of VEGF-C (rather than cell-bound or cytoplasmic forms) dispersed within connective tissue was only observed in 5-9 week regenerates. Associations of gVEGF-C staining with lymphatic vessels show binding or expression of this ligand by lymphatic vasculature in early-mid tail regeneration providing further evidence of a lymphangiogenic role. Protein expression of VEGF-C in gecko tail extracts, while potentially unreliable, further corroborates mRNA expression data by revealing a pattern of early up-regulation during tail regeneration (Chapter 5). Western blotting confirmed the presence of unprocessed and partially processed forms of VEGF-C protein in regenerates and original tailed geckos. No fully processed, mature, forms of gVEGF-C were detected by western blotting (Chapter 5), despite cleavage sites being available in the gecko protein sequence for full proteolysis (Chapter 4). Unprocessed and partially processed VEGF-C is capable of binding VEGFR-3, however, if mature forms of

gVEGF-C are not present in gecko tails, this protein would not be capable of binding gVEGFR-2 (if present). Unprocessed forms of VEGF-C show reduced affinity for VEGFR-2 (Joukov et al. 1996; McColl et al. 2007) and therefore would be unlikely to be involved in angiogenesis. Activation of VEGFR-2 can also guide lymphangiogenesis (if expressed on LECs) but this pathway is generally considered primarily angiogenic (via expression on BECs).

gVEGF-D mRNA expression data indicate a lack of function in early tail regeneration and initiation of lymphangiogenesis. gVEGF-D mRNA expression was up-regulated in late regeneration (Chapter 3) during the time where the lymphatic network was developing functional maturity (Chapter 2), suggesting a potential role for VEGF-D in lymphatic vessel organisation and maturation. Given that VEGF-D mRNA expression has been shown in mice fibroblasts to be up-regulated by cell contact (Orlandini and Oliviero 2001), the up-regulation observed in this study may be a result of increased cell-density within the tail at this time, a tissue state suggested by functional data obtained in Chapter 2, and expected as the tail reaches the final stages of regeneration. Some fibroblast expression of VEGF-D in gecko tail tissue was observed via immunostaining, but only up to 6 weeks of regeneration (Chapter 3). Beyond 6 weeks VEGF-D is primarily localised to keratinocytes. Tissue expression patterns show greater staining intensities in keratinocytes of early regenerates, which is not consistent with the mRNA profile. However, quantitative analysis was not performed on tissue sections and so images may be misleading. Results for protein expression of VEGF-D in gecko tail extracts were inconclusive (discussed in Chapter 5) and so it is unclear if increased mRNA expression in late regeneration correlates with increased protein expression and hence with functional responses generated by ligand binding. It is therefore unclear whether up-regulation of VEGF-D mRNA in late regeneration is indicative of a role for this protein during this time.

Localisation of VEGF-C and VEGF-D was observed primarily in subcutaneous tissues, a region previously described as being rich in lymphatic vasculature (Daniels et al. 2003). Associations of gVEGF-C and gVEGF-D with lymphatic and blood endothelia respectively within the subcutaneous region were observed and are thought to be due to interactions with receptors on LEC and BEC surfaces. Confirmation of the lymphatic identity of suspected lymph vessels was provided by LYVE-1 immunostaining, although LYVE-1 positive vessels were observed in full regenerates only (Chapter 3). In particular within subcutaneous tissues, VEGF-C and VEGF-D expression was generally observed in keratinocytes and fibroblasts and this is consistent with mammalian studies which have suggested that these cells play an important role in the regulation of angiogenesis and lymphangiogenesis in the skin, both physiologically and pathologically (Trompezinski et al. 2004). Similarly, expression of VEGF-C and VEGF-D by keratinocytes in mammalian studies triggers lymphangiogenesis in the skin (Jeltsch et al. 1997; Veikkola et al. 2001) and therefore expression of these factors by keratinocytes in regenerating gecko tail tissues suggests lymphangiogenic capabilities.

gVEGFR-3 mRNA expression is up-regulated in the mid-phase of gecko tail regeneration, occurring towards the end of up-regulated gVEGF-C expression and therefore likely a result of increased demand for receptors by increased presence of ligand (Enholm et al. 2001). Increased VEGFR-3, if expressed on LECs and activated by ligand binding, would result in cell migration and proliferation (Makinen et al. 2001b) and hence lymphangiogenesis. gVEGFR-3 expression in protein extracts does not show the same pattern as for the mRNA, however this may be due, as for VEGF-D, to the apparent issues with antibody affinity and so may not accurately represent the true situation. Localisation of gVEGFR-3 in regenerating and original gecko tails provided unexpected and interesting results (Chapter 5). Specific and intense immunostaining was observed only in adipose tissue

in original, full regenerate and regenerating gecko tail tissues. This is consistent with observations of VEGF-C immunostaining in adipose tissue (Chapter 3), and may indicate that VEGF-C staining in this region was due to associations of the protein with the receptor on adipocyte cell surfaces. Alternatively, adipocytes may be capable of both expressing and binding VEGF-C in an autocrine manner. Adipose tissue is highly vascularised (in terms of both blood and lymphatic vasculature) and it has been suggested that adipose tissue serves as an endocrine organ to stimulate angiogenesis and lymphangiogenesis during times of fat store expansion (discussed in Chapters 3 and 5). Furthermore, there is evidence in mammals of close associations of adipocytes and endothelial cells along with paracrine/autocrine interactions between them (Hausman and Richardson 2004). However, VEGFR-3 expression does not appear to be on vessels or cells surrounding adipose deposits but rather directly surrounding or within the cytoplasm of adipocytes themselves. If it is the case that adipocytes directly express VEGFR-3 then VEGF-C overexpression and binding in these tissues may stimulate adipogenesis rather than have any lymphangiogenic role. Much more speculatively, perhaps VEGFR-3 positive staining in adipose tissue may be associated with progenitor cells with both LEC and adipocyte properties. Human adipose tissue contains cells that are capable of differentiating along a number of different lineages (Nakagami et al. 2006; Schaffler and Buchler 2007; Sengenès et al. 2005; Zuk et al. 2001). Studies examining these adipose tissue-derived stromal or stem cell (ADSC) populations show they can be stimulated to differentiate into lineages including mature adipocytes, chondrocytes, osteoblasts, neuronal cells, endothelial cells, and cardiomyocytes (reviewed in (Witkowska-Zimny and Walenko 2011)). Several studies have shown differentiation of ADSCs to endothelial cells that can participate in blood vessel formation, are functionally connected to the pre-existing vascular network and secrete angiogenic growth factors such as VEGF and PDGF (Cao et al. 2005; Kang et al. 2010; Madonna and De Caterina 2008; Miranville et al. 2004; Planat-Benard et al. 2004;

Rehman et al. 2004). In contrast, ADSCs have been shown to play a role in vascular stabilisation, acting as components of the vascular wall via structural and functional interactions with endothelial cells rather than by differentiation into endothelial cells themselves (Traktuev et al. 2008). In this case it is suggested the ADSCs are cells with pericytic properties rather than progenitor cells for endothelia (Traktuev et al. 2008). Pericytic ADSCs not only cooperatively assemble with microvascular endothelial cells, but they also express growth, inflammatory and mobilisation factors to promote endothelial cell survival and angiogenesis. No work has specifically looked at adipocyte interactions with LECs, whether LEC progenitor populations are present in adipose tissue or the capabilities of ADSCs to differentiate into LECs. Furthermore, the cells within adipose tissue displaying positive immunostaining for VEGF-C and VEGFR-3 seem to have the appearance of mature adipocytes containing large lipid vacuoles rather than that of a mesenchymal stem cell or pericyte-like cell associated with lymphatic endothelia. If VEGFR-3 positive staining in gecko tail adipose tissue was indicative of LEC progenitor cell populations then this could serve as both a store of growth factor (particularly in original tails) and readily available cells such that there is a ready source following tail loss or injury for rapid lymphatic regeneration. Much work needs to be performed to address this speculation and determine the significance behind adipose expression of VEGFR-3 and VEGF-C.

A lack of VEGFR-3 expression by obvious LECs and BECs, the two common VEGFR-3 expressing cell-types, was apparent (Chapter 5). This finding does not reflect a lack of these cell types within gecko tails as LYVE-1 positive lymphatic endothelial cells are present within tail tissues and obvious blood vessels can be seen in tissue sections, lined by cells with endothelial characteristics (Chapters 3 and 5). The absence of VEGFR-3 staining on LECs and BECs, along with the strongly specific adipocyte staining (following troubleshooting of the immunohistochemical method, Chapter 5) suggests that either these

cells do not express VEGFR-3 in the gecko, that there is cross reactivity of the mammalian antibody with a different protein found in adipose tissue or that something in the tissue preparation and/or staining method is blocking the antigenic site in endothelial cells but not in adipocytes. It is unlikely that gecko LECs and/or BECs do not express VEGFR-3, as LECs are the primary cell type for expression of this receptor following embryonic development (Kaipainen et al. 1995) and BECs are found to express this receptor when actively undergoing angiogenesis (Laakkonen et al. 2007; Petrova et al. 2008; Tammela et al. 2008; Witmer et al. 2001). Further investigations as to whether gecko endothelial cells do express VEGFR-3 are required to accurately determine whether this receptor is involved in lymphangiogenesis and/or angiogenesis throughout tail regeneration.

6.3. LIMITATIONS OF THE STUDY/ PROBLEMS ENCOUNTERED

This study has focused on the unique model of the regenerating gecko tail, which is obviously not a standard laboratory animal and as such is widely understudied. The lack of information, and hence data and molecular tools (e.g. sequence information, antibodies), placed constraints on what the study could achieve with the time, funding and resources available. For example, many techniques had to be vigorously troubleshooted and validated before results could be deemed trustworthy (or not). Furthermore, mammalian derived antibodies were relied upon with the hope that there would be sufficient cross-reactivity to reptilian proteins.

The greatest limitation of this study is that the major hypothesis of 'lymphangiogenesis in regenerating gecko tails is driven by the VEGF-C/ -D and VEGFR-3 pathway' could not be definitively confirmed. I was unable to positively identify lymphatic vessels in early-mid regeneration and original tail states using LYVE-1 immunostaining and similarly was unable to identify VEGFR-3 expression on endothelial cells. While these issues are presumably due to a lack of antibody specificity, without conclusively showing increases

in lymphatic vessel density throughout early regeneration (which has been shown previously using basic histological analysis (Daniels et al. 2003) but has not been established using molecular markers) and without proving that VEGFR-3 is expressed by LECs and hence VEGF-C and VEGF-D binding would elicit a response in LECs, I cannot conclusively say that this pathway functions in lymphangiogenesis.

The source of these limitations, along with the issues encountered with densitometry analysis of western blots and the ELISAs (variability and inaccuracy of results), is assumed to be due to a lack of sufficient antibody specificity. However, it needs to be confirmed whether lack of antigen recognition is the primary cause of these problems or whether it is a truthful reflection of the expression of these molecules in tissues and protein extracts (e.g. LECs only express LYVE-1 in full regenerate tissues and do not express VEGFR-3 at all) or more to do with issues in the specific protocols used. Generating reptilian specific antibodies would be necessary for future studies to determine the accuracy of this assumption.

6.4. FUTURE DIRECTIONS

Given the limitations described above, this thesis has ultimately resulted in a descriptive study of the functional characteristics of the lymphatic system along with sequence analysis and expression profiles of the VEGF-C, VEGF-D and VEGFR-3 pathway during tail regeneration. Therefore, a number of future studies need to be performed to fully characterise lymphangiogenesis in regenerating gecko tails and to confirm the hypothesis that the VEGF-C/D/R3 pathway is responsible for the molecular regulation of this process.

An obvious first step would be to produce gecko specific antibodies against synthesised recombinant proteins (generated from sequence information gained in this study). Repeating IHC, western blot analysis and ELISA experiments using specific antibodies would determine whether the issues identified in the current study were due to problems with

antibody specificity, as presumed. If antibody specificity and affinity were the causative factors behind a lack of VEGFR-3 immunostaining on gecko endothelial cells (Chapters 3 and 5), variability and inaccuracy of western blotting densitometry (Chapter 5) and failure of ELISAs to evaluate gecko protein extracts (Chapter 5) then using antibodies specifically generated against the gecko antigens should resolve these difficulties. Similarly, if the fat present in extracted protein was responsible for variations in total protein quantification along with western blotting and ELISA difficulties then repeating these experiments in a lizard species (capable of comparable autotomy and regeneration processes to *C. marmoratus*) with fewer tail lipid stores may eliminate these technical difficulties and allow quantification. Many skink species would fit these criteria and should therefore be investigated.

In the present study, LYVE-1 expression was observed only on lymphatic endothelia in full regenerate gecko tail tissues (Chapter 3) and VEGFR-3 expression was not observed on lymphatic or blood endothelia in any of the tissues examined as would have been expected (Chapters 3 and 5). The phenotype of gecko lymphatic endothelial cells throughout the different stages of regeneration (early, mid, late and full) as well as in original gecko tails needs to be elucidated. Phenotyping lymphatic cells could be attempted using immunohistochemistry on isolated gecko LECs with a wider variety of molecular markers for LECs (commercially available and specifically synthesised for gecko proteins if sequence data is available). Alternatively, laser capturing of lymphatic vessels within regenerating tails and subsequent screening using genomics (microarray) and proteomics (protein array) approaches (if they can be optimised specifically for use in geckos) may identify molecular targets present within gecko lymphatic endothelia. LEC cells do display significant heterogeneity (Lee et al. 2010) and thus will not necessarily express the same markers at each stage of regeneration. The use of gecko specific antibodies in the immunohistochemistry technique may aid this discovery. Knowledge on the presence or absence of VEGFR-3

expression on gecko LECs would determine if activation of this receptor is, or is not capable of regulating lymphangiogenesis and thus would allow confirmation or rejection of the hypothesis that the VEGF-C/D/R3 pathway plays a role in the molecular regulation of this process. Furthermore, examining the localisation of lymphatic endothelia throughout regeneration could identify the source of the LECs throughout regeneration. Specifically, do cells arise from LEC progenitors from the blastema, via sprouting from pre-existing vasculature or a combination of both?

Sequence analysis performed in this study (Chapter 4) suggests that gVEGF-C and gVEGF-D would bind gVEGFR-3 and that the receptor is capable of autophosphorylation upon ligand binding. However, these actions were not specifically tested in the current study. *In vitro* studies examining the binding, affinity and activation properties of recombinantly expressed gVEGF-C (rgVEGF-C) and rgVEGF-D to rgVEGFR-3 are therefore imperative in determining the role of these proteins in lymphangiogenesis within regenerating gecko tails. Likewise, investigating the mitogenic and proliferative capabilities of rgVEGF-C and rgVEGF-D on isolated gecko LECs would be useful. Such experiments have been performed previously using mammalian proteins and cells in the identification of the roles and functions of VEGF-C, VEGF-D and VEGFR-3 in mammals (Achen et al. 1998; Jeltsch et al. 2006). In vivo studies into this pathway in gecko tail regeneration are also relevant. Chorioallantoic membrane (CAM) analysis has been used previously to determine angiogenic and lymphangiogenic properties of recombinant VEGF-C molecules (Jeltsch et al. 2006) and gecko recombinant proteins could likewise be tested in this setting. Introducing ligand blocking peptides, VEGFR-3 neutralising antibodies (Pytowski et al. 2005) and/or specific antagonists (such as the soluble splice variant of VEGFR-2, sVEGFR-2, which is a specific inhibitor of VEGF-C (Albuquerque et al. 2009)) into gecko tails and determining if

lymphangiogenesis is blocked and lymphoedema stimulated would also provide direct evidence of this pathway in the re-growth of lymphatic vessels during tail regeneration.

Observations of VEGF-C and VEGFR-3 localisation in adipose tissue in regenerating, full regenerate and original tails (Chapters 3 and 5) warrant further study. It was undetermined whether immunostaining of these proteins within adipose tissue could have resulted from associations of adipocytes with lymphatic vasculature, expression by adipocytes themselves or whether it indicates the presence of progenitor cells with LEC and adipocyte properties. The phenotype of these VEGFR-3 positive cells within gecko tail adipose tissue therefore needs to be determined. Of particular interest is determining whether gecko tail adipose tissue contains progenitor/stem cells as is the case for human adipose tissue and whether the VEGFR-3 positive cells identified fall into this category. ADSCs would be particularly advantageous in the gecko tail for rapid supply of pluripotent cells ready to contribute to regeneration (along with dedifferentiated cells that arise in the blastema) upon tail loss. Additionally, gene expression profiles and biochemical analysis of gVEGF-C, gVEGF-D and gVEGFR-3 could be performed on extracts from tail adipose tissue only, and potentially isolated adipocytes, rather than whole tails to determine the links between adipose tissue, lymphatic vasculature and lymphangiogenic growth factors, if any. Adipose tissue could serve as an important source of lymphangiogenic factors for secretion upon tail loss and regeneration or during fat deposition/ expansion.

Finally, several other genes have recently been identified as being crucial to the lymphangiogenic process and therefore their contributions within regenerating gecko tails also need to be established. For example, the angiopoietins (Ang-1 and Ang-2), ligands for the receptor tyrosine kinase Tie2, have recently been described as having roles in lymphangiogenesis and angiogenesis both during development and postnatally (Saharinen et al. 2010). Mice deficient in Ang-2 show defects in lymphatic vasculature patterning and

function (Gale et al. 2002). These defects can be rescued by Ang-1 administration, suggesting redundant roles for these genes in developing lymphatic vasculature (Gale et al. 2002). In adult mice, overexpression of Ang-1 induces lymphangiogenesis (Tammela et al. 2005). However, the action of Ang-1 in this setting is dependent on up-regulation of VEGFR-3 on LECs and can be blocked by inhibition of VEGFR-3 signalling (Tammela et al. 2005). Ephrin-B2, a transmembrane ligand for Eph receptor tyrosine kinases, may also control lymphatic and blood vessel growth in mice and zebrafish (Wang et al. 2010). However, this is also dependent on VEGFR-3 signalling.

6.5. CRITIQUE OF THE PROPOSAL OF THE REGENERATING GECKO TAIL AS A MODEL FOR LYMPHANGIOGENESIS

One of the initial aims of this thesis was to highlight the potential of the regenerating gecko tail as a new model to investigate lymphangiogenesis given that the precise mechanisms behind this process remain unclear. A greater understanding of lymphangiogenesis and how it can be manipulated has potential therapeutic benefits and research into all forms of lymphangiogenesis (wound healing, development, tumour related etc.) over a variety of different adult models may aid in our understanding. From this study several advantages and disadvantages of the regenerating gecko tail model versus other models of lymphangiogenesis have become apparent.

The biggest advantage of the gecko tail system is that it is an adult model of regeneration. Many previous studies on lymphangiogenesis have focused on transgenic mouse models, xenopus tadpoles or zebrafish embryos (Ny et al. 2006; Shin and Rockson 2008). This thesis has shown that the regenerating gecko tail provides a model of adult lymphangiogenesis whereby a functional lymphatic network (Chapter 2) is re-grown following autotomy and new lymphatic vessels are present in the regenerated tail (Chapter 3).

This model therefore provides opportunities to study the mechanisms (molecular, structural, and functional) behind the re-establishment of a functional lymphatic network, particularly following tissue trauma.

Although at first glance autotomy may appear to be completely different than for instance surgical amputation (and so the regenerating gecko tail may not adequately reflect mammalian wound healing), in the case of the lymphatic vessels these are severed by the force of contraction of the caudal muscles and splitting of the vertebral fracture plane. Given that these tissues are torn, some form of wound healing must take place, particularly in the lymphatics as the connection to the venous circulation is outside of the tail region and thus lymph would not be able to drain from the tail if some form of vessel regeneration and re-connection did not occur. The regenerating gecko tail is therefore a model for regenerating lymphatics. The observed changes in functional characteristics of the lymphatic network described in Chapter 2 suggest not only lymph flow re-establishment but also a level of maturation and organisation of lymphatic vessels into appropriate hierarchical arrangements. This model may therefore be particularly advantageous in studying the regulation of the final stages of lymphangiogenesis including terminal differentiation/maturation and vascular remodelling.

Lymphangiogenesis following autotomy in the regenerating gecko tail may or may not be under the same molecular control as is seen in mammalian lymphatic regeneration. However given the mRNA expression profiles of gVEGF-C, gVEGF-D and gVEGFR-3, tissue localisation of gVEGF-C and gVEGF-D in regenerating gecko tails (Chapter 3) and the high level of sequence conservation between mammalian and gecko VEGF-C, VEGF-D and VEGFR-3 (Chapter 4) it is not unreasonable to hypothesise that these factors would have a role in gecko tail lymphangiogenesis. The regenerating gecko tail model is therefore useful to further explore the VEGF-C/D/R3 pathway along with their interactions with other molecules

and cells. A high level of sequence conservation is another advantage of the gecko model versus other non-mammalian models such as *Xenopus* and zebrafish. Geckos are more closely related to mammals and share more VEGF-C, VEGF-D and VEGFR-3 sequence homology to humans and other mammals than *Xenopus* and zebrafish (Chapters 3 and 4). Furthermore, the structure of the lymphatic system in lizards is reported to be more similar to mammals than that of amphibians and fish (Ottaviani and Tazzi 1977).

Disadvantages of the gecko tail model include a lack of genetic information (the genome has not been sequenced, and few genes are characterised), a lack of specific molecular tools (e.g. antibodies) and that these animals are not as readily available (purchase and/ or capture) compared to other animal models. However, once obtained the geckos are easy and cheap to care for and handle. The capacity of the animals to regenerate their tails multiple times means that only one colony needs to be obtained which is then self-replenishing to obtain sufficient tissue for analysis. Furthermore, as autotomy and tail regeneration occur naturally, surgery is not required to sever the lymphatic vessels. This reduces costs given that surgery often requires anaesthetics, analgesics, specialised contained sterile animal housing etc. The gecko as a model warrants further research and could potentially provide further knowledge into not only the lymphangiogenic response but also into the regenerative capacity in general. As tail loss and regeneration are natural processes, the mechanisms behind the regeneration of tissues within the tail have evolved to ensure that the capacity for regeneration is maintained. Therefore, many tissues, including the lymphatic vessels must be subject to molecular control mechanisms that specifically promote re-growth. While these mechanisms may be similar or different to those in mammals, information from this model may help in identifying ways to promote vessel re-growth in cases where this is limited, for example in lymphoedema.

6.6. CONCLUSION

In conclusion, this study has shown that lymphatic transport is restored by tail regeneration in the Australian marbled gecko as early as 6 weeks following autotomy. It was presumed that this restoration of lymphatic function was a result of the growth of new lymphatic vessels within the regenerating tail. This study has conclusively proven the presence of lymphatic vessels within regenerated tails using a known lymphatic molecular marker, which demonstrates that lymphangiogenesis does indeed occur during tail regeneration. This study is also the first to identify and characterise the lymphangiogenic factors VEGF-C, VEGF-D and VEGFR-3 in a reptile, partly confirming the initial hypothesis in determining the presence of these factors in the gecko tail. Gecko VEGF-C, VEGF-D and VEGFR-3 genes are highly similar to those in other vertebrate species, and are particularly homologous to chicken sequences. However, limitations with protein analysis, presumably as a result of antibody specificity, have prevented definitive confirmation of the hypothesis that VEGF-C and VEGF-D via binding to and activation of VEGFR-3 is the key molecular pathway responsible for lymphangiogenesis in the regenerating gecko tail. Nevertheless, sequence analysis, mRNA and tissue expression profiles of gecko VEGF-C, VEGF-D and VEGFR-3 are consistent with lymphangiogenic functions and thus this study has provided significant evidence for the roles of these genes in lymphangiogenesis within the regenerating gecko tail.

APPENDICIES

APPENDIX ONE: MATERIALS SUPPLIERS

AbCam, Cambridge, UK

Alpha Innotech, San Leandro, CA

Ambion, Applied Biosystems, Foster City, USA

Applied Biosystems, Foster City, USA

Astral Scientific Pty Ltd, Caringbah, Australia

Bio-Rad, Herculus, CA, USA

Daintree Scientific, Tasmania, Australia

Dako Australia Pty Ltd, NSW, Australia

Geneworks, Adelaide, Australia

Greiner Bio-One, Frickenhausen, Germany

Invitrogen, Carlsbad, CA

Millipore, MA, USA

MJ Research, Reno, MV, USA

NanoDrop Technologies Inc., Wilmington, USA

New England Biolabs, MA, USA

Pierce, Thermo Fisher Scientific, Rockford, IL, USA

Promega, Madison, WI, USA

QIAGEN, Hilden, Germany

R&D Systems Inc., Minneapolis, USA

Roche Diagnostics Australia Pty Ltd, NSW, Australia

Santa Cruz Biotechnology, Santa Cruz, CA, USA

Sigma-Aldrich, St. Louis, MO

TECAN, Männedorf, Switzerland

APPENDIX TWO: AMINO ACID CODE

Amino acid name	***Abbreviation***	***Single letter code***
Arginine	Arg	R
Histidine	His	H
Lysine	Lys	K
Aspartic acid	Asp	D
Glutamic acid	Glu	E
Serine	Ser	S
Threonine	Thr	T
Asparagine	Asn	N
Glutamine	Gln	Q
Cysteine	Cys	C
Selenocysteine	Sec	U
Glycine	Gly	G
Proline	Pro	P
Alanine	Ala	A
Valine	Val	V
Isoleucine	Ile	I
Leucine	Leu	L
Methionine	Met	M
Phenylalanine	Phe	F
Tyrosine	Tyr	Y
Trytophan	Trp	W

APPENDIX THREE: LUMINOL SOLUTION

Reagents

Coumaric acid (Sigma) 90 mM

Luminol (Sigma) 250 mM

Prepare in DMSO store at -20°C

Tris 100mM, pH 8.0

Hydrogen peroxide

Luminol solution for chemiluminescence

Add together:

100 ml 100mM Tris, pH 8.0

220 µl coumaric acid

500 µl luminal

Mix well, store at room temperature until needed (maximum 1 week)

For use:

To 10 ml add 4 µl of 40 % hydrogen peroxide, cover blot and incubate for 3 min in the dark

Remove blot from solution and remove excess luminal solution with paper towel

Wrap blot tightly in glad wrap ensuring there are no creases

Expose to film

REFERENCES: CHAPTERS 1, 4, 5 AND 6

Absolom DR, van Oss CJ (1986) The nature of the antigen-antibody bond and the factors affecting its association and dissociation. CRC Crit Rev Immunol 6:1-46

Achen MG, Jeltsch M, Kukk E, Makinen T, Vitali A, Wilks AF, Alitalo K, Stacker SA (1998) Vascular endothelial growth factor D (VEGF-D) is a ligand for the tyrosine kinases VEGF receptor 2 (Flk1) and VEGF receptor 3 (Flt4). Proc Natl Acad Sci U S A 95:548-553

Achen MG, Stacker SA (2008) Molecular control of lymphatic metastasis. Ann N Y Acad Sci 1131:225-234

Achen MG, Williams RA, Minekus MP, Thornton GE, Stenvers K, Rogers PA, Lederman F, Roufail S, Stacker SA (2001) Localization of vascular endothelial growth factor-D in malignant melanoma suggests a role in tumour angiogenesis. J Pathol 193:147-154

Akahane M, Akahane T, Matheny SL, Shah A, Okajima E, Thorgeirsson UP (2006) Vascular endothelial growth factor-D is a survival factor for human breast carcinoma cells. Int J Cancer 118:841-849

Albuquerque RJC, Hayashi T, Cho WG, Kleinman ME, Dridi S, Takeda A, Baffi JZ, Yamada K, Kaneko H, Green MG, Chappell J, Wilting J, Weich HA, Yamagami S, Amano S, Mizuki N, Alexander JS, Peterson ML, Brekken RA, Hirashima M, Capoor S, Usui T, Ambati BK, Ambati J (2009) Alternatively spliced vascular endothelial growth factor receptor-2 is an essential endogenous inhibitor of lymphatic vessel growth. Nat Med 15:1023-1030

Alibardi L (2010) Morphological and cellular aspects of tail and limb regeneration in lizards. A model system with implications for tissue regeneration in mammals. Adv Anat Embryol Cell Biol 207:iii, v-x, 1-109

Alibardi L, Gibbons J, Simpson SB, Jr. (1993) 3H-GABA administration during tail regeneration of lizards and autoradiographical localization. J Hirnforsch 34:67-77

Alibardi L, Lovicu FJ (2010) Immunolocalization of FGF1 and FGF2 in the regenerating tail of the lizard *Lampropholis guichenoti*: implications for FGFs as trophic factors in lizard tail regeneration. Acta Histochem 112:459-473

Alibardi L, Maurizii MG, Taddei C (2000) Immunocytochemical and electrophoretic distribution of cytokeratins in the regenerating epidermis of the lizard *Podarcis muralis*. J Morphol 246:179-191.

Alitalo K, Mohla S, Ruoslahti E (2004) Lymphangiogenesis and cancer: meeting report. Cancer Res 64:9225-9229

Alitalo K, Tammela T, Petrova TV (2005) Lymphangiogenesis in development and human disease. Nature 438:946-953

Anisimov A, Alitalo A, Korpisalo P, Soronen J, Kaijalainen S, Leppanen VM, Jeltsch M, Yla-Herttuala S, Alitalo K (2009) Activated forms of VEGF-C and VEGF-D provide improved vascular function in skeletal muscle. Circ Res 104:1302-U1156

Anthony JP, Foster RD, Price DC, Mahdavian M, Inoue Y (1997) Lymphatic regeneration following microvascular limb replantation: a qualitative and quantitative animal study. J Reconstr Microsurg 13:327-330.

Arnold EN (1984) Evolutionary aspects of tail shedding in lizards and their relatives. J Nat History 18:127-169

Arnold EN (1988) Caudal autotomy as a defence. In: Gans C, Huey R (eds) Biology of the Reptilia. Alan R. Liss, New York, pp 235-273

Arnold K, Bordoli L, Kopp Jr, Schwede T (2006) The SWISS-MODEL workspace: a web-based environment for protein structure homology modelling. Bioinformatics 22:195-201

Asplund A, Gry Bjorklund M, Sundquist C, Stromberg S, Edlund K, Ostman A, Nilsson P, Ponten F, Lundeberg J (2008) Expression profiling of microdissected cell populations selected from basal cells in normal epidermis and basal cell carcinoma. Br J Dermatol 158:527-538

Badger CM, Peacock JL, Mortimer PS (2000) A randomized, controlled, parallel-group clinical trial comparing multilayer bandaging followed by hosiery versus hosiery alone in the treatment of patients with lymphedema of the limb. Cancer 88:2832-2837

Baldwin ME, Catimel B, Nice EC, Roufail S, Hall NE, Stenvers KL, Karkkainen MJ, Alitalo K, Stacker SA, Achen MG (2001) The specificity of receptor binding by vascular endothelial growth factor-d is different in mouse and man. J Biol Chem 276:19166-19171

Baldwin ME, Halford MM, Roufail S, Williams RA, Hibbs ML, Grail D, Kubo H, Stacker SA, Achen MG (2005) Vascular endothelial growth factor D is dispensable for development of the lymphatic system. Mol Cell Biol 25:2441-2449

Baldwin ME, Stacker SA, Achen MG (2002) Molecular control of lymphangiogenesis. Bioessays 24:1030-1040

Baluk P, Fuxe J, Hashizume H, Romano T, Lashnits E, Butz S, Vestweber D, Corada M, Molendini C, Dejana E, McDonald DM (2007) Functionally specialized junctions between endothelial cells of lymphatic vessels. J Exp Med 204:2349-2362

Baluk P, Tammela T, Ator E, Lyubynska N, Achen MG, Hicklin DJ, Jeltsch M, Petrova TV, Pytowski B, Stacker SA, Yla-Herttuala S, Jackson DG, Alitalo K, McDonald DM (2005) Pathogenesis of persistent lymphatic vessel hyperplasia in chronic airway inflammation. J Clin Invest 115:247-257

Bando H, Brokelmann M, Toi M, Alitalo K, Sleeman JP, Sipos B, Grone HJ, Weich HA (2004) Immunodetection and quantification of vascular endothelial growth factor receptor-3 in human malignant tumor tissues. Int J Cancer 111:184-191.

Banerji S, Ni J, Wang SX, Clasper S, Su J, Tammi R, Jones M, Jackson DG (1999) LYVE-1, a new homologue of the CD44 glycoprotein, is a lymph-specific receptor for hyaluronan. J Cell Biol 144:789-801

Bateman PW, Fleming PA (2009) To cut a long tail short: a review of lizard caudal autotomy studies carried out over the last 20 years. J Zool 277:1-14

Bauer SM, Bauer RJ, Liu ZJ, Chen H, Goldstein L, Velazquez OC (2005) Vascular endothelial growth factor-C promotes vasculogenesis, angiogenesis, and collagen constriction in three-dimensional collagen gels. J Vasc Surg 41:699-707

Beasley NJ, Prevo R, Banerji S, Leek RD, Moore J, van Trappen P, Cox G, Harris AL, Jackson DG (2002) Intratumoral lymphangiogenesis and lymph node metastasis in head and neck cancer. Cancer Res 62:1315-1320

Bellairs AdA, Bryant SV (1985) Autotomy and Regeneration in Reptiles. In: Gans C, Billett F (eds) Biology of the Reptilia. John Wiley & Sons, New York, pp 301-410

Bellman S, Oden B (1959) Regeneration of surgically divided lymph vessels; an experimental study on the rabbit's ear. Acta Chir Scand 116:99-117.

Benkert P, Tosatto SC, Schomburg D (2008) QMEAN: A comprehensive scoring function for model quality assessment. Proteins 71:261-277

Berggreen E, Haug SR, Mkonyi LE, Bletsa A (2009) Characterization of the dental lymphatic system and identification of cells immunopositive to specific lymphatic markers. Eur J Oral Sci 117:34-42

Bianchi J, Todd M (2000) The management of a patient with lymphoedema of the legs. Nurs Stand 14:51-52, 55-56

Blomhoff R, Green MH, Berg T, Norum KR (1990) Transport and storage of vitamin A. Science 250:399-404

Board J, Harlow W (2002a) Lymphoedema 1: components and function of the lymphatic system. Br J Nurs 11:304-309

Board J, Harlow W (2002b) Lymphoedema 3: the available treatments for lymphoedema. Br J Nurs 11:438-450

Boardman KC, Swartz MA (2003) Interstitial flow as a guide for lymphangiogenesis. Circ Res 92:801-808

Braden BC, Poljak RJ (1995) Structural features of the reactions between antibodies and protein antigens. FASEB J 9:9-16

Breslin JW, Yuan SY, Wu MH (2007) VEGF-C alters barrier function of cultured lymphatic endothelial cells through a VEGFR-3-dependent mechanism. Lymphat Res Biol 5:105-113

Brice G, Child AH, Evans A, Bell R, Mansour S, Burnand K, Sarfarazi M, Jeffery S, Mortimer P (2005) Milroy disease and the VEGFR-3 mutation phenotype. J Med Genet 42:98-102

Bridenbaugh EA, Gashev AA, Zawieja DC (2003) Lymphatic muscle: a review of contractile function. Lymphat Res Biol 1:147-158

Bryant SV (1970) Regeneration in amphibians and reptiles. Endeavour 29:12-17

Butler MG, Dagenais SL, Rockson SG, Glover TW (2007) A novel VEGFR3 mutation causes Milroy disease. Am J Med Genet A 143A:1212-1217

Byzova TV, Goldman CK, Jankau J, Chen JH, Cabrera G, Achen MG, Stacker SA, Carnevale KA, Slemionow M, Deitcher SR, DiCorleto PE (2002) Adenovirus encoding vascular endothelial growth factor-D induces tissue-specific vascular patterns in vivo. Blood 99:4434-4442

Cao R, Eriksson A, Kubo H, Alitalo K, Cao Y, Thyberg J (2004) Comparative evaluation of FGF-2-, VEGF-A-, and VEGF-C-induced angiogenesis, lymphangiogenesis, vascular fenestrations, and permeability. Circ Res 94:664-670

Cao Y (2008) Why and how do tumors stimulate lymphangiogenesis? Lymphat Res Biol 6:145-148

Cao Y, Linden P, Farnebo J, Cao R, Eriksson A, Kumar V, Qi JH, Claesson-Welsh L, Alitalo K (1998) Vascular endothelial growth factor C induces angiogenesis in vivo. Proc Natl Acad Sci U S A 95:14389-14394

Cao Y, Sun Z, Liao LM, Meng Y, Han Q, Zhao RCH (2005) Human adipose tissue-derived stem cells differentiate into endothelial cells in vitro and improve postnatal neovascularization in vivo. Biochem Biophys Res Commun 332:370-379

Casley-Smith JR (1962) The identification of chylomicra and lipoproteins in tissue sections and their passage into jejunal lacteals. J Cell Biol 15:259-277

Casley-Smith JR (1980) The fine structure and functioning of tissue channels and lymphatics. Lymphology 13:177-183

Cavanagh LL, Von Andrian UH (2002) Travellers in many guises: the origins and destinations of dendritic cells. Immunol Cell Biol 80:448-462

Chapman SW, Conklin RE (1935) The lymphatic system of the snake. J Morphol 58:385-417

Chen G, Gharib TG, Huang CC, Taylor JM, Misek DE, Kardia SL, Giordano TJ, Iannettoni MD, Orringer MB, Hanash SM, Beer DG (2002) Discordant protein and mRNA expression in lung adenocarcinomas. Mol Cell Proteomics 1:304-313

Chilov D, Kukk E, Taira S, Jeltsch M, Kaukonen J, Palotie A, Joukov V, Alitalo K (1997) Genomic organization of human and mouse genes for vascular endothelial growth factor C. J Biol Chem 272:25176-25183

Clark ER, Clark EL (1932) Observations on the new growth of lymphatic vessels as seen in transparent chambers introduced into the rabbit's ear. Am J Anat 51:49-87

Collawn JF, Wallace CJ, Proudfoot AE, Paterson Y (1988) Monoclonal antibodies as probes of conformational changes in protein-engineered cytochrome c. J Biol Chem 263:8625-8634

Cox PG (1969) Some aspects of tail regeneration in the lizard, *Anolis carolinensis*. II. The role of the peripheral nerves. J exp Zool 171:151-160

Cueni LN, Detmar M (2006) New insights into the molecular control of the lymphatic vascular system and its role in disease. J Invest Dermatol 126:2167-2177

Cursiefen C, Chen L, Borges LP, Jackson D, Cao JT, Radziejewski C, D'Amore PA, Dana MR, Wiegand SJ, Streilein JW (2004) VEGF-A stimulates lymphangiogenesis and hemangiogenesis in inflammatory neovascularization via macrophage recruitment. J Clin Invest 113:1040-1050

Cursiefen C, Chen L, Dana MR, Streilein JW (2003) Corneal lymphangiogenesis: evidence, mechanisms, and implications for corneal transplant immunology. Cornea 22:273-281

Cursiefen C, Schlotzer-Schrehardt U, Kuchle M, Sorokin L, Breiteneder-Geleff S, Alitalo K, Jackson D (2002) Lymphatic vessels in vascularized human corneas: immunohistochemical investigation using LYVE-1 and podoplanin. Invest Ophthalmol Vis Sci 43:2127-2135

Dadras SS, Paul T, Bertoncini J, Brown LF, Muzikansky A, Jackson DG, Ellwanger U, Garbe C, Mihm MC, Detmar M (2003) Tumor lymphangiogenesis: a novel prognostic indicator for cutaneous melanoma metastasis and survival. Am J Pathol 162:1951-1960

Dalla Valle L, Toffolo V, Belvedere P, Alibardi L (2005) Isolation of a mRNA encoding a glycine-proline-rich beta-keratin expressed in the regenerating epidermis of lizard. Dev Dyn 234:934-947

Daniels CB (1983) Running: an escape strategy enhanced by autotomy. Herpetologica 39:162-165

Daniels CB (1984a) The importance of caudal lipid in the gecko *Phyllodactylus marmoratus*. Herpetologica 40:337-344

Daniels CB (1984b) The role of caudal lipid in the adaptive strategy of tail autotomy in the gekkonid *Phyllodactylus marmoratus*. Department of Zoology. University of Adelaide, Adelaide

Daniels CB (1985) Economy of autotomy as a lipid conserving mechanism: an hypothesis rejected for the gecko *Phylladactylus marmoratus*. Copeia 1985:468-472

Daniels CB, Flaherty SP, Simbotwe MP (1986) Tail size and effectiveness of autotomy in a lizard. J Herpetol 20:93-96

Daniels CB, Lewis BC, Tsopelas C, Munns SL, Orgeig S, Baldwin ME, Stacker SA, Achen MG, Chatterton BE, Cooter RD (2003) Regenerating lizard tails: a new model for investigating lymphangiogenesis. FASEB J 17:479-481

Danussi C, Spessotto P, Petrucco A, Wassermann B, Sabatelli P, Montesi M, Doliana R, Bressan GM, Colombatti A (2008) Emilin1 deficiency causes structural and functional defects of lymphatic vasculature. Mol Cell Biol 28:4026-4039

Dhanasekaran SM, Barrette TR, Ghosh D, Shah R, Varambally S, Kurachi K, Pienta KJ, Rubin MA, Chinnaiyan AM (2001) Delineation of prognostic biomarkers in prostate cancer. Nature 412:822-826

Dial BE, Fitzpatrick LC (1983) Lizard tail autotomy: function and energetics of postautotomy tail movement in *Scincella lateralis*. Science 219:391-393

Dixelius J, Makinen T, Wirzenius M, Karkkainen MJ, Wernstedt C, Alitalo K, Claesson-Welsh L (2003a) Ligand-induced vascular endothelial growth factor receptor-3 (VEGFR-3) heterodimerization with VEGFR-2 in primary lymphatic endothelial cells regulates tyrosine phosphorylation sites. J Biol Chem 278:40973-40979

Dixelius J, Makinen T, Wirzenius M, Karkkainen MJ, Wernstedt C, Alitalo K, Claesson-Welsh L (2003b) Ligand-induced vascular endothelial growth factor receptor-3 (VEGFR-3) heterodimerization with VEGFR-2 in primary lymphatic endothelial cells regulates tyrosine phosphorylation sites. J Biol Chem 278:40973-40979

Dumont DJ, Jussila L, Taipale J, Lymboussaki A, Mustonen T, Pajusola K, Breitman M, Alitalo K (1998) Cardiovascular failure in mouse embryos deficient in VEGF receptor-3. Science 282:946-949

Eichmann A, Corbel C, Jaffredo T, Breant C, Joukov V, Kumar V, Alitalo K, le Douarin NM (1998) Avian VEGF-C: cloning, embryonic expression pattern and stimulation of the differentiation of VEGFR2-expressing endothelial cell precursors. Development 125:743-752.

Eisenberg D, Luthy R, Bowie JU (1997) VERIFY3D: assessment of protein models with three-dimensional profiles. Methods Enzymol 277:396-404

Enholm B, Karpanen T, Jeltsch M, Kubo H, Stenback F, Prevo R, Jackson DG, Yla-Herttuala S, Alitalo K (2001) Adenoviral expression of vascular endothelial growth factor-C induces lymphangiogenesis in the skin. Circ Res 88:623-629

Epstein SE, Fuchs S, Zhou YF, Baffour R, Kornowski R (2001a) Therapeutic interventions for enhancing collateral development by administration of growth factors: basic principles, early results and potential hazards. Cardiovasc Res 49:532-542

Epstein SE, Kornowski R, Fuchs S, Dvorak HF (2001b) Angiogenesis therapy - Amidst the hype, the neglected potential for serious side effects. Circulation 104:115-119

Etheridge R (1967) Lizard caudal vertebrae. Copeia:699-721

Fernandez MI, Bolenz C, Trojan L, Steidler A, Weiss C, Alken P, Grobholz R, Michel MS (2008) Prognostic implications of lymphangiogenesis in muscle-invasive transitional cell carcinoma of the bladder. Eur Urol 53:571-578

Ferrara N (2001) Role of vascular endothelial growth factor in regulation of physiological angiogenesis. Am J Physiol Cell Physiol 280:C1358-1366

Fitz LJ, Morris JC, Towler P, Long A, Burgess P, Greco R, Wang J, Gassaway R, Nickbarg E, Kovacic S, Ciarletta A, Giannotti J, Finnerty H, Zollner R, Beier DR, Leak LV, Turner KJ, Wood CR (1997) Characterization of murine Flt4 ligand VEGF-C. Oncogene 15:613-618

Flister MJ, Wilber A, Hall KL, Iwata C, Miyazono K, Nisato RE, Pepper MS, Zawieja DC, Ran S (2010) Inflammation induces lymphangiogenesis through up-regulation of VEGFR-3 mediated by NF-kappa B and Prox1. Blood 115:418-429

Fournier E, Dubreuil P, Birnbaum D, Borg JP (1995) Mutation at tyrosine residue 1337 abrogates ligand-dependent transforming capacity of the FLT4 receptor. Oncogene 11:921-931

Fu N, Drinnenberg I, Kelso J, Wu JR, Paabo S, Zeng R, Khaitovich P (2007) Comparison of protein and mRNA expression evolution in humans and chimpanzees. PLoS One 2:e216

Gale NW, Thurston G, Hackett SF, Renard R, Wang Q, McClain J, Martin C, Witte C, Witte MH, Jackson D, Suri C, Campochiaro PA, Wiegand SJ, Yancopoulos GD (2002) Angiopoietin-2 is required for postnatal angiogenesis and lymphatic patterning, and only the latter role is rescued by angiopoietin-1. Dev Cell 3:411-423

Gerhardt H, Golding M, Fruttiger M, Ruhrberg C, Lundkvist A, Abramsson A, Jeltsch M, Mitchell C, Alitalo K, Shima D, Betsholtz C (2003) VEGF guides angiogenic sprouting utilizing endothelial tip cell filopodia. J Cell Biol 161:1163-1177

Gerli R, Ibba L, Fruschelli C (1991) Ultrastructural cytochemistry of anchoring filaments of human lymphatic capillaries and their relation to elastic fibers. Lymphology 24:105-112.

Goldman J, Conley KA, Raehl A, Bondy DM, Pytowski B, Swartz MA, Rutkowski JM, Jaroch DB, Ongstad EL (2007) Regulation of lymphatic capillary regeneration by interstitial flow in skin. Am J Physiol Heart Circ Physiol 292:H2176-H2183

Gry M, Rimini R, Stromberg S, Asplund A, Ponten F, Uhlen M, Nilsson P (2009) Correlations between RNA and protein expression profiles in 23 human cell lines. BMC Genomics 10:365

Guo Y, Xiao P, Lei S, Deng F, Xiao GG, Liu Y, Chen X, Li L, Wu S, Chen Y, Jiang H, Tan L, Xie J, Zhu X, Liang S, Deng H (2008) How is mRNA expression predictive for protein expression? A correlation study on human circulating monocytes. Acta Biochim Biophys Sin (Shanghai) 40:426-436

Hall TA (1999) BioEdit a user-friendly biological sequence alignment editor and analysis program for Windows 95/98/NT. Nucl Acids Symp Ser 41:95-98

Hamrah P, Chen L, Zhang Q, Dana MR (2003) Novel expression of vascular endothelial growth factor receptor (VEGFR)-3 and VEGF-C on corneal dendritic cells. Am J Pathol 163:57-68

Harvey NL (2008) The link between lymphatic function and adipose biology. Ann N Y Acad Sci 1131:82-88

Harvey NL, Oliver G (2004) Choose your fate: artery, vein or lymphatic vessel? Curr Opin Genet Dev 14:499-505

Harvey NL, Srinivasan RS, Dillard ME, Johnson NC, Witte MH, Boyd K, Sleeman MW, Oliver G (2005) Lymphatic vascular defects promoted by Prox1 haploinsufficiency cause adult-onset obesity. Nat Genet 37:1072-1081

Hasegawa M, Nishigaki N, Washio Y, Kano K, Harris PA, Sato H, Mori I, West RI, Shibahara M, Toyoda H, Wang L, Nolte RT, Veal JM, Cheung M (2007) Discovery of Novel Benzimidazoles as Potent

Inhibitors of TIE-2 and VEGFR-2 Tyrosine Kinase Receptors. Journal of Medicinal Chemistry 50:4453-4470

Hausman GJ, Richardson RL (2004) Adipose tissue angiogenesis. J Anim Sci 82:925-934

He YL, Karpanen T, Alitalo K (2004) Role of lymphangiogenic factors in tumor metastasis. Biochimica Et Biophysica Acta-Reviews on Cancer 1654:3-12

Hedges SB (1994) Molecular evidence for the origin of birds. Proc Natl Acad Sci U S A 91:2621-2624

Hirakawa S, Brown LF, Kodama S, Paavonen K, Alitalo K, Detmar M (2007) VEGF-C-induced lymphangiogenesis in sentinel lymph nodes promotes tumor metastasis to distant sites. Blood 109:1010-1017

Hirakawa S, Kodama S, Kunstfeld R, Kajiya K, Brown LF, Detmar M (2005) VEGF-A induces tumor and sentinel lymph node lymphangiogenesis and promotes lymphatic metastasis. J Exp Med 201:1089-1099

Hoffstetter R, Gasc J-P (1969) Vertebrae and ribs of modern reptiles. In: Gans C, Bellairs AdA, Parsons S (eds) Biology of the Reptilia. Academic Press, London, pp 201-310

Hong YK, Harvey N, Noh YH, Schacht V, Hirakawa S, Detmar M, Oliver G (2002) Prox1 is a master control gene in the program specifying lymphatic endothelial cell fate. Dev Dyn 225:351-357

Houck KA, Leung DW, Rowland AM, Winer J, Ferrara N (1992) Dual regulation of vascular endothelial growth factor bioavailability by genetic and proteolytic mechanisms. J Biol Chem 267:26031-26037

Hughes A, New D (1959) Tail regeneration in the geckonid lizard, *Sphaerodactylus*. J Embryol Exp Morphol 7:281-302

Huntington GS, McClure CFW (1910) The anatomy and development of the jugular lymph sacs in the domestic cat (*Felis domestica*). Am J Anat 10:177-312

Irrthum A, Karkkainen MJ, Devriendt K, Alitalo K, Vikkula M (2000) Congenital hereditary lymphedema caused by a mutation that inactivates VEGFR3 tyrosine kinase. Am J Hum Genet 67:295-301

Ishii H, Yazawa T, Sato H, Suzuki T, Ikeda M, Hayashi Y, Takanashi Y, Kitamura H (2004) Enhancement of pleural dissemination and lymph node metastasis of intrathoracic lung cancer cells by vascular endothelial growth factors (VEGFs). Lung Cancer 45:325-337

Isogai S, Hitomi J, Yaniv K, Weinstein BM (2009) Zebrafish as a new animal model to study lymphangiogenesis. Anat Sci Int 14:14

Jackson DG, Prevo R, Clasper S, Banerji S (2001) LYVE-1, the lymphatic system and tumor lymphangiogenesis. Trends Immunol 22:317-321

Jeltsch M, Kaipainen A, Joukov V, Meng X, Lakso M, Rauvala H, Swartz M, Fukumura D, Jain RK, Alitalo K (1997) Hyperplasia of lymphatic vessels in VEGF-C transgenic mice. Science 276:1423-1425

Jeltsch M, Karpanen T, Strandin T, Aho K, Lankinen H, Alitalo K (2006) Vascular endothelial growth factor (VEGF)/VEGF-C mosaic molecules reveal specificity determinants and feature novel receptor binding patterns. J Biol Chem 281:12187-12195

Jeltsch M, Tammela T, Alitalo K, Wilting J (2003) Genesis and pathogenesis of lymphatic vessels. Cell Tissue Res 314:69-84

Ji RC (2005) Characteristics of lymphatic endothelial cells in physiological and pathological conditions. Histol Histopathol 20:155-175

Ji RC (2006) Lymphatic endothelial cells, lymphangiogenesis, and extracellular matrix. Lymphat Res Biol 4:83-100

Ji RC (2007) Lymphatic endothelial cells, inflammatory lymphangiogenesis, and prospective players. Curr Med Chem 14:2359-2368

Ji RC, Miura M, Qu P, Kato S (2004) Expression of VEGFR-3 and 5'-nase in regenerating lymphatic vessels of the cutaneous wound healing. Microsc Res Tech 64:279-286

Jiang MR, Gu XS, Feng X, Fan Z, Ding F, Liu Y (2009) The molecular characterization of the brain protein 44-like (Brp44l) gene of *Gekko japonicus* and its expression changes in spinal cord after tail amputation. Mol Biol Rep 36:215-220

Jin da P, An A, Liu J, Nakamura K, Rockson SG (2009) Therapeutic responses to exogenous VEGF-C administration in experimental lymphedema: immunohistochemical and molecular characterization. Lymphat Res Biol 7:47-57

Joukov V, Kaipainen A, Jeltsch M, Pajusola K, Olofsson B, Kumar V, Eriksson U, Alitalo K (1997a) Vascular endothelial growth factors VEGF-B and VEGF-C. J Cell Physiol 173:211-215.

Joukov V, Kumar V, Sorsa T, Arighi E, Weich H, Saksela O, Alitalo K (1998) A recombinant mutant vascular endothelial growth factor-c that has lost vascular endothelial growth factor receptor-2 binding, activation, and vascular permeability activities. J Biol Chem 273:6599-6602

Joukov V, Pajusola K, Kaipainen A, Chilov D, Lahtinen I, Kukk E, Saksela O, Kalkkinen N, Alitalo K (1996) A novel vascular endothelial growth factor, VEGF-C, is a ligand for the Flt4 (VEGFR-3) and KDR (VEGFR-2) receptor tyrosine kinases. EMBO J 15:1751

Joukov V, Sorsa T, Kumar V, Jeltsch M, Claesson-Welsh L, Cao Y, Saksela O, Kalkkinen N, Alitalo K (1997b) Proteolytic processing regulates receptor specificity and activity of VEGF-C. EMBO J 16:3898-3911

Jussila L, Alitalo K (2002) Vascular growth factors and lymphangiogenesis. Physiol Rev 82:673-700

Kaipainen A, Korhonen J, Mustonen T, van Hinsbergh VW, Fang GH, Dumont D, Breitman M, Alitalo K (1995) Expression of the fms-like tyrosine kinase 4 gene becomes restricted to lymphatic endothelium during development. Proc Natl Acad Sci U S A 92:3566-3570

Kajiya K, Detmar M (2006) An important role of lymphatic vessels in the control of UVB-induced edema formation and inflammation. J Invest Dermatol 126:919-921

Kalin RE, Banziger-Tobler NE, Detmar M, Brandli AW (2009) An in vivo chemical library screen in Xenopus tadpoles reveals novel pathways involved in angiogenesis and lymphangiogenesis. Blood 114:1110-1122

Kampmeier OF (1969) Evolution and comparative morphology of the lymphatic system. Charles C Thomas Publisher, Springfield

Kamrin RP, Singer M (1955) The influence of the spinal cord in regeneration of the tail of the lizard, *Anolis carolinensis*. J exp Zool 128:611-627

Kang Y, Park C, Kim D, Seong CM, Kwon K, Choi C (2010) Unsorted human adipose tissue-derived stem cells promote angiogenesis and myogenesis in murine ischemic hindlimb model. Microvasc Res 80:310-316

Karkkainen MJ, Ferrell RE, Lawrence EC, Kimak MA, Levinson KL, McTigue MA, Alitalo K, Finegold DN (2000) Missense mutations interfere with VEGFR-3 signalling in primary lymphoedema. Nat Genet 25:153-159

Karkkainen MJ, Haiko P, Sainio K, Partanen J, Taipale J, Petrova TV, Jeltsch M, Jackson DG, Talikka M, Rauvala H, Betsholtz C, Alitalo K (2004) Vascular endothelial growth factor C is required for sprouting of the first lymphatic vessels from embryonic veins. Nat Immunol 5:74-80

Karkkainen MJ, Saaristo A, Jussila L, Karila KA, Lawrence EC, Pajusola K, Bueler H, Eichmann A, Kauppinen R, Kettunen MI, Yla-Herttuala S, Finegold DN, Ferrell RE, Alitalo K (2001) A model for gene therapy of human hereditary lymphedema. Proc Natl Acad Sci U S A 98:12677-12682

Karpanen T, Alitalo K (2008) Molecular biology and pathology of lymphangiogenesis. Annu Rev Pathol 3:367-397

Karpanen T, Egeblad M, Karkkainen MJ, Kubo H, Yla-Herttuala S, Jaattela M, Alitalo K (2001) Vascular endothelial growth factor C promotes tumor lymphangiogenesis and intralymphatic tumor growth. Cancer Res 61:1786-1790

Kawakami M, Yanai Y, Hata F, Hirata K (2005) Vascular endothelial growth factor C promotes lymph node metastasis in a rectal cancer orthotopic model. Surg Today 35:131-138

Kerjaschki D (2005) The crucial role of macrophages in lymphangiogenesis. J Clin Invest 115:2316-2319

Kerjaschki D, Huttary N, Raab I, Regele H, Bojarski-Nagy K, Bartel G, Krober SM, Greinix H, Rosenmaier A, Karlhofer F, Wick N, Mazal PR (2006) Lymphatic endothelial progenitor cells contribute to de novo lymphangiogenesis in human renal transplants. Nat Med 12:230-234

Khatib AM, Lahlil R, Scamuffa N, Akimenko MA, Ernest S, Lomri A, Lalou C, Seidah NG, Villoutreix BO, Calvo F, Siegfried G (2010) Zebrafish ProVEGF-C expression, proteolytic processing and inhibitory effect of unprocessed ProVEGF-C during fin regeneration. PLoS One 5:e11438

Kivelä R, Havas E, Vihko V (2007) Localisation of lymphatic vessels and vascular endothelial growth factors-C and -D in human and mouse skeletal muscle with immunohistochemistry. Histochem cell biol 127:31-40

Kleespies A, Bruns CJ, Jauch KW (2005) Clinical significance of VEGF-A, -C and -D expression in esophageal malignancies. Onkologie 28:281-288

Kotani M (1959) [Lymphatic vessels, lymphatic system and extravascular lymph tracts of the snake (*Elaphe quadrivirgata* Boie)]. Acta Sch Med Univ Kioto 36:121-171

Kotani M (1990) New concepts related to the evolution of lymphatics. In: Nishi M, Uchino S, Yabuki S (eds) Progress in Lymphology. Elsevier, Amsterdam, pp 113-115

Kriederman BM, Myloyde TL, Witte MH, Dagenais SL, Witte CL, Rennels M, Bernas MJ, Lynch MT, Erickson RP, Caulder MS, Miura N, Jackson D, Brooks BP, Glover TW (2003) FOXC2 haploinsufficient mice are a model for human autosomal dominant lymphedema-distichiasis syndrome. Hum Mol Genet 12:1179-1185

Kubo H, Fujiwara T, Jussila L, Hashi H, Ogawa M, Shimizu K, Awane M, Sakai Y, Takabayashi A, Alitalo K, Yamaoka Y, Nishikawa SI (2000) Involvement of vascular endothelial growth factor receptor-3 in maintenance of integrity of endothelial cell lining during tumor angiogenesis. Blood 96:546-553

Kuchler AM, Gjini E, Peterson-Maduro J, Cancilla B, Wolburg H, Schulte-Merker S (2006) Development of the zebrafish lymphatic system requires VEGFC signaling. Curr Biol 16:1244-1248

Kuhn G, Gruber P, Müller R, Rühli F (2008) Three-dimensional evaluation of structures in small bones by Micro- CT: tail fracture planes of autotomizing lizards (Scincidae and Gecconidae families). Internet J Biol Anthrop 1

Kukk E, Lymboussaki A, Taira S, Kaipainen A, Jeltsch M, Joukov V, Alitalo K (1996) VEGF-C receptor binding and pattern of expression with VEGFR-3 suggests a role in lymphatic vascular development. Development 122:3829-3837

Kunstfeld R, Hirakawa S, Hong Y, Lange-Asschenfeldt B, Velasco P, Fiebiger E, Wu Y, Hicklin D, Bohlen P, Detmar M (2004) VEGF-A induced psoriatic skin inflammation and the associated lymphangiogenic response are ameliorated by systemic blockage of VEGF receptor-1 and-2. J Invest Dermatol 122:009

Laakkonen P, Waltari M, Holopainen T, Takahashi T, Pytowski B, Steiner P, Hicklin D, Persaud K, Tonra JR, Witte L, Alitalo K (2007) Vascular endothelial growth factor receptor 3 is involved in tumor angiogenesis and growth. Cancer Res 67:593-599

Lahat G, Lazar A, Wang X, Wang WL, Zhu QS, Hunt KK, Pollock RE, Lev D (2009) Increased vascular endothelial growth factor-C expression is insufficient to induce lymphatic metastasis in human soft-tissue sarcomas. Clin Cancer Res 15:2637-2646

Landis EM, Pappenheimer JR (1963) Exchange of substances through the capillary wall. In: Pow P (ed) Handbook of Physiology. American Physiological Society, Washington, pp 961-1073

Leak LV (1976) The structure of lymphatic capillaries in lymph formation. Fed Proc 35:1863-1871

Leak LV, Burke JF (1968) Ultrastructural studies on the lymphatic anchoring filaments. J Cell Biol 36:129-149

Leduc O, Leduc A, Bourgeois P, Belgrado JP (1998) The physical treatment of upper limb edema. Cancer 83:2835-2839

Lee S, Choi I, Hong Y-K (2010) Heterogeneity and plasticity of lymphatic endothelial cells. Semin Thromb Hemost 36:352,361

Leppänen V-M, Prota AE, Jeltsch M, Anisimov A, Kalkkinen N, Strandin T, Lankinen H, Goldman A, Ballmer-Hofer K, Alitalo K (2010) Structural determinants of growth factor binding and specificity by VEGF receptor 2. Proc Natl Acad Sci U S A 107:2425-2430

Leung DW, Cachianes G, Kuang WJ, Goeddel DV, Ferrara N (1989) Vascular endothelial growth factor is a secreted angiogenic mitogen. Science 246:1306-1309

Licht P, Howe NR (1969) Hormonal dependence of tail regeneration in the lizard *Anolis carolinensis*. J exp Zool 171:75-84

Ling S, Lin H, Liang L, Xu J, Xu C, Zhao W, Liu Z (2009) Development of new lymphatic vessels in alkali-burned corneas. Acta Ophthalmol 87:315-322

Liu Y, Fan Z, Zhou YL, Liu M, Ding F, Gu XS (2009) The molecular cloning of platelet-derived growth factor-c (PDGF-C) gene of *Gekko japonicus* and its expression change in the spinal cord after tail amputation. Cell Mol Neurobiol 29:263-271

Lyttle DJ, Fraser KM, Fleming SB, Mercer AA, Robinson AJ (1994) Homologs of vascular endothelial growth factor are encoded by the poxvirus orf virus. J Virol 68:84-92

Madonna R, De Caterina R (2008) In vitro neovasculogenic potential of resident adipose tissue precursors. Am J Physiol Cell Physiol 295:C1271-C1280

Maglione D, Guerriero V, Viglietto G, Delli-Bovi P, Persico MG (1991) Isolation of a human placenta cDNA coding for a protein related to the vascular permeability factor. Proc Natl Acad Sci U S A 88:9267-9271

Maisonpierre PC, Suri C, Jones PF, Bartunkova S, Wiegand S, Radziejewski C, Compton D, McClain J, Aldrich TH, Papadopoulos N, Daly TJ, Davis S, Sato TN, Yancopoulos GD (1997) Angiopoietin-2, a natural antagonist for Tie2 that disrupts in vivo angiogenesis. Science 277:55-60

Makinen T, Jussila L, Veikkola T, Karpanen T, Kettunen MI, Pulkkanen KJ, Kauppinen R, Jackson DG, Kubo H, Nishikawa S, Yla-Herttuala S, Alitalo K (2001a) Inhibition of lymphangiogenesis with resulting lymphedema in transgenic mice expressing soluble VEGF receptor-3. Nat Med 7:199-205

Makinen T, Norrmen C, Petrova TV (2007) Molecular mechanisms of lymphatic vascular development. Cellular and Molecular Life Sciences 64:1915-1929

Makinen T, Veikkola T, Mustjoki S, Karpanen T, Catimel B, Nice EC, Wise L, Mercer A, Kowalski H, Kerjaschki D, Stacker SA, Achen MG, Alitalo K (2001b) Isolated lymphatic endothelial cells transduce growth, survival and migratory signals via the VEGF-C/D receptor VEGFR-3. EMBO J 20:4762-4773.

Mandriota SJ, Jussila L, Jeltsch M, Compagni A, Baetens D, Prevo R, Banerji S, Huarte J, Montesano R, Jackson DG, Orci L, Alitalo K, Christofori G, Pepper MS (2001) Vascular endothelial growth factor-C-mediated lymphangiogenesis promotes tumour metastasis. EMBO J 20:672-682

Marconcini L, Marchio S, Morbidelli L, Cartocci E, Albini A, Ziche M, Bussolino F, Oliviero S (1999) c-fos-induced growth factor/vascular endothelial growth factor D induces angiogenesis in vivo and in vitro. Proc Natl Acad Sci U S A 96:9671-9676

Maruyama K, Li M, Cursiefen C, Jackson DG, Keino H, Tomita M, Van Rooijen N, Takenaka H, D'Amore PA, Stein-Streilein J, Losordo DW, Streilein JW (2005) Inflammation-induced lymphangiogenesis in the cornea arises from CD11 b-positive macrophages. J Clin Invest 115:2363-2372

Mattila MM, Ruohola JK, Karpanen T, Jackson DG, Alitalo K, Harkonen PL (2002) VEGF-C induced lymphangiogenesis is associated with lymph node metastasis in orthotopic MCF-7 tumors. Int J Cancer 98:946-951

McColl BK, Baldwin ME, Roufail S, Freeman C, Moritz RL, Simpson RJ, Alitalo K, Stacker SA, Achen MG (2003) Plasmin activates the lymphangiogenic growth factors VEGF-C and VEGF-D. J Exp Med 198:863-868

McColl BK, Paavonen K, Karnezis T, Harris NC, Davydova N, Rothacker J, Nice EC, Harder KW, Roufail S, Hibbs ML, Rogers PA, Alitalo K, Stacker SA, Achen MG (2007) Proprotein convertases promote processing of VEGF-D, a critical step for binding the angiogenic receptor VEGFR-2. FASEB J 21:1088-1098

McColl BK, Stacker SA, Achen MG (2004) Molecular regulation of the VEGF family -- inducers of angiogenesis and lymphangiogenesis. APMIS 112:463-480.

McConnachie S, Whiting M (2003) Costs associated with tail autotomy in an ambush foraging lizard, *Cordylus melanotus melanotus.* Afr Zool 38:57-65

Melo F, Feytmans E (1998) Assessing protein structures with a non-local atomic interaction energy. J Mol Biol 277:1141-1152

Mescher AL (1996) The cellular basis of limb regeneration in urodeles. Int J Dev Biol 40:785-795

Milroy WF (1892) An undescribed variety of hereditory oedema. N Y Med J 56:505-508

Miranville A, Heeschen C, Sengenes C, Curat CA, Busse R, Bouloumie A (2004) Improvement of postnatal neovascularization by human adipose tissue-derived stem cells. Circulation 110:349-355

Mortimer PS (1990) Investigation and management of lymphoedema. Vasc Med Rev 1:1-20

Mortimer PS, Bates SO, Brassington HD, Stanton AWB, Strachan DP, Levick JR (1996) The prevalence of arm edema following treatment for breast cancer. Q J Med 89:377-380

Mousses S, Bubendorf L, Wagner U, Hostetter G, Kononen J, Cornelison R, Goldberger N, Elkahloun AG, Willi N, Koivisto P, Ferhle W, Raffeld M, Sauter G, Kallioniemi OP (2002) Clinical validation of candidate genes associated with prostate cancer progression in the CWR22 model system using tissue microarrays. Cancer Res 62:1256-1260

Muller YA, Heiring C, Misselwitz R, Welfle K, Welfle H (2002) The cystine knot promotes folding and not thermodynamic stability in vascular endothelial growth factor. J Biol Chem 277:43410-43416

Mustonen T, Alitalo K (1995) Endothelial receptor tyrosine kinases involved in angiogenesis. J Cell Biol 129:895-898

Nakagami H, Morishita R, Maeda K, Kikuchi Y, Ogihara T, Kaneda Y (2006) Adipose tissue-derived stromal cells as a novel option for regenerative cell therapy. J Atheroscler Thromb 13:77-81

Ny A, Autiero M, Carmeliet P (2006) Zebrafish and *Xenopus* tadpoles: Small animal models to study angiogenesis and lymphangiogenesis. Exp Cell Res 312:684-693

Ny A, Koch M, Schneider M, Neven E, Tong RT, Maity S, Fischer C, Plaisance S, Lambrechts D, Heligon C, Terclavers S, Ciesiolka M, Kalin R, Man WY, Senn I, Wyns S, Lupu F, Brandli A, Vleminckx K, Collen D, Dewerchin M, Conway EM, Moons L, Jain RK, Carmeliet P (2005) A genetic *Xenopus laevis* tadpole model to study lymphangiogenesis. Nat Med 11:998-1004

Ny A, Koch M, Vandevelde W, Schneider M, Fischer C, Diez-Juan A, Neven E, Geudens I, Maity S, Moons L, Plaisance S, Lambrechts D, Carmeliet P, Dewerchin M (2008) Role of VEGF-D and VEGFR-3 in developmental lymphangiogenesis, a chemicogenetic study in *Xenopus* tadpoles. Blood 112:1740-1749

Ober EA, Olofsson B, Makinen T, Jin SW, Shoji W, Koh GY, Alitalo K, Stainier DY (2004) Vegfc is required for vascular development and endoderm morphogenesis in zebrafish. EMBO Rep 5:78-84

Odelberg SJ (2005) Cellular plasticity in vertebrate regeneration. Anat Rec B New Anat 287:25-35

Oden B (1960) A micro-lymphangiographic study of experimental wounds healing by second intention. Acta Chir Scand 120:100-114.

Oh SJ, Jeltsch MM, Birkenhager R, McCarthy JE, Weich HA, Christ B, Alitalo K, Wilting J (1997) VEGF and VEGF-C: specific induction of angiogenesis and lymphangiogenesis in the differentiated avian chorioallantoic membrane. Dev Biol 188:96-109

Oliver G (2004) Lymphatic vasculature development. Nat Rev Immunol 4:35-45

Oliver G, Alitalo K (2005) The lymphatic vasculature: recent progress and paradigms. Annu Rev Cell Dev Biol 21:457-483

Oliver G, Harvey N (2002) A stepwise model of the development of lymphatic vasculature. Ann N Y Acad Sci 979:159-165

Olofsson B, Pajusola K, Kaipainen A, von Euler G, Joukov V, Saksela O, Orpana A, Pettersson RF, Alitalo K, Eriksson U (1996) Vascular endothelial growth factor B, a novel growth factor for endothelial cells. Proc Natl Acad Sci U S A 93:2576-2581

Olsson AK, Dimberg A, Kreuger J, Claesson-Welsh L (2006) VEGF receptor signalling - in control of vascular function. Nat Rev Mol Cell Biol 7:359-371

Orlandini M, Oliviero S (2001) In fibroblasts Vegf-D expression is induced by cell-cell contact mediated by cadherin-11. J Biol Chem 276:6576-6581

Otrock ZK, Makarem JA, Shamseddine AI (2007) Vascular endothelial growth factor family of ligands and receptors: Review. Blood Cell Mol Dis 38:258-268

Ottaviani G, Tazzi A (1977) The Lymphatic System. In: Gans C (ed) Biology of the Reptilia. Academic Press, London, pp 315-462

Paavonen K, Mandelin J, Partanen T, Jussila L, Li TF, Ristimaki A, Alitalo K, Konttinen YT (2002) Vascular endothelial growth factors C and D and their VEGFR-2 and 3 receptors in blood and lymphatic vessels in healthy and arthritic synovium. J Rheumatol 29:39-45

Paavonen K, Puolakkainen P, Jussila L, Jahkola T, Alitalo K (2000) Vascular endothelial growth factor receptor-3 in lymphangiogenesis in wound healing. Am J Pathol 156:1499-1504.

Pajusola K, Aprelikova O, Pelicci G, Weich H, Claesson-Welsh L, Alitalo K (1994) Signalling properties of FLT4, a proteolytically processed receptor tyrosine kinase related to two VEGF receptors. Oncogene 9:3545-3555

Panizza B (1833) Sopra il sistema linfatico dei rettili, ricerche zootomiche. Typographia Fusi, Pavia

Papoutsi M, Tomarev SI, Eichmann A, Prols F, Christ B, Wilting J (2001) Endogenous origin of the lymphatics in the avian chorioallantoic membrane. Dev Dyn 222:238-251

Partanen TA, Alitalo K, Miettinen M (1999) Lack of lymphatic vascular specificity of vascular endothelial growth factor receptor 3 in 185 vascular tumors. Cancer 86:2406-2412

Partanen TA, Arola J, Saaristo A, Jussila L, Ora A, Miettinen M, Stacker SA, Achen MG, Alitalo K (2000) VEGF-C and VEGF-D expression in neuroendocrine cells and their receptor, VEGFR-3, in fenestrated blood vessels in human tissues. FASEB J 14:2087-2096

Partanen TA, Paavonen K (2001) Lymphatic versus blood vascular endothelial growth factors and receptors in humans. Microsc Res Tech 55:108-121

Pennisi D, Gardner J, Chambers D, Hosking B, Peters J, Muscat G, Abbott C, Koopman P (2000) Mutations in Sox18 underlie cardiovascular and hair follicle defects in ragged mice. Nat Genet 24:434-437

Pepper MS, Tille JC, Nisato R, Skobe M (2003) Lymphangiogenesis and tumor metastasis. Cell Tissue Res 314:167-177

Petrek JA, Pressman PI, Smith RA (2000) Lymphedema: Current issues in research and management. CA Cancer J Clin 50:292-307

Petrova TV, Bono P, Holnthoner W, Chesnes J, Pytowski B, Sihto H, Laakkonen P, Heikkila P, Joensuu H, Alitalo K (2008) VEGFR-3 expression is restricted to blood and lymphatic vessels in solid tumors. Cancer Cell 13:554-556

Petrova TV, Karpanen T, Norrmen C, Mellor R, Tamakoshi T, Finegold D, Ferrell R, Kerjaschki D, Mortimer P, Yla-Herttuala S, Miura N, Alitalo K (2004) Defective valves and abnormal mural cell recruitment underlie lymphatic vascular failure in lymphedema distichiasis. Nat Med 10:974-981

Petrova TV, Makinen T, Makela TP, Saarela J, Virtanen I, Ferrell RE, Finegold DN, Kerjaschki D, Yla-Herttuala S, Alitalo K (2002) Lymphatic endothelial reprogramming of vascular endothelial cells by the Prox-1 homeobox transcription factor. Embo Journal 21:4593-4599

Pettersen EF, Goddard TD, Huang CC, Couch GS, Greenblatt DM, Meng EC, Ferrin TE (2004) UCSF Chimera--a visualization system for exploratory research and analysis. J Comput Chem 25:1605-1612

Planat-Benard V, Silvestre JS, Cousin B, Andre M, Nibbelink M, Tamarat R, Clergue M, Manneville C, Saillan-Barreau C, Duriez M, Tedgui A, Levy B, Penicaud L, Casteilla L (2004) Plasticity of human adipose lineage cells toward endothelial cells - Physiological and therapeutic perspectives. Circulation 109:656-663

Poltorak Z, Cohen T, Sivan R, Kandelis Y, Spira G, Vlodavsky I, Keshet E, Neufeld G (1997) VEGF145, a secreted vascular endothelial growth factor isoform that binds to extracellular matrix. J Biol Chem 272:7151-7158

Pratt CW (1946) The plane of fracture of the caudal vertebrae of certain lacertilians. J Anat 80:184-188

Pytowski B, Goldman J, Persaud K, Wu Y, Witte L, Hicklin DJ, Skobe M, Boardman KC, Swartz MA (2005) Complete and specific inhibition of adult lymphatic regeneration by a novel VEGFR-3 neutralizing antibody. J Natl Cancer Inst 97:14-21

Quattrini D (1954) Piano di autotomia e rigenerazione della coda nei Sauri. Archo ital Anat Embriol 59:225-282

Quattrini D (1955) Richerche sperimentali sulla rigenerazione della coda dei Sauri (Osservazioni in *Lacerta sicula campestris* de betta e . *muralis Brueggemanni* Bedr.). Monit Zool Ital 62:210-222

Rafii S (2000) Circulating endothelial precursors: mystery, reality, and promise. J Clin Invest 105:17-19

Rehman J, Traktuev D, Li JL, Merfeld-Clauss S, Temm-Grove CJ, Bovenkerk JE, Pell CL, Johnstone BH, Considine RV, March KL (2004) Secretion of angiogenic and antiapoptotic factors by human adipose stromal cells. Circulation 109:1292-1298

Renyi-Vamos F, Tovari J, Fillinger J, Timar J, Paku S, Kenessey I, Ostoros G, Agocs L, Soltesz I, Dome B (2005) Lymphangiogenesis correlates with lymph node metastasis, prognosis, and angiogenic phenotype in human non-small cell lung cancer. Clin Cancer Res 11:7344-7353

Reverberi R, Reverberi L (2007) Factors affecting the antigen-antibody reaction. Blood Transfus 5:227-240

Risau W (1997) Mechanisms of angiogenesis. Nature 386:671-674

Rissanen TT, Markkanen JE, Gruchala M, Heikura T, Puranen A, Kettunen MI, Kholova I, Kauppinen RA, Achen MG, Stacker SA, Alitalo K, Yla-Herttuala S (2003) VEGF-D is the strongest angiogenic and lymphangiogenic effector among VEGFs delivered into skeletal muscle via adenoviruses. Circ Res 92:1098-1106

Ristimaki A, Narko K, Enholm B, Joukov V, Alitalo K (1998) Proinflammatory cytokines regulate expression of the lymphatic endothelial mitogen vascular endothelial growth factor-C. J Biol Chem 273:8413-8418

Rossi A, Weber E, Sacchi G, Maestrini D, Di Cintio F, Gerli R (2007) Mechanotransduction in lymphatic endothelial cells. Lymphology 40:102-113

Routh HB, Bhowmik KR (1994) Filariasis. Dermatol Clin 12:719-727

Rutkowski JM, Boardman KC, Swartz MA (2006) Characterization of lymphangiogenesis in a model of adult skin regeneration. Am J Physiol Heart Circ Physiol 28:28

Ryan TJ (1989) Structure and function of lymphatics. J Invest Dermatol 93:18S-24S

Saaristo A, Karpanen T, Alitalo K (2000) Mechanisms of angiogenesis and their use in the inhibition of tumor growth and metastasis. Oncogene 19:6122-6129

Saaristo A, Tammela T, Farkkila A, Karkkainen M, Suominen E, Yla-Herttuala S, Alitalo K (2006) Vascular endothelial growth factor-C accelerates diabetic wound healing. Am J Pathol 169:1080-1087

Saaristo A, Tammela T, Timonen J, Yla-Herttuala S, Tukiainen E, Asko-Seljavaara S, Alitalo K (2004) Vascular endothelial growth factor-C gene therapy restores lymphatic flow across incision wounds. FASEB J 18:1707-1709

Saaristo A, Veikkola T, Enholm B, Hytonen M, Arola J, Pajusola K, Turunen P, Jeltsch M, Karkkainen MJ, Kerjaschki D, Bueler H, Yla-Herttuala S, Alitalo K (2002a) Adenoviral VEGF-C overexpression induces blood vessel enlargement, tortuosity, and leakiness but no sprouting angiogenesis in the skin or mucous membranes. FASEB J 16:1041-1049

Saaristo A, Veikkola T, Tammela T, Enholm B, Karkkainen MJ, Pajusola K, Bueler H, Yla-Herttuala S, Alitalo K (2002b) Lymphangiogenic gene therapy with minimal blood vascular side effects. J Exp Med 196:719-730

Sabin FR (1902) On the origin of the lymphatic system from the veins and the development of the lymph hearts and thoracic duct in the pig. Am J Anat 1:367-389

Saharinen P, Bry M, Alitalo K (2010) How do angiopoietins Tie in with vascular endothelial growth factors? Curr Opin Hematol 17:198-205

Saharinen P, Tammela T, Karkkainen MJ, Alitalo K (2004) Lymphatic vasculature: development, molecular regulation and role in tumor metastasis and inflammation. Trends Immunol 25:387-395

Sasisekharan R, Venkataraman G (2000) Heparin and heparan sulfate: biosynthesis, structure and function. Curr Opin Chem Biol 4:626-631

Schacht V, Ramirez MI, Hong YK, Hirakawa S, Feng D, Harvey N, Williams M, Dvorak AM, Dvorak HF, Oliver G, Detmar M (2003) T1alpha/podoplanin deficiency disrupts normal lymphatic vasculature formation and causes lymphedema. EMBO J 22:3546-3556

Schaffler A, Buchler C (2007) Concise review: Adipose tissue-derived stromal cells - Basic and clinical implications for novel cell-based therapies. Stem Cells 25:818-827

Schledzewski K, Falkowski M, Moldenhauer G, Metharom P, Kzhyshkowska J, Ganss R, Demory A, Falkowska-Hansen B, Kurzen H, Ugurel S, Geginat G, Arnold B, Goerdt S (2006) Lymphatic endothelium-specific hyaluronan receptor LYVE-1 is expressed by stabilin-1(+), F4/80(+), CD11b(+) macrophages in malignant tumours and wound healing tissue in vivo and in bone marrow cultures in vitro: implications for the assessment of lymphangiogenesis. J Pathol 209:67-77

Schmid-Schonbein GW (2003) The second valve system in lymphatics. Lymphat Res Biol 1:25-31

Schneider M, Othman-Hassan K, Christ B, Wilting J (1999) Lymphangioblasts in the avian wing bud. Dev Dyn 216:311-319

Schoppmann SF, Birner P, Stockl J, Kalt R, Ullrich R, Caucig C, Kriehuber E, Nagy K, Alitalo K, Kerjaschki D (2002a) Tumor-associated macrophages express lymphatic endothelial growth factors and are related to peritumoral lymphangiogenesis. Am J Pathol 161:947-956.

Schoppmann SF, Birner P, Stockl J, Kalt R, Ullrich R, Caucig C, Kriehuber E, Nagy K, Alitalo K, Kerjaschki D (2002b) Tumor-associated macrophages express lymphatic endothelial growth factors and are related to peritumoral lymphangiogenesis. Am J Pathol 161:947-956

Sengenès C, Lolmède K, Zakaroff-Girard A, Busse R, Bouloumié A (2005) Preadipocytes in the human subcutaneous adipose tissue display distinct features from the adult mesenchymal and hematopoietic stem cells. J Cell Physiol 205:114-122

Sheppard L, Bellairs AdA (1972) The mechanism of tail autotomy in *Lacerta*. British Journal of Herpetology 4:276-286

Shimoda H, Takahashi Y, Kato S (2004) Regrowth of lymphatic vessels following transection of the muscle coat in the rat small intestine. Cell Tissue Res 316:325-338

Shin WS, Rockson SG (2008) Animal models for the molecular and mechanistic study of lymphatic biology and disease. Ann N Y Acad Sci 1131:50-74

Siegfried G, Basak A, Cromlish JA, Benjannet S, Marcinkiewicz J, Chretien M, Seidah NG, Khatib AM (2003) The secretory proprotein convertases furin, PC5, and PC7 activate VEGF-C to induce tumorigenesis. J Clin Invest 111:1723-1732

Simpson SB, Jr. (1964) Analysis of tail regeneration in the lizard *Lygosoma Laterale*. I. Initiation of regeneration and cartilage differentiation: The role of ependyma. J Morphol 114:425-435

Simpson SB, Jr. (1970) Studies on regeneration of the lizard's tail. Am Zool 10:157-165

Simpson SB, Jr. (1977) Nerves, trophic factors and limb regeneration. In: Ede DA, Hinchliffe JR, Balls M (eds) British Society for Developmental Symposium No 3. Cambridge University Press, pp 329-346

Singer M (1980) The influence of nerves in amphibian regeneration, with special emphasis on the relationship between nerves and epidermis. In: Spearman RIC, Riley PA (eds) The Skin of Vertebrates. Academic Press, London, pp 151-159

Skobe M, Detmar M (2000) Structure, function, and molecular control of the skin lymphatic system. J Invest Dermatol Symp Proc 5:14-19.

Skobe M, Hamberg LM, Hawighorst T, Schirner M, Wolf GL, Alitalo K, Detmar M (2001a) Concurrent induction of lymphangiogenesis, angiogenesis, and macrophage recruitment by vascular endothelial growth factor-C in melanoma. Am J Pathol 159:893-903

Skobe M, Hawighorst T, Jackson DG, Prevo R, Janes L, Velasco P, Riccardi L, Alitalo K, Claffey K, Detmar M (2001b) Induction of tumor lymphangiogenesis by VEGF-C promotes breast cancer metastasis. Nat Med 7:192-198

Slavin SA, Upton J, Kaplan WD, Van den Abbeele AD (1997) An investigation of lymphatic function following free-tissue transfer. Plast Reconstr Surg 99:730-741

Sleeman J, Schmid A, Thiele W (2009) Tumor lymphatics. Semin Cancer Biol 19:285-297

Sleeman JP, Thiele W (2009) Tumor metastasis and the lymphatic vasculature. Int J Cancer 125:2747-2756

Smith AR, van Alphen WA, van der Pompe WB (1987) Lymphatic drainage in patients after replantation of extremities. Plast Reconstr Surg 79:163-170.

Song M, Yang H, Yao S, Ma F, Li Z, Deng Y, Deng H, Zhou Q, Lin S, Wei Y (2007) A critical role of vascular endothelial growth factor D in zebrafish embryonic vasculogenesis and angiogenesis. Biochem Biophys Res Commun 357:924-930

Spanner R (1929) Über die Wurzelgebiete der Nieren-,Nebennieren und Leberpfortader bei Reptilien. Morph Jb 63:314-358

Stacker SA, Achen MG (1999) The vascular endothelial growth factor family: signalling for vascular development. Growth Factors 17:1-11

Stacker SA, Achen MG, Jussila L, Baldwin ME, Alitalo K (2002a) Metastasis: Lymphangiogenesis and cancer metastasis. Nat Rev Cancer 2:573-583

Stacker SA, Baldwin ME, Achen MG (2002b) The role of tumor lymphangiogenesis in metastatic spread. FASEB J 16:922-934

Stacker SA, Caesar C, Baldwin ME, Thornton GE, Williams RA, Prevo R, Jackson DG, Nishikawa S, Kubo H, Achen MG (2001) VEGF-D promotes the metastatic spread of tumor cells via the lymphatics. Nat Med 7:186-191

Stacker SA, Stenvers K, Caesar C, Vitali A, Domagala T, Nice E, Roufail S, Simpson RJ, Moritz R, Karpanen T, Alitalo K, Achen MG (1999) Biosynthesis of vascular endothelial growth factor-D involves proteolytic processing which generates non-covalent homodimers. J Biol Chem 274:32127-32136

Steffensen JF, Lomholt JP (1992) The Secondary Vascular System. In: Hoar WS, Randall DJ, Farrell AP (eds) Fish Physiology. Academic Press, New York, pp 185-217

Steffensen JF, Lomholt JP, Vogel WOP (1986) In vivo observations on a specialized microvasculature, the primary and secondary vessels in fishes. Acta Zool 67:193-200

Su JL, Yen CJ, Chen PS, Chuang SE, Hong CC, Kuo IH, Chen HY, Hung MC, Kuo ML (2007) The role of the VEGF-C/VEGFR-3 axis in cancer progression. Br J Cancer 96:541-545

Suto K, Yamazaki Y, Morita T, Mizuno H (2005) Crystal structures of novel vascular endothelial growth factors (VEGF) from snake venoms: insight into selective VEGF binding to kinase insert domain-containing receptor but not to fms-like tyrosine kinase-1. J Biol Chem 280:2126-2131

Swartz MA (2001) The physiology of the lymphatic system. Adv Drug Deliv Rev 50:3-20

Sybert VP, Dale BA, Holbrook KA (1985) *Ichthyosis vulgaris*: identification of a defect in synthesis of filaggrin correlated with an absence of keratohyaline granules. J Invest Dermatol 84:191-194

Szuba A, Rockson SG (1997) Lymphedema: anatomy, physiology and pathogenesis. Vasc Med 2:321-326

Szuba A, Skobe M, Karkkainen MJ, Shin WS, Beynet DP, Rockson NB, Dakhil N, Spilman S, Goris ML, Strauss HW, Quertermous T, Alitalo K, Rockson SG (2002) Therapeutic lymphangiogenesis with human recombinant VEGF-C. FASEB J 16:1985-1987

Tabibiazar R, Cheung L, Han J, Swanson J, Beilhack A, An A, Dadras SS, Rockson N, Joshi S, Wagner R, Rockson SG (2006) Inflammatory manifestations of experimental lymphatic insufficiency. PLoS Med 3:1114-1139

Taipale J, Makinen T, Arighi E, Kukk E, Karkkainen M, Alitalo K (1999) Vascular endothelial growth factor receptor-3. Curr Top Microbiol Immunol 237:85-96

Tammela T, Alitalo K (2010) Lymphangiogenesis: molecular mechanisms and future promise. Cell 140:460-476

Tammela T, Saaristo A, Holopainen T, Lyytikka J, Kotronen A, Pitkonen M, Abo-Ramadan U, Yla-Herttuala S, Petrova TV, Alitalo K (2007) Therapeutic differentiation and maturation of lymphatic vessels after lymph node dissection and transplantation. Nat Med 13:1458-1466

Tammela T, Saaristo A, Lohela M, Morisada T, Tornberg J, Norrmen C, Oike Y, Pajusola K, Thurston G, Suda T, Yla-Herttuala S, Alitalo K (2005) Angiopoietin-1 promotes lymphatic sprouting and hyperplasia. Blood 105:4642-4648

Tammela T, Zarkada G, Wallgard E, Murtomaki A, Suchting S, Wirzenius M, Waltari M, Hellstrom M, Schomber T, Peltonen R, Freitas C, Duarte A, Isoniemi H, Laakkonen P, Christofori G, Yla-Herttuala S, Shibuya M, Pytowski B, Eichmann A, Betsholtz C, Alitalo K (2008) Blocking VEGFR-3 suppresses angiogenic sprouting and vascular network formation. Nature 454:656-660

Tamura K, Dudley J, Nei M, Kumar S (2007) MEGA4: Molecular Evolutionary Genetics Analysis (MEGA) software version 4.0. Mol Biol Evol 24:1596-1599

Tamura K, Nei M, Kumar S (2004) Prospects for inferring very large phylogenies by using the neighbor-joining method. Proc Natl Acad Sci U S A 101:11030-11035

Tarsitano M, De Falco S, Colonna V, McGhee JD, Persico MG (2006) The C. elegans pvf-1 gene encodes a PDGF/VEGF-like factor able to bind mammalian VEGF receptors and to induce angiogenesis. FASEB J 20:227-233

Todd J (2000) Containment in the management of lymphoedema. In: Twycross R, Jenns K, Todd J (eds) Lymphoedema. Radcliffe Medical Press, Oxford, pp 165-202

Toivanen PI, Nieminen T, Viitanen L, Alitalo A, Roschier M, Jauhiainen S, Markkanen JE, Laitinen OH, Airenne TT, Salminen TA, Johnson MS, Airenne KJ, Yla-Herttuala S (2009) Novel Vascular Endothelial Growth Factor D Variants with Increased Biological Activity. J Biol Chem 284:16037-16048

Traktuev DO, Merfeld-Clauss S, Li J, Kolonin M, Arap W, Pasqualini R, Johnstone BH, March KL (2008) A population of multipotent CD34-positive adipose stromal cells share pericyte and mesenchymal surface markers, reside in a periendothelial location, and stabilize endothelial networks. Circ Res 102:77-85

Trompezinski S, Berthier-Vergnes O, Denis A, Schmitt D, Viac J (2004) Comparative expression of vascular endothelial growth factor family members, VEGF-B, -C and -D, by normal human keratinocytes and fibroblasts. Exp Dermatol 13:98-105

Trzewik J, Mallipattu SK, Artmann GM, Delano FA, Schmid-Schonbein GW (2001) Evidence for a second valve system in lymphatics: endothelial microvalves. FASEB J 15:1711-1717

Tsopelas C, Munns SL, Daniels CB, Lai C, Cooter RD, Chatterton BE (2002) Biodistribution and lymphatic speed of ^{99m}Tc-Antinomy Trisulphide Colloid in the Lizard *Pogona vitticeps*. Hellenike Pyrenike Iatr 1:42-45

Turgut M, Koca YB, Kaplan S, Metin K, Uzum N, Soylu E, Avc A, Ragbetli MC, Beytas EP, Olgun K (2007) Effects of Ca2+channel blocker verapamil on tissue regeneration in a lizard tail autotomy model: a biochemical and histological study. Amphibia-Reptilia 28:7-15

Uzarski J, Drelles MB, Gibbs SE, Ongstad EL, Goral JC, McKeown KK, Raehl AM, Roberts MA, Pytowski B, Smith MR, Goldman J (2008) The resolution of lymphedema by interstitial flow in the mouse tail skin. Am J Physiol Heart Circ Physiol 294:H1326-H1334

Valtola R, Salven P, Heikkila P, Taipale J, Joensuu H, Rehn M, Pihlajaniemi T, Weich H, deWaal R, Alitalo K (1999) VEGFR-3 and its ligand VEGF-C are associated with angiogenesis in breast cancer. Am J Pathol 154:1381-1390

Van der Auwera I, Van den Eynden GG, Colpaert CG, Van Laere SJ, van Dam P, Van Marck EA, Dirix LY, Vermeulen PB (2005) Tumor lymphangiogenesis in inflammatory breast carcinoma: a histomorphometric study. Clin Cancer Res 11:7637-7642

Veikkola T, Alitalo K (2002) Dual role of Ang2 in postnatal angiogenesis and lymphangiogenesis. Dev Cell 3:302-304

Veikkola T, Jussila L, Makinen T, Karpanen T, Jeltsch M, Petrova TV, Kubo H, Thurston G, McDonald DM, Achen MG, Stacker SA, Alitalo K (2001) Signalling via vascular endothelial growth factor receptor-3 is sufficient for lymphangiogenesis in transgenic mice. EMBO J 20:1223-1231

Vogel WO (1985) The caudal heart of fish: not a lymph heart. Acta Anat (Basel) 121:41-45

Von Marschall Z, Scholz A, Stacker SA, Achen MG, Jackson DG, Alves F, Schirner M, Haberey M, Thierauch KH, Wiedenmann B, Rosewicz S (2005) Vascular endothelial growth factor-D induces lymphangiogenesis and lymphatic metastasis in models of ductal pancreatic cancer. Int J Oncol 27:669-679

Voros G, Maquoi E, Demeulemeester D, Clerx N, Collen D, Lijnen HR (2005) Modulation of angiogenesis during adipose tissue development in murine models of obesity. Endocrinology 146:4545-4554

Wake DB, Dresner IG (1967) Functional morphology and evolution of tail autotomy in salamanders. J Morphol 122:265-305

Wang YD, Nakayama M, Pitulescu ME, Schmidt TS, Bochenek ML, Sakakibara A, Adams S, Davy A, Deutsch U, Luthi U, Barberis A, Benjamin LE, Makinen T, Nobes CD, Adams RH (2010) Ephrin-B2 controls VEGF-induced angiogenesis and lymphangiogenesis. Nature 465:483-486

Watari K, Nakao S, Fotovati A, Basaki Y, Hosoi F, Bereczky B, Higuchi R, Miyamoto T, Kuwano M, Ono M (2008) Role of macrophages in inflammatory lymphangiogenesis: Enhanced production of vascular endothelial growth factor C and D through NF-kappaB activation. Biochem Biophys Res Commun 377:826-831

Werner YL (1967) Regeneration of the caudial axial skeleton in a gekkonid lizard (*Hemidactylus*) with particular reference to the 'latent' period. Acta Zool 48:103-125

Whimster IW (1978) Nerve supply as a stimulator of the growth of tissues including skin. II. Animal evidence. Clin Exp Dermatol 3:389-410

Wigle JT, Harvey N, Detmar M, Lagutina I, Grosveld G, Gunn MD, Jackson DG, Oliver G (2002) An essential role for Prox1 in the induction of the lymphatic endothelial cell phenotype. EMBO J 21:1505-1513

Wigle JT, Oliver G (1999) Prox1 function is required for the development of the murine lymphatic system. Cell 98:769-778

Wilting J, Aref Y, Huang R, Tomarev SI, Schweigerer L, Christ B, Valasek P, Papoutsi M (2006) Dual origin of avian lymphatics. Dev Biol 292:165-173

Wilting J, Papoutsi M, Othman-Hassan K, Rodriguez-Niedenfuhr M, Prols F, Tomarev SI, Eichmann A (2001) Development of the avian lymphatic system. Microsc Res Tech 55:81-91.

Wilting J, Schneider M, Papoutski M, Alitalo K, Christ B (2000) An avian model for studies of embryonic lymphangiogenesis. Lymphology 33:81-94

Witkowska-Zimny M, Walenko K (2011) Stem cells from adipose tissue. Cell Mol Biol Lett 16:236-257

Witmer AN, van Blijswijk BC, Dai J, Hofman P, Partanen TA, Vrensen GFJM, Schlingemann RO (2001) VEGFR-3 in adult angiogenesis. J Pathol 195:490-497

Witzenbichler B, Asahara T, Murohara T, Silver M, Spyridopoulos I, Magner M, Principe N, Kearney M, Hu JS, Isner JM (1998) Vascular endothelial growth factor-C (VEGF-C/VEGF-2) promotes angiogenesis in the setting of tissue ischemia. Am J Pathol 153:381-394

Wong SY, Haack H, Crowley D, Barry M, Bronson RT, Hynes RO (2005) Tumor-secreted vascular endothelial growth factor-C is necessary for prostate cancer lymphangiogenesis, but lymphangiogenesis is unnecessary for lymph node metastasis. Cancer Res 65:9789-9798

Yamada Y, Nezu J, Shimane M, Hirata Y (1997) Molecular cloning of a novel vascular endothelial growth factor, VEGF-D. Genomics 42:483-488

Yaniv K, Isogai S, Castranova D, Dye L, Hitomi J, Weinstein BM (2006) Live imaging of lymphatic development in the zebrafish. Nat Med 12:711-716

Yaniv K, Isogai S, Castranova D, Weinstein BM (2007) Live imaging of lymphatic development in the zebralish embryo. FASEB J 21:A87-A88

Yoon YS, Murayama T, Gravereaux E, Tkebuchava T, Silver M, Curry C, Wecker A, Kirchmair R, Hu CS, Kearney M, Ashare A, Jackson DG, Kubo H, Isner JM, Losordo DW (2003) VEGF-C gene therapy augments postnatal lymphangiogenesis and ameliorates secondary lymphedema. J Clin Invest 111:717-725

Zeng Y, Opeskin K, Baldwin ME, Horvath LG, Achen MG, Stacker SA, Sutherland RL, Williams ED (2004) Expression of vascular endothelial growth factor receptor-3 by lymphatic endothelial cells is associated with lymph node metastasis in prostate cancer. Clin Cancer Res 10:5137-5144

Zhang QX, Magovern CJ, Mack CA, Budenbender KT, Ko W, Rosengart TK (1997) Vascular endothelial growth factor is the major angiogenic factor in omentum: mechanism of the omentum-mediated angiogenesis. J Surg Res 67:147-154

Zhou H, Zhou Y (2002) Distance-scaled, finite ideal-gas reference state improves structure-derived potentials of mean force for structure selection and stability prediction. Protein Sci 11:2714-2726

Zuckerlandl E, Pauling L (1965) Evolutionary divergence and convergence in proteins. In: Bryson V, Vogel HJ (eds) Evolving Genes and Proteins. Academic Press, New York, pp 97-166

Zuk PA, Zhu M, Mizuno H, Huang J, Futrell JW, Katz AJ, Benhaim P, Lorenz HP, Hedrick MH (2001) Multilineage cells from human adipose tissue: Implications for cell-based therapies. Tissue Eng 7:211-228